THE UNIVERSITY OF
SYDNEY

THE UNIVERSITY OF SYDNEY

CRYPTOCOCCOSIS:

A PROTEOMIC INVESTIGATION OF AN EMERGING FUNGAL DISEASE

Michael David Sivell

Bachelor of Biotechnology (Honours)

University of Technology, Sydney

A thesis submitted in fulfilment of the requirements of the degree of Doctor of Philosophy

Discipline of Microbiology

School of Molecular and Microbial Biosciences

Faculty of Science

University of Sydney

2014

Declaration

I certify that the research presented in this thesis is original and entirely my own work, except where otherwise acknowledged. The research was completed between February 2009 and September 2013 while I was enrolled in the degree of Doctor of Philosophy in the Faculty of Science at the University of Sydney, Sydney, Australia under the guidance of Associate Professor Dee Carter. Parts of the research described here were undertaken at the Biomolecular Frontiers Research Centre, Macquarie University, Sydney, Australia under the guidance of Associate Professor Ben Herbert. This thesis has not been previously submitted for examination, either wholly or in part for any other degree at any university or institution. Any assistance revived in the preparation of this thesis and all sources have been duly acknowledged.

The University of Sydney Animal Ethics Committee approved the research presented in this thesis.

Animal ethics approval number: **N00/10-2008/2/4810**

……..

Michael David Sivell

September 2013

Abstract

Fungal infections are increasing in frequency throughout the world. The development of new diagnostic and treatment strategies has not kept pace with this increase. Anti-fungal treatment options are limited to azoles and echinocandins, which are limited in spectrum, and the polyenes, which are toxic to human cells [1]. As treatments are limited in efficacy, there is a high incidence of recurrence and high mortality. The pathogenic yeasts *Cryptococcus neoformans* and *Cryptococcus gattii*, provide an excellent system for determining the spectrum of fungal growth and infection, from environmental saprotrophic growth, to self-limiting infection and through to severe primary infection. *C. neoformans* and *C. gattii* are the primary causative agents of cryptococcosis [2], however, the biological processes of *in vivo Cryptococcus* pathogenesis, and the host response to infection, at the molecular level remain a mystery.

Unlike bacterial pathogens, where a single gene can determine virulence, fungal pathogens require a minimum set of interacting virulence-associated properties for establishing and maintaining infection [3, 4]. The interplay between these during the infectious process is difficult to unravel by conventional genetic methods. Global approaches using proteomics allow differential gene expression to be investigated at a whole organism level. Furthermore, as proteins are targets for diagnostic tests and drug interventions, proteome approaches are the most rapid, reliable and powerful means of identifying potentially useful targets [5-9]. However, at this point in time, there is an absence of proteomic analyses of *in vivo* fungal infection. This is likely a result of the inherent technical issues associated with the fungal proteomics and mammalian pulmonary infection models.

This study focused on using comparative proteomic techniques to elucidate the proteins vital to *Cryptococcus* pathogenesis and the mammalian host response to pulmonary infection. *Cryptococcus* cells obtained from pulmonary infection and rat lung tissue represented technically challenging sample types that required significant protocol development prior to comparative analysis. Combined with the use of a mammalian model of infection, this subjected the data that were obtained to a number of experimental caveats. Despite the impediments to experimentation, the advances made in protocol development by this study allowed for the first *in vivo* analysis of intracellular *Cryptococcus* protein expression. This result provided proof of concept for global "–omics" analysis of *Cryptococcu*s from an *in vivo* sample. In addition, qualitative data were obtained that offered insights into fungal pathogenesis at the protein level and highlighted a number of *Cryptococcus* proteins that could be exploited as drug targets.

The application of iTRAQ to rat lung tissue provided the first demonstration of the global host lung protein response to pulmonary infection with *Cryptococcus* of differing species and virulence levels. iTRAQ comparative proteomic analysis suggested that the basic responses to pulmonary infection with *Cryptococcus* of different species and different virulence levels are uniform, regardless of disease outcome. While the identified lung proteins did not indicate the eventual outcome of disease, the analysis permitted inferences to be drawn regarding the potential therapeutic use of a number of differentially expressed proteins. The elucidation of the host response to infection with *Cryptococcus* was further pursued via Bio-Plex comparative cytokine analysis. This analysis found that pulmonary infection with virulent *Cryptococcus* progressed despite increased expression of cytokines, chemokines and growth factors that classically result in infection inhibition and/or

eradication. This study indicates that protection from the threat of infection and disease progression with highly virulent strains of *Cryptococcus* requires the development of novel anti-*Cryptococcus* therapeutic agents.

The identification of intracellular *Cryptococcus* proteins and host lung proteins and systemic cytokines of biological relevance to pulmonary cryptococcosis provides proof of the ability of comparative proteomics to elucidate future drug targets, biomarkers and diagnostic markers from *in vivo* mammalian infection models. The studies' most significant achievement has been the advances made in protocol development. It is hoped that these advances will lead to further, potentially quantitative, analysis of fungal pathogens under *in vivo* conditions, along with continued development of novel therapeutic and diagnostic options for pathogenic fungi.

Abbreviations

1-D SDS-PAGE	One dimensional/sodium dodecyl sulphate/polyacrylamide gel electrophoresis
2-D PAGE	Two dimensional/polyacrylamide gel electrophoresis
2-D nanoLC ESI MS/MS	Two dimensional/nano-liquid chromatography/electrospray ionization/tandem mass spectrometry
ACN	Acetonitrile
AIDS	Acquired immunodeficiency syndrome
C7BzO	3-(4-Heptyl)phenyl-3-hydroxypropyl)dimethylammoniopropanesulfonate
cm	Centimetre(s)
ddH_2O	Double distilled water
DIGE	Difference gel electrophoresis
DMSO	Dimethyl sulfoxide
DNA	Deoxyribonucleic acid
DTT	Dithiothreitol
ELISA	Enzyme-linked immunosorbent assay
G-CSF	Granulocyte-colony stimulating factor
GalXM	Galactoxylomannan
GM-CSF	Granulocyte macrophage-colony stimulating factor
GXM	Glucuronoxylomannan
HIV	Human immunodeficiency virus
IDA	Information dependent acquisition mode
IEF	Isoelectric focusing
IFN	Interferon
IL	Interleukin
IPG	Immobilised pH gradient
iTRAQ	Isobaric tags for relative and absolute quantitation
kDa	Kilodalton(s)
LDS	Lithium dodecyl sulphate
LiCl	Lithium chloride
LPS	Lipopolysaccharide
M	Molar
m/z	Mass to charge ratio
MES	2-(*N*-morpholino)ethanesulfonic acid
MHC	Major histocompatibility complex
min(s)	Minute(s)
MIP	Macrophage inflammatory protein
mL	Millilitre
mm	Millimetre
mM	Millimolar
MMTS	Methyl methanethiosulfonate
mRNA	Messenger ribonucleic acid
NK cells	Natural Killer cells
PBS	Phosphate buffered saline
PBS-T	Phosphate buffered saline with Tween 20
pI	Isoelectric point
PVDF	Polyvinylidene fluoride

RANTES	Regulated upon activation, normal T cell expressed and secreted
RNA	Ribonucleic acid
SCX HPLC	Strong cation-exchange/high-performance liquid chromatography
SD	Standard deviation
SDS	Sodium dodecyl sulphate
TBP	Tributylphosphine
TBS	Tris-buffered saline
TCEP	Tris(2-carboxyethyl)phosphine
TEAB	Tetraethylammonium bromide
TGF	Transforming growth factor
TNF	Tumour necrosis factor
TOF-MS	Time-of flight mass spectrometer
VEGF	Vascular endothelial growth factor
x g	Units of centrifugal force, i.e. earth's gravitational acceleration
α	Alpha
β	Beta
γ	Gamma
δ	Delta
µm	Micron
µM	Micromolar

Table of contents

Declaration ..... **i**

Abstract ..... **ii**

Abbreviations ..... **v**

Introduction **1**

1.1. The *C. neoformans-C. gattii* species complex **2**

1.2. *C. gattii* and the cryptococcosis outbreak on Vancouver Island **7**

1.3. The association between the global environment and the emergence of fungal pathogens **9**

1.4. Cryptococcal pathogenesis **10**

1.4.1. Host invasion 10

1.4.2. Intracellular survival and dissemination 10

1.4.3. Invasion of the central nervous system 12

1.5. Factors key to cryptococcal infection **14**

1.5.1. Basic characteristics of pathogenesis 14

1.5.2. Virulence factors 16

1.6. The origin and maintenance of virulence factors: Is cryptococcal infection a case of readymade virulence? **25**

1.7. The host response to infection **26**

1.7.1. Physical barriers of the lung 26

1.7.2. The innate immune response 27

1.7.3. The complement system 28

1.7.4. Cell mediated immunity 29

1.7.5. Antibodies 31

1.7.6. The direct antifungal effects of T lymphocytes 32

1.8. Cryptococcosis diagnosis, therapy and treatment **33**

1.8.1. Diagnosis 33
1.8.2. Therapy and treatment 33
1.8.3. Antifungal agents 34
1.8.4. Resolving cryptococcosis requires the development of novel antifungals and therapies 34
1.9. Proteomics: the study of protein structure and function 35
1.9.1. Comparative proteomics 37
1.9.2. Two-dimensional polyacrylamide gel electrophoresis: a fundamental proteomic technology 38
1.9.3. Difference in Gel Electrophoresis (DIGE) 39
1.9.4. Further general limitations to the 2-D PAGE analysis platform 42
1.9.5. Alternative comparative proteomics techniques 43
1.9.6. Isobaric tag for relative and absolute quantification (iTRAQ) 44
1.9.7. Analysis of the host immune response 48
1.9.8. The Bio-Plex suspension array system 49
1.10. Project outline 51
1.10.1. Hypothesis and aims – fungal pathogenesis 52
1.10.2. Hypothesis and aims - host response 53
Materials and Methods 54
2.1. Fungal strains 55
2.2. Materials and equipment, reagents and chemicals and solution formulations 56
2.3. General methods 59
2.3.1. *In vitro* growth conditions 59
2.3.2. Pulmonary infection model 59
2.3.3. Pulmonary tissue homogenisation 61

2.3.4. Isolation of *Cryptococcus* from pulmonary tissue and lyophilisation of *Cryptococcus* ... 62
2.3.5. *In vitro*/*in vivo Cryptococcus* cellular disruption and phenol protein extraction ... 63
2.3.6. 2-D PAGE ... 64
2.3.7. 1-D SDS-PAGE ... 65
2.3.8. Fluorescent staining and image analysis ... 66
2.3.9. Mass spectrometry (completed by the Australian Proteome Analysis Facility at Macquarie University) ... 66
2.4. Study Specific Methods: ... 68
Development of proteomic protocols for the analysis of pulmonary infection with *Cryptococcus* ... 69
3.1. Technical issues are inherent to the fungal sample type ... 70
3.2. Methods ... 71
3.2.1. *In vitro* growth conditions ... 71
3.2.2. Pulmonary infection model ... 71
3.2.3. Pulmonary tissue homogenisation ... 71
3.2.4. Isolation of *Cryptococcus* from pulmonary tissue and lyophilisation of *Cryptococcus* ... 71
3.2.5. *In vitro*/*in vivo Cryptococcus* cellular disruption and phenol protein extraction ... 72
3.2.6. 2-D PAGE ... 72
3.2.7. 1-D SDS-PAGE ... 72
3.2.8. 2-D PAGE Western blotting ... 72
3.3. Results: ... 76
3.3.1. Separating *Cryptococcus* from pulmonary tissue ... 76

3.3.2. Cell disruption, decapsulation and protein purification for *Cryptococcus* from pulmonary infection 77
3.3.3. Lyophilisation prior to mechanical disruption is essential for the disruption of *Cryptococcus* cells from pulmonary infection 78
3.3.4. Phenol extraction for cultured *Cryptococcus* 79
3.3.5. Phenol protein extraction of *Cryptococcus* cells obtained from pulmonary infection 80
3.3.6. Exopolysaccharides in pulmonary supernatants 82
3.3.7. 2-D PAGE Western blot complexity issues 82
3.3.8. Non-specific binding does not cause 2-D PAGE Western blot complexity 83
3.4. Discussion 84
3.4.1. Issues with the proteomic investigation of pulmonary infections 84
3.4.2. Development of an efficient protocol for *in vivo* Cryptococcus cell lysis 86
3.3.3. Cellular disruption techniques 86
3.4.4. Contaminating capsular polysaccharides 88
3.4.5. Dissociating *Cryptococcus* capsule and proteins from pulmonary infection requires the stronger dissociating agent Phenol 90
3.4.6. Phenol protein extraction for *in vitro Cryptococcus*: a litmus test 92
3.4.7. Phenol protein extraction for *in vivo Cryptococcus* 93
3.4.8. Exopolysaccharides in the lung material 94
3.4.9. 2-D PAGE Western blot analysis 95
3.5. Conclusions 97
Comparative proteomics of *Cryptococcus* 99
4.1. Introduction 100
4.2. Methods 103
4.2.1. *In vitro* growth conditions 103
4.2.2. Pulmonary infection model 103

4.2.3. Pulmonary tissue homogenisation 103
4.2.4. Isolation of *Cryptococcus* from pulmonary tissue and lyophilisation of *Cryptococcus* 103
4.2.5. *In vitro*/*in vivo Cryptococcus* cellular disruption and phenol protein extraction 104
4.2.6. 1-D SDS-PAGE 104
4.2.7. 1-D SDS-PAGE manual lane excision and trypsin in-gel digestion for mass spectrometry protein identification 104
4.2.8. Mass spectrometry (completed by the Australian Proteome Analysis Facility at Macquarie University) 106
4.2.9. Codon adaptation index calculation 106
4.3. Results 107
4.3.1. Macroscopic observation of rats infected with *C. gattii* R265 107
4.3.2. *In vitro* and *in vivo Cryptococcus* mass spectrometry results 108
4.3.3. Host proteins co-purified with *Cryptococcus* proteins from pulmonary infection 109
4.3.4. Proteins 'unique' to *Cryptococcus* cells obtained from pulmonary infection 111
4.4. Discussion 114
4.4.1. Experimental design "Catch 22" 114
4.4.2. 1-D SDS-PAGE NanoLC ESI MS/MS can detect *Cryptococcus* proteins expressed during rat pulmonary infection 114
4.4.3. The persistence of contaminating rat proteins 116
4.4.4. Contaminating host proteins are non-specific 116
4.4.5. The selection of biologically relevant proteins from proteomics datasets ... 118
4.4.6. Protein function as a selection criterion and the danger of using automated systems to assign function 119
4.4.7. Protein abundance as an indicator of biological relevance 120

4.4.8. Codon usage bias as a predictor of protein abundance 122
4.4.9. Fungal response to hypoxia and stress during infection 122
4.4.10. Low abundance *Cryptococcus* proteins from cells obtained from pulmonary infection as potential drug targets 124
4.4.11. From biologically relevant protein to drug target 128
4.5. Conclusions 130

Elucidating the rat host protein response to pulmonary infection with *Cryptococcus* 131

5.1. Introduction 132
5.2. Methods 135
5.2.1. *Cryptococcus* strains and number of rats infected 135
5.2.2. Pulmonary infection model 136
5.2.3. Pulmonary tissue homogenisation 136
5.2.4. Pulmonary sample preparation for iTRAQ analysis 136
5.2.5. 4-plex iTRAQ sample design 137
5.2.6. iTRAQ labelling (completed by the Australian Proteome Analysis Facility at Macquarie University) 138
5.2.7. Mass spectrometry (completed by the Australian Proteome Analysis Facility at Macquarie University) 139
5.3. Results 139
5.3.1. Rat lung weights pre and post infection 139
5.3.2. Inoculation resulted in strain specific lesion formation in rat lungs 139
5.3.3. Global comparative quantitative analysis of control and infected lungs 142
5.3.4. Differentially expressed proteins common to infected lungs 142
5.3.5. Biologically relevant differentially expressed proteins 144
5.3.6. Proteins that are marginally outside the selection criteria 145
5.3.7. Ambiguous interesting proteins 147

5.4. Discussion 149

5.4.1. An observable strain hierarchy in response to infection 149

5.4.2. The selection of biologically proteins from datasets generated by iTRAQ 150

5.4.3. Protein function as a selection criterion 151

5.4.4. Differentially expressed proteins common to infected lungs 151

5.4.5. Differentially expressed proteins that increased in expression 152

5.4.6. Differentially expressed proteins that decreased in expression 157

5.4.7. The case of proteins that fall outside of the selection criteria 162

5.4.8. Proteins with one or more biological replicates that was not significant 164

5.4.9. Experimental design constrains the elucidation of the host response to infection 165

5.4.10. An observable increase in ambiguity at the late stage infection time-point 167

5.5. Conclusions 168

The systemic response to pulmonary infection with *Cryptococcus* 170

6.1. Introduction 171

6.2. Methods 175

6.2.1. *In vitro* growth conditions 175

6.2.2. Pulmonary infection model 175

6.2.3. Bio-Plex Pro Rat Cytokine, Chemokine, and Growth Factor Assay 175

6.2.4. Linear regression models 178

6.2.5. Data analysis 180

6.3. Results 181

6.3.1. Cytokine response to pulmonary cryptococcosis: global trends 181

6.3.2. Pro-inflammatory cytokine expression during pulmonary infection 182

6.3.3. Anti-inflammatory cytokine, chemokine, growth factor and dual role cytokine expression during pulmonary infection 183

6.3.4. Differentially expressed cytokines as a result of pulmonary infection with *Cryptococcus* 184

6.4. Discussion 187

6.4.1. Experimental design considerations 187

6.4.2. Linear regression models and the cytokine response to infection 188

6.4.3. More than regression models 190

6.4. Conclusions 199

General discussion 202

7.1. Fungal pathogens - the emerging threat 203

7.2. The elucidation of *Cryptococcus* pathogenesis and the host response to infection requires a holistic approach 204

7.3. *Cryptococcus* protein extraction protocols - a work in progress 206

7.4. Comparative proteomics revealed lung proteins of biological relevance . 207

7.5. The systemic cytokine response to infection 208

7.6. Is there a relationship between pulmonary *Cryptococcus* infection and COPD? 209

7.7. Conclusions 211

References 212

List of Figures

Figure 1.1: Scanning electron microscopy of *C. neoformans* 3

Figure 1.2: The cryptococcal virulence pathway 4

Figure 1.3: Schematic phylogeny of the *C. neoformans*-*C. gattii* species complex 6

Figure 1.4: Map of the Pacific Northwest 8

Figure 1.5: Cell-to-cell transfer of *C. neoformans* leads to infection of previously uninfected cells 12

Figure 1.6: Possible methods that *Cryptococcus* uses to transverse the endothelium of the blood-brain barrier or the epithelium of the blood cerebrospinal fluid barrier 13

Figure 1.7: Model of the *Cryptococcus* lifecycle showing basidiospore production 15

Figure 1.8: *C. gattii* obtained from pulmonary infection showing the very large *Cryptococcus* capsule 18

Figure 1.9: Electron microscopy of the cell wall-capsule interface 19

Figure 1.10: Images depicting cryptococcal cells with different capsule sizes and a schematic representation of capsule enlargement 21

Figure 1.11: Non-melanin- and melanin-forming colonies of *C. gattii* on 3,4-dihydroxyphenylalanine (L-DOPA) media after 7 days at 25 °C 22

Figure 1.12: Macrophage parasitism by *Cryptococcus* 30

Figure 1.13: An example of the fractionation power of 2-D PAGE 39

Figure 1.14: iTRAQ reagent structure 45

Figure 1.15: iTRAQ workflow 46

Figure 1.16: Bio-Plex sandwich immunoassay 50

Figure 1.17: Bio-Plex suspension array system workflow 50

Figure 3.1: Semi-dry blotting stack for reverse polarity protein transfer 74

Figure 3.2: Semi-dry blotting stack for traditional polarity protein transfer 75

Figure 3.3: Sucrose density cushion centrifugation separates *Cryptococcus* cells from host pulmonary material 77

Figure 3.4: A) Hydrated *C. gattii* cells isolated from late stage pulmonary infection; B) the same cells post lyophilisation and beat beating 79

Figure 3.5: 2-D PAGE gel images showing the separation of proteins obtained from *C. gattii* 80

Figure 3.6: 1-D SDS-PAGE gel images of *C. gattii* proteins 81

Figure 3.7: 2-D PAGE images showing separated lung proteins from rats infected with *C. gattii* R265 (late stage infection) 82

Figure 3.8: Representative Western blot showing complexity of protein spots 83

Figure 3.9: Anode membrane generated following the previously described Western blot (section 3.2.8.) protocol without primary antibody 84

Figure 3.10: Removal of lung tissue using an Ultra-turrax to wash the *Cryptococcus* cells 85

Figure 3.11: Phenol protein extraction protocol 91

Figure 4.1: Images of uninfected and infected lungs and *Cryptococcus* cells obtained from pulmonary infection 108

Figure 5.1: Schematic of the mammalian respiratory structures 132

Figure 6.1: Magnetic microsphere architecture 172

Figure 6.2: Plot generated by RStudio after fitting a linear regression model to the global cytokine, chemokine and growth factor expression data for control and infected rat lung 182

Figure 6.3: Plot generated by RStudio after fitting a linear regression model to the pro-inflammatory cytokine expression data for control and infected rat lung 183

Figure 6.4: Plots generated by RStudio after fitting linear regression models to the anti-inflammatory, chemokine, growth factors and dual role cytokine expression data for control and infected rat lung 184

Figure 6.5: Cytokines, chemokines and growth factors found to be significantly different in expression when comparing serum from rats with pulmonary *Cryptococcus* infection to serum from naïve rats 186

List of Tables

Table 2.1: Fungal strains 55

Table 2.2: Materials and equipment 56

Table 2.3: Reagents and chemicals 57

Table 2.4: Solution formulations 58

Table 2.5: Study specific methods 68

Table 3.1: Techniques attempted for *Cryptococcus* from pulmonary infection 78

Table 4.1: Rat lung weights 107

Table 4.2: Mass spectrometric data obtained from cultured *Cryptococcus* and *Cryptococcus* from pulmonary infection 109

Table 4.3: Biologically relevant *Rattus norvegicus* proteins co-purified with *Cryptococcus* proteins from cells obtained from pulmonary infection 110

Table 4.4: Biologically relevant *in vivo Cryptococcus* proteins 112

Table 5.1: *Cryptococcus* strains and number of rats infected 135

Table 5.2: 4-plex iTRAQ sample design for pulmonary infection with KN99α 137

Table 5.3: 4-plex iTRAQ sample design for pulmonary infection with R265 137

Table 5.4: 4-plex iTRAQ sample design for pulmonary infection with R272 138

Table 5.5: Rat lung weights 139

Table 5.6: iTRAQ mass spectrometry results 142

Table 5.7: Differentially expressed proteins common to the pulmonary infection datasets 143

Table 5.8: Biologically relevant proteins with increased expression 144

Table 5.9: Biologically relevant proteins with decreased expression 145

Table 5.10: Differentially expressed proteins marginally outside the selection criteria 146

Table 5.11: Proteins with ambiguous expression states among biological replicates 148

Chapter One

Introduction

This introduction includes a brief description of the current understanding of the C. neoformans-C. gattii *species complex including the basic characteristics required for pathogenesis and the major virulence factors involved in pathogenesis. In addition, this introduction will encompass a brief review of the proteomic techniques applicable to the study of the* C. neoformans-C. gattii *species complex during both* in vitro *growth and* in vivo *mammalian infection.*

1.1. The *C. neoformans-C. gattii* species complex

Fungi are ubiquitous in both the natural and urban environment. It has been estimated that the fungal Kingdom contains 1.5 million fungal species [10] of which approximately 140,000 have been formally identified by taxonomists [11]. Despite their ubiquitous nature, less than 0.01% of fungi species are capable of causing human disease [12, 13]. Included in this selective group of pathogenic fungi are the *Cryptococcus neoformans* and *Cryptococcus gattii* yeast species. *Cryptococcus* belongs to the *Filobasidella* clade of the Tremellales (Order Tremellomycetes) (figure 1.1) [14]. The genus *Cryptococcus* contains around 37 recognised fungal species, the majority of which do not cause disease in mammals [15]. The *C. neoformans-C. gattii* species complex includes *C. neoformans* var. *neoformans*, *C. neoformans* var. *grubii* and *C. gattii*, which are the most common causative agents of cryptococcosis [16, 17]. *C. neoformans* and *C. gattii* are free-living in the environment and do not require an infective step in their lifecycle to propagate. *C. neoformans* and *C. gattii* are not considered zoonotic pathogens [18] and this appears to be true apart from a handful of zoonotic transfer cases involving immune-suppressed patients [19, 20]. Rather, mammals acquire the organism from environmental sources. Disease as a result of *C. neoformans* or *C. gattii* infection, known as cryptococcosis, generally begins in the lungs before haematogenous dissemination to other organs, with a predilection for the central nervous system (figure 1.2) [16, 21]. The result of brain invasion is cryptococcal meningoencephalitis that is always fatal without antifungal therapy. In fact, mortality remains at almost 20% despite aggressive antifungal therapy [22].

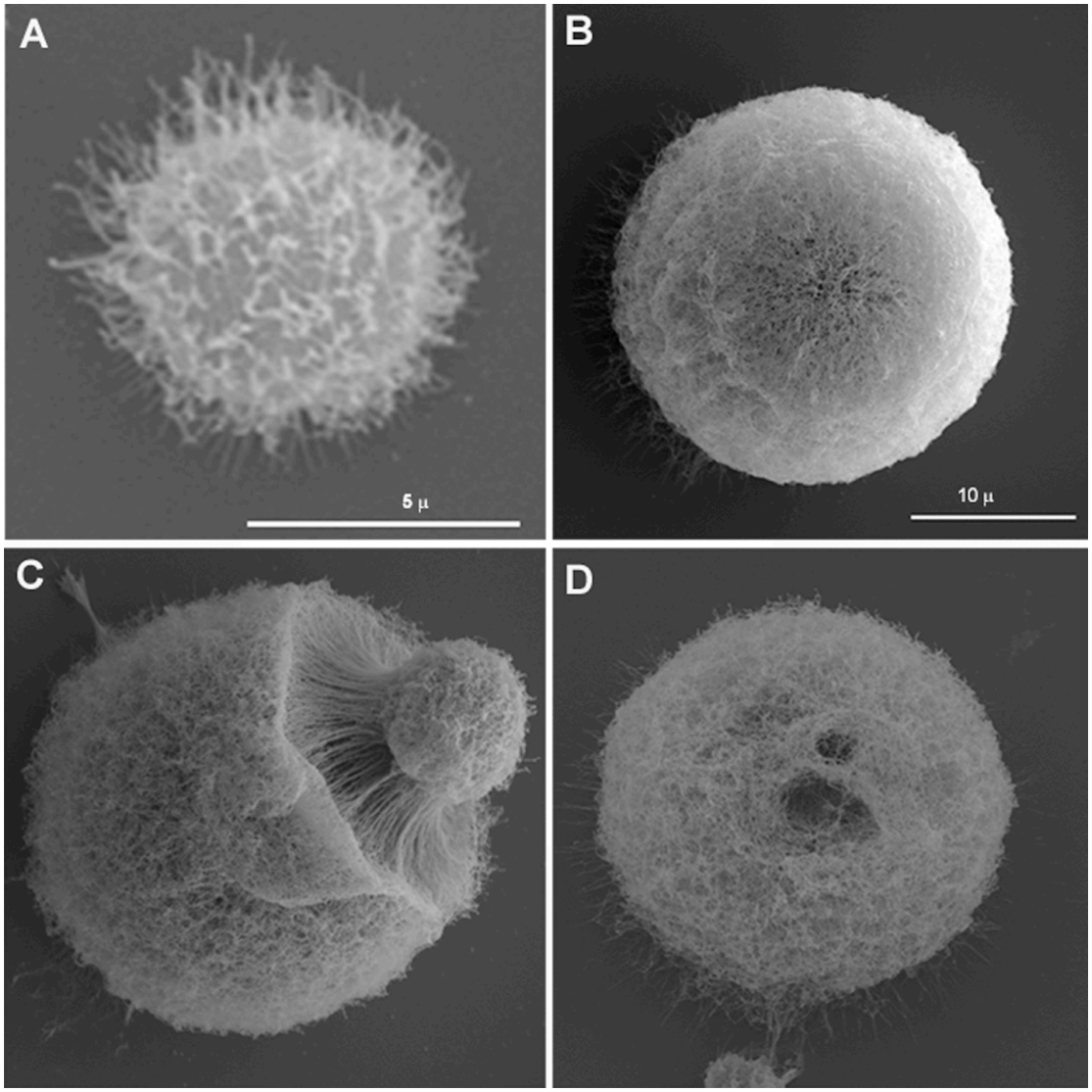

Figure 1.1: Scanning electron microscopy of *C. neoformans*

Scanning electron microscopy of A) *C. neoformans* grown in rich media, B – D) *C. neoformans* obtained from pulmonary infection (scale bar from B applies to C and D) (from [23]).

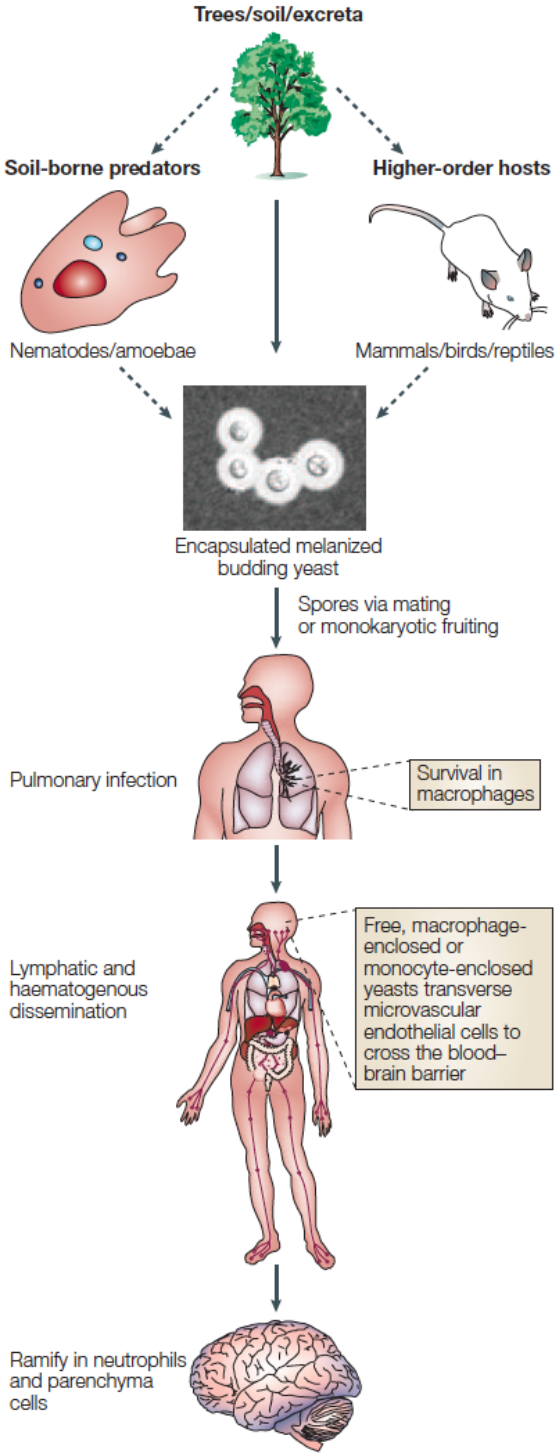

Figure 1.2: The cryptococcal virulence pathway

Cryptococcus survives in the environment where it can interact with animals or microbial predators. Inhaled desiccated yeast cells or spores establish mammalian pulmonary infection. The fungus can then spread from the lungs and enter the central nervous system (CNS) through the microcapillaries of the blood–brain barrier. Dashed arrows indicate that pathways are hypothetical (from [24]).

C. neoformans and *C. gattii* are so closely related, having diverged from each other approximately 37-49 million years ago [25], that until recently they were considered varieties of a single species (figure 1.3) [26-28]. Despite the fact that the two species share all known major virulence factors [16], there are numerous differences between the species with regard to ecology, epidemiology, pathobiology, biochemistry and genetics [27]. A clear distinction between the two *Cryptococcus* species is that *C. neoformans* is primarily an opportunistic pathogen that causes a self-limiting asymptomatic, chronic disease whereas *C. gattii* produces a relentlessly progressive infection that readily results in the death of otherwise healthy hosts [29, 30]. *C. gattii* is therefore classified as a primary pathogen. A further defining discrepancy between the two species is that *C. neoformans* has a worldwide distribution in association with avian guano while *C. gattii* has traditionally been considered to be geographically restricted to tropical and sub-tropical climates in association with Eucalypt trees [31-33]. However, a recent outbreak of *C. gattii* induced cryptococcosis in the temperate climate of Vancouver Island, British Columbia, Canada is challenging this proposed geographical restriction [32, 34].

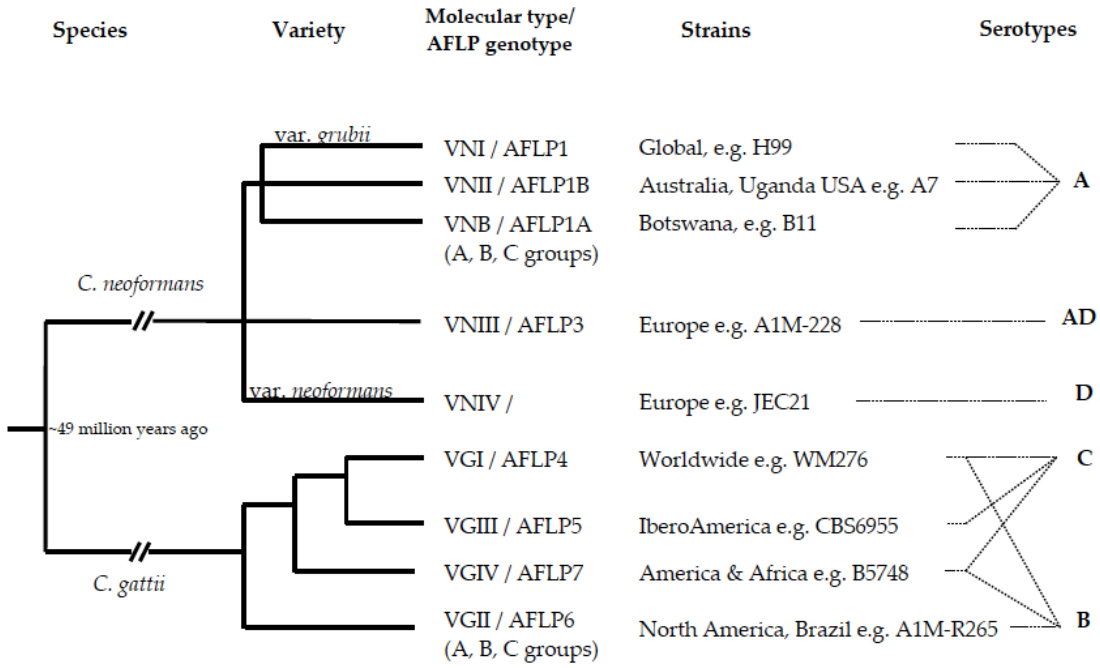

Figure 1.3: Schematic phylogeny of the *C. neoformans-C. gattii* species complex

For *C. neoformans*, two monophyletic lineages, corresponding to variety *grubii* and *neoformans* consistently present along with the hybrid population. Serotypes correspond to genotypes. For *C. gattii*, four monophyletic lineages corresponding to the previously described genotypic groups are consistently found. Serotypes and genotype do not correlate. The molecular types VNIV and VGII form the basal clades within the *C. neoformans* and *C. gattii* branches of the phylogenetic tree, respectively (from [35]).

Cryptococcus classification is based on serotype, as determined by specific capsular antigens, and by molecular genotyping, which further defines diversity at the sub-species and sub-variety level. The *C. neoformans-C. gattii* species complex is divided into the following serotypes: *C. neoformans* var. *neoformans* = serotype D, *C. neoformans* var. *grubii* = serotype A, a mixed *C. neoformans* = serotype AD (diploid hybrid) and *C. gattii* = serotype B or C. The development of modern molecular technologies and genomic analyses resulted in the confirmation of *C. neoformans* and *C. gattii* as separate species [36]. Genotyping has been performed using a variety of

molecular techniques such as PCR fingerprinting, AFLP, RFLP, RAPD and MLST. Molecular genotyping further defines diversity within serotypes. *C. neoformans* var. *grubii* (serotype A) includes molecular types VNI and VNII. *C. neoformans* var. *neoformans* (serotype D) comprises molecular type VNIV and the hybrid serotype AD is molecular type VNIII. *C. gattii* (serotypes B and C) is divided into molecular types VGI, VGII, VGIII and VGIV [37], with no clear correlation between the serotypes and genotypes. Genetic subtypes exist within some molecular types, for example VGII is subdivided into subtypes VGIIa, VGIIb and VGIIc. The molecular genotyping of the *C. neoformans*-*C. gattii* species complex not only provides a more precise classification method, it also provides the scientific community with a tool to aid our understanding of the relationships both within and between geographic areas.

1.2. *C. gattii* and the cryptococcosis outbreak on Vancouver Island

C. gattii was first identified in 1970 after being isolated from a leukemic patient [38]. Since that time it has been shown to differ from *C. neoformans* in phenotypic characteristics, natural habitat, epidemiology, clinical manifestations of disease and response to antifungal therapy [28]. Despite increasing evidence of *C. gattii* as an emerging primary human pathogen, during the past 4 decades this pathogenic organism has remained understudied. This can be largely attributed to the fact that less than 1% of cryptococcosis cases worldwide are a result of infection with *C. gattii* [35]. Furthermore, it was previously believed that the organism was geographically restricted to tropical and subtropical environs. A recent outbreak of cryptococcosis in human and animal hosts as a result of *C. gattii* has increased the rate of *C. gattii* related cryptococcosis cases and has resulted in the reassessment of the geographic

range limits of this fungal pathogen. The outbreak and spread of what appears to be a hyper-virulent clone of *C. gattii* has stimulated interest in the scientific investigation of this pathogenic organism. The outbreak was first acknowledged in 1999 on Vancouver Island, British Columbia, Canada, and is continuing to spread into northwestern United States of America with fatal consequences (figure 1.4) [32, 39-41]. The vast majority of *C. gattii* isolates involved in the outbreak have been identified as belonging to the VGII molecular type [35]. These VGII isolates have been further separated into two subtypes, a major hyper-virulent form that is common in environmental and clinical isolates (VGIIa) and a rare, less virulent minor form (VGIIb) [37, 42, 43]. The obvious question arises as to how and why these subtypes, and especially VGIIa, have become such a pathogenic threat in relatively recent times.

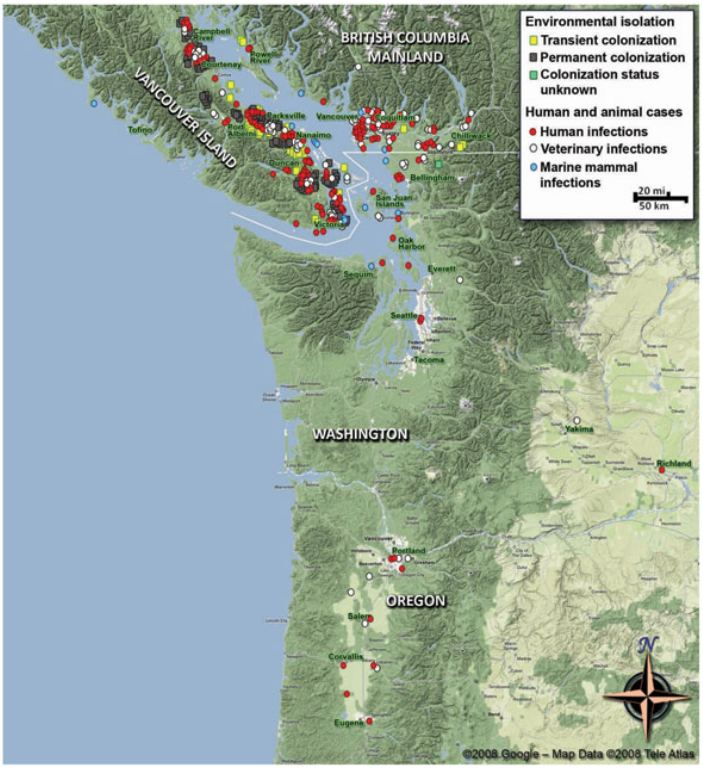

Figure 1.4: Map of the Pacific Northwest

Shows human and veterinary *C. gattii* cases (including marine mammals) by place of residence or detection, and locations of environmental isolation of *C. gattii* during 1999–2008 (from [40]).

1.3. The association between the global environment and the emergence of fungal pathogens

Human infections and diseases are intricately linked to the global environment [44]. The exact consequences of the alteration of the global environment via the effects of global warming on the emergence, or re-emergence, of infectious diseases are as to this date only theoretical and are heavily dependent on the complex interaction between the host population and the causative agent [44, 45]. It is postulated that global warming could lead to human migration, crowding, famine, water contamination, changes in vector ecology, the spread of infectious diseases to environs which where previously unsuitable and the straining/breakdown of public health services [44, 46]. Global warming could have some very real detrimental effects to mammalian hosts in the case of fungal diseases, such as cryptococcosis. Fungi cause relatively few diseases in mammals, despite being major pathogens of plants, other fungi, rotifers, insects and amphibians [47]. Mammals have a high resistance to fungal infections as a result of a combination of possessing a complex immune system and endothermy. Body temperatures above that of environmental temperatures create a thermally restrictive barrier for the majority of fungi. Fungi have only come into prevalence as human pathogens as a result of increasing rates of impaired immunity due to medical interventions and the onset of the HIV/AIDS epidemic in the late 20th century. It has been hypothesised that global warming could increase geographic range of pathogenic species and select for adaptive thermotolerance, that is, the ability to grow at and above mammalian body temperatures [48]. Both *C. gattii* and *C. neoformans* are infective organisms that display thermotolerance, and the opening of new environmental niches to these potentially deadly organisms could have serious consequences for public health. The

risk of newly emerging fungal pathogens will be magnified by the apparent lack of effective antifungal drugs and the absolute lack of vaccines. A better understanding of fungal pathogenesis is paramount to the identification of novel drug targets and the development of antifungal drugs and possibly vaccines.

1.4. Cryptococcal pathogenesis

1.4.1. Host invasion

There is a general consensus that cryptococcal cells most commonly enter the host via the respiratory tract. Infection is initiated when the fungal propagules enter the alveolar space. Infections can also be initiated in other tissues via trauma and may also be acquired via the gastrointestinal tract [49]. Fungal propagules 1-2 μm in diameter result in the highest rate of deposition in the respiratory spaces of the lungs [50]. Above this size penetration and deposition efficiency decreases due to the fact that fewer particles escape upper respiratory trapping and expulsion. Below this size lobular deposition is retarded due to the fact that gravitational settlement within the alveolar space decreases. Cryptococcal cells fit this size criterion when in the form of desiccated haploid yeast cells (<2 μm diameter) or as basidiospores (1-3 μm diameter) [51].

1.4.2. Intracellular survival and dissemination

Many aspects of cryptococcal pathogenesis are poorly understood. This is especially true of *C. gattii* pathogenesis. However, there is broad consensus in the literature that subsequent to deposition in the alveolar spaces, highly virulent strains of

Cryptococcus are able to surmount the initial host defence barrier, namely alveolar macrophages, and disseminate utilising unique pathogenic strategies. It has been demonstrated experimentally that the interaction of cryptococcal cells with host phagocytes, including macrophages and monocytes, is vital for the persistence and proliferation of cryptococcal disease. Indeed it has been determined that these pathogenic fungi replicate inside and escape alive from phagocytic cells, the very cells that are designed to eradicate infection [52-54]. It is during facultative intracellular infection that cryptococcal cells undergo microevolution and phenotypic switching resulting in the enhanced expression of key virulence factors that increase the pathogenicity of the infectious particles [55]. These virulence factors are paramount to cryptococcal host infection and dissemination. These aspects of cryptococcal infection will be discussed at greater length in a following section.

In addition to replication within phagocytes, it has been recently demonstrated that cryptococcal cells have the ability to undergo lateral transfer between phagocytes, moving directly from infected to uninfected phagocytes (figure 1.5). Although this is a rare event that has only been observed within *in vitro* systems, it has been hypothesised that direct cell-to-cell spread may occur repeatedly during *Cryptococcus* infections, allowing the pathogen to remain concealed from the immune system and protecting it from exposure to antifungal agents [56, 57]. This strategy would not only allow the fungus to persist within the host during latent infections, but also provides a plausible model for the mode of the spread of infection, whereby phagocytes act as the vehicle for dissemination of *Cryptococcus* cells throughout the host [58, 59].

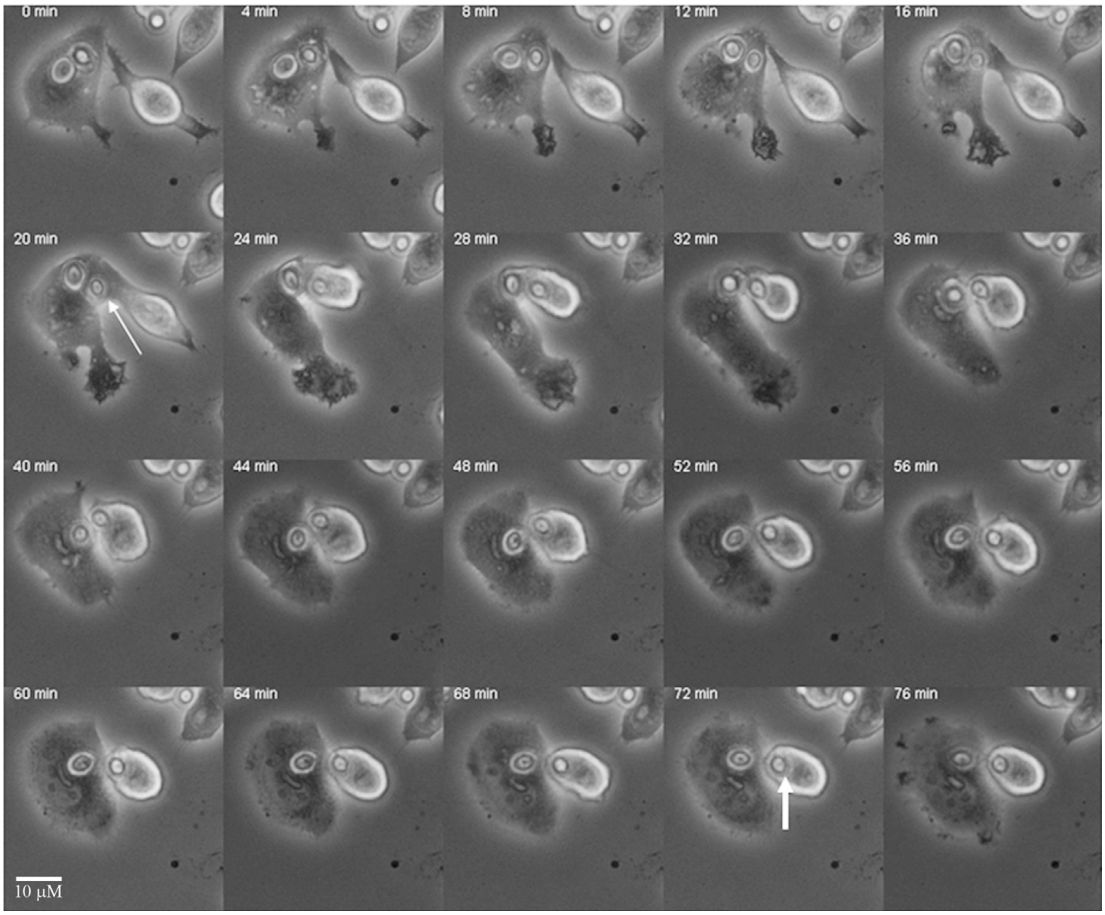

Figure 1.5: Cell-to-cell transfer of *C. neoformans* leads to infection of previously uninfected cells

The thin arrow indicates the cryptococcal cell that is being transferred while the wide arrow points to the cryptococcal cell that has been fully transferred to the previously uninfected macrophage cell (from [56]).

1.4.3. Invasion of the central nervous system

Although cryptococcal cells have the capability to infect any organ, the infection of the central nervous system is one of the most common clinical manifestations and is the leading cause of death from cryptococcosis. The apparent neurotropism observed during cryptococcal infection is the result of *C. neoformans* and *C. gattii* being able to utilise catecholamines, a compound the brain is rich in, as a carbon source.

Cryptococcus cells are thought to invade the brain and cerebrospinal fluid via circulating blood [60]. In order to penetrate into the brain, cryptococcal cells must transverse the endothelium of the blood-brain barrier or the epithelium of the blood-cerebrospinal fluid barrier. The exact method by which this process occurs is one of the least understood steps of cryptococcosis. It is known that microbial pathogens may cross the blood-brain barrier transcellularly (passage through the brain micro-vascular endothelial cells), paracellularly (passage between the cells of an epithelium) and/or by means of infected immune cells (also known as the Trojan horse mechanism whereby infected immune cells carry the pathogen across the blood brain barrier) (figure 1.6) [61]. Multiple studies have provided evidence for both the transcellular [62] and Trojan horse mechanism [58, 59] of brain invasion, however the role of paracellular passage remains uncertain.

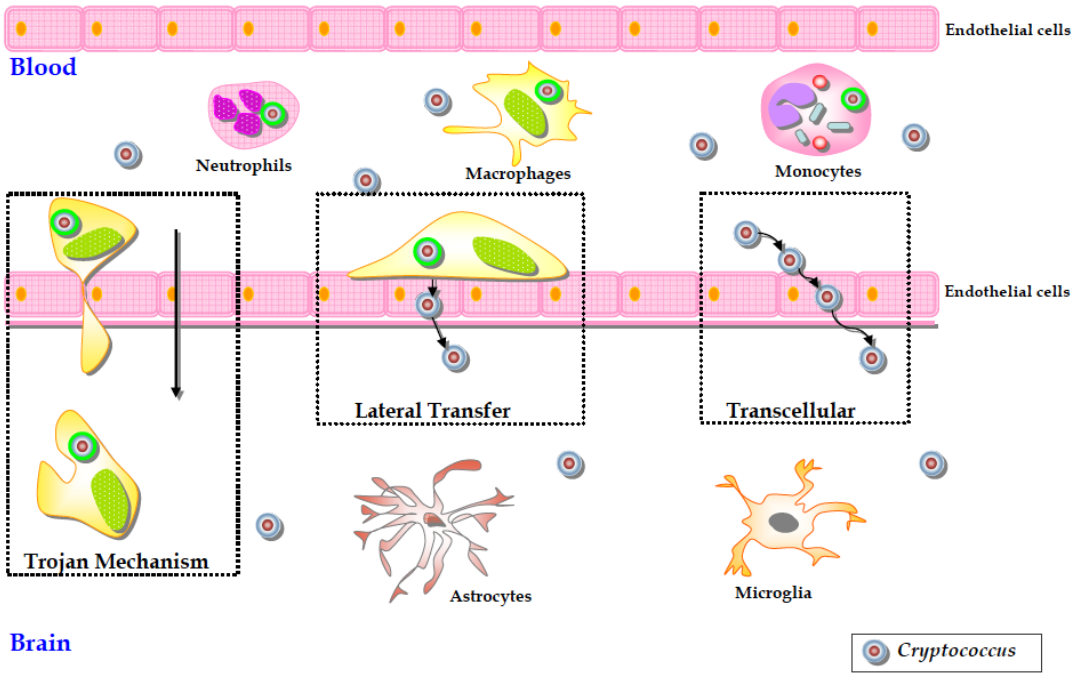

Figure 1.6: Possible methods that *Cryptococcus* uses to transverse the endothelium of the blood-brain barrier or the epithelium of the blood-cerebrospinal fluid barrier (from [35]).

1.5. Factors key to cryptococcal infection

The factors that make *C. neoformans* and *C. gattii* a pathogen are divided into two major groups, namely the characteristics required for the fungi to establish infection and survive in the human host and the virulence factors that increase the degree of pathogenicity [51]. The basic characteristics for pathogenicity are absolutely essential for the survival of *C. gattii* and *C. neoformans* within animal and human hosts. Thus, these basic characteristics are paramount for the initiation and progression of cryptococcal disease.

1.5.1. Basic characteristics of pathogenesis

1.5.1.1. The infectious propagule

To enter the alveolar spaces of the lungs, so as to establish pulmonary infection, an organism must produce viable forms that are smaller than 4 μm in diameter. Although the exact nature of the infectious propagules responsible for cryptococcosis remains unknown, they have been hypothesised to be dehydrated yeast cells or basidiospores [63]. The typical vegetative form of *C. neoformans* and *C. gattii* is the yeast form with a cell diameter ranging from 2.5 - 10 μm, depending on environmental conditions [16]. Thus, cells in the lower region of this size range are capable of entering the alveolar spaces of the lungs. Basidiospores range in size from 1 - 3 μm and hence are also capable of entering the alveolar spaces of the lungs. Basidiospores are produced during sexual reproduction between α- and a-mating types, an event that has not been observed directly in nature but readily occurs on appropriate media [63].

An organism's ability to generate spores depends on the presence of appropriate mating partners and the fertility of the strains (figure 1.7). In specific cases, the degree

of strain fertility, and thus its ability to undergo sexual reproduction, has been correlated to the virulence of the strain [64-66]. There is also evidence that an organism's ability to undergo sexual reproduction and thus sexual recombination facilitates its ability to adapt to new environments and be more tolerant of harsh environs via an increased capability of generating genetic diversity [66-68]. Thus, there is a direct relationship between fertility and virulence in *Cryptococcus*. This concept is especially interesting with regard to *C. gattii* virulence and the Vancouver Island outbreak. It has also been demonstrated that viable basidiospores are produced during monokaryotic fruiting events that occur when cells are under nitrogen starvation (figure 1.7) [69]. Monokaryotic fruiting was once believed to be linked exclusively to the *MAT*α locus and thus a-mating type strains, which posses the *MAT*a locus, were once thought to be unable to produce haploid fruiting bodies. Recent research has proven that this is not the case, rather that both α- and a-mating types can undergo monokaryotic fruiting events [70]. Regardless of the nature of the infectious propagule, it is known that if a cryptococcal strain is unable to produce small infectious propagules it cannot be pathogenic [51].

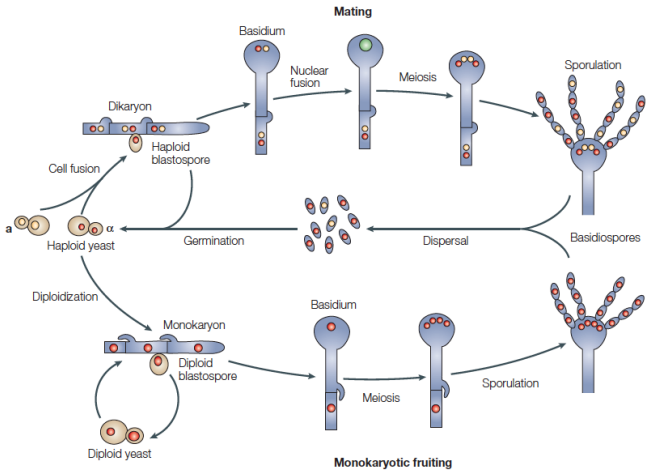

Figure 1.7: Model of the *Cryptococcus* lifecycle showing basidiospore production (from [24]).

1.5.1.2. Growth under in vivo conditions

In order to cause infection in humans, *C. neoformans* and *C. gattii* isolates must be able to efficiently grow at 37 °C in an atmosphere of approximately 5 % CO_2 at a pH of 7.3 to 7.4. It has been established that many cryptococcal genes are regulated by temperature; however, the exact mechanisms by which cryptococcal species tolerate high-temperature growth are not entirely understood. A number of studies have identified approximately 50 genes that are either induced or up-regulated by high temperature growth, of which over a dozen have been identified as being necessary for high-temperature growth [71-73]. The gene encoding the calcineurin A catalytic subunit is one such essential gene. This serine-threonine specific phosphatase is activated by Ca^{2+}-calmodulin and is involved in stress responses in yeasts. Calcineurin A mutants are unable to survive at 37 °C, in 5 % CO_2 or at alkaline pH [74]. It has been predicted that calcineurin A would not represent a likely candidate for drug therapy due to *Cryptococcus* calcineurin sharing striking identity with other calcineurins, including human calcineurin [74]. Calcineurin inhibitors, which are the mainstay of post-transplantation immunosuppression [75], are inherently toxic, especially to the kidneys [76]. However, the fact that calcineurin A is a basic requirement of *Cryptococcus* survival in the host and thus an absolutely necessary feature for the pathogenicity of the organism continues to drive research attempting to harness calcineurin as an anti-fungal agent [74, 77].

1.5.2. Virulence factors

Virulence factors act to increase the degree of pathogenicity of a microbe. *C. neoformans* and *C. gattii* have been found to share all known major virulence factors,

a number of which have been well defined. Although virulence factors do not serve as potential targets in the hunt for a definitive cure for cryptococcal disease, inhibitors and vaccines designed to act upon the components of the cryptococcal virulence phenotype may be useful in the treatment and/or prevention of cryptococcosis [78]. There appears to be a general consensus that capsule synthesis, cryptococcal products (exopolysaccharides, mannoproteins etc.), melanin production, mannitol production and phenotypic switching are the major virulence factors during cryptococcal infection. Cryptococcal infection has been further associated with phospholipase [78], a myriad of proteases, urease [79], thiol peroxidise [80] and superoxide dismutase activity [81]. A review of every potential virulence factor is beyond the scope of this introduction. Thus, the focus will be on the major virulence factors of cryptococcal infection.

1.5.2.1. The Cryptococcus capsule

The capsule is widely regarded as the main virulence factor of *C. neoformans* and *C. gattii* (figure 1.8). Indeed, experimental evidence demonstrates that acapsular mutant strains are typically avirulent whilst encapsulated isolates have varying degrees of virulence [82, 83]. Until recently there had been no identified correlation between capsule thickness and the virulence of a strain [84]. Pool *et al. (2013)* demonstrated that, in the context of neuro-pathogenesis, hypercapsular strains of *Cryptococcus* were less virulent that strains that produced less capsule, and that neuro-virulence is related to total capsule accumulation rates and total capsule volume rather than the amount of capsule produced per organism [85]. The correlation between capsule thickness and *Cryptococcus* virulence during pulmonary infection, however, remains enigmatic.

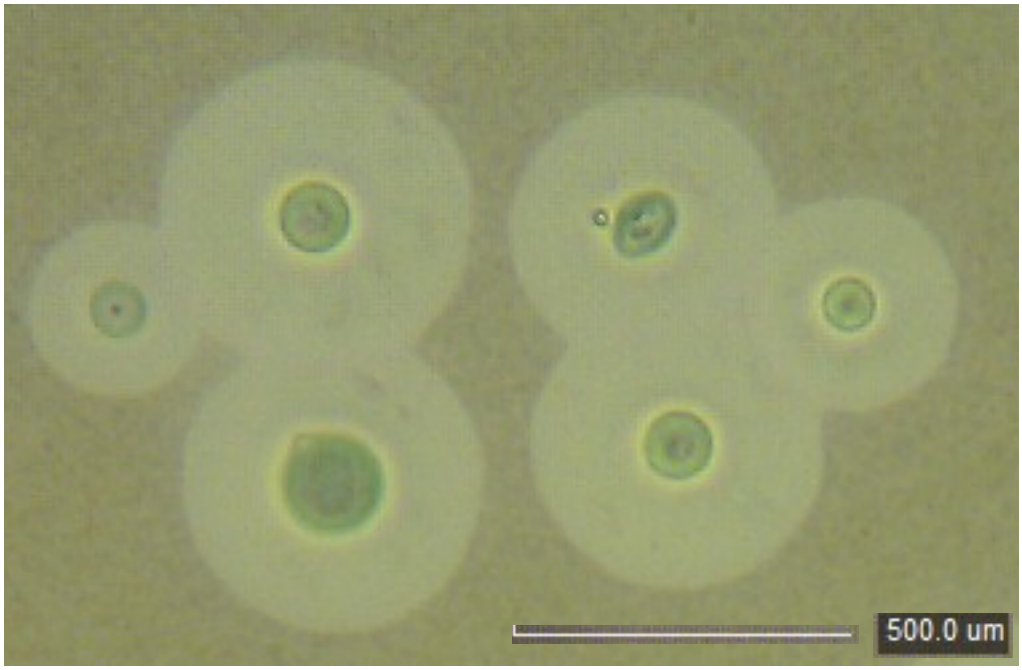

Figure 1.8: *C. gattii* obtained from pulmonary infection showing the very large *Cryptococcus* capsule.

The cryptococcal capsule has been associated with chemotactic effects on leukocytes that protect the organism from host defences, with complement depletion in the host that creates a favourable environment for the cryptococcal cells, and also with altered cytokine production, which compromises the protective responses of the host [86]. It has also been determined that glucuronoxylomannan (GXM), the major component of the cryptococcal capsule, has immunosuppressive effects. GXM promotes T-cell apoptosis, indicating that GXM is a negative regulator that suppresses self-reactive lymphocytes [87].

The cryptococcal capsule is a complex structure that displays variable density and porosity and is highly plastic depending on the ionic strength of the aqueous environment [88, 89]. The capsule is composed primarily of polysaccharides. The major polysaccharide component is the high molecular weight GXM ($1.2\text{-}1.5 \times 10^6$

Da), which accounts for approximately 88 % of the capsule mass. The polysaccharide galactoxylomannan (GalXM) (1.5×10^5 Da) accounts for roughly 7 % of capsule mass and is considered a minor capsular component along with mannoproteins. *Cryptococcus* capsule synthesis strategies could theoretically generate an infinite number of structural combinations. This structural heterogeneity is a result of differing molar ratios of xylose, the extent of *O*-acetylation and the glucuronic acid positional differences in the primary capsule constituent GXM. The biological consequence is the production of a powerful avoidance strategy for interactions with host immune systems and phagocytic environmental predators [90]. The polysaccharide capsule is non-covalently anchored to the cell wall via α-1,3-glucan (figure 1.9) [91]. This was demonstrated via the observation that mutants lacking cell wall α-1,3-glucan no longer display capsule polysaccharide on their surfaces, although they do continue to shed this material into the environment. These mutant cells were further found to grow slowly and were temperature sensitive. These results strongly suggest that the cryptococcal capsule is important for cellular survival [92].

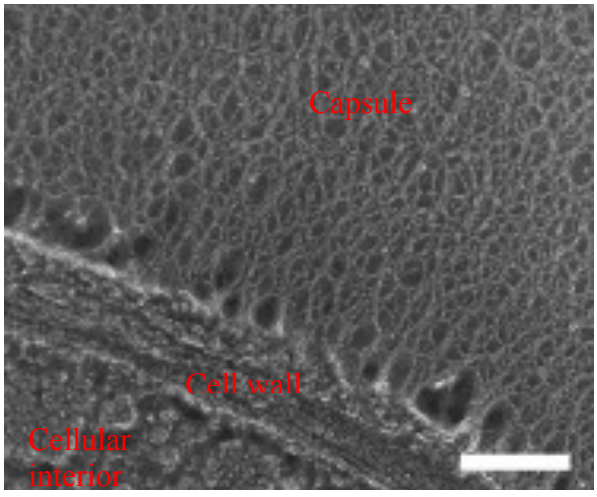

Figure 1.9: Electron microscopy of the cell wall-capsule interface.

Depicts an arc of cell wall separating the cellular interior from the capsule fibres emanating upwards (from [93])

The cryptococcal capsule is also a dynamic structure, the thickness of which is modulated in response to environmental conditions. In typical environmental conditions and under standard *in vitro* conditions the capsule thickness is often 2.5 - 10 μm. However, during *in vivo* infection, or under specific capsule-inducing conditions *in vitro* [94, 95], capsule thickness can be up to 100 μm [96]. It is thought that capsule enlargement is mediated at the level of individual polysaccharide molecules whereby new polysaccharide molecules, with larger effective diameter, are added near the capsule edge (figure 1.10) [97-99]. Capsule enlargement is associated with reduced susceptibility to both oxidative and antifungal killing, demonstrating the importance of capsule enlargement as a mechanism of intracellular survival [100]. The *CAP59* gene has been identified to be essential for the extracellular trafficking and/or secretion of polysaccharides, however, the exact mechanism of CAP59 remains unknown [101]. The high-energy cost of capsule growth is offset by a significant reduction of fungal susceptibility to oxidative and antifungal killing [102]. This demonstrates the importance of capsule enlargement as a mechanism of intracellular survival [100].

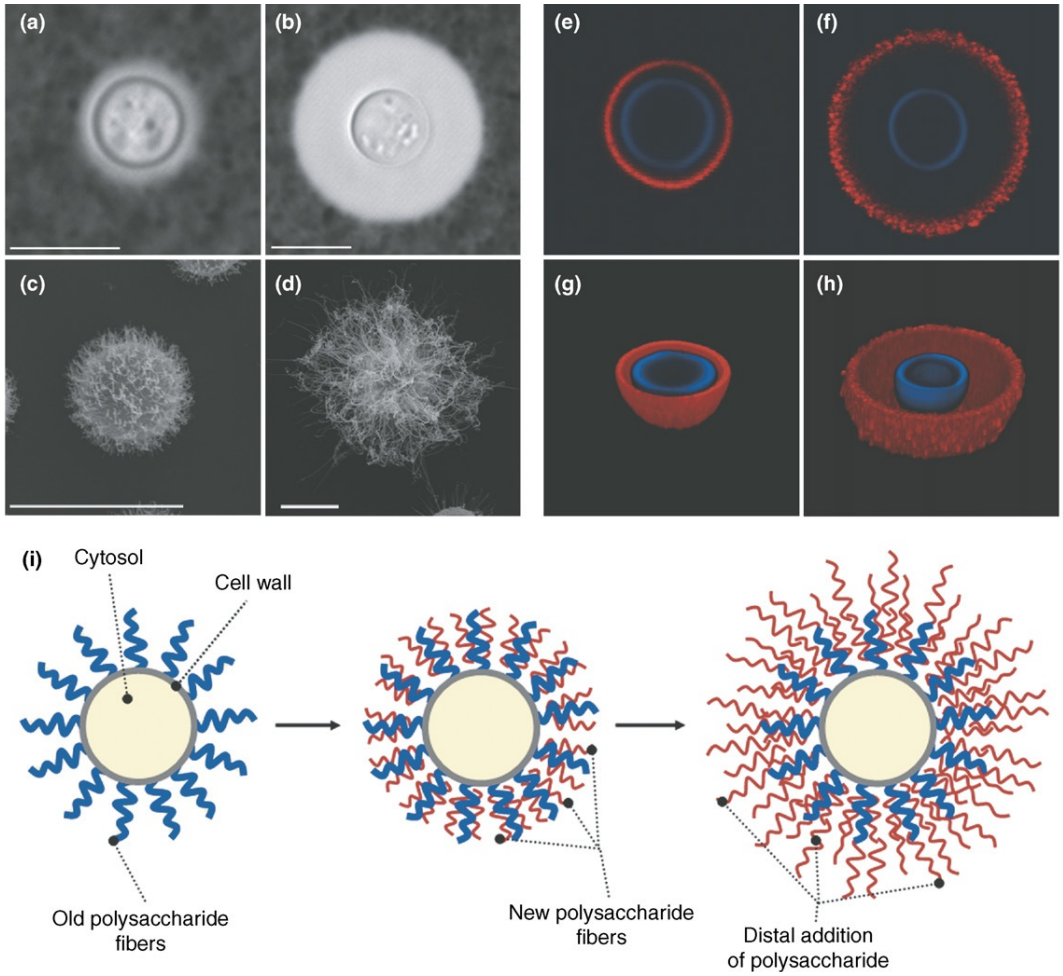

Figure 1.10: Images depicting cryptococcal cells with different capsule sizes and a schematic representation of capsule enlargement.

India ink staining of a) cells with a small capsule and b) cells with an enlarged capsule. Scanning electron microscopy of c) small-capsule cells and d) enlarged-capsule cells. Scale bars = 5 μm. Confocal microscopy of e) small-capsule cells and f) enlarged-capsule cells after coating the capsule with an IgM mAb to GXM (12A1) and detection with a goat anti-mouse IgM antibody conjugated to rhodamine (red fluorescence). The cell wall is visible by staining with calcofluor (blue fluorescence). 3D image reconstruction of g) small-capsule cells shown in part e); and h) enlarged-capsule cells shown in part f). i) Schematic showing the self-assembly and distal elongation of the capsule. New polysaccharide (red) is added to existing polysaccharide (blue) (from [103]).

1.5.2.2. Melanin production

Melanin production has been described as one of the three major *Cryptococcus* virulence factors, along with polysaccharide capsule and growth at 37 °C. The brown-to-black melanin-like pigment was first described by Staib in 1962 [104] and is a result of phenoloxidase (also known as laccase) activity (figure 1.11) [105]. Melanin production has been correlated to a number of functions involved in fungal protection including protection from oxygen and nitrogen derived oxidants, impeding phagocytosis, impeding the T-cell mediated immune response, maintaining cell wall structure and protecting *Cryptococcus* from UV light, X-ray or gamma radiation, heat, cold and amphotericin B [106]. Ngamskulrungroj and Meyer *(2009)* demonstrated that the major Vancouver Island outbreak genotype, VGIIa, produced more melanin at *in vitro* physiological temperature than the minor Vancouver Island outbreak genotype, VGIIb [106].

Figure 1.11: Non-melanin- and melanin-forming colonies of *C. gattii* on 3,4-dihydroxyphenylalanine (L-DOPA) media after 7 days at 25 °C (from [35]).

Another intriguing element regarding melanin production and pathogenesis is that the melanin synthesis pathway has the ability to utilise catecholamines, a compound that

is enriched in the brain. This may provide an explanation for the evident neurotropism observed during *C. neoformans* and *C. gattii* infection. Catecholamines, however, cannot act as a sole carbon source, suggesting that the brain serves as a survival niche rather than a preferred nutritional niche during cryptococcosis [107]. To date, the role of melanin as a virulence factor has been limited to *in vitro* studies and there is little evidence demonstrating the presence of melanin *in vivo*. Further investigation is required to delineate the role of melanin production regarding virulence in mammals.

1.5.2.3. Mannitol production

Wong *et al. (1990)* demonstrated that *C. neoformans* produces large amounts of mannitol *in vitro* and *in vivo* [108]. Mannitol expression has been associated with increased resistance to heat, osmotic stress and damage by reactive oxygen intermediates. Moreover, low mannitol production has been linked to decreased pathogenicity [109]. Mannitol has been hypothesised to contribute to pathogenicity by two means. Firstly, high concentrations of mannitol in the central nervous system may contribute to brain oedema. Secondly, mannitol is an effective free hydroxyl radical scavenger, providing a link to mannitol production as a means to protect the organism against oxidative damage [51, 108]. Further studies are required to deduce the exact role of mannitol during cryptococcal infection.

1.5.2.4. Cryptococcal products

Measurable levels of cryptococcal products, including glucuronoxylomannan, galactoxylomannan and mannoproteins, are present in bodily fluids during cryptococcal infection. Indeed, the detection of cryptococcal antigens in serum or

spinal fluid is diagnostic for cryptococcosis and it has been demonstrated that there is a direct correlation between cryptococcal antigen levels in body fluids and severity of disease [110]. Cryptococcal exopolysaccharides, which are structurally different from capsular polysaccharides, have been found to exhibit potent immunosuppressive properties *in vitro* and *in vivo* [111]. These specific cryptococcal products have been demonstrated to negatively affect leukocyte migration to the site of infection, and to induce T-cell apoptosis and regulatory T-cells, resulting in dampened anti-cryptococcal humoral as well as cell-mediated immune responses [87]. Moreover, high concentrations of cryptococcal products have the potential to alter the osmolarity of the cerebral spinal fluid leading to increased intracranial pressure resulting in headaches, visual loss and early death [112]. Thus, is has been suggested that more consideration should be given to the impact of high levels of cryptococcal products in body fluids on the progression of disease [51].

1.5.2.5. Phenotypic switching

Phenotypic switching has been observed in both prokaryotes and eukaryotes. It involves the stochastic switching between two or more alternative and heritable phenotypes. It results from spontaneous alterations in gene expression that arises at higher frequencies than standard spontaneous mutation rates. It differs from random spontaneous mutations in that the process is reversible and readily detectable. Phenotypic switching is usually adopted by pathogens to escape recognition by the host immune system and/or to adapt to a novel, hostile host environment [113].

Fries and Casadevall *(1998)* first observed phenotypic switching in *C. neoformans* [114]. They showed that *C. neoformans* has the ability to undergo microevolution

during chronic infections. The most crucial aspect of phenotypic switching to fungal pathogenesis is that the microevolutionary changes that occur have lead to observable changes in virulence by causing changes in capsule or cell wall morphology [115-118]. Phenotypic switching is clearly observable in *C. gattii* pulmonary infections where the cells are found to switch reversibly between two colony/cell morphologies. During pulmonary infection, cells switch to a mucoid colony phenotype that reflects enlargement of the polysaccharide capsule, which affords the cells with enhanced intracellular survival. The ability of *Cryptococcus* to cause chronic infections even after prolonged antifungal treatment therapy has been attributed to phenotypic switching [118]. It should be noted at this point that the process of phenotypic switching during pulmonary infection in *C. gattii* was the cause of significant technical issues encountered during this project.

1.6. The origin and maintenance of virulence factors: Is cryptococcal infection a case of readymade virulence?

C. neoformans and *C. gattii* do not require host cellular machinery for replication, dissemination and survival [55, 119]. However, these environmental saprotrophs, which are typically found in soil and trees, have the incredibly rare ability to cause respiratory disease and a potentially fatal meningoencephalitis in both human and animal hosts. Thus, the question arises as to why these organisms possess an unusual and sophisticated strategy for the facultative intracellular parasitism observed during cryptococcosis [120].

To date a significant amount of evidence has been gathered that suggests that *Cryptococcus* virulence originated as a result of environmental selective pressure.

Firstly, it has been proposed that the intracellular replication and dissemination of *C. neoformans* and *C. gattii* within animal hosts may have evolved from the ability of the fungus to survive inside amoebae. Amoebae feed on microorganisms in a similar way to phagocytosis by macrophages. Indeed, it has been hypothesised that amoebae could be the earliest form of macrophage and perhaps gave rise, by an undetermined evolutionary pathway, to the modern macrophage [121]. Thus, it has been proposed that *C. neoformans* and *C. gattii* acquired the ability to cause disease in human and animal hosts as the result of the defence mechanisms developed to evade environmental predators [122]. Secondly, the fact that environmental isolates can cause animal infections indicates that virulence factors have been developed in the absence of prior interaction with host animals [119]. Furthermore, a multitude of 'virulence factors' appear to have 'dual use' capabilities that afford survival advantages in both animal hosts and in the environment [35]. Thus, it is becoming increasingly evident that virulence factors were probably not specially developed to enable host infection; rather, they are 'ready made' due to environmental selective pressures. It is likely that animals represent an inadvertent host rather than a primary niche.

1.7. The host response to infection

1.7.1. Physical barriers of the lung

The inhalation of *Cryptococcus* propagules is considered the initial point of exposure of *Cryptococcus* to the host immune system. Physical protection from pulmonary infection is provided by airway turbulence and proper ciliary function [16, 123]. Combined, these physical barriers retain the majority of inhaled yeast forms in the

upper airways, preventing fungal deposition in the alveoli. Fungal basidiospores and/or hypocapsular forms of *Cryptococcus* are able to circumvent these physical barriers and reach the alveolar space [124]. Fungi that do reach the lung parenchyma are normally controlled by the host immune response without extra-pulmonary dissemination. The immune system either eliminates the infective agent completely or restricts it to the lung within granulomas, where it has been found to persist in a latent state indefinitely. If the infection is not eliminated or contained, pneumonitis and/or dissemination may result [123]. This part of the introduction will briefly discuss how the innate and adaptive immune system responds to cryptococcal infection.

1.7.2. The innate immune response

The innate immune response acts as a major barrier to cryptococcal infection. This is especially true for immune compromised individuals. Physical barriers, such as the skin and nasal mucosa, and the anti-cryptococcal activity of serum and saliva, have been identified as innate immune factors that inhibit the establishment of infection [125-131]. Specifically for the lung, antimicrobial substances in surfactant have been identified to contribute to innate resistance against inhaled *Cryptococcus*. The exact role of surfactant and collectins (primitive opsonins found in surfactant and serum found to bind acapsular but not encapsulated cells) in innate immunity remains enigmatic, however, evidence suggests that these proteins play a role in the early pulmonary antifungal defence mechanisms [132]. While these innate factors have the potential to discourage cryptococcal infection, the complement system and the phagocytic effector cells resident in the lung have been identified as the major contributors in the nonspecific host immune system response to pulmonary infection.

It is the interaction of the pathogen with these innate immune factors that determines the outcome of infection [86, 133].

1.7.3. The complement system

The complement system is an anti-pathogen cascade of serum proteins that can be activated by the classical (antibody mediated), lectin or alternative (microbial-surface-mediated) pathway. The complement system plays a vital role in host defence from infection of the lung. Local complement sources in the lung appear to play an important role in the very early stages of infection, providing immediate protection from infection along the delicate epithelium of the lung [134]. By opsonising the infective agent, the lung complement system attracts both immune effector cells and serum complement. The disruption of the complement system, especially the alternative pathway [135], has been found to result in reduced survival time during cryptococcal infection for a number of animal models. Thus, the lung complement system performs vitally important preparations for the subsequent host defence response.

The cryptococcal capsule appears to act as an inhibitor of complement induced host immune responses [136, 137]. Interestingly, studies have demonstrated that total C3 (which plays a central role in the complement system) accumulation on the cellular surface of *C. gattii* strains is half that of *C. neoformans* strains [138, 139], despite having an overall higher binding efficiency [140]. These observable differences in complement activation between *C. gattii* and *C. neoformans* have been suggested to be influential with regard to the increased virulence observed for *C. gattii*.

1.7.4. Cell mediated immunity

The success or failure of the host defence against cryptococcal infection is critically regulated by cell-mediated immunity and especially T lymphocytes [35, 141-144]. The exact mechanisms of cryptococcal elimination by T lymphocytes remains enigmatic, however it is thought that lymphocytes act to indirectly clear the infection via the production of cytokines (produced mainly by CD4+ T cells) that enhance the elimination of the pathogen by natural effector cells, in particular macrophages [145, 146]. The balance between Th1 (a proinflammatory response that stimulates the cellular immune system), Th2 (an anti-inflammatory response that stimulates the humoral immune system) and Th17 (recruitment, activation and migration of neutrophils) patterns of cytokine production in response to cryptococcal exposure to the immune system markedly influences the outcome of infection [86]. It has become apparent that the predominant synthesis of Th1 and Th17 cytokines over Th2 cytokines protects mice from cryptococcal infection. The loss of the Th1 response, either as a result of HIV infection [147] or experimental depletion [148], leads to a high susceptibility to cryptococcal infection. Similarly, Th2-dominant anti-inflammatory conditions exacerbate infection [149]. Phagocytic effector cells and primary lymphocytes such as natural killer T cells and γδ T cells maintain the balance of Th1/Th2/Th17 cytokine production during cryptococcal infection [150-153].

Macrophages are involved in antigen presentation, cytokine production and phagocytosis during cryptococcosis. Macrophages have been established as the phagocyte that initially encounters inhaled *Cryptococcus* and acts as the primary phagocytic cell at all times during infection [154-157]. There are three distinct outcomes of *Cryptococcus* phagocytosis by macrophages: 1) the yeast is killed; 2) the yeast remains latent inside the macrophage; or 3) the yeast grows unchecked within

the macrophage leading to macrophage lysis (figure 1.12) [35]. The outcome is a direct result of the presence or absence of T-cell mediated immune response and whether the macrophages have been activated by Th1 cytokines or Th2 cytokines.

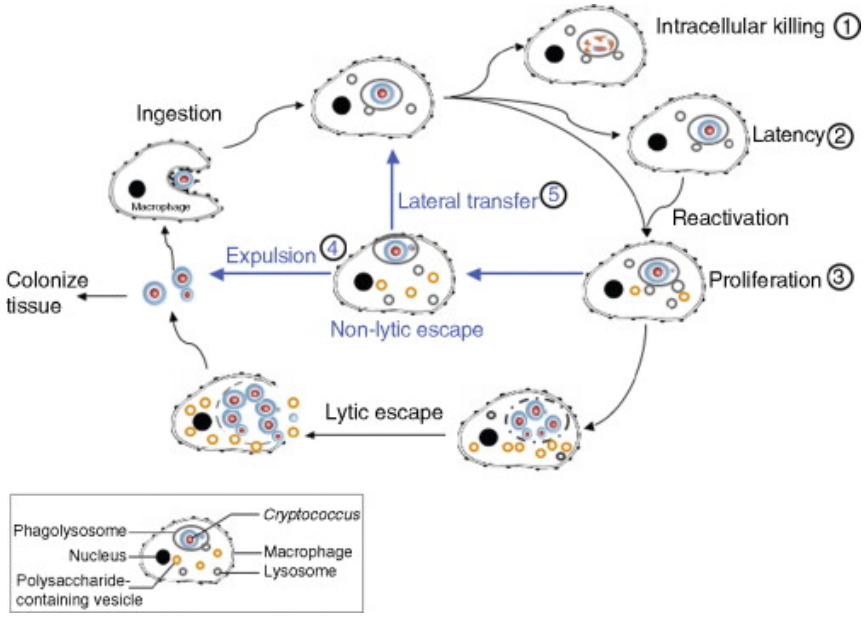

Figure 1.12: Macrophage parasitism by *Cryptococcus*.

Following phagocytosis, there are three distinct outcomes; 1) the yeast is killed; 2) the yeast remains latent inside the macrophage; or 3) the yeast grows unchecked within the macrophage leading to macrophage lysis. Released cells can infect more macrophages or establish extracellular dominance. Non-lytic escape pathways are also observed for *Cryptococcus*, during which the yeast cells are expelled by macrophages without causing death of either party 4) or the intracellular yeast cells are directly delivered to a neighbouring macrophage via lateral transfer 5) (from [158]).

Th1 cytokine activated macrophages are more efficient at eliminating intracellular cryptococcal cells than macrophages activated by Th2 cytokines [123, 159, 160]. Macrophages activated by Th1 cytokines possess a variety of antifungal mechanisms, including oxidative and nitrosative bursts and granuloma formation. Granulomatous inflammation is a prerequisite for the successful resolution of infection with

Cryptococcus [16, 161]. Granuloma formation is a result of intact T cell function (and thus is common in non-HIV associated cryptococcosis) where macrophages form a histiocytic ring around *Cryptococcus* cells. These macrophages also have the potential to from multinucleated cells to engulf heavily encapsulated fungal cells [35]. Granuloma formation has been found to be the most effective host response to localise the infection and prevent dissemination [162]. The Th2-polarised host response, which up-regulates the expression of genes involved in tissue repair and results in activation changes in phagocytic effector cells, leads to the inhibition of phagocyte activity and increased susceptibility to infection. The absence of a T-cell mediated immune response results in the intracellular survival and proliferation of *Cryptococcus* cells [86].

1.7.5. Antibodies

Antibodies produced against *Cryptococcus* have been found to enhance the fungistatic and fungicidal activity of macrophages. For instance, antibody produced against capsular GXM increases nitric oxide production in macrophages [163] and antibody-treated mice have a more intense granulomatous inflammatory response than control animals [16, 35]. Despite the presence of Th1 cytokines and antibody in immune competent individuals, certain strains of *Cryptococcus* are able to survive inside macrophages. This is most likely a result of the survival advantages provided by cryptococcal virulence factors and the host switching to a Th2 polarised response during late stage infection to avoid tissue damage as a result of the early proinflammatory Th1 response [35]. It is this persistence of this latent population of *Cryptococcus* cells that can lead to the development of cryptococcosis later in life if the host immune system becomes compromised [30].

1.7.6. The direct antifungal effects of T lymphocytes

It is well established that as well as acting as vital regulators of the immune response, NK cells and T lymphocytes (CD4+ and CD8+) function as cytotoxic cells during cryptococcosis. Studies have observed that these cells have the ability to directly bind to and inhibit the growth of *Cryptococcus* in the absence of MHC restriction [155, 164]. This antifungal activity is dependent on the production and secretion of the proteins granulysin and perforin. These proteins are pore-forming effector molecules that are stored in secretory vesicles (granules) of T lymphocytes and NK cells [35]. The expression and insertion of these proteins into the target cell's plasma membrane leads to apoptosis. NK cells utilise perforin as the main contributor to the elimination of *Cryptococcus* cells [165] while CD4+ and CD8+ cells utilise granulysin [166, 167].

Successful immune defence against *Cryptococcus* infection is dependent on complement opsonisation of the pathogen, a functioning T-cell mediated immune response driven by CD4+ cells, and the direct antifungal/cytotoxic activity of lymphocytes. Normally the efficient activation of these immune effector functions results in either the destruction of the infectious agent or containment of the fungus in a latent state. Proliferation and possible dissemination can result if an individual becomes immuno-compromised or the specific cryptococcal strain possesses virulence factors (capsule, phenotypic switching) that are able to circumvent or overcome the host immune responses.

1.8. Cryptococcosis diagnosis, therapy and treatment

1.8.1. Diagnosis

There are several methods for the diagnosis of cryptococcosis that can be grouped into two classes: radiological diagnosis and laboratory diagnosis. Body imaging via radiography, CT and MRI scans can provide the first indication/evidence of disease and can also identify the focus of infection [168]. When using radiological methods of diagnosis it must be taken into account that pulmonary cryptococcosis caused by *C. gattii* can mimic lung cancer [169]. The laboratory diagnostic techniques include the direct examination of the fungus in body fluids or tissue, histopathology of infected tissues [170, 171], serological studies and culture of the fungus from body fluids or tissue [49].

1.8.2. Therapy and treatment

The *Clinical Practice Guidelines for the Management of Cryptococcal Disease: 2010 Update* by the Infectious Diseases Society of America provides excellent guidelines for specific therapeutic options during cryptococcal infection [172]. Preliminary guidelines were first produced in 2000 [173]. The 2010-updated version provides detailed discussions on management, therapy and treatment recommendations for specific sites of infection and risk groups/populations. This document suggests that the principles for induction, consolidation and suppressive/maintenance treatment are the same for *C. neoformans* and *C. gattii*. It does state, however, that "the management of *C. gattii* infection in immunocompetent hosts needs to be specifically addressed" with more intensive diagnostic and follow-up examination recommended [174].

1.8.3. Antifungal agents

To date amphotericin B combined with flucytosine represents the most potent fungicidal regimen and as such remains the treatment option of choice for disseminated or constrained severe cryptococcal disease [173, 175]. Despite their effectiveness both amphotericin B and flucytosine have severe and potentially lethal side effects. Therapeutic doses of intravenously administered amphotericin B are associated with multiple organ damage, especially severe and irreversible nephrotoxicity [176]. When delivered via liposomes, which causes the drug to be fungal specific, the side effects associated with amphotericin B are much reduced. Liposomes are disrupted upon binding to fungal cell walls and since mammalian cells lack a cell wall, lipid formulations of amphotericin B are significantly less toxic to mammals [177, 178]. Flucytosine has adverse effects on liver function, renal function, the central nervous system, causing skin reactions and anaphylaxis [179]. The antifungal advantages of the amphotericin B and flucytosine drug combination are offset by the generation of potentially lethal side effects.

1.8.4. Resolving cryptococcosis requires the development of novel antifungals and therapies

Since the first independent isolation of *C. neoformans*, from peach juice in Italy by Sanfelice [180] and from the tibial lesion of a patient in Germany by Busse [181] and Buschke [182] in 1894, the clinical relevance of cryptococcal disease has continued to gain in prominence. In 2009, Park *et al.* estimated that 957,900 cases of cryptococcal meningitis occur each year with approximately 624,700 of the cases resulting in death at 3 months post infection [183]. Coupled with the emergence of hyper-virulent strains of *C. gattii* that have the ability to proliferate outside of their predicted

ecological niche, it is evident that the pathogenic yeasts *C. neoformans* and *C. gattii* deserve further investigation [184]. Treating fungal disease remains a challenge due to the numerous similarities between the cellular machinery of fungi and humans that result in the majority of effective antifungal drugs having toxic side effects. As a result there are fewer drugs available for the treatment of fungal diseases compared with bacterial and viral diseases. There is a growing demand for the discovery of novel anti-*Cryptococcus* drug targets that are non-toxic or have a low toxicity to mammals. The discovery of these targets requires the elucidation of the molecular responses of the fungal and host responses to pulmonary infection. In this study, a proteomic approach was used to acquire a better understanding of these complex responses to fungal infection. What follows is a description of the proteomic techniques applicable to this endeavour.

1.9. Proteomics: the study of protein structure and function

Genetic information provided by genome sequences can be analysed utilising three distinct approaches: - the monitoring of the genome (genes) via genomics, the transcriptome (mRNA) via transcriptomics and the proteome (proteins) via proteomics. Although the genome and the transcriptome are relatively easy to analyse employing high-throughput techniques, it is evident that such analyses do not directly describe the molecules that function and interact in the cell, the proteins [185]. Hence genomic and transcriptomic approaches may lack the capability to comprehensively analyse the multifactorial process that is fungal pathogenesis during mammalian infection. Furthermore, transcriptomics suffers as a global investigative tool for gene expression due to its inability to detect posttranslational modifications and the fact

that the correlation between mRNA and protein expression levels is not always perfect [186-190].

These shortcomings of genomic and transcriptomic analyses are addressed by proteomics, which encompasses the study of the functional output of the genome, that is, the proteome [191]. In the broadest sense, proteomics aims to systematically determine the amount, structure and function of the entire protein complement expressed by a genome, cell, tissue or organism, including their posttranslational modifications [185]. Theoretically proteomics allows the qualitative and quantitative analysis of the proteins that directly influence cellular biochemistry. Proteomics is presenting itself as the key technology for the study of complex and dynamic biological systems as it has the potential to provide a snapshot of the cellular state and/or system changes during growth, development and response to environmental factors.

Despite the theoretical advantages, experimental proteomics represents a much greater technological challenge than genomics and transcriptomics. Consequently, to date, proteome-based studies have not yet been widely applied to pathogenic fungi [192]. This is a result of a multitude of factors, the most detrimental element being the extreme chemical complexity of the proteome. Furthermore, proteomics lacks a polymerase chain reaction equivalent and thus proteins cannot be amplified. As a result, comprehensive proteomic analysis requires highly sophisticated analytical machinery and software in order to detect a wide range of protein species that can be present at minute amounts. In practice, comprehensive ‘whole-cell’ proteomics is beyond the capacity of any combination of current proteomic technologies and consequently the identification and quantification of all the proteins in a biological system remains elusive [193]. Most proteomic studies adopt a simplification via

prefractionation approach based on either chemical attributes, such as solubility, or biological attributes, such as membrane preparations [194]. The nature of sample preparation and prefractionation is determined by the project aims and hypotheses and sample availability, however, the biological and medical importance of membrane proteins means that membrane preparation and analysis is a major part of many proteomic studies.

The sheer number of prefractionation methods precludes any attempt at a review here, but the main goal of these techniques is complexity reduction [195]. Even the simplest organisms produce proteomes that are too complex and wide ranging in protein abundance to be analysed by a single separation step. Prefractionation methods aim to reduce the complexity from thousands to hundreds of proteins in each fraction. Subsequently, the core of most proteomics strategies is a protein or peptide separation method designed to further reduce the complexity of each fraction prior to mass spectrometry analysis. The goal at this stage is to present the mass spectrometer with a single protein at a time or a mixture of only a few proteins [194]. The two main separation approaches are based on liquid chromatography (LC) [196] or two-dimensional electrophoresis (2-D PAGE) [197].

1.9.1. Comparative proteomics

The primary goal of comparative proteomics is to discover the quantitative and qualitative changes that underlie the cellular changes in response to a given experimental or biological scenario [198]. Traditional comparative proteomic experimental platforms have utilised dyes, fluorophores or radioactivity coupled with high-resolution protein separation to identify quantitative and qualitative changes

between protein samples. For the past four decades, two dimensional polyacrylamide gel electrophoresis (2-D PAGE) has been the technique of choice for the separation of the protein composition of a given sample [199]. This technique was first described by O'Farrell in 1975 [200]. 2-D PAGE utilises the orthogonal protein fractionation procedures of isoelectric focusing (IEF), where proteins are separated according to their isoelectric point, in the first dimension and sodium dodecyl sulphate polyacrylamide gel electrophoresis, where proteins are separated according to their molecular weight, in the second dimension.

1.9.2. Two-dimensional polyacrylamide gel electrophoresis: a fundamental proteomic technology

The 2-D PAGE analysis platform was, until recent times, the most widely employed protein separation technique as it offers the unparalleled resolution of intact proteins coupled with the ability to simultaneously separate many thousands of proteins, and their modified forms, to homogeneity (figure 1.13). Furthermore, a number of groups have demonstrated that by applying the correct sample preparation and fractionation techniques it is possible to obtain large numbers of low abundance, membrane and alkaline proteins on 2-D PAGE gels [201, 202]. More importantly, the seemingly small number of genes in the human genome has reinforced the *one gene-many post-translational products* paradigm and 2-D PAGE remains the only technique which offers sufficient resolution and quantitative range to address this at a proteomic level [203]. 2-D PAGE coupled with fluorescent staining provides an ideal image-based method for quantitative comparative proteomics [204].

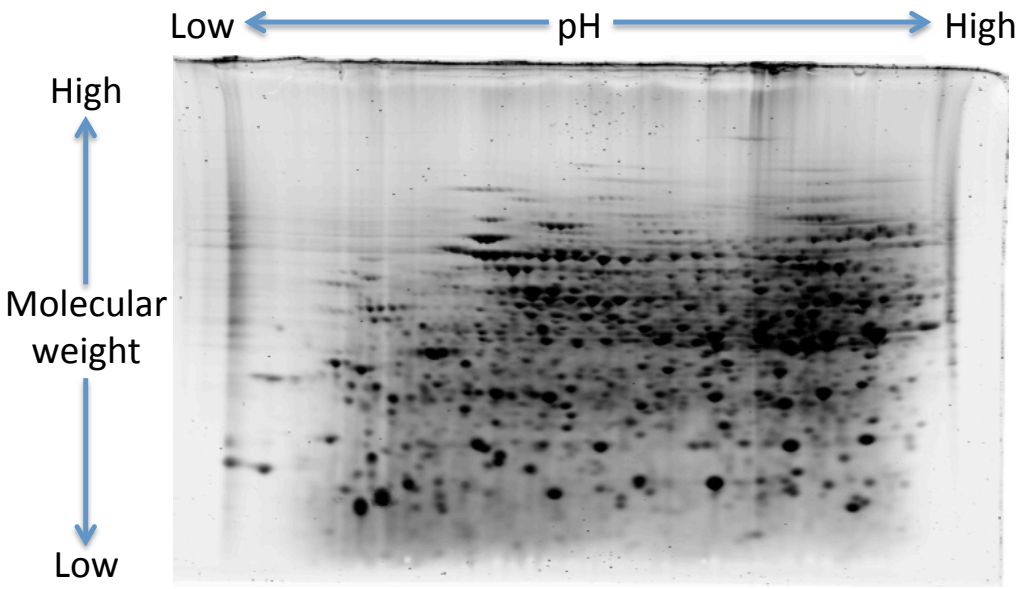

Figure 1.13: An example of the fractionation power of 2-D PAGE.

This image shows separated *Cryptococcus* proteins from cultured *C. gattii*. Each spot represents an individual protein species.

1.9.3. Difference in Gel Electrophoresis (DIGE)

In 1997 Unlu *et al.* [205] introduced difference in gel electrophoresis (DIGE). This technology was designed to directly limit the amount of technical variation associated with comparative 2-D PAGE proteomics. DIGE is based on the fluorescence pre-labelling of protein mixtures prior to 2-D PAGE [206]. Protein samples to be compared are labelled with up to three spectrally distinct, charge and mass-matched cyanine dyes known as CyDye DIGE fluors (which includes Cy2, Cy3 and Cy5) [207]. The labelled proteins samples are mixed and separated simultaneously on the same 2-D PAGE gel and visualised separately by exciting the different CyDyes at their specific excitation wavelengths [206]. Protein samples can be labelled via two markedly different methods. The first technique developed was minimal labelling that used amine reactive dye to label lysine residues. This method is referred to as minimal

labelling as the ratio of dye to protein is kept very low so that the only proteins visualised on a gel are those labelled with a single dye molecule; indeed only 1 to 5 % of total protein is labelled [205, 206]. The next generation of DIGE dyes targeted cysteine residues. This technique is known as saturation labelling as a high dye to protein ratio is used so as to label all available cysteine residues. Saturation dyes possess a maleimide reactive group that covalently binds to the thiol group of cysteine residues on a protein via a thioether linkage [208]. The saturation technique is far more sensitive than minimal labelling, being able to visualise proteins from a 5 μg protein sample. Indeed, saturation dyes are sensitive down to 15 pg of protein. In comparison 50 μg of protein sample is required for minimal labelling. Thus, the saturation method of labelling is also referred to as scarce sample labelling.

The ability of DIGE to substantially reduce the effects of gel-to-gel variation is a result of the technology being able to separate more than one sample on a single two-dimensional gel. Thus, samples of interest are separated and proteins detected and identified on a medium that has experienced identical experimental conditions. The capability of DIGE to include an internal standard during electrophoresis further increases the confidence that an observed difference is genuine [209]. The internal standard is a mixture of equal amounts of protein from each biological sample in the experiment. The internal standard is run on every gel, meaning that every sample within a gel can be normalised to the internal standard on that gel. Furthermore, every protein spot can be measured as a ratio to its corresponding spot present in the internal standard. Therefore, the confidence that a difference in fluorescence intensity between two samples is due to biological rather than experimental variation is increased. As a result, DIGE has the capability to generate statistically significant data using fewer 2-D gels than conventional comparative differential display 2-D PAGE methods.

1.9.3.1. Technical issues associated with DIGE

Despite the advantages of DIGE, the technique remains hampered by the inherent technical limitations associated with any 2-D PAGE analysis. These limitations include variable protein solubility [210], protein expression dynamic range problems [211] and low protein abundance issues [212]. Coupled with these global 2-D PAGE analysis issues, both minimal and saturation labelling techniques are subject to a number of significant DIGE-specific technical limitations. During minimal labelling, high dye substitutions result in significantly decreased protein solubility [205]. Therefore, the dye to protein ratio is very kept low in order to maintain protein solubility during electrophoresis [206]. Furthermore, it has been demonstrated that SYPRO Ruby dye staining detects 40 % more protein spots than minimal protein labelling with CyDye [213]. It is almost certain that the undetected proteins represent the lowest abundant species in the sample. These undetected proteins could include the very proteins that the researcher is attempting to detect [213]. The saturation labelling method also faces some significant limitations. The most evident issue is that not all protein species contain a cysteine residue. A protein that does not contain a cysteine residue cannot be labelled and will thus remain undetected. Furthermore, studies have found that saturation labelling can result in significantly increased protein insolubility [208]. Up to 40 % of high molecular weight proteins become insoluble upon labelling and on average 25 % of all protein material can be lost due to precipitation during the labelling process [208]. Moreover, detection sensitivity for both the minimal and saturation labelling techniques can also be hampered via fluorescence cross-talk between excitation/emission band-pass filters. The result is Cy5 labelled proteins being detected when illuminating at the optimal Cy3 excitation wavelength [214]. Thus, the ability of DIGE labelling systems to complete

meaningful comparative proteomics has been brought into question. If the technique is to become an efficient and effective method of comparative proteomics it is quite obvious that further research and development is required to optimise this technique.

1.9.4. Further general limitations to the 2-D PAGE analysis platform

Despite the advantages of the 2-D PAGE analysis platform, as with all experimental procedures there are a number of drawbacks to the fractionation technique. As with all proteomic procedures, 2-D PAGE is limited by low protein abundance and dynamic range issues. These issues can be combated with the use of a number of prefractionation techniques such as the use of narrow-range IPG strips that allow higher protein loads and improved resolution [215]. The overriding issue with 2-D PAGE is that this protein separation technique is sample greedy. 2-D gels of adequate protein spot intensity require at least 300 μg of protein, which may not be obtainable from *in vivo* experiments. For samples where obtainable protein yields are minimal, alternative techniques must be utilised. A further complicating factor for the 2-D PAGE experimental platform is that approximately 10% of the proteins in a typical proteome fall outside the 2-D PAGE solubility window. Additionally, very acidic and very alkaline proteins are notoriously difficult to focus during IEF [215]. Finally, 2-D PAGE has a generally low throughput of protein identifications when compared to alternative approaches such as liquid chromatography-mass spectrometry (LC-MS). Differential display comparative proteomics using the 2-D PAGE platform requires an individual MS run per spot identified with the differential display software. When compared to the hundreds of proteins identified with LC-MS the throughput limitations of the 2-D PAGE experimental platforms are obvious. These significant

inherent technical challenges, together with the low throughput nature of traditional 2-D PAGE based comparative proteomic techniques, means there is an emerging trend towards using liquid chromatography coupled with tandem mass spectrometry (LC-MS/MS) based technology platforms [193].

1.9.5. Alternative comparative proteomics techniques

A hybrid approach to comparative proteomics that has gained favour in recent years is the combination of one-dimensional SDS-PAGE (1-D SDS-PAGE) with reversed phase LC-MS of peptides from in-gel digests. The advantages of this type of non-2-D PAGE gel approach include a reduced demand for sample compared to 2-D PAGE, an increased number of identifications, and the ability to combine highly solubilising techniques like 1-D SDS-PAGE as a separation method prior to LC-MS.

The primary shortcoming of the LC-MS/MS platform is that mass spectrometry is not inherently quantitative. Accurate quantification requires the comparison of each individual peptide between experiments. This can be achieved in a number of ways. The most widely adopted approach, introduced in 1999 by three independent laboratories [216-218], is based on stable isotope labelling of peptides. This approach relies on the theory that a stable isotope-labelled peptide is chemically identical to its native counterpart and thus the two peptides also behave identically during chromatography and mass spectrometry. Isotope labels can be introduced metabolically, chemically, enzymatically or via the use of external standards using spiked synthetic peptides. A mass spectrometer has the ability to recognise the mass difference between the labelled and unlabelled peptides, and thus, quantification is achieved via comparing the respective signal intensities [193].

In the last five years the use of stable isotope labelling methods has driven an increase in non-gel approaches to quantitative proteomics. Both metabolic labelling and post-extraction labelling target certain amino acids that are 'mass-tagged' using stable isotopes. Multiple samples can then be mixed and subsequently fractionated, separated and analysed by MS. The advantage of this is that several procedural and instrumental factors such as signal suppression are cancelled out when the compared samples are run under exactly the same conditions [219]. In the most automated approaches to these forms of proteomics, there are no protein separations at all. The entire sample, or multiplexed labelled sample, is enzymatically digested with trypsin and the complex mixture of peptides separated by two-dimensional LC. This usually involves strong cation exchange as the first dimension, followed by reversed phase LC-MS of each ion exchange fraction. Whilst this approach requires relatively low sample amounts and provides large numbers of peptides to the MS and can confirm that particular genes were expressed, the proteins are never observed as intact molecules. In addition, it does not adequately resolve multiple isoforms of proteins, thus under-estimating the complexity of any given proteome [220]. In recent times alternative strategies utilising label-free methods have been introduced [221-223]. These techniques compare multiple experiments via comparing the direct mass spectrometric signal intensity for a given peptide or by using the number of spectra matching to a peptide or protein as an indication of their respective amounts in a given sample.

1.9.6. Isobaric tag for relative and absolute quantification (iTRAQ)

iTRAQ is a novel mass spectrometry based technique that can accurately quantify proteins in absolute and relative terms [224]. iTRAQ is a post-extraction approach

that involves mass-tagging protein or peptide amino groups using the iTRAQ® reagents from Applied Biosystems (figure 1.14). The utilisation of iTRAQ overcomes the problem of low total protein yield encountered during sample preparation as it requires only 100 µg compared to the 300 µg demanded by the 2-D PAGE analysis platform. Furthermore, the iTRAQ reagent comes as a four-plex and eight-plex kit allowing several protein samples to be analysed simultaneously and compared on the same spectra. In comparison, the spectral counting analysis platform requires that each sample be run on the MS individually. This necessitates the inclusion of technical replicates due to the inherent variability associated with multiple MS/MS analyses over an extended time period. The multiplex nature of the iTRAQ technology removes the need to run technical replicates, improving time efficiency and lowering cost (at least in terms of MS runs).

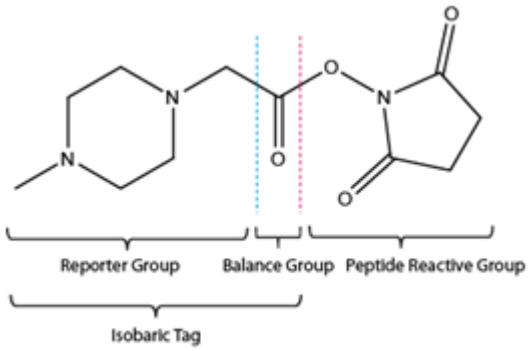

Figure 1.14: iTRAQ reagent structure (from [225]).

The basic principle of the iTRAQ technology consists of the chemical derivatisation of proteolytic peptide mixtures using a set of amine-reactive reagents with distinct isotopic mass designs. The iTRAQ reagent 'tags' are isobaric, meaning they will not affect the overall protein sample mass across different samples as all changes in each

individual protein mass are effectively the same. The iTRAQ reagent covalently attaches to the primary amine on amino acids such as those found in lysine and free N-terminal amines[226]. The isobaric 'tags' consist of a mass balance group, which provides the covalent link to primary amines, and a reporter group, that is released during MS/MS fragmentation and which provides the quantitative ion for each tag [226]. Once the labelling has occurred, the differentially labelled samples are combined and the peptides are separated by liquid chromatography and then analysed by tandem mass spectrometry (figure 1.15).

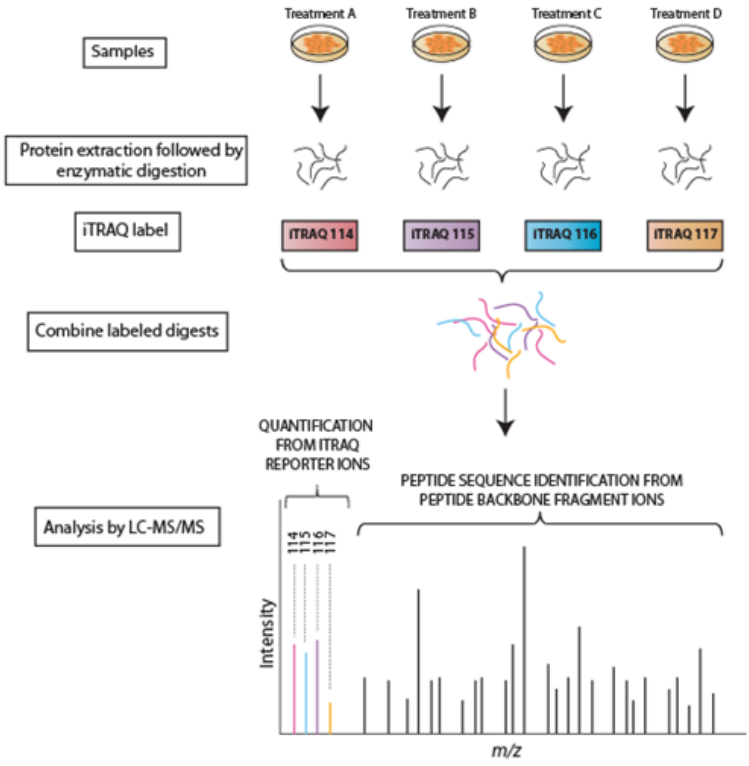

Figure 1.15: iTRAQ workflow (from [225]).

The reporter tags have differing mass to charge (m/z) ratios ranging from 113 to 121 (excluding 120) and peptides of the same sequence from different samples, which are labelled with different tags, are eluted at the same chromatographic retention time

[227]. Differentially labelled peptides of the same sequence therefore appear as a single peak in MS scans. Relative quantitative information on iTRAQ-tagged peptides is obtained in MS/MS scans liberating the reporter groups as distinct isotope-encoded fragments [226]. Isotopic labelling at the peptide level, coupled with the specific mass design of the label, enables the simultaneous acquisition of qualitative and quantitative information [226].

1.9.6.1. Limitations of the iTRAQ technology

As with all experimental protocols, the iTRAQ technology is not without its limitations. Pichler *et al. (2010)* found that the iTRAQ 4-plex identified a significantly higher number of peptides and proteins than the iTRAQ 8-plex [228]. It was concluded that the observed differences in peptide detection was a result of a combination of several factors, including the cleavage of the label itself and the possible disparate physiochemical properties of peptides depending on the type of derivatisation (iTRAQ labeled peptides are both bulkier and more hydrophobic than their underivatised counterparts – especially for the 8-plex). Protein ratios are calculated from the median of peptide ratios; thus, higher numbers of identified peptides improves the precision of protein ratios and the accuracy of protein quantification. It was concluded that due to its superior ability to identify peptides and proteins, 4-plex iTRAQ should be used in the place of the 8-plex iTRAQ [228]. This revelation reduces the high-throughput nature of the iTRAQ technology and demands more convoluted experimental design in the case of experiments with high sample number. However, the technique still has higher throughput and sensitivity than 2-D PAGE analysis and other comparative proteomic techniques.

1.9.7. Analysis of the host immune response

Immunoproteomics is defined as the analysis of circulating antibodies that reflect the molecular imprint of antigens. These antibodies represent the subset of proteins that induce an immune response in the host [229, 230]. Immunoproteomic-based technologies are grouped into three broad groups: gel-based, gel-free (gel-free fractionation such as liquid chromatography followed by protein array) and inverse immunoproteomics. As this project will focus on gel-based techniques only these will be described. Gel-based techniques use either 1-D PAGE or 2-D PAGE for protein separation followed by protein transfer to a nitrocellulose or polyvinylidene fluoride membrane. Towbin *et al. (1979)* first introduced gel-to-membrane protein transfer, also known as immunoblotting or Western blotting [231].

The selective identification of proteins that react with the host immune system reduces the necessity of examining the entire proteome. Immunoproteomics, however, is heavily dependent on optimised protein isolation techniques and is also highly sensitive to non-protein contaminants (cell wall, polysaccharide, DNA etc.) [232]. This sensitivity is especially relevant for the analysis of pathogenic *Cryptococcus* species, which produce polysaccharide capsule, especially during *in vivo* pulmonary infection. The technical limitations of coupling immunoproteomics with the *Cryptococcus* sample type were identified and resolved by Jobbins *et al.* [232], who used circulating antibodies from an infected host to detect 31 disease-associated antigens from *Cryptococcus* proteins separated by 2-D PAGE. The identification of disease-associated antigens can be used to identify targets for therapy, diagnostic biomarkers and indicators of prognosis.

1.9.8. The Bio-Plex suspension array system

The Bio-Plex suspension array system was developed by Bio-Rad for the detection and measurement of cytokines, chemokines and growth factors. These cell-signalling proteins are expressed and secreted by a myriad of cells, including those of the immune system. The detection and quantitative measurement of these proteins can provide insight to the physiological state/responses of the host to cryptococcal infection. This technology is based on the flow cytometric analysis of fluorescently dyed microspheres (6.5 μm magnetic beads) that possess distinct spectral addresses. The assay is essentially an immunoassay, similar in principle to a sandwich ELISA, formatted on magnetic beads (figure 1.16). Capture antibodies, which target the desired biomarker, are covalently bound to the magnetic beads that react with sample containing the biomarker of interest. After washing, a biotinylated detection antibody is then introduced and subsequently reacts with the biomarker of interest to form the sandwich complex. The detection of the complex is achieved by the addition of the fluorescent indicator phycoerythrin in the form of a streptavidin-phycoerythrin conjugate. Data from these reactions are acquired by dual laser flow cytometery. A red laser (635 nm) illuminates the specific fluorescent dyes within each bead so as to provide assay identification while a green laser (532 nm) excites the phycoerythrin to generate a reporter signal that is detected by a photomultiplier tube. The Bio-Plex manager software then presents the data as median fluorescence intensity and concentration (pg/mL) (figure 1.17).

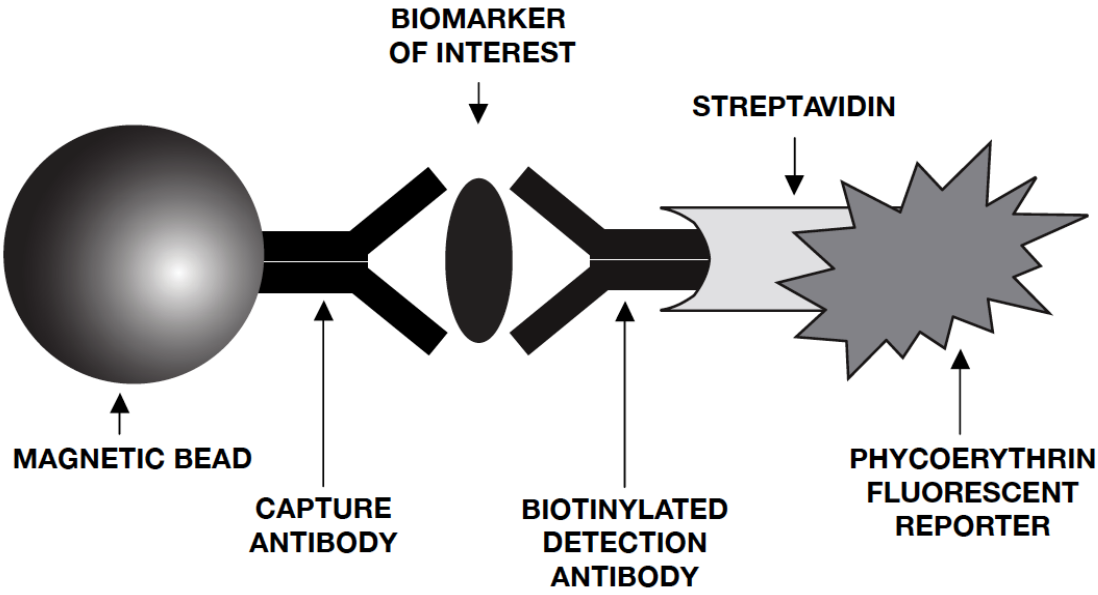

Figure 1.16: Bio-Plex sandwich immunoassay (from [233]).

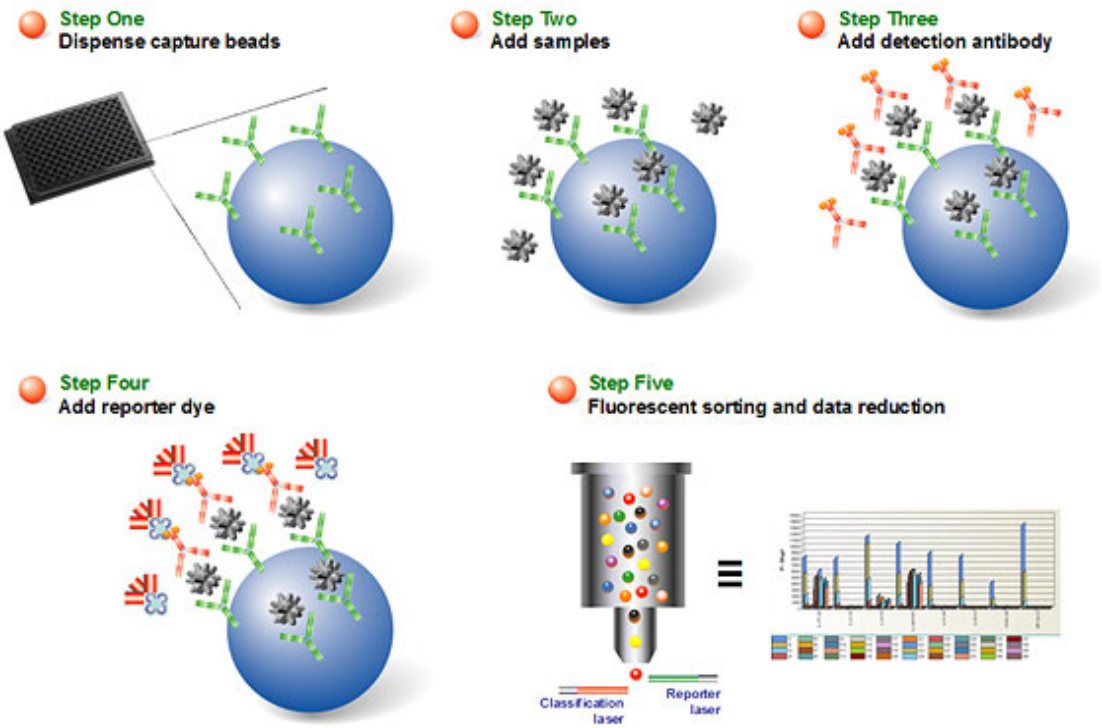

Figure 1.17: Bio-Plex suspension array system workflow (from [234]).

The Bio-Plex suspension array system allows for the simultaneous detection and measurement of over 100 different molecules in a single well of a 96 well microplate. The clear advantages of Bio-Plex are that the assay is a multiplex system (the rat cytokine kit can essentially run 23 ELISAs at once), it is not greedy on sample (requiring only 50 μL of serum per sample while Western blots require at least 250 μL serum per sample) and it generates results in a time frame of hours rather than approximately three days to complete the 2-D PAGE Western blot protocol.

1.10. Project outline

Fungal infection and disease are increasing on a worldwide scale. The outbreak of a hypervirulent strain of *C. gattii* on Vancouver Island in 1999 highlighted the need for the development of novel, more effective *Cryptococcus*-specific antifungal agents [235]. Current antifungal therapies are limited in scope and spectrum, are frequently toxic [236] and are very expensive. Furthermore, treatment does not always completely eradicate the pathogen and antifungal drug resistance is an emerging issue. The development of novel antifungal agents requires the elucidation of the *in vivo* molecular responses of both the fungus and the host to pulmonary fungal infection. Pulmonary infection with *C. neoformans* and *C. gattii* provided a suitable model to investigate these molecular processes as inoculation resulted in the development of fungal burdens large enough to permit the use of comparative proteomic analysis techniques. Furthermore, this study had access to *Cryptococcus* strains of differing virulence, which resulted in different levels of pulmonary infection.

The aim of this thesis was to use the pulmonary infection model to provide insight as to how virulent *Cryptococcus* establishes and maintains infection in the mammalian

host. More specifically, this project attempted to identify the fungal proteins that promote pathogenesis during pulmonary infection via comparative quantitative proteomics. In addition to studying changes in *Cryptococcus* protein expression during infection, the work described in this thesis attempted to identify the proteins involved in the host response to fungal pulmonary infection via the comparative quantitative analysis of host lung proteins and serum cytokines. This thesis provides the first attempt at the comparative proteomic analysis of a pathogenic fungal species and the dynamic host response during mammalian infection.

1.10.1. Hypothesis and aims – fungal pathogenesis

The work outlined in this thesis was undertaken with the hypotheses that:

1. Mammalian pulmonary infection would induce specific protein changes in the intracellular proteome of *Cryptococcus*;
2. A comparative proteomic analyses would identify specific proteins that provide virulent *Cryptococcus* strains with survival advantages over less virulent strains; and
3. This analysis would lead to the development of novel therapeutic or diagnostic targets.

The aims of this study were therefore:

- To investigate and develop suitable proteomic techniques for the analysis of *Cryptococcus* from pulmonary infection.

- To use these techniques to identify and describe the fungal proteins essential for the establishment and progression of *Cryptococcus* pulmonary infection.

1.10.2. Hypothesis and aims - host response

The work outlined in this thesis was undertaken with the hypotheses that:

1. Pulmonary infection with *Cryptococcus* would induce specific changes in the lung proteome and systemic changes in cytokine expression that would vary according to the virulence of the infecting strain; and
2. Comparative proteomic analyses would identify specific host proteins and serum cytokines that could form future therapeutic or diagnostic targets.

The aims of this study were therefore:

- To use iTRAQ to detect and quantify lung proteins that change in expression in response to pulmonary infection by *Cryptococcus* strains of different virulence levels.
- To use the Bio-Plex suspension array system to detect and quantify the systemic cytokines that change in expression in response to pulmonary *Cryptococcus* infection.

Chapter Two

Materials and Methods

This chapter lists the materials and equipment, reagents and chemicals and the solution formulations used in this project. This chapter also contains a description of the general methods used and cross-references to the appropriate sections of the results chapters that detail the specifics of the methodology used.

2.1. Fungal strains

The fungal strains utilised to complete the work presented in this doctoral thesis are listed in Table 2.1.

Table 2.1: Fungal strains

Isolate designation	Source/host	Geographic source	Serotype	Molecular Type
A1M R265	Bronchial alveolar lavage	Duncan, Vancouver Island (B.C., Canada)	B	VGIIa
A1M R272	Bronchial alveolar lavage	Ladysmith, Vancouver Island (B.C., Canada)	B	VGIIb
KN99α	A cross of KNA14 and H99 crg1 (αA) backcrossed 10 times to H99 - bred to be a congenic α mating type strain of H99 [237]	Duke University Medical Center, Durham (North Carolina, USA)	A	VNI

2.2. Materials and equipment, reagents and chemicals and solution formulations

The materials and equipment used to complete the work presented in this thesis are contained in Table 2.2. Table 2.3 contains the source of the reagents and chemicals. The solution formulations are listed in Table 2.4.

Table 2.2: Materials and equipment

Materials/Equipment	Company
11 cm focusing tray with lid	Proteome Systems, Australia
11 cm IPG strip rehydration/equilibration tray	Bio-Rad, USA
Alpha 1-4 LDplus Freeze Dryer	Christ, Germany
Bio-Plex 200 system with version 5.0 software	Bio-Rad, USA
Bio-Plex Pro II magnetic wash station	Bio-Rad, USA
Bio-Plex Pro™ Rat Cytokine 24-plex Assay	Bio-Rad, USA
Criterion™ Cell gel running apparatus	Bio-Rad, USA
Criterion™ XT Bis-Tris One Dimensional Precast, 4-12%, 12 well, 40 µl, 1.0 mm polyacrylamide gel	Bio-Rad, USA
Criterion™ XT Bis-Tris Precast, 4-12%, IPG + 1 well, 11 cm, 1.0mm polyacrylamide gel	Bio-Rad, USA
DT-50 tube with rotor-stator element	IKA, Germany
Extra thick blot paper	Bio-Rad, USA
Micro Bio-Spin 6 columns, P6 in saline sodium citrate	Bio-Rad, USA
Micromax 230 centrifuge	IEC, USA
Nanosep 100K Omega centrifugal devices	Pall Scientific, USA
PROTEAN® IEF Cell	Bio-Rad, USA
0.45 µm PVDF Immobiline-P Transfer Membrane	Millipore Corporation, USA
Ratek Orbital Mixer Incubator	Ratek Instruments Pty. Ltd., Australia
ROTANTA 96 R centrifuge	Hettich Zentrifugen, Germany
Sonicator 3000	Misonix, USA
Trans-Blot® SD Semi-Dry Transfer Cell	Bio-Rad, USA
Typhoon Trio laser scanners	GE Healthcare, UK
ULTRA-TURRAX® tube drive workstation	IKA, Germany
Vacufuge™ Concentrator 5301	Eppendorf, Germany

Table 2.3: Reagents and chemicals

Reagent/Chemical	Supplier
10X Flamingo™ protein staining solution	Bio-Rad, USA
20 XT MES running buffer	Bio-Rad, USA
Acetic Acid	Chem-supply, Australia
Acetone	Sigma-Aldrich Co, USA
Acetonitrile, LC-MS grade (ACN)	Sigma-Aldrich Co, USA
Acrylamide	Bio-Rad, USA
Agar	Sigma-Aldrich Co, USA
Amino-caproic acid	Sigma-Aldrich Co, USA
Ammonium Bicarbonate	Sigma-Aldrich Co, USA
Ammonium sulphate	Sigma-Aldrich Co, USA
Bacteriological Peptone	Oxoid, England
Bromophenol blue	Sigma-Aldrich Co, USA
C7BzO	Sigma-Aldrich Co, USA
Citric acid	Sigma-Aldrich Co, USA
Complete protease inhibitor cocktail tablets	Roche, Germany
Coomassie brilliant blue G250	Sigma-Aldrich Co, USA
Dextrose	Univar, USA
Direct blue 71	Sigma-Aldrich Co, USA
Dithiothreitol (DTT)	Bio-Rad, USA
Ethanol	Sigma-Aldrich Co, USA
Formic acid	Sigma-Aldrich Co, USA
Lithium Chloride	Sigma-Aldrich Co, USA
Methanol	Sigma-Aldrich Co, USA
Mineral oil, Biotechnology grade	Bio-Rad, USA
NuPAGE® 4X LDS Sample Buffer (pH 8.4)	Invitrogen Corporation, USA
Orange G IEF Dye	Proteome Systems, Australia
Phosphoric acid	Sigma-Aldrich Co, USA
Phosphate buffered saline	Amresco, USA
Precision Plus Unstained Protein Standards	Bio-Rad, USA
Sodium dodecyl sulphate (SDS)	Sigma-Aldrich Co, USA
Sucrose	Univar, USA
Thiourea	Sigma-Aldrich Co, USA
Tributylphosphine (TBP)	Sigma-Aldrich Co, USA
Triethylammonium bicarbonate (TEAB)	Sigma-Aldrich Co, USA
Tris buffered Phenol, pH 8	Sigma-Aldrich Co, USA
Tris-HCl, pH 6.8	Sigma-Aldrich Co, USA
Tris(hydroxymethyl)aminomethane	Sigma-Aldrich Co, USA
Trypsin Gold, Mass spectrometry grade	Promega Corporation, USA
Urea	Sigma-Aldrich Co, USA
Yeast Extract	Oxoid, England

Table 2.4: Solution formulations

Solutions	Formulation
1X Flamingo™ protein staining solution	10X Flamingo™ protein staining solution diluted to 1X with ddH_2O
1X NuPAGE® LDS Sample Buffer (pH 8.4)	NuPAGE® 4X LDS Sample Buffer (pH 8.4) diluted to 1X with ddH_2O
1X XT MES running buffer	20X XT MES running buffer diluted to 1X with ddH_2O
2-D PAGE sample buffer	1% C7BzO (w/v), complete protease inhibitor cocktail in 2 M thiourea, 7 M urea, 40 mM Tris, 50 mM LiCl
Acrylamide stock	1 M Acrylamide in ddH_2O
Coomassie brilliant blue G250 staining solution 1	0.12% Coomassie brilliant blue G250 (w/v), 20% Methanol (v/v), 10% Phosphoric acid (v/v) in ddH_2O
Coomassie brilliant blue G250 staining solution 2	50% Ammonium sulphate in ddH_2O
Coomassie de-staining solution	1% Acetic acid (v/v) in ddH_2O
Direct blue 71 stock	0.01% (w/v) in ddH_2O
Dithiothreitol stock	1 M Dithiothreitol in ddH_2O
In-gel trypsin digestion Coomassie de-stain solution	50% Acetonitrile (v/v) in 50 mM Ammonium bicarbonate
In-gel trypsin digestion enzyme solution	5 µL trypsin per 395 µL of 50 mM NH_4HCO_3
In-gel trypsin digestion peptide extraction solution	50% Acetonitrile (v/v), 2% Formic acid (v/v) in ddH_2O
IPG equilibration solution	6 M urea, 0.25 M Tris-HCl (pH 6.8), Bromophenol blue, 10% SDS (w/v) in ddH_2O
iTRAQ sample buffer	1% SDS (w/v) in 100 mM TEAB
Polyacrylamide gel fixing solution	40% methanol (v/v), 10% Acetic acid (v/v) in ddH_2O
Pulmonary tissue homogenisation sample buffer	1% C7BzO (w/v), complete protease inhibitor cocktail in 2 M thiourea, 7 M urea, 80 mM citric acid, 50 mM LiCl
PVDF membrane washing solution	40% Ethanol (v/v), 10% Acetic acid (v/v) in ddH_2O
Sucrose density cushion centrifugation	0.5 g/mL in ddH_2O
Western blot buffer 1 10X stock	400 mM Amino-caproic acid, 250 mM Tris in ddH_2O
Western blot buffer 2 10X stock	250 mM Tris in ddH_2O
Western blot buffer 3 10X stock	3 M Tris in ddH_2O
Yeast peptone dextrose agar	1% yeast (w/v), 2% peptone (w/v), 2% glucose (w/v), 2% agar (w/v) in ddH_2O
Yeast peptone dextrose broth	1% yeast (w/v), 2% peptone (w/v), 2% glucose (w/v) in ddH_2O

2.3. General methods

This thesis presents individual studies that used a number of general experimental techniques. What follows is a description of these techniques.

2.3.1. *In vitro* growth conditions

Cryptococcus colonies were grown on yeast extract peptone dextrose (YPD) agar plates for two days at 37 °C (or until sufficient colonies had developed). The cells were then sub-cultured in 100 mL of YPD broth in a Ratek Orbital Mixer Incubator (Ratek Instruments Pty. Ltd., Victoria, Australia) at 37 °C, 200 rpm to mid-logarithmic phase. Cells were then isolated from the YPD broth via slow speed centrifugation and washed three times in 50 mL volumes of 1 X PBS.

2.3.2. Pulmonary infection model

2.3.2.1 Animals used

A number of mammals have been used to study cryptococcosis including mice, rats, rabbits and guinea pigs [238]. There are two clear advantages of the rat model compared to the other mammalian model organisms. First, the rat reproduces many of the histopathological and serologic features of human cryptococcosis [239]. Second, the rat provides a size advantage over the popular mouse model. The mouse model would not be able to produce the fungal load required to complete global proteomics analyses. Inbred female Fisher-344 rats (body weight approximately 150 g) were obtained from the Animal Resource Centre (W.A., Australia) and maintained in individually ventilated cages in groups of two (care was taken to ensure that rats were

grouped according to inoculation type). Rats had access to food and water ad libitum from a top loaded food hopper and water bottle.

2.3.2.2 Inoculation of rats with Cryptococcus

Cryptococcus cells were cultured on yeast peptone dextrose (YPD) agar for at least 48 hours at 37 °C. Fungal colonies were then transferred to sterile saline solution. Yeast cells were counted on a Neubauer-improved haemocytometer and the cell number adjusted to the appropriate concentration. Intratracheal inoculation with 0.1 mL of 10^7 CFU, the minimal inoculum concentration demonstrated by Krockenberger *et al. (2010)* to produce progressive pneumonia [239], resulted in poor lesion development and limited disease progression. Thus, intratracheal inoculations of 0.1 mL of 10^8 CFU were administered through a flexible plastic catheter that had been passed over the epiglottis and into the rat trachea. An otoscope was used to assist the insertion of the catheter into the trachea. An intranasal method of inoculation was used when the intratracheal route proved difficult. Intranasal inoculation involved the insertion of a flexible plastic catheter into the nasal passage. A 1 mL volume of air was administered via the inserted catheter immediately after the *Cryptococcus* inoculum to ensure that the maximal dose of *Cryptococcus* cells was administered and to ensure that the lungs were flushed with cells. Post inoculation, the rats were allowed to recover from anaesthesia of their own accord under a heating lamp. For this study the control was naïve lung, the rats being neither anesthetised nor subject to mock inoculations. The inoculum concentration was confirmed by back plating, whereby an aliquot of the inoculum was diluted, spread plated onto YPD agar plates and cultured at 37 °C until colonies formed.

Infected rats were monitored according to the University of Sydney animal ethics guidelines (ethics approval number: N00/10-2008/2/4810). Pulmonary infection was allowed to progress for 14 days (equating to early infection) and 42 days (equating to late infection) at which time the rats were euthanized. Prior to harvesting the rat lung, as much blood as possible was extracted via heart puncture with a 2 mL syringe. The extracted blood was allowed to coagulate at room temperature. During coagulation the lungs were harvested, weighed and then stored at -80 °C until required. Rat serum was then isolated via low speed centrifugation, aliquoted and frozen at -80 ºC until required.

2.3.3. Pulmonary tissue homogenisation

Control or infected lung tissue was homogenized in a 15-50 mL Ultra-turrax tube (IKA, Germany) with 40 mL of 1 % C7BzO, 2 M thiourea, 7 M urea, 80 mM citric acid, 50 mM LiCl and a complete protease inhibitor cocktail for three bursts of one minute at maximum speed (6,000 rpm). In between homogenization bursts the sample was kept on ice to prevent overheating. Processing a severely infected lung sample resulted in a highly viscous homogenate. To reduce viscosity the sample was divided into aliquots (the number of aliquots was dependent on the degree of viscosity observed) and diluted with 40 mL of 1 % C7BzO, 80 mM citric acid and 50 mM LiCl. The samples were then further Ultra-turraxed for 2 x 1 minute bursts to ensure complete tissue homogenization. The sample was transferred to a suitable number of 50 mL Falcon tubes and ultra-sonicated with a probe for four bursts of 30 seconds. During sonication the sample was kept on ice to prevent a significant rise in sample temperature. The samples were then centrifuged at 4,000 *g* for ten minutes at 4 °C to

remove connective tissue, cell debris and to isolate the *Cryptococcus* cells. The supernatants were retained for the investigation of the host lung proteome and the pellet was retained for *Cryptococcus* isolation and lyophilisation.

2.3.4. Isolation of *Cryptococcus* from pulmonary tissue and lyophilisation of *Cryptococcus*

The pellet retained after the low speed spin (containing connective tissue, cell debris and *Cryptococcus* cells) was resuspended in 2 volumes of 1 x PBS containing a protease inhibitor cocktail. The sample was then carefully pippetted on the top of a 3 mL sucrose density cushion (0.5 g/mL) in a 15 mL Falcon tube. Special care was taken to ensure that the sample did not mix with the sucrose density cushion. The sample/sucrose cushion was then centrifuged at 1,500 *g* for 20 minutes. Post centrifugation the sample differentiated into three distinct partitions:

1. A top layer of lung supernatant
2. An interface of *C. gattii* cells
3. A pellet of pulmonary connective tissue and cell debris

The *Cryptococcus* interface was carefully transferred to a 50 mL Falcon tube and the cells washed with 50 mL of PBS containing a protease inhibitor cocktail to remove excess sucrose. The wash step was repeated twice. The washed cells were then resuspended in 5 mL of 1% C7BzO, 2 M thiourea, 7 M urea, 80 mM citric acid, 50 mM LiCl and a protease inhibitor cocktail and ultra-sonicated with a probe for four bursts of 30 seconds. During the sonication process the sample was kept on ice. The sample was then centrifuged at 4,000 *g* for 10 minutes at 4 °C. The supernatant was

then transferred to a 15 mL Falcon and retained. This process was repeated and the supernatant pooled and retained. This repeated wash/ultra-sonication step in denaturing conditions was completed in an attempt to remove any proteins non-covalently bound to the outer surface of the *Cryptococcus* capsule. The washed cells were then resuspended in a minimal volume of PBS (volume varied in accordance to the total volume of cells obtained from individual infected lungs) and transferred to the required number of lyophilisation/bead beating tubes (maximum of 500 μL per 2 mL tube). The samples were immediately placed at -80 °C for at least 20 minutes or until completely frozen and were then placed in the Alpha 1-4 LDplus Freeze Dryer (Christ, Germany) and lyophilized overnight.

2.3.5. *In vitro*/*in vivo Cryptococcus* cellular disruption and phenol protein extraction

After the lyophilisation of *Cryptococcus* cells the equivalent of a 500 μL volume of 3 mm glass beads were added to the sample tubes. The sample was then dry bead beaten in a Fast-prep Instrument for 5 bursts of 30 seconds at maximum speed. After each bead beating round the samples were kept on ice to prevent them from over heating. Samples were then resuspended in 1 mL of 1% C7BzO, 2 M thiourea, 7 M urea, 50 mM LiCl, 40 mM Tris and containing a protease inhibitor cocktail (Roche Applied Science). Further bead-beating of the sample for two x 30 second bursts at maximum speed was done to ensure resuspension and to promote maximal cell lysis. The disrupted samples were pooled in a 50 mL Falcon tube and centrifuged at 4,000 *g* for 5 minutes to remove excessive bubbles. The sample was then ultra-sonicated on ice

with a probe for four bursts of 30 seconds and centrifuged at 4,000 *g* for ten minutes at 4 °C to remove cell debris and any un-lysed cells.

This solution was made to 30 % sucrose and vortexed to ensure a homogenous mixture. An equal volume of Tris buffered phenol (10 mM Tris HCl, pH 8.0) was added to the protein solution and the sample mixed thoroughly for ten minutes. The sample was then centrifuged at 20,000 *g* for 10 minutes to ensure the separation of the organic and aqueous phases. The top organic phase (which contains the protein) was transferred to a suitably sized Falcon tube and the proteins precipitated by incubation with a 5 x volume of 100 % acetone for 30 minutes at room temperature. The precipitated proteins were pelleted at 4,000 *g* for 10 minutes at room temperature and the acetone discarded. The protein pellet was briefly air-dried and then resuspended in a suitable volume of 1 x LDS sample buffer for 1-D SDS-PAGE or 1% C7BzO, 2 M thiourea, 7 M urea, 50 mM LiCl, and 40 mM Tris for 2-D PAGE. Post resolubilisation, the sample was reduced and alkylated via 1-hour room temperature incubation with 10 mM TBP and 10 mM acrylamide. The reduction/alkylation reaction was then quenched with the addition of 10 mM DTT.

2.3.6. 2-D PAGE

To visualise the extracted lung proteome 2-D PAGE was performed [200] with the following modifications. 11 cm immobilised pH gradient (IPG) strips, pH 4-7 (Bio-Rad, USA), were rehydrated with 210 µL of sample solution pipetted under the strips. Isoelectric focusing (IEF) was performed using a Protean IEF Cell apparatus (Bio-Rad, USA) at 20 ºC (Slow ramp to 5,000 V over four hours, linear gradient reaching 10,000V over four hours, fast gradient at 10,000 V for a maximum of 150,000 kVhrs;

current limit set at 50 μA per strip). Prior to second dimension protein separation the IPG strips were equilibrated for 20 minutes in 6 M urea, 0.25 M tris-HCl pH 6.8, bromophenol blue and 10 % SDS (v/v). The equilibrated strips were then transferred onto Criterion XT Bis-Tris Precast gels, 4-12% (Bio-Rad, USA). Second dimension separation was carried out using a Criterion Cell apparatus (Bio-Rad, USA) at a constant voltage of 150 V. The gel was then removed from its casing and transferred into a fixing tray.

2.3.7. 1-D SDS-PAGE

In preparation for 1-D SDS-PAGE, the sample was heated at 95 °C for 10 minutes to maximise protein denaturation and solubilisation. The sample was centrifuged at 16,000 *g* for 10 minutes to remove any insoluble particulates prior to gel loading. During sample heating and centrifugation, a Criterion XT Bis-Tris One Dimensional Precast gel and a Criterion gel running apparatus were prepared for use. The upper buffer chamber of the Criterion XT Bis-Tris One Dimensional Precast gel and the Criterion gel tank were filled with 1 x XT MES running buffer (500 mL per gel). For Criterion XT Bis-Tris One Dimensional Precast 12 well gels, 30 μL of the sample was loaded into the appropriate well/s. In addition to sample loading, 5 μL of Precision Plus Unstained Protein Standards (molecular weight markers) were loaded into the appropriate well of every sample gel. Electrophoresis performed at 160 V until the Precision Plus Unstained Protein Standards dye-front had reached the very end of the gel. The gel was then removed from its casing and transferred into a fixing tray.

2.3.8. Fluorescent staining and image analysis

Protein was fixed in the polyacrylamide gel matrix via incubation in fixing solution for a minimum of 30 minutes. The fixing solution was then decanted and the gel was rinsed with ddH_2O and stained with 50 mL of 1 X Flamingo™ staining solution (Bio-Rad, USA) for a minimum of 60 minutes while wrapped in foil. All fixing and staining was undertaken on an orbital shaker (50 rpm) to encourage mixing of solutions and to expose the entire gel to each solution. The gel was imaged with a Typhoon TRIO (GE Healthcare, UK) gel imager using pre-set scanning wavelengths designed for the Flamingo™ protein stain. Scans were completed on all gels at a resolution of 50 μm assuming low sample intensity.

2.3.9. Mass spectrometry (completed by the Australian Proteome Analysis Facility at Macquarie University)

2.3.9.1. SCX HPLC

Samples (iTRAQ labelled pulmonary material and unlabelled *Cryptococcus*) were cleaned and fractionated by SCX HPLC. The dried samples were re-suspended in buffer A (5 mM phosphate, 25 % acetonitrile (v/v), pH 2.7). After sample loading and washing with buffer A, buffer B (5 mM phosphate, 350 mM KCl, 25 % acetonitrile (v/v), pH 2.7) concentration increased from 10 % to 45 % over 70 minutes and then increased quickly to 100 % where it stayed for 10 minutes at a flow rate of 300 μL/min. The eluent of SCX was collected every 2 minutes at the beginning of the gradient and at 4-minute intervals thereafter.

2.3.9.2. NanoLC ESI MS/MS data acquisition

The SCX fractions were resuspended in 100 μL of loading/desalting solution (0.1 % trifluoroacetic acid (v/v) and 2 % acetonitrile (v/v) in ddH_2O). 39 μL of the resuspended solution was loaded on a reverse phase peptide Captrap (Michrom Bioresources) and desalted with 0.1 % formic acid, 2% ACN (v/v) at 10 μL/min for 13 minutes. After desalting, the trap was switched on line with a 150 μm x 10 cm C18 3 μm 300 A ProteCol column (SGE Analytical Science, Australia). Buffer B (90 % ACN (v/v) / 9.9 % ddH_2O (v/v) / 0.1 % formic acid (v/v)) concentration was increased from 5 % to 90 % over 120 minutes in three linear gradient steps to elute peptides. After peptide elution, the column was cleaned with 100 % buffer B for 15 minutes and then equilibrated with buffer A (99.9 % ddH_2O (v/v) / 0.1 % formic acid (v/v)) for 30 minutes before next sample injection.

The reverse phase nanoLC eluent was subject to positive ion nanoflow electrospray analysis in an information dependent acquisition mode (IDA). In IDA mode a TOFMS survey scan was acquired (m/z 370-1600, 0.5 second), with the three most intense multiply charged ions (counts >70) in the survey scan sequentially subjected to MS/MS analysis. MS/MS spectra were acquired in the mass range m/z 100-1,600.

2.3.9.3. Data processing

The experimental MS data were submitted to ProteinPilot V4.0 (AB Sciex, USA) for data processing using SwissProt database and *Rattus norvegicus* species. All reported data were based on 95 % confidence for protein identification as determined by ProteinPilot (ProtScore ≥ 1.3). A further requirement was a protein *p*-value, which ensured protein identification and quantitation was not based on a single peptide hit.

2.4. Study Specific Methods:

This thesis presents detailed descriptions of methods unique to individual studies in a chapter specific manner. Table 2.5 contains an index of these study specific methodologies.

Table 2.5: Study specific methods

Method	Refer to section
2-D PAGE Western blotting	3.2.8.
1-D SDS-PAGE manual lane excision and trypsin in-gel digestion for mass spectrometry protein identification	4.2.7.
Pulmonary sample preparation for iTRAQ analysis	5.2.4.
4-plex iTRAQ sample design	5.2.5.
iTRAQ labelling (completed by the Australian Proteome Analysis Facility at Macquarie University)	5.2.6.
Bio-Plex Pro Rat Cytokine, Chemokine, and Growth Factor Assay	6.2.3.
Linear regression models	6.2.4.

Chapter Three

Development of proteomic protocols for the analysis of pulmonary infection with *Cryptococcus*

The proteomic data presented in this study were the result of a significant amount of protocol development. This chapter presents a description and analysis of the experimental work undertaken to develop the study-specific protocols required for the proteomic investigation of pulmonary infection with Cryptococcus.

3.1. Technical issues are inherent to the fungal sample type

Despite the importance of fungi to both industry and biomedicine, the proteomic analysis of these organisms is only just beginning. This is a direct result of the technical challenges associated with fungal proteomics. Protein extraction from fungi, and especially filamentous fungi, is difficult, largely due to the robust fungal cell wall that increases the structural integrity of the cell [240-242]. A number of studies have been undertaken to overcome the cell lysis challenges that fungal organisms pose, with a vast number of mechanical, chemical and enzymatic extraction methods being investigated. Some research groups have gone so far as to generate protoplasts (cell wall removed) [242], however, it is generally agreed that meaningful proteomic data can only be obtained when pre-lysis handling and manipulation is kept to a minimum.

Gene expression and gene transcript changes during infection have been investigated in a number pathogenic fungi including *Cryptococcus neoformans, Candida albicans* and *Aspergillus fumigatus* [243], but there have been no studies in *C. gattii*. Additionally, to date there are no publications investigating the proteome of pathogenic fungi during infection. Studying fungal proteomes using animal models is technically challenging. The *Cryptococcus* model was chosen because 1) it is an important fungal pathogen with a suitable animal model; 2) it produces robust infection and was predicted to provide enough material for proteomics; and 3) as a yeast it was possible to purify intact infecting cells from contaminating host material. However, the polysaccharide capsule specific to virulent *Cryptococcus* species provided its own difficulties and using this model for proteomic analysis required extensive optimisation. What follows is the description of the technical difficulties encountered in this study and the measures taken to overcome them.

3.2. Methods

3.2.1. *In vitro* growth conditions

The *in vitro* growth conditions used were described in section 2.3.1.

Note: *C. gattii* R265 (molecular type VGIIa), both cultured and obtained from pulmonary infection, was used for the development of protein extraction protocols.

3.2.2. Pulmonary infection model

The pulmonary infection model used was described in section 2.3.2.

3.2.3. Pulmonary tissue homogenisation

Pulmonary tissue homogenisation was completed using the method described in section 2.3.3.

3.2.4. Isolation of *Cryptococcus* from pulmonary tissue and lyophilisation of *Cryptococcus*

Cryptococcus cells were isolated from pulmonary tissue and lyophilised using the methods described in section 2.3.4.

3.2.5. *In vitro*/*in vivo Cryptococcus* cellular disruption and phenol protein extraction

Cryptococcus cells were lysed and intracellular proteins extracted using the methods described in section 2.3.5.

3.2.6. 2-D PAGE

2-D PAGE was completed using the methods described in section 2.3.6.

3.2.7. 1-D SDS-PAGE

1-D SDS-PAGE was completed using the methods described in section 2.3.7.

3.2.8. 2-D PAGE Western blotting

Proteins separated by 2-D PAGE were transferred onto 0.45µm PVDF Immobilon-P Transfer Membrane (Millipore Corporation, USA) following the semi-dry method developed by Khyse-Anderson [244] with the following modifications. Prior to the completion of 2-D PAGE seven extra thick blot papers (Bio-Rad, USA) and two membranes were cut to the size of the 2-D PAGE gel (approximately 12 cm x 8 cm). The following three buffers were also prepared and cooled to 4 °C:

Buffer 1: SDS aids the elution of proteins from the gel matrix [245]. Amino-caproic acid acts as the terminating ion in the isotachophoresis 'train' that cleans up the proteins from the polyacrylamide gel [244, 246].

- 200 mL required per gel: 20 mL of Western blot buffer 1 10X stock, 20 mL of 100 % methanol and 500 μL of 20 % SDS made up to 200 mL with ddH_2O.

Buffer 2: Methanol increases protein affinity for the membrane by removing SDS from proteins [245].

- 100 mL required per gel: 10 mL of Western blot buffer 2 10X stock and 20 mL of 100 % methanol made up to 100 mL with ddH_2O.

Buffer 3: Tris acts as a conductive strong buffering agent that maintains the conductivity and pH of the system during transfer [247].

- 50 mL required per gel: 5 mL of Western blot buffer 3 10X stock made up to 50 mL with ddH_2O.

Just prior to the completion of 2-D PAGE, 100 mL of buffer 1 was decanted into a clean plastic tray. All of buffer 2 and buffer 3 were decanted into additional individual clean plastic trays. Two blot papers were then placed into the tray containing buffer 1, four into the tray containing buffer 2 and one into the tray containing buffer 3. The membranes were soaked in 100 % methanol until completely wet before being transferred to the tray containing buffer 2 (placed under the blot papers). Upon completion of 2-D PAGE, the gel was removed from its cassette and placed in a clean tray containing ddH_2O for two minutes. The ddH_2O was then decanted from the

plastic tray and replaced with the remainder of buffer 1 and the gel equilibrated with buffer 1 for five minutes. When equilibrated the blot stack was assembled in a bottom up manner as shown below in figure 3.1:

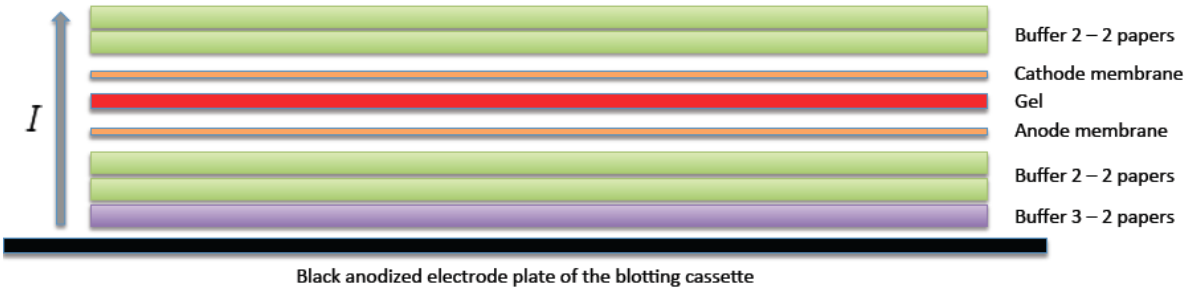

Figure 3.1: Semi-dry blotting stack for reverse polarity protein transfer

This blotting stack differs from that described by Khyse-Anderson [244] in that the stack was initially formed with an additional membrane on the cathode side of the protein gel. Also, two blotting papers soaked in buffer 2 were in place of the standard two blotting papers soaked in buffer 1.

After the gel was placed onto the membrane it was carefully inspected to ensure that there were no trapped air bubbles, which would prevent the transfer of protein. Once the stack was assembled it was carefully rolled with a plastic roller to remove excess buffer and any residual air bubbles. The blotting cassette was then closed and the instrument programmed to run at 300 mA constant for 5 minutes in the reverse polarity. The two blotting papers soaked in buffer 2 were then removed and discarded. The cathode membrane was carefully removed from the blotting stack and stained with direct blue 71 (DB71) for at least 5 minutes and anywhere up to an hour [248]. The membrane was then briefly washed with washing solution to remove excess DB71. The membrane was then allowed to air dry.

After the transfer of protein in the cathode direction, the blotting stack was reassembled as described by Khyse-Anderson [244], with two blotting papers soaked in buffer 1 in place of the two discarded blotting papers soaked in buffer 2 as shown below in figure 3.2:

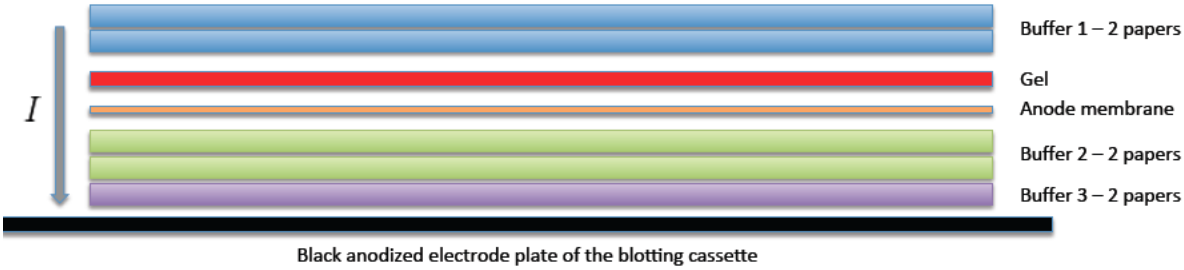

Figure 3.2: Semi-dry blotting stack for traditional polarity protein transfer

The polarity was reset to the traditional orientation and the proteins transferred onto the anode membrane at 300 mA for an additional 25 minutes. Protein transfers in both the cathode and anode direction were completed in a 4 °C cold room. This is especially crucial when transferring proteins in the reverse polarity cathode direction. This process generates a significant amount of heat that would melt the gel into the membrane, resulting in poor protein transfer and high background staining.

The anode membrane was then incubated with 5 % non-fat milk powder in PBS containing 0.1 % (v/v) Tween-20 (PBS-T) for 1 hour at 4 °C, in preparation for hybridization with sera. The blocked membrane was washed with PBS-T 5 times, for 6 minutes each wash, and incubated with patient sera (1:20 dilution with PBS) overnight at 4 °C. Following another 5 washes in PBS-T, the membrane was incubated with alkaline phosphatase-conjugated anti-rat IgG (heavy and light chain) antibody (Sigma-Aldrich, 1:1000 dilution with PBS) for 1.5 hours at ambient

temperature. The membrane was then washed 5 times in TBS containing 0.1 % (v/v) Tween-20 (TBS-T).

Colorimetric development of the immunoblot was achieved using an Alkaline Phosphatase Conjugate Substrate Kit (Bio-Rad, USA). 25 mL of 1 x colour development buffer was prepared and allowed to warm to room temperature. Immediately before use 250 μL of alkaline phosphatase colour reagent A and B were added to the 1 x colour development buffer. The anode membrane was then immersed in the colour development solution and incubated at room temperature on an orbital shaker until colour development was completed (approximately 5 minutes). The membrane was then washed with ddH_20 for five minutes to stop colour development and then allowed to air dry.

3.3. Results:

3.3.1. Separating *Cryptococcus* from pulmonary tissue

Mixed proteomes represented a serious technical issue to this study. The fulfilment of the aims of this thesis, the independent analysis of the host and infective agent proteomes during infection, required the separation of the host material from *Cryptococcus* and vice versa. The low-density nature of the *Cryptococcus* cells from pulmonary infection was exploited to achieve this separation via the use of sucrose cushion density centrifugation (figure 3.3).

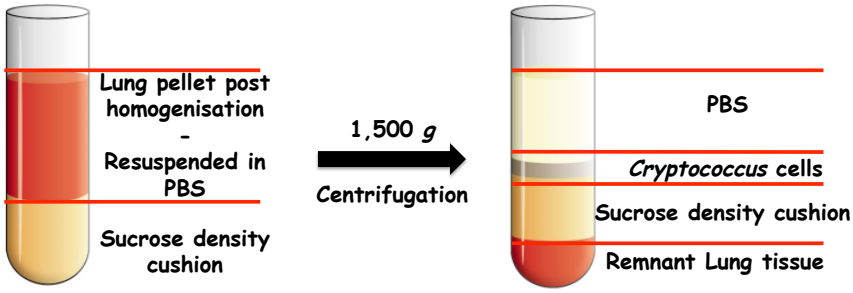

Figure 3.3: Sucrose density cushion centrifugation separates *Cryptococcus* cells from host pulmonary material.

3.3.2. Cell disruption, decapsulation and protein purification for *Cryptococcus* from pulmonary infection

Protein extraction methods progressed from attempts to disrupt cells, to attempts at cell decapsulation from intact cells and finally to attempts at protein purification from cell lysates. Table 3.1 represents the techniques attempted for *Cryptococcus* from pulmonary infection. This table provides a brief description of the effect of the specific technique on the *Cryptococcus* cell or lysate, and whether the resulting sample was suitable for proteomic analysis platforms post-treatment.

Table 3.1: Techniques attempted for *Cryptococcus* from pulmonary infection

Cell lysis technique	Lysis/sample buffer	Outcome/Comments
Ultrasonication	1% SDS	• No cell lysis
Ultrasonication	1% C7BzO, 7 M urea, 2 M thiourea, 40 mM tris	• No cell lysis
Boiling	1% SDS	• No cell lysis
Bead beating	1% SDS	• No cell lysis
Beat beating	1% C7BzO, 7 M urea, 2 M thiourea	• Standard method for cultured material • No cell lysis
Liquid nitrogen + bead beating	1% C7, 7 M urea, 2 M thiourea	• No cell lysis
Chemical	DMSO	• Common method of *Cryptococcus* decapsulation • No detected decapsulation
Enzymatic	Glucanex	• No detected decapsulation
Lyophilisation + bead beating	1% C7BzO, 7 M urea, 2 M thiourea, 40 mM tris	• Cell lysis achieved • Large amount of non-protein contamination generated • Samples not suitable for proteomics analysis platforms
Lyophilisation + bead beating + acidic extraction	1% C7BzO, 7 M urea, 2 M thiourea, 80 mM citric acid	• Cell lysis achieved • Acidic extraction unable to remove non-protein contamination • Samples not suitable for proteomics analysis platforms
Lyophilisation + bead beating + phenol extraction	1% C7BzO, 7 M urea, 2 M thiourea, 40 mM tris followed by phenol extraction	• Cell lysis achieved • Phenol extraction removed significant amounts of non-protein contaminant • Samples suitable for proteomics analysis platforms

3.3.3. Lyophilisation prior to mechanical disruption is essential for the disruption of *Cryptococcus* cells from pulmonary infection

Finding the most suitable cellular disruption technique for *Cryptococcus* cells isolated from pulmonary infection required significant trial and error. It was determined that *Cryptococcus* cell lysis required drying and shrinking of the capsular polysaccharide structure via lyophilisation. Lysis was then achieved using bead beating with 3 mm glass beads (figure 3.4).

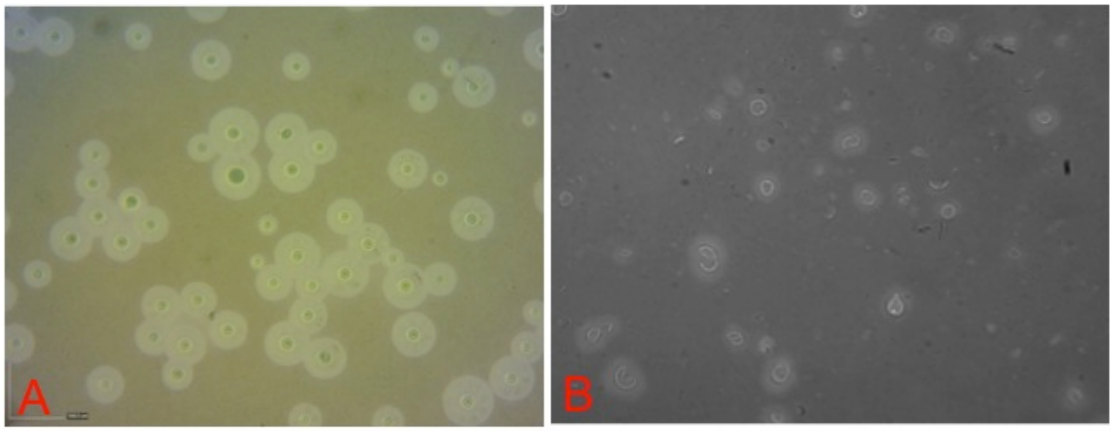

Figure 3.4: A) Hydrated *C. gattii* cells isolated from late stage pulmonary infection; B) the same cells post lyophilisation and beat beating.

Image B shows the broad spectrum of cellular disruption evident post lyophilisation and beat beating, from complete cellular destruction to intact cells. Image B also shows the high level of cellular debris post lyophilisation and bead beating.

3.3.4. Phenol extraction for cultured *Cryptococcus*

Cellular disruption using lyophilisation coupled with bead beating generated large amounts of non-protein contaminants with the 2-D PAGE gel image showing poor protein migration/separation during IEF coupled with significant vertical streaking. (figure 3.5A). Phenol is one of the strongest protein-polysaccharide dissociating agents [249] and initial experiments with cultured *Cryptococcus* indicated that phenol could prove to be an effective sample preparation technique for *Cryptococcus* from pulmonary infection. Phenol protein extraction ameliorated the inhibitory effects non-protein contaminants, improving protein separation during IEF and eliminating the majority of vertical streaking. These experiments also indicated that LiCl, the agent used by Jobbins *et al.* to dissociate protein from non-protein contaminants [232], is

not required as a dissociating agent when using phenol protein extraction (figures 3.5B and 3.5C).

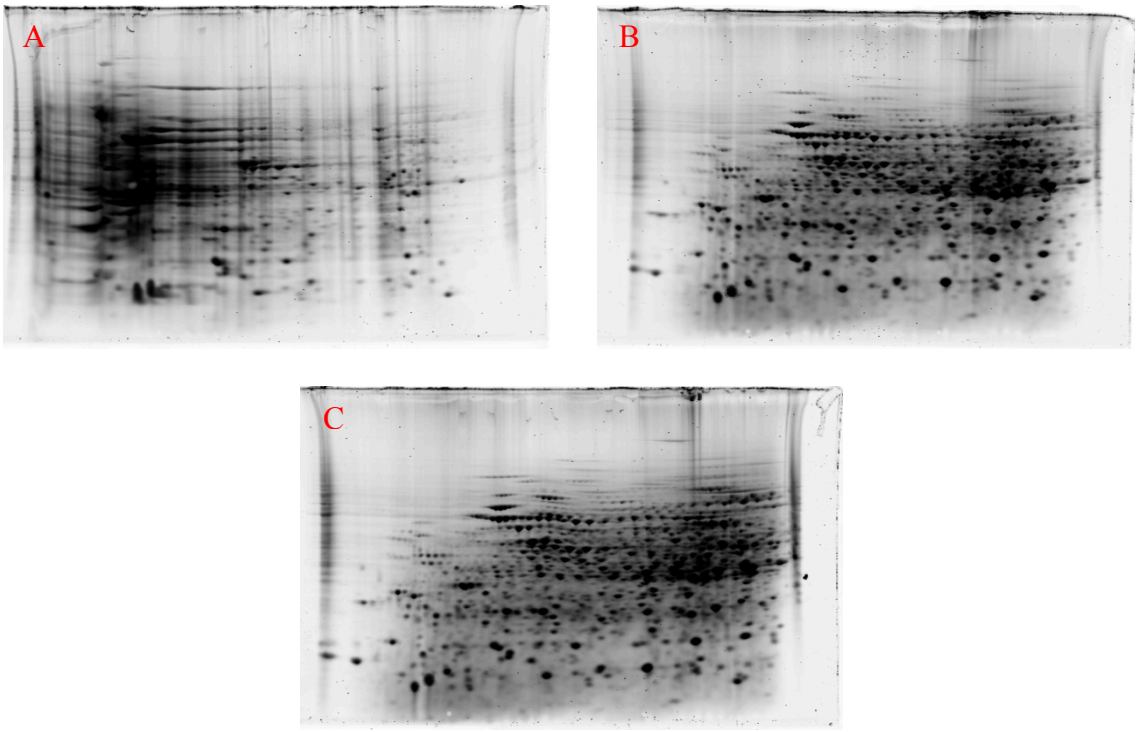

Figure 3.5: 2-D PAGE gel images showing the separation of proteins obtained from *C. gattii*.

A) Cultured *C. gattii* cells prepared using standard alkaline protein extraction; B) cultured *C. gattii* prepared using phenol protein extraction without 50 mM LiCl; and C) cultured *C. gattii* prepared using phenol protein extraction with 50 mM LiCl. There are no observable differences between the migration/separation of proteins in B and C.

3.3.5. Phenol protein extraction of *Cryptococcus* cells obtained from pulmonary infection

The results of lyophilisation followed by bead beating and phenol protein extraction of *Cryptococcus* cells from pulmonary infection is shown in figure 3.6. While not

completely removing the non-protein contamination (observable as inhibited protein migration in figure 3.6C), phenol protein extraction was able to improve protein migration and separation for 1-D SDS-PAGE to the extent that mass spectrometry could be attempted.

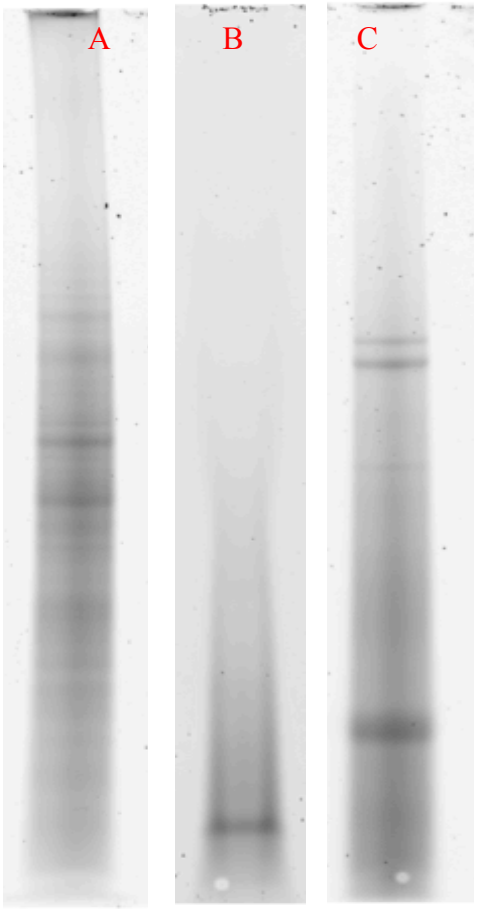

Figure 3.6: 1-D SDS-PAGE gel images of *C. gattii* proteins.

1-D SDS-PAGE gel image of proteins from A) cultured *C. gattii* and B) *C. gattii* obtained from pulmonary infection prepared using the techniques developed by Jobbins *et al. (2010)*. C) *C. gattii* obtained from pulmonary infection prepared using phenol protein extraction. This set of images demonstrates that the techniques developed by Jobbins *et al. (2010)* are ineffective for *in vivo* sample types and that phenol protein extraction improves protein migration, separation and resolution.

3.3.6. Exopolysaccharides in pulmonary supernatants

Pulmonary infection with *Cryptococcus* resulted in the generation of large amounts of exopolysaccharides, which are secreted into the pulmonary spaces. This non-protein contaminant must be accounted for prior to the iTRAQ analysis of pulmonary proteins. It was determined that the application of acidic protein extraction, coupled with 100 kDa MWCO filtration, was readily applicable to this sample type and effectively removed the non-protein contaminant (figure 3.7).

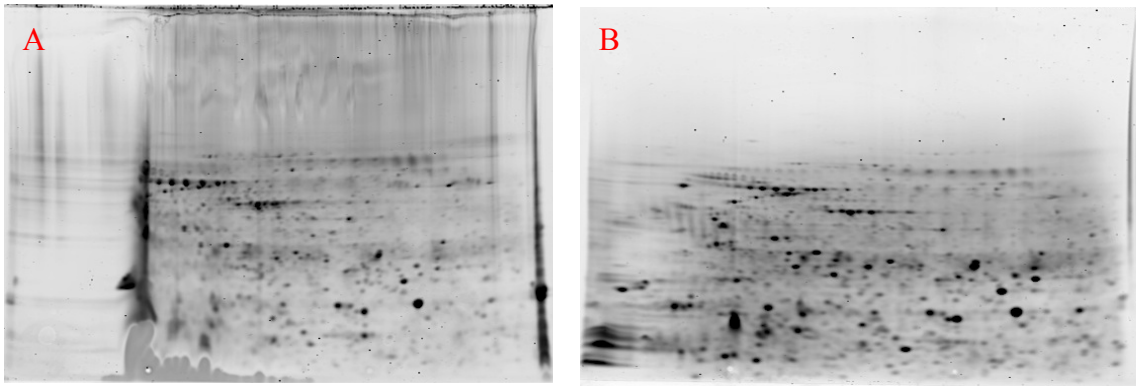

Figure 3.7: 2-D PAGE images showing separated lung proteins from rats infected with *C. gattii* R265 (late stage infection).

Prepared with A) standard alkaline extraction protocol plus treatment with 50 mM LiCl and 100 kDa MWCO filtration and B) acidic extraction protocol plus treatment with 50 mM LiCl and 100 kDa MWCO filtration. A) shows the presence of non-protein contamination, observable as inhibited IEF in the acidic portion of the gel. B) shows that the inhibition of IEF inhibition has been rectified.

3.3.7. 2-D PAGE Western blot complexity issues

The Western blots generated by this study were far more complex than those generated by a similar study conducted by Jobbins *et al. (2010)*. This introduced

difficulties during the alignment of protein spots of interest across the three protein visualisation formats (figure 3.8). Ultimately the result was the re-evaluation of the experimental design for this element of the study.

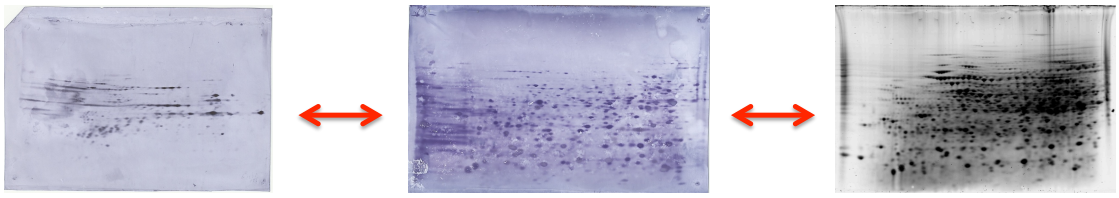

Anode membrane – transferred proteins probed with primary & secondary antibody - colorimetric development

Cathode membrane – transferred proteins stained with Direct Blue 71

2-D PAGE image – stained with Flamingo fluorescent protein stain

Figure 3.8: Representative Western blot showing complexity of protein spots.

This complexity caused difficulties when attempting to align specific protein spots across the three elements of the 2-D PAGE Western blot detection system.

3.3.8. Non-specific binding does not cause 2-D PAGE Western blot complexity

To ensure that the complexity of spots on the 2-D PAGE Western blots was not caused by non-specific binding the Western blot protocol was repeated without primary antibody (figure 3.9). The negative detection of any proteins post secondary antibody incubation and colourimetric development indicated that non-specific binding is not the cause for the observed 2-D PAGE Western blot complexity.

Figure 3.9: Anode membrane generated following the previously described Western blot (section 3.2.8.) protocol without primary antibody.

Negative protein detection indicates that the secondary antibody is not suffering from non-specific binding.

3.4. Discussion

3.4.1. Issues with the proteomic investigation of pulmonary infections

In the simplest terms proteomics can be defined as the context driven search for protein purity. This is a difficult pursuit with regard to *in vivo* infectious diseases, and pulmonary infection with *Cryptococcus* proved particularly challenging. The initial concern in preparing *Cryptococcus* cells from pulmonary infection was the separation of the fungal sample from the host material, and vice versa, prior to independent protein identification. Previous work presented in the NHMRC grant application for this study demonstrated that host proteins can be removed from intact *Cryptococcus* cell obtained from murine pulmonary infection in less than 30 minutes using an Ultra-turrax blender and 1% C7BzO, 7 M urea, 2 M thiourea, 40 mM tris buffer (figure

3.10) [3]. The use of repeated Ultra-turrax washes represents a very aggressive method of host protein removal. For this study, the physicochemical nature of the *Cryptococcus* capsule was exploited, as the increase in capsule size as a result of pulmonary infection, coupled with the generally low-density nature of the capsule, reduced the mass per unit volume ratio of the cell. In comparison, the residual lung material post homogenisation was tightly bound dense connective tissue. Thus, the overall density of the *Cryptococcus* cells was lower than that of the remnant pulmonary tissue. A density cushion (sucrose at a density of approximately 1.2 g/cm^3), which inhibited the passage of fungal cells but permitted the pelleting of the denser connective tissue during low speed centrifugation, was effective for separating the two sample types from each other (figure 3.3). This procedure was gentler on the *Cryptococcus* cells than the technique described in the NHMRC grant and also proved to be faster, approximately 15 minutes as opposed to 30 minutes for repeated Ultra-turrax washes.

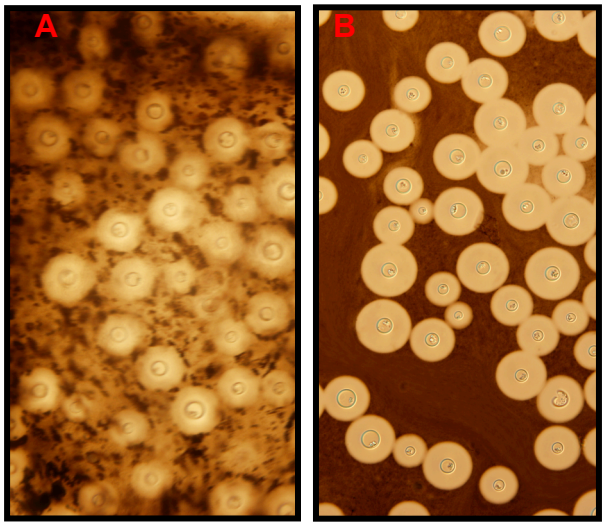

Figure 3.10: Removal of lung tissue using an Ultra-turrax to wash the *Cryptococcus* cells.

A) 1st extraction with residual lung material; B) pure intact *C. gattii* cells after 5th extraction (from [3]).

3.4.2. Development of an efficient protocol for *in vivo Cryptococcus* cell lysis

Taking into consideration the effect that experimental procedures have on sample proteomes is paramount for comparative and quantitative proteomic analyses. Minimal sample manipulation is essential for the most accurate comparative proteomic data. Unfortunately, this proved to be extremely difficult for the *Cryptococcus* cells obtained from pulmonary infection. The major complicating factor was the physiochemical nature of the *Cryptococcus* polysaccharide capsule and its dynamic response to pulmonary infection, resulting in a drastic increase in capsule volume. The capsule resulted in three major challenges to protein isolation and purification: increased structural integrity of the *C. gattii* cells; non-protein contamination and associated problems with 2-D PAGE and 1-D SDS-PAGE resolution; and the direct binding and depletion of cryptococcal proteins.

3.3.3. Cellular disruption techniques

A number of cell lysis techniques were experimentally investigated with limited success (Table 3.6), including the cell lysis technique developed for cultured *C. gattii* by Jobbins *et al. (2010)*. Jobbins *et al. (2010)* used bead beating in 2-D PAGE sample buffer coupled with ultra-sonication to achieve efficient cell disruption of cultured *Cryptococcus* cells [232]. This methodology proved to be completely inadequate for *Cryptococcus* obtained from pulmonary infection. A more aggressive cell disruption technique than that utilised by Jobbins *et al. (2010),* or sample pre-treatment to partially or totally decapsulate cells prior to cell disruption, was required. Dimethyl

sulfoxide (DMSO), a polar aprotic solvent that dissolves both polar and nonpolar compounds, has been previously found to remove a significant portion of the *Cryptococcus* polysaccharide capsule [250]. The removal of capsular polysaccharides with DMSO requires fungal cells to be incubated at room temperature for at least an hour, which ultimately kills the cells [96, 250, 251]. However, the resulting effects of the conditions necessary for decapsulation with DMSO on the proteome far outweigh any decapsulation that may be achieved. Additionally, DMSO decapsulation proved to be completely ineffective for *Cryptococcus* obtained from pulmonary infection (data not shown).

Maxson *et al. (2007)* estimated that water could account for approximately 95% of the weight of the polysaccharide capsule of *C. neoformans* cells grown under capsule inducing conditions [252]. High water retention is a result of the acidic nature of the polysaccharide structure, imparted by the high content of glucuronic acid. Maxson *et al. (2007)* also established that the capsule was not a rigid boundary but is in fact compressible, thus capsule has the ability to absorb the shear forces created by mechanical disruption techniques. The compressible nature of the capsule, coupled with its extremely large size during pulmonary infection, explains why this sample type was highly resistant to mechanical cellular disruption.

Dehydration of the capsule, via lyophilisation, resulted in the loss of its compressible nature, enabling mechanical cellular disruption via dry bead beating. While hydrated cells were uniformly unaffected by bead beating, the lyophilised sample exhibited a heterogeneous cell population (figure 3.2). Cellular integrity ranged from minimally damaged cells, to cells broken in half, to cells with varying degrees of capsule loss, to cells exhibiting complete fragmentation. Whilst not achieving 100% cell disruption,

lyophilisation followed by dry bead beating represents the most effective cellular disruption technique for *Cryptococcus* obtained from pulmonary infections attempted to date.

3.4.4. Contaminating capsular polysaccharides

For cultured *C. gattii* sample preparation, Jobbins *et al.* determined that standard protein extraction protocols resulted in the loss of high molecular weight proteins and significant streaking in the acidic portion of 2-D PAGE [232]. These results were attributed to the inability of standard extraction/sample preparation methods to deal with the large volumes of polysaccharide capsular material inherent to the *Cryptococcus* sample type, the components of which are small enough to enter IPG strips. Solubilised polysaccharides pose a major problem for IEF. They behave as polyanions, which are capable of binding proteins via electrostatic interactions [253]. The result is significant horizontal streaking at the acidic end of the 2-D PAGE gel. Obtaining the most complete snapshot of the *Cryptococcus* proteome requires the disassociation of proteins from capsular material and the subsequent removal of the capsular material from the sample.

In 1888 Franz Hofmeister defined the series of anions and cations, known as the Hofmeister or lyotropic series, in order of their ability to change water structure via interactions between ion-protein and ion-water [254]. Anions have a larger effect than cations, and ions later in the series increase the solubility of non-polar molecules while ions earlier in the series decrease their solubility [255, 256]. Jobbins *et al. (2010)* found that lithium chloride (LiCl) was best at disrupting protein-capsule

interactions for cultured *Cryptococcus* samples, increasing the representation of high molecular weight proteins and improving total protein yield [232]. Lithium ions and chloride ions both appear towards the middle of the Hofmeister series for cations and anions respectively. As a result the use of this compound did not skew the data towards polar or non-polar proteins. Jobbins *et al. (2010)* concluded that the use of LiCl to disrupt the electrostatic interactions between protein and polysaccharide followed by 100 kDa molecular weight cut off (MWCO) filtration to remove capsular fragments eliminated the majority of artifacts from the acidic end of 2-D PAGE.

This protocol proved ineffective at eliminating the vast amount of contaminants produced by the mechanical disruption of lyophilised *Cryptococcus* from pulmonary infection. For *in vivo* cells the capsule accounts for the majority of cell volume and mass. Furthermore, the physiochemical nature of the *in vivo* polysaccharide capsule, which is produced under nutrient and oxidative stress, is far more complex than the capsule produced following growth in rich culture media. Capsular enlargement results from the addition of new polysaccharide molecules near the capsule edge [96, 257-259]. This mode of enlargement means the architecture of the capsule consists of multiple zones defined by their relative polysaccharide density, with the densest zone closest to the cell and decreasing with distance from the cell [96, 258]. It is therefore possible that as well as more capsular material overall, the *Cryptococcus* cells from pulmonary infection had larger amounts of polysaccharide subtypes that more readily and strongly associated with protein. This may have rendered LiCl ineffective at disassociating proteins from capsule.

3.4.5. Dissociating *Cryptococcus* capsule and proteins from pulmonary infection requires the stronger dissociating agent Phenol

Phenol is the simplest aromatic alcohol, containing a polar (OH) group bound to an aromatic ring [260]. Phenol selectively solubilizes proteins, having little tendency to dissolve polysaccharides and nucleic acids. In addition to its selectivity as a solvent, phenol is one of the strongest dissociating agents for decreasing the molecular interaction between proteins and non-proteins [249]. The phenol protein extraction protocol was initially developed to deproteinise carbohydrates and became the standard procedure for removal of proteins from nucleic acid samples [261]. Hurkman and Tanaka *(1986)* were the first to discuss phenol extraction for proteomic studies [262]. This study, along with later studies conducted by Carpentier *et al. (2005)* [249] and Saravanan and Rose *(2004)* [263], established that phenol extraction was highly efficient at removing nucleic acids and other carbohydrate non-protein contaminants from protein extractions. The use of phenol extraction for protein samples has the added advantage of minimizing protein degradation via the denaturation and deactivation of endogenous proteolytic enzymes.

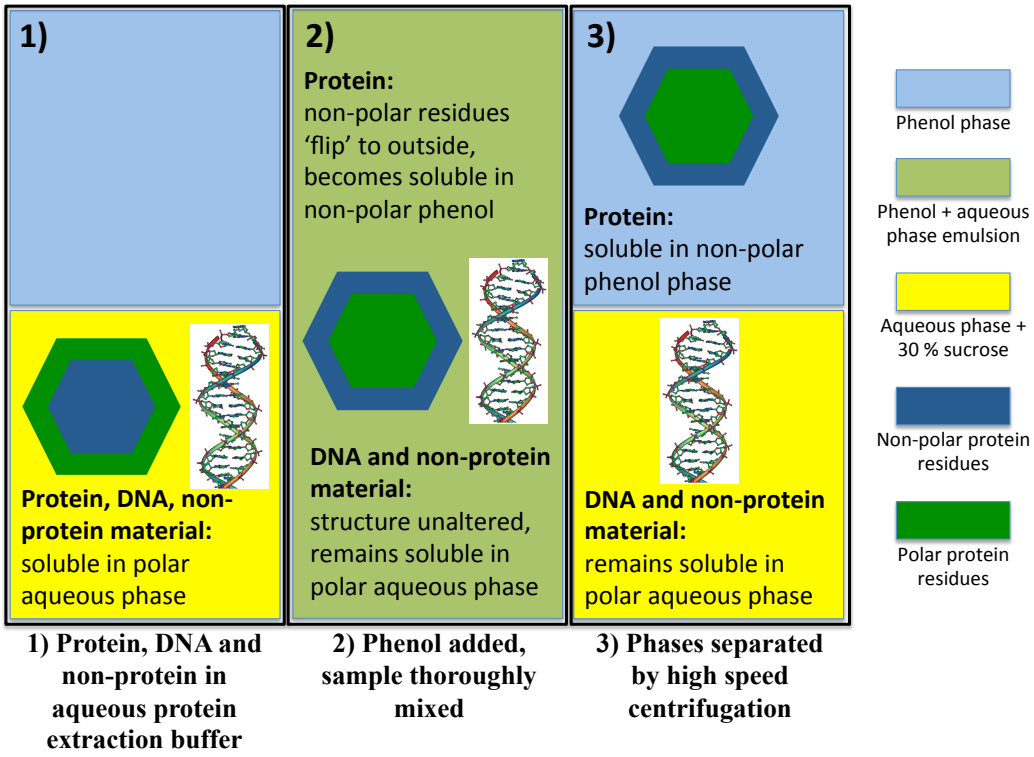

Figure 3.11: Phenol protein extraction protocol.

The phenol protein extraction protocol is based on a two-phase partition principle (figure 3.11). The protocol couples the ability of phenol to selectively solubilize proteins with the immiscible nature of phenol (the organic phase) and water (the aqueous phase) to isolate protein from non-protein contaminants. Phenol causes proteins in the aqueous layer to denature via hydrogen bond interactions, effectively forcing the non-polar residues to the outside of the protein structure. It is this protein denaturation that is key to the successful isolation of protein from carbohydrates. The proteins become soluble in the phenol phase and less soluble in the aqueous phase while, crucially, the polar carbohydrate molecules remain in the polar aqueous phase.

3.4.6. Phenol protein extraction for *in vitro Cryptococcus*: a litmus test

Preliminary experiments with the phenol protein extraction technique were conducted with *C. gattii* cultured in rich media. While this sample type is not indicative of the issues encountered with cells from pulmonary infection, coupled with 2-D PAGE it provided an effective diagnosis of the ability of phenol protein extraction to remove non-protein contaminants. 2-D PAGE is highly sensitive to non-protein contaminants (e.g. cell wall, polysaccharide, DNA etc.) [232]. Thus, a gross assessment of the efficiency of protein purification via phenol protein extraction can be judged on the quality of 2-D PAGE gel images.

Comparison of the control gel image with that of the phenol protein extraction gel images indicates the potential of phenol protein extraction as a suitable sample preparation technique for *Cryptococcus* from pulmonary infection (figure 3.5). The control gel, prepared via standard alkaline extraction procedures without the inclusion of a disassociating agent or MWCO filtration, was of poor quality. This gel exhibits clear indications of polysaccharide contamination, observable as an acidic bias of protein migration and significant vertical and horizontal streaking. The acidic bias of protein separation results from the association of poly-anionic polysaccharides with the proteins in the sample. This association alters the natural pI of the proteins to a more acidic one, thus the observed bias of “acidic” proteins. The application of phenol protein extraction resulted in an amelioration of the acidic bias of protein migration along with an improvement in overall protein separation and resolution for cultured *Cryptococcus*. This improvement was achieved without the use of MWCO filtration, which was previously considered essential for *C. gattii* samples. It was also interesting to observe that the inclusion or exclusion of the disassociating agent LiCl

appeared to have no observable effect on the quality of protein separation by 2-D PAGE. The drastic improvement in gel image quality without the use of LiCl or MWCO filtration indicates that phenol protein extraction far exceeds the capability of the techniques developed by Jobbins *et al. (2010)* to isolate protein from non-protein contaminants and to subsequently remove these contaminants.

3.4.7. Phenol protein extraction for *in vivo Cryptococcus*

1-D SDS-PAGE was used as a diagnostic to determine the efficiency and effectiveness of phenol protein extraction to purify *Cryptococcus* from pulmonary infection. While not as sensitive to non-protein contaminants as 2-D PAGE, the key advantage of 1-D SDS-PAGE is that this technique requires significantly lower protein loads than 2-D PAGE. The application of *Cryptococcus* from pulmonary infection to 2-D PAGE would require the use of an entire infected lung sample per 2-D PAGE run. This would eliminate the use of the sample for alternative proteomic investigations (i.e. iTRAQ) if phenol protein extraction proved effective.

The 1-D SDS-PAGE image of *C. gattii* from pulmonary infection prepared using the techniques developed by Jobbins *et al. (2010)* demonstrates an inhibition and distortion of protein migration (figure 3.6B). This indicates that the sample preparation techniques utilized by Jobbins *et al. (2010)* are inadequate for the highly contaminated *in vivo* samples. Applying the phenol protein extraction protocol to the *in vivo* sample resulted in the marked improvement in protein separation (figure 3.6C). While not completely removing the smearing associated with non-protein contamination the application of phenol protein extraction increased the total number

of protein bands observable and limited the degree of distortion observable in the gel lane. Additionally, phenol protein extraction ameliorated non-protein contamination to the extant that the cryptococcal proteins obtained following pulmonary infection were pure enough to be applied to mass spectrometric protein identification (see chapter 4).

3.4.8. Exopolysaccharides in the lung material

During culture, and especially during infection, *C. neoformans* and *C. gattii* continuously release soluble capsular material, termed exopolysaccharide, into the culture media [111]. While *in vitro* conditions stimulate capsule production, the extent of capsular development is much reduced compared to that observed during pulmonary infection. It is likely that, in accordance with an observable increase in capsular production, a vast amount of capsular material is released during pulmonary infection.

The existing sample preparation protocols [232] were unable to eliminate the non-protein contaminant associated with the pulmonary sample type. As with the cryptococcal proteins, application of extracted pulmonary proteins to 2-D PAGE resulted in the inhibition of IEF in the acidic portion of the gel (figure 3.7A). This is a result of acidic proteins remaining associated with soluble exopolysaccharides that were able to pass through the 100 kDa MWCO filters. The removal of soluble exopolysaccharide required the use of acidic protein extraction [253]. Acidic protein extraction exploits the principle that material close to or at its pI is at its lowest solubility and can be removed from solution via high-speed centrifugation. Acidic

protein extraction is readily applicable to the contaminated pulmonary protein sample as capsular polysaccharides act as poly-anions. Changing the pH buffer used during homogenisation from 40 mM tris (alkaline, pH ≈ 8) to 80 mM citric acid (acidic pH ≈ 3) and increasing the duration of high-speed centrifugation to 20 minutes improved isoelectric focusing in the acidic portion of 2-D PAGE and eliminated the majority of vertical streaking (figure 3.7B). Reducing the pH of the pulmonary protein sample had the added advantage increasing the solubility of the majority of the pulmonary proteins in the sample, increasing total protein yield.

3.4.9. 2-D PAGE Western blot analysis

The identification of experimentally relevant protein spots via 2-D PAGE Western blot analysis required the alignment of individual protein spots across the three protein visualisation formats. A protein identified on the anode membrane probed with antibody must align with its corresponding protein on the cathode membrane and finally with its corresponding protein on the 2-D PAGE image prior to protein spot excision, trypsin digestion and identification via mass spectrometry (figure 3.8). Despite utilising automated systems (PDQuest, Bio-Rad, USA)) and manual techniques the accurate alignment of the three aspects of the 2-D PAGE western detection system proved problematic. The primary source of the difficulties was a higher than expected complexity of the Western blots (figure 3.8).

Jobbins *et al. (2010)* successfully identified 37 unique cryptococcal proteins from sera obtained from Koalas presenting with clinical cryptococcosis. The 2-D PAGE Western blots presented by Jobbins *et al. (2010)* exhibited approximately ten

identifiable protein spots per anode membrane. In comparison, the work presented in this study detected hundreds of protein spots per anode membrane, for both control and disease samples. At first it was suspected that the high number of detectable protein spots was the result of non-specific secondary antibody binding, however, probing with secondary antibody in the absence of prior primary antibody resulted in no protein detection (figure 3.9). The differences in observable protein spots is most likely a result of the differences in the protocols utilised by Jobbins *et al. (2010)* and by this study to generate the 2-D PAGE Western blots.

Jobbins *et al. (2010)* were forced to utilise a three-step detection system (primary, secondary and tertiary antibodies) for their koala infection model as alkaline phosphatase-conjugated anti-koala IgG is not commercially produced. In their study, following incubation with the koala sera, the anode membrane was incubated with an intermediate rabbit anti-opossum IgG antibody that was then followed by incubation with alkaline phosphatase-conjugated anti-rabbit IgG [232]. In contrast, the current study using a rat model was able to use the commercially available alkaline phosphatase-conjugated anti-rat IgG antibody and did not require an intermediate secondary antibody.

In terms of taxonomic hierarchical classification opossums and koalas are species from the same Kingdom (Animalia), Phylum (Chordata), Class (Mammalia), Infraclass (Marsupialia) but are from different Orders (koala: Diprotodontia, opossum: Didelphimorphia). It is likely that the use of an antibody generated in a species that is similar but not identical to that of the species being analysed would result in both false positives and false negatives during 2-D PAGE Western blot analysis. Hence the intermediate anti-opossum antibody used by Jobbins *et al. (2010)*

to detect koala protein is a likely cause for the lower number of detected proteins compared to this study.

In addition to protein alignment issues, Western blots could not be completed for rats infected with KN99α for this study. These rats were in such poor health that extracting enough blood to generate the required volume of serum for 2-D PAGE Western blots analysis proved impossible. Together, the technical limitations associated with the 2-D PAGE Western blot detection system forced a reassessment of the direction of this study to a more applicable detection system (see chapter 6).

3.5. Conclusions

This aim of this aspect of the thesis was to describe the technical issues and limitations encountered during this study and to highlight the progress made in protocol development that eventually ameliorated these significant technical difficulties. The majority of the technical difficulties encountered during this study were associated with the physiochemical nature of the capsular polysaccharides and exopolysaccharides that are inherent to *Cryptococcus* obtained from pulmonary infection. This study determined that cellular disruption via lyophilisation followed by dry bead beating and sample preparation using phenol protein extraction is most effective for *Cryptococcus* samples, including for cells obtained from pulmonary infection. Additional experimental investigation is required to improve protein purity in order to apply *Cryptococcus* from pulmonary infection to comparative proteomics techniques. Inhibited protein migration post-phenol protein extraction indicates that non-protein contaminants remain in cryptococcal protein samples obtained from

pulmonary infection (figure 3.6). The effect that these non-protein contaminants have on iTRAQ and other comparative proteomic techniques remains enigmatic. This study, however, has proven that such an endeavour may be possible and has made advancements towards this goal. An effective acidic protein extraction technique to reduce exopolysaccharide contamination of infected pulmonary protein samples was also identified. However, the application of phenol protein extraction to this sample type could prove to be more effective than acidic protein extraction at removing non-protein contaminants. The use of phenol protein extraction would also remove the requirement of 100 kDa MWCO filtration, which was time consuming and possibly inhibited the detection of high molecular weight proteins. Unfortunately the work conducted on the lung proteome was completed prior to the commencement of experimentation focused on *Cryptococcus* sample preparation that resulted in the development of the phenol protein extraction procedure. This study also found the systemic analysis of the host response to infection via 2-D PAGE Western blot analysis to be far more complicated than observed in previous studies. Consequently, the Bio-Plex suspension array system was used instead of Western blotting (see Chapter 6).

Chapter Four

Comparative proteomics of *Cryptococcus*

One of the major aims of this PhD thesis was to compare clinically significant strains of Cryptococcus *from* in vitro *and* in vivo *sources using quantitative proteomic techniques. The elucidation of the quantitative protein differences between cultured cells and cells obtained from pulmonary infection was expected to shed light on the biological processes of* Cryptococcus *pathogenesis at the molecular level. The technical challenges related to cell lysis and protein extraction from* Cryptococcus *obtained from pulmonary infection have been documented in Chapter 3. As a result of these challenges, the focus of this study shifted to performing qualitative mass spectrometry to compare the proteomes of cultured* Cryptococcus *cells and cells obtained from pulmonary infection. The results of this study indicate that future quantitative experiments with* Cryptococcus *from* in vivo *infections are achievable, although further protocol development will be required (see Chapter 3). Time limits restricted the focus of this study to* C. gattii*, which has been classified as a highly virulent primary pathogen. Despite limitations, this study detected a number of theoretically low abundance proteins from* Cryptococcus *obtained from pulmonary infection that are relevant to fungal pathogenesis.*

4.1. Introduction

Quantitative genomic and proteomic approaches are utilised to capture and monitor an organism's transcriptional and translational outputs, respectively. These methods permit the elucidation of a pathogen's response to varying external conditions via the simultaneous quantitative analysis of numerous genes or proteins. As fungal virulence is a multifactorial process, these approaches are particularly valuable for identifying the integrated expression of the different factors involved in the infection process. Transcriptional approaches have been applied to a number of fungal pathogens and significantly up- and down-regulated genes have been identified as potential virulence factors [1, 264-267].

The proteome-based investigation of human-pathogenic fungi, such as *C. albicans*, *A. fumigates, P. boydii* and *C. neoformans* [7, 268, 269], is a growing area of interest. A significant constraint to proteomics technologies is their limited ability to detect and quantify low abundance proteins. Ghaemmaghami *et al. (2003)* demonstrated that the range of protein expression for *Saccharomyces cerevisiae* proteins expressed during normal growth was from fewer than 50 to more than 10^6 molecules per cell [212]. Low abundance proteins can be detected, down to hundreds of copies per cell, but fractionation coupled with milligram amounts of starting material are usually required in these cases. This amount of protein is rarely obtainable for *in vivo* studies using rat infection models. Pedersen *et al. (2003)* demonstrated that low abundance proteins make up approximately 80% of the yeast proteome [203]. The phylogenetic distance between *Cryptococcus*, a basidiomycete, and *Saccharomyces*, a ascomycete [270], questions whether *Saccharomyces* protein expression values represent a true reflection of the protein expression levels in *Cryptococcus*. Despite this, the studies by

Ghaemmaghami *et al. (2003)* and Pedersen *et al. (2003)* indicate that it is likely that a number of potentially interesting low abundance proteins will remain undetected by global proteomic investigations.

Missall *et al. (2004)* published the first global examination of the *Cryptococcus* proteome. Their study used differential 2-D PAGE in an attempt to elucidate the proteins required for *C. neoformans* growth at high temperatures (37 °C). Missall *et al. (2004)* determined that the thiol peroxidases Tsa1 and Tsa3 were increased in expression at 37 °C and found Tsa1 is vital for growth of *C. neoformans* at high temperatures [80]. Since the Missall *et al. (2004)* study there have been a growing number of published studies analysing the *C. neoformans* proteome, however, it was not until recently that the *C. gattii* proteome was investigated. Jobbins *et al. (2010)* published the first examination of the global proteome of cultured *C. gattii*. Their study used immunoproteomics, 2-D PAGE Western blotting, to elucidate the key proteins and pathways involved in early and late stage *C. gattii* pathogenesis using the naturally occurring koala model of cryptococcosis [232]. The authors hypothesised that the disease-associated antigens that were identified could form future targets for therapy or be useful diagnostic biomarkers and indicators of prognosis. The detection and identification of 31 disease-associated antigens, in this case cryptococcal proteins, required the generation of novel sample preparation protocols. Similarly, Martins *et al. (2013)* identified 68 immunoreactive *C. gattii* proteins using 2-D PAGE Western blotting, a number of which were identified as potential targets for the development of immunodiagnostic tools for cryptococcosis [271]. Chong *et al. (2012)* used the *C. gattii* sample preparation techniques developed by Jobbins *et al. (2010)* to investigate the global response of cultured *C. gattii* to fluconazole treatment using a 1-D SDS-PAGE 2-D nanoLC ESI MS/MS approach [272]. Their study hypothesised that fungal

proteins identified to be involved in the response to the fluconazole antifungal agent might be useful targets in future therapeutics. Crestani *et al. (2012)* investigated *C. gattii* protein expression during culture with varied levels of iron. Using multidimensional protein identification technology (MudPIT) and differential display 2-D PAGE Crestani *et al. (2012)* found that iron deprivation affected capsule production, cAMP-signalling pathway, response to stress and metabolic pathways related to mitochondrial function [273].

These studies attempt to elucidate potential therapeutic and diagnostic markers using *in vitro* experimental models that are far removed from the reality of infection with *Cryptococcus*. While these *in vitro* studies have been able to identify proteins and pathways of relevance to the *Cryptococcus* cell, to date, no study has attempted the analysis of how *Cryptococcus* regulates protein expression in the process of *in vivo* infection. The aim of this study was to compare the proteome of *Cryptococcus* during saprophytic growth to the proteome generated during pulmonary infection using global comparative proteomic techniques. The underlying hypotheses of the study were that:

- Fungal growth in the pulmonary environment would induce specific protein changes in the intracellular proteome of *Cryptococcus*
- Comparative proteomic analyses would identify these specific proteins highlighting:
    - The proteins that permit *Cryptococcus* to overcome host immune responses and establish disease.
    - The proteins that could form future targets for therapy or be useful diagnostic biomarkers and indicators of prognosis.

4.2. Methods

4.2.1. *In vitro* growth conditions

The *in vitro* growth conditions used were described in section 2.3.1.

- Note: only *C. gattii* (R265) cells were used for this study.

4.2.2. Pulmonary infection model

The pulmonary infection model used was described in section 2.3.2.

- Note: The *C. gattii* (R265) cells used for this study were obtained from late stage infection (42 days post infection).

4.2.3. Pulmonary tissue homogenisation

Pulmonary tissue homogenisation was completed using the method described in section 2.3.3.

4.2.4. Isolation of *Cryptococcus* from pulmonary tissue and lyophilisation of *Cryptococcus*

Cryptococcus cells were isolated from pulmonary tissue and lyophilised using the methods described in section 2.3.4.

4.2.5. *In vitro*/*in vivo Cryptococcus* cellular disruption and phenol protein extraction

Cryptococcus cells were lysed and intracellular proteins extracted using the methods described in section 2.3.5.

4.2.6. 1-D SDS-PAGE

1-D SDS-PAGE was completed using the methods described in section 2.3.7.

4.2.7. 1-D SDS-PAGE manual lane excision and trypsin in-gel digestion for mass spectrometry protein identification

Post 1-D SDS-PAGE the sample gel was stained with Coomassie G250 to facilitate the manual cutting of protein lanes. After fixation or Flamingo™ (Bio-Rad, USA) staining, the sample gel was washed for five minutes in ddH_2O in a fixing tray. The ddH_2O was then decanted and Coomassie staining solutions 1 and 2 were added in a 4:1 ratio. The tray was covered and incubated on an orbital shaker (50 rpm) for a minimum of 8 hours. After staining, the gel was de-stained with 1 % acetic acid (v/v) solution until the gel background was clear and the protein bands were clearly defined. Once de-staining was complete an image of the gel was taken with a flatbed scanner.

The de-stained gel was then placed on a clean white light illuminator. Using a printed and labelled image of the gel to be cut, the appropriate gel lanes were excised with a

scalpel. Each gel lane was cut lengthwise into 10 uniformly sized segments. These segments were further cut into ≈1 mm squares and transferred to 0.65 mL Eppendorf tubes. The gel pieces were briefly washed with 100 mM ammonium bicarbonate solution to ensure that the gel pieces were at the correct pH (above pH 8) and were then de-stained by the addition of 400 µL of 50% acetonitrile (ACN) (v/v) in 100 mM ammonium bicarbonate. The samples were vortexed and incubated for 10 minutes and the blue de-stain solution was removed and discarded. This de-staining process was repeated until the gel pieces were thoroughly de-stained. For heavily stained gel pieces complete de-staining was rarely achieved and instead de-staining was repeated until the de-stain solution no longer appeared blue.

The samples were then washed with 200 µL of 100 % ACN to completely dehydrate the gel pieces. The excess ACN was removed and the gel pieces air-dried in a fume hood until the gel pieces appeared shrunken and white. Enough trypsin solution was then added to cover the dehydrated gel pieces. The gel pieces were re-hydrated at 4 °C for a minimum of 30 minutes to limit auto-digestion and ensure that trypsin remained active as it was absorbed into the gel. After rehydration, 100 mM ammonium bicarbonate solution was added to re-cover the gel pieces. The gel pieces were then digested overnight in a 37 °C incubator.

After overnight digestion, the gel pieces were incubated in a sonicating bath for 5 minutes and then centrifuged in a microfuge. The digest supernatant was transferred to a clean 0.65 mL Eppendorf tube. Enough 50 % acetonitrile (v/v) / 2 % formic acid (v/v) solution was then added to cover the gel pieces. The samples were then incubated for 30 minutes with occasional vortexing, incubated for 5 minutes in the sonicating bath and briefly centrifuged in the microfuge. The resulting supernatant

was removed and pooled with the initial digest solution supernatant. This process was repeated once more to ensure maximal peptide extraction from the gel pieces.

The sample digest solutions were vortexed and then placed in a Vacufuge™ Concentrator 5301 (Eppendorf, Germany), with caps off, until completely dry. The samples were resuspended with 10 µL of loading buffer (Buffer A: 5mM phosphate 25% acetonitrile (v/v), pH 2.7) and centrifuged at 16,000 *g* for 10 minutes to remove any extraneous insoluble particulates. 15 µL of each sample was then loaded into auto-sampler tubes for MS processing and subsequent protein identification. Alternatively, samples were stored at -20 °C until MS protein identification could be completed.

4.2.8. Mass spectrometry (completed by the Australian Proteome Analysis Facility at Macquarie University)

Mass spectrometry was completed using the methods described in section 2.3.9.

4.2.9. Codon adaptation index calculation

Codon adaptation index values were calculated using the E-CAI calculator at the following website http://genomes.urv.es/CAIcal/E-CAI/. FASTA sequence (from Uniprot) and the codon usage table and %G+C content (from http://www.kazusa.or.jp/codon/cgi-bin/showcodon.cgi?species=292817) data were entered in the designated fields. Using the Markov method and the alternative yeast genetic code the CAI was automatically calculated.

4.3. Results

4.3.1. Macroscopic observation of rats infected with *C. gattii* R265

Table 4.1: Rat lung weights

Infection time point	Mean control lung weight (±SD)	Mean infected lung weight (±SD)
14 days post infection	0.88 g (0.035)	5.00 g (1.700)
42 days post infection	0.88 g (0.035)	4.79 g (1.676)

Early stage infection: At the 14-day time point rats displayed symptoms typical of cryptococcosis. Rats infected with R265 demonstrated ruffled fur, lethargy and laboured breathing. Infected lungs were greatly increased in size compared to control lungs due to the development of large, multifocal gelatinous lesions (table 4.1). Infected lungs demonstrated extensive consolidation of lung fields, with little normal lung material remaining.

Late stage infection: At the 42 day time-point rats displayed a similar degree of cryptococcosis-associated symptoms as observed at 14 days post infection. Similarly, lung weights, the extent of lesion development and the degree of lung field consolidation were comparable to the observations made at the 14 day time-point, however, the lungs were lighter at 42 days than at 14 days. Figure 4.1 shows lungs and cryptococcal cells isolated from infected rats at 42 days post infection.

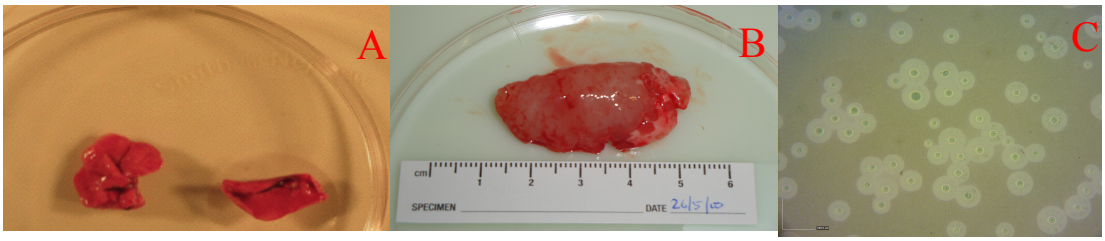

Figure 4.1: Images of uninfected and infected lungs and *Cryptococcus* cells obtained from pulmonary infection.

A) Typical, uninfected Fisher-344 rat lungs; B) Fisher-344 rats lungs at 42 days (late stage infection) post inoculation with 0.1 mL of 10^8 CFU of *C. gattii* R265; C) *C. gattii* R265 cells isolated from pulmonary tissue 42 days post inoculation. Note the drastic physical changes to lung tissue and *Cryptococcus* capsule as a result of pulmonary infection.

4.3.2. *In vitro* and *in vivo Cryptococcus* mass spectrometry results

1-D SDS-PAGE nanoLC ESI MS/MS qualitative proteomics was used to compare proteins expressed by *C. gattii* grown in culture (overnight in YPD broth) versus those expressed by *C. gattii* from late stage of pulmonary infection. This technique identified 1,164 non-redundant *Cryptococcus* proteins expressed in rich medium culture, 114 non-redundant *Cryptococcus* proteins expressed during late stage pulmonary infection and 470 *Rattus norvegicus* proteins co-identified with *Cryptococcus* proteins obtained from cells during late stage pulmonary infection (Table 4.2). Due to the identification of a significantly higher number of *Cryptococcus* proteins from culture than from pulmonary infection, it was hypothesized that any proteins unique to the pulmonary infection sample type would be of significance during infection. Despite using sample preparation methods designed to remove host contaminants from *Cryptococcus* cells obtained from

pulmonary infection, far more *Rattus norvegicus* proteins were identified than *Cryptococcus* proteins. This indicates that sample preparation for *Cryptococcus* cells obtained from pulmonary infection remains a work in progress.

Table 4.2: Mass spectrometric data obtained from cultured *Cryptococcus* and *Cryptococcus* from pulmonary infection

***Cryptococcus* Sample Type**	**Database searched**	**Matched Spectra**	**Distinct Peptides**	**Proteins Detected**
In vitro	*Filobasidiella/Cryptococcus neoformans* species complex	73522	21300	1164
In vivo	*Filobasidiella/Cryptococcus neoformans* species complex	11276	6174	114
In vivo	*Rattus norvegicus*	45238	10640	470

4.3.3. Host proteins co-purified with *Cryptococcus* proteins from pulmonary infection

Table 4.3 represents biologically relevant *Rattus norvegicus* proteins, based on biological function, that were co-purified with *Cryptococcus* proteins obtained from cells from pulmonary infection. The proteins listed in this table exhibit an array of different biological and molecular functions. This indicates that during infection the *Cryptococcus* capsule does not associate with any particular class of proteins but instead appears to bind proteins randomly.

Table 4.3: Biologically relevant *Rattus norvegicus* proteins co-purified with *Cryptococcus* proteins from cells obtained from pulmonary infection

Accession number	Protein name	Function
P08426	Cationic trypsin-3	Involved in the degradation of dietary trypsin inhibitors; the premature activation of mesotrypsinogen could contribute to the pathogenesis of human pancreatitis [274]
O08837	Cell division cycle 5-related protein	Cell cycle regulator important for G2/M transition, acts as a positive regulator of cell cycle G2/M progression
Q3B7D0	Coproporphyrinogen-III oxidase, mitochondrial	Involved in the sixth step of porphyrin metabolism in the haem and chlorophyll biosynthetic pathways
P23965	Enoyl-CoA delta isomerase 1, mitochondrial	Involved in beta-oxidation of unsaturated fatty acids with double bonds at odd-numbered carbon positions.
Q64625	Glutathione peroxidase 6	Catalyses the reduction of hydrogen peroxide and other peroxides, generated during normal metabolism or oxidative stress, to their corresponding alcohols using glutathione as a substrate
P84586	Heterogeneous nuclear ribonucleoprotein G retrogene-like	RNA-binding protein that plays several role in the regulation of pre- and post-transcriptional processes.
Q99PS8	Histidine-rich glycoprotein	Involved in innate immunity, ex vivo, HRG-containing plasma as well as fibrin clots exert antifungal effects. In vivo, Hrg−/− mice were susceptible to infection by C. albicans, in contrast to wild-type mice, which were highly resistant to infection [275]
Q63692	Hsp90 co-chaperone Cdc37	Cdc37is involved in tau (a protein associated with microtubules) stability and perhaps pathobiology by multiple mechanisms [276]
P22791	Hydroxymethylglutaryl-CoA synthase, mitochondrial	An intermediate in both cholesterol synthesis and ketogenesis
D3ZHV2	Microtubule-actin cross-linking factor 1	MACF1 null endodermal cells exhibit defects in microtubule dynamics. MACF1 is important for guiding microtubules on actin filaments. Essential for microtubule rearrangement during trauma/wound healing. [277]
F1LP90	Misshapen-like kinase 1	Is known to regulate cytoskeletal organization and oncogene-induced cell senescence. MINK1 is essential for cytokinesis [278]
Q9Z2J4	Nexilin	Loss of nexilin function induces Z-disk damage and heart failure [279]
B4F7E8	Niban-like protein 1	May play a role in apoptosis suppression, may promote melanoma cell invasion in vitro.

P48679	Prelamin-A/C	Implicated in various functions, including nuclear stability, transcriptional control, cell cycle regulation, nucleo-cytoplasmic interplay, cellular signalling, and heterochromatin dynamics[280]
Q63639	Retinal dehydrogenase 2	Vitamin A (retinol) is a critical factor in protective immunity, retinol synthesis is dependent on the three retinal dehydrogenases (Raldh1-3) [281]
Q62868	Rho-associated protein kinase 2	Involved in regulating the shape and movement of cells by acting on the cytoskeleton, regulates actin filament organisation and contractility
P04774	Sodium channel protein type 1 subunit alpha	Essential for the generation and propagation of action potentials, chiefly in nerve and muscle.
Q9ERH3	WD repeat-containing protein 7	Perform a wide range of cellular functions including; signal transduction, RNA synthesis/processing, chromatin assembly, vesicular trafficking, cytoskeletal assembly, cell cycle control and apoptosis [282].

4.3.4. Proteins 'unique' to *Cryptococcus* cells obtained from pulmonary infection

Table 4.4 lists the biologically relevant proteins identified from *Cryptococcus* cells obtained from pulmonary infection that were not identified from cultured *Cryptococcus*. The majority of these proteins were found to have functions relevant to fungal pathogenesis. Where possible the likely abundance of these proteins, expressed as protein molecules per cell, was estimated by cross-referencing protein homologs to the *Sacchromyces* protein abundance work completed by Ghaemmaghami *et al. (2003)* [212].

Table 4.4: Biologically relevant *in vivo Cryptococcus* proteins

Accession number	Protein Name	Function	Estimated number of protein molecules per cell (yeast data from [212])
E6R936	Adenylate cyclase (ATP pyrophosphate-lyase), putative	Capsule biosynthesis in C. neoformans, a major virulence factor, is dependent upon adenylyl cyclase activity [283]	<50
E6R0R2	Alpha tubulin, putative	Cytoskeleton, a component of *C. neoformans* "virulence bags" [232, 284]	5.59E+03
E6QYP5	ATP-binding cassette transporter protein YOR1, putative	Functions to regulate Tat2 endocytosis, loss of the multidrug transporter Yor1 from cells induces a strong increase in phytosphingosine tolerance [285]	3.61E+03
Q5K7W2	ATP:ADP antiporter, putative	Appears to be involved in energy parasitism [286]	No identifiable homolog
Q5KIC0	Calcium-transporting ATPase, putative	Functions to remove Ca2+ ions from the cytosol, transporting them to internal stores and avoiding calcium toxicity [287]	6.90E+03
E6REF5	Cell wall integrity protein scw1, putative	Regulation of fungal septation and cell wall structure. Acts in opposition to the septation initiation network as a negative regulator of cell-wall/septum deposition [288]	5.73E+03
Q5KER6	Clathrin-coated vesicle protein, putative	Involved in Clathrin-mediated endocytosis, the uptake of material into the cell from the surface using clathrin-coated vesicles	No identifiable homolog
E6RC32	Extracellular elastinolytic metalloproteinase, putative	Possibly involved in fungal invasion of lung tissue due to its ability to hydrolyze elastin [289]	No identifiable homolog
E6R7S2	Formin binding protein 3, putative	Regulator of actin polymerization machineries, presumably critical for the production of different organizations of actin filaments, e.g. at the leading edge of migrating cells [290]	No identifiable homolog
E6RCU9	Glycolipid mannosyltransferase, putative	Involved in O-glycosylation of cell wall and secreted proteins, important for adherence to host surfaces and for virulence [291]	No identifiable homolog

E6R2Q4	Nonmuscle myosin heavy chain b, putative	Fundamental roles in a number of different biological events such as cell division, alteration of cell shape and protein synthesis and secretion [292]	No identifiable homolog
E6RAV5	Phosphatidylinositol 4-kinase, putative	Involved in the maintenance of vacuole morphology by controlling membrane channels or transporters required for osmotic control. Potential role in the regulation of vacuole fusion and/or fission [293]	No identifiable homolog
Q5KB69	Phosphoenolpyruvate carboxykinase, putative	An enzyme in the metabolic pathway of gluconeogenesis. A key player of part of the *C. albicans* metabolic programming that allows fungal persistence after phagocytosis by host cells and during systemic disease [294]	No detected expression
E6R9V4	Polyamine transport-related protein, putative	Binds polyamines and other related molecules (the uptake of environmental polyamines is crucial for full expression of virulence *in vivo*). Expression is increased in response to oxidative and temperature stress, choline limitation and during murine bacteremia. Systemic immunization with recombinant protein results in a vigorous antibody response in mice that protects against invasive pneumococcal infections [295]	No detected expression
E6R1W0	Response to drug-related protein, putative	Function unknown	3.86E+02
E6R9B8	Serine/threonine protein kinase, putative; (SOK-1) (Ste20-like kinase)	Activated by oxidative stress and chemical anoxia, regulates cell death in stressed cells. Its down-regulation by RNA interference enhances cell survival. Induces death when overexpressed [296]	No detected expression
E6RBT4	STE20	Plays evolutionarily conserved functions in cellular volume sensing and regulation. Yeast Ste20 initiates a shrinkage activated MAPK cascade that regulates organic osmolyte accumulation. May also function in systemic osmotic homeostasis and to link cell-cycle events with cell volume [297]	2.59E+02
E6RE09	Thioredoxin peroxidase, putative	Defence against oxidative and nitrosative stress, survival inside macrophages, *C. neoformans* virulence in mice [80]	3.78E+05
E6R9F2	UDP-glucuronic acid decarboxylase Uxs1p	Converts UDP-glucuronic acid to UDP-xylose, capsule synthesis in *C. neoformans* [284]	No identifiable homolog

4.4. Discussion

4.4.1. Experimental design "Catch 22"

A caveat to the experimental design of this study is that the inoculation of rats with 0.1 mL of 10^8 CFU of *Cryptococcus* cells is exceptionally high and does not represent a natural infection. Initial experiments with inoculums of 0.1 mL of 10^7 CFU, the minimal inoculum concentration demonstrated by Krockenberger *et al. (2010)* to produce progressive pneumonia [239], resulted in poor lesion development and limited disease progression. Since the goal of this thesis was to obtain sufficient fungal burdens, and thus fungal protein yields, for comparative proteomic analyses it was decided that a high inoculum would be required. As proteomics lacks an equivalent to the PCR amplification technique utilized by genomics and transcriptomics there was no alternative to this approach. The data presented in this chapter, and the subsequent chapters of this thesis, should be interpreted in the light of this caveat.

4.4.2. 1-D SDS-PAGE NanoLC ESI MS/MS can detect *Cryptococcus* proteins expressed during rat pulmonary infection

Chapter 2 demonstrated that phenol protein extraction purified *C. gattii* samples to the extent that cultured samples can be applied to 2-D PAGE and that samples from pulmonary infection can be applied to 1-D SDS-PAGE. The identification of *Cryptococcus* proteins via mass spectrometry post protein fractionation provides strong evidence of the effectiveness of the proteomic sample purification techniques developed for this analysis. Prior to this study, mass spectrometry protein detection

and identification had not been achieved for *C. gattii* cells from pulmonary infections. Here a 1-D SDS-PAGE nanoLC ESI MS/MS qualitative proteomics approach was used to determine if intracellular *Cryptococcus* proteins from cells obtained from pulmonary infection could be identified. This protocol was chosen to provide evidence of whether sample preparation techniques were efficient, rather than to identify the maximal number of proteins.

1-D SDS-PAGE nanoLC ESI MS/MS resulted in the detection and identification of 114 non-redundant intracellular *in vivo Cryptococcus* proteins. This is the first successful extraction and identification of intracellular proteins from *Cryptococcus* sourced from mammalian pulmonary infection. In addition, the current study detected and identified 1,164 non-redundant intracellular proteins from cultured *C. gattii*. In comparison, Chong *et al. (2012)*, who also used 1-D SDS-PAGE nanoLC ESI MS/MS to investigate the global response of cultured *C. gattii* to fluconazole treatment, identified a total of 195 non-redundant intracellular proteins. Using MudPIT, a shotgun proteomic technique that uses the combination of strong cation exchange with reverse phase chromatography, Crestani *et al. (2012)* identified 1,080 non-redundant *C. gattii* proteins from low iron media culture conditions and 1,135 from low iron media plus iron culture conditions [273]. The current study, which used techniques similar to Crestani *et al. (2012),* provides one of the most comprehensive snapshots of the *in vitro C. gattii* proteome achieved to date.

4.4.3. The persistence of contaminating rat proteins

Despite incorporating a number of steps aimed at preventing the carry-over of host proteins there was persistent contamination of the sample with a significant number of *Rattus norvegicus* proteins. Indeed, the number of identified non-redundant rat proteins (470) in this sample was considerably greater than the number of non-redundant *Cryptococcus* proteins identified (114). One consideration, given the skew towards rat proteins, was that host proteins overloaded the MS and suppressed *Cryptococcus* protein detection. This does not appear to be case, however, because the total number of rat proteins identified (584) was well below the totals observed in many LC-MS experiments, where thousands of proteins can be identified [298, 299]. This is a technical issue inherent to *in vivo* sample types and indicates the purification methods were unable to completely disrupt the association of host proteins with the porous polysaccharide capsular matrix.

4.4.4. Contaminating host proteins are non-specific

The majority of the 470 *Rattus norvegicus* proteins co-identified with *Cryptococcus* proteins from cells obtained from pulmonary infection were also identified in the iTRAQ experimentation on rat lungs described in Chapter 5 of this thesis and only 33 (7 %) were unique. The suite of *Rattus norvegicus* proteins identified in the *Cryptococcus* sample were largely representative of the protein groupings exhibited by the iTRAQ data and included antioxidants and antifungals as well as proteins involved in tissue modification and metabolism. These results indicate that *Cryptococcus* does not selectively associate with host proteins with particular

functions during the infective process, but instead randomly binds with an assortment of relatively abundant host proteins. The most likely source of host protein contamination is serum proteins and leakage from damaged lung cells.

Jobbins *et al. (2010)* established that protein and capsular polysaccharides are capable of forming strong associations with each other. During infection the cryptococcal polysaccharide capsule is surrounded by and saturated with host proteins. It is very likely that a significant amount of these host proteins are incorporated into the polysaccharide matrix of the capsule. It is also possible that these proteins remain associated, and effectively 'trapped', in this matrix until liberation during fungal cell lysis, leading to the subsequent co-identification of host proteins with fungal proteins during mass spectrometry. The resolution of this issue would require the development of a cellular de-capsulation technique that is compatible with comparative proteomics. Such a technique has yet to be developed for *Cryptococcus* cells from pulmonary infections. Until the mixed proteome issue is satisfactorily addressed global quantitative proteomics comparing cultured *Cryptococcus* with cells obtained from pulmonary infection remains problematic.

While the persistence of a mixed proteome represents a significant technical problem, the biological consequence of host protein association with fungal polysaccharide capsular material is of interest. The capsule is the external component of the fungal surface and is the primary site of interaction between fungus and host. Capsular structures have been found to mediate interactions between *Cryptococcus* and the host and are involved in evasion of the host immune system and promotion of pathogenesis [16]. The capsule provides *Cryptococcus* with powerful immune avoidance strategies including masking of pathogen-associated molecular patterns,

inhibition of fungal opsonisation, structural heterogeneity and inhibition of phagocytosis [16, 90]. The co-identification of significant numbers of host proteins with *Cryptococcus* proteins from cells obtained from pulmonary infection could be evidence of a further complementary host immune system avoidance strategy in antigenic masking. This avoidance strategy has been suggested for various species of trypanosomes where host immunoglobulin has been observed to become associated with the protozoan cell surface [300]. It has been suggested that these antibodies may prevent immune recognition of the parasite by the host, but this has not been conclusively demonstrated. It is possible that incorporation of extensive amounts of host proteins on the outside and within the matrix of the *Cryptococcus* polysaccharide capsule could act to mask the pathogen from the host immune system. This theory requires further extensive investigation to determine its validity for virulent *Cryptococcus*.

4.4.5. The selection of biologically relevant proteins from proteomics datasets

The disparity between the numbers of proteins identified from cultured *Cryptococcus* grown and cells obtained from pulmonary infection restricted comparative quantitative proteomics. Instead, the analysis of differences between the *Cryptococcus* proteomes focused on unique proteins, rather than differential protein expression level, as the primary selection criterion for identifying biologically relevant fungal proteins. Since the detected *in vivo* proteome represents approximately 10 % of the detected *in vitro* proteome, it was considered likely that any proteins identified exclusively in the *in vivo* sample would be biologically relevant. Qualitative

proteomics, although generally used in tandem with quantitative proteomics, can provide in-depth sample analysis and has been exploited in the search for biomarkers and drug targets [301, 302].

4.4.6. Protein function as a selection criterion and the danger of using automated systems to assign function

A further selection criterion used to identify proteins of interest was determination of their specific function in the context of both fungal proteins in general and fungal pulmonary infection/trauma. However, significant limitations were encountered when using automated computer algorithms to apply gene ontology terms/protein functions to the *C. gattii* dataset. The use of these systems is a standard method of assigning biological functions to large data sets of identified proteins. While these systems are rapidly able to provide relevant information regarding the general function of a given protein, they lack the disease or infection context needed to provide the most relevant information for the function of a specific protein in the particular biological system that is being investigated. For example, Gene Ontology assigned seven different biological processes or functions for fatty acid-binding protein, epidermal (E-FABP), while the DAVID Bioinformatics Database provided over 20 different biological processes or functions. There is no straightforward way to filter those functions by relevance to infectious disease.

The idea that one gene encodes for one protein with one function has been superseded by the identification of proteins that exhibit multiple functions [303-305]. The multifunctional ability of “moonlighting” proteins is not a result of gene fusion,

homologous proteins, splice variants or non-specific enzyme activity. Nor are they proteins that have the same function in different cell types or sub-cellular location. Rather, moonlighting proteins are defined as single polypeptide chains that exhibit two or more functions. The identification of moonlighting proteins is crucial in assigning correct functions to the thousands of proteins that have been identified by the ever-growing number of genome projects being undertaken. Furthermore, the identification and improved understanding of this important class of proteins could influence the selection of target proteins during drug development, where it may be crucial to selectively inhibit one or more of the functions of a multifunctional protein. The assignment of protein function is a far from straightforward process given the complexity associated with moonlighting proteins and proteins that have very similar functions. For this study, proteins were assigned biological and molecular function based on information available in the literature concerning the broad field of fungal pathogens. While this proved to be a laborious procedure, determining the specific role of a given protein in the context of lung ailments is far more accurate than a general search for function without restriction to this particular niche.

4.4.7. Protein abundance as an indicator of biological relevance

In 2003 Ghaemmaghami *et al.* published a study that investigated global protein expression in *Saccharomyces cerevisiae* during log phase growth [212]. This study involved the creation of a *Saccharomyces cerevisiae* fusion library, where each open reading frame was tagged with a high-affinity epitope and expressed from its natural chromosomal location. The absolute level of protein expression (as protein molecules per cell) was then measured via immunodetection of the common tag. The study

found that about 80% of the *Saccharomyces cerevisiae* proteome was expressed under normal growth conditions, with the abundance of proteins ranging from fewer than 50 to more than 10^6 molecules per cell.

In general, global proteomic analysis techniques, even with high sensitivity MS, are limited to detecting and quantifying abundant and hydrophilic non-membrane proteins with isoelectric points below pH 8. It is unusual to identify proteins present at less than 10^4 copies per cell in an unfractionated LC-MS experiment. It has been predicted that low abundance proteins make up 80% of the yeast proteome [203]; thus, the majority of the proteome remains undetectable by conventional proteomic experimental platforms. It was interesting to find that the majority of the unique *in vivo Cryptococcus* proteins that had *Saccharomyces* homologs were predicted to be of low abundance. For example, adenylate cyclase (ATP pyrophosphate-lyase), a protein that functions as a CO_2 chemosensor in *C. albicans* and *C. neoformans* [283], is expressed at less than 50 protein molecules per cell in *Saccharomyces*. Similarly, the putative "response to drug-related protein" and Ste20 were found to be expressed at approximately 10^2 protein molecules per cell in *Saccharomyces* and are considered to be of low abundance. This study also detected proteins, such as phosphoenolpyruvate carboxykinase, polyamine transport-related protein and serine/threonine protein kinase, whose expression could not be detected by *Ghaemmaghami et al. (2003)* in yeast. Although an obvious caveat of using protein abundance measurements made for *Saccharomyces* to estimate those in *Cryptococcus* is that the cellular machinery and physiochemical nature of these two species are markedly different, the fact that they were also not seen in cultured *Cryptococcus* suggests they have been increased in expression in response to the infection process.

4.4.8. Codon usage bias as a predictor of protein abundance

Codon usage bias is based on the probability that only one of several possible codons will be used in coding DNA. Until recently the accepted dogma was that proteins from genes with codon bias indices (CBI) or codon adaptation indices (CAI) of less than 0.2 are usually poorly transcribed and therefore likely to be found in low abundance [188]. Despite an established correlation of codon bias and gene expression, it has recently been suggest that mRNA structure rather than CAI affects protein expression, and thus protein abundance, levels [306, 307]. The codon bias figures for the unique *Cryptococcus* proteins from cells obtained from pulmonary infection in this study were calculated to be greater than 0.8 (indicating high abundance) and there are no literature to suggest that protein expression would be inefficient. It is more likely that they are found in low abundance during *in vitro* growth because they are not required for growth in rich medium and low-stress normoxic conditions.

4.4.9. Fungal response to hypoxia and stress during infection

A number of fungal pathogens are capable of anaerobic fermentation during culture in rich media. However, molecular oxygen continues to be thought of as essential for the synthesis of ergosterol, NAD and heme, molecules that are likely to be in short supply in the host [308]. Thus, *Cryptococcus* is considered to be an obligate aerobic pathogen. The conditions encountered during early stage lung infection will be partially hypoxic and less favourable than the usual planktonic culture. After infection is established the lung environment becomes inflammatory and severely hypoxic.

Inflammatory sites such as those found in infected lung tissue contain many immune cells that metabolise available oxygen and obstruct blood vessels, creating an oxygen-depleted environment. In theory hypoxia represents a greater challenge to fungi than bacteria, and bacterial pathogens have alternative, oxygen independent pathways to synthesize NAD and heme and do not synthesise sterol [308]. To infect tissue fungal pathogens must be able to adapt to a hypoxic environment. Chun *et al. (2007)* demonstrated that *C. neoformans* mutants in either the SREBP pathway (cholesterol biosynthesis regulatory pathway) or the Tco1 pathway (fungal-specific hybrid histidine kinase family member) were less virulent and unable to proliferate in murine host tissue [308]. The authors suggest that targeting the components of the hypoxia response could yield more effective treatments for infections with *Cryptococcus*.

The likely explanation for the induced expression of some *in vivo Cryptococcus* proteins is a coordinated response to the stress and hypoxia during pulmonary infection. Adenylate cyclase (ATP pyrophosphate-lyase) represents a perfect example of a *Cryptococcus* protein likely to be increased in expression during infection. The *Cryptococcus* capsule significantly increases in thickness in response to pulmonary infection and adenylate cyclase activity is essential for capsular biosynthesis in *C. neoformans* [283]. In addition, phosphoenolpyruvate carboxykinase (a key player in *C. albicans* metabolic programming that allows fungal persistence after phagocytosis by host cells and during systemic disease [294]), polyamine transport-related protein (the uptake of environmental polyamines is crucial for full expression of virulence *in vivo* [295]) and serine/threonine protein kinase (activated by oxidant stress and chemical anoxia, regulates cell death in stressed cells [296]) all represent proteins that are likely be up-regulated in response to fungal pulmonary infection.

4.4.10. Low abundance *Cryptococcus* proteins from cells obtained from pulmonary infection as potential drug targets

An investigation of the literature indicated that a number of theoretically low abundance (as predicted by [212]) *Cryptococcus* proteins from cells obtained from pulmonary infection represent potential drug and/or inhibition targets. Included in this select group are adenylate cyclase, elastinolytic metalloproteinase, glycolipid mannosyltransferase, enolpyruvate carboxykinase and polyamine transport-related protein.

4.4.10.1. Adenylate cyclase

Adenylate cyclase functions in a conserved signal transduction pathway that has been demonstrated to be responsible for the regulation of cyclic AMP production, hyphal differentiation and virulence in *Cryptococcus* [309]. Klengel *et al.* demonstrated a conserved link between cyclic AMP signalling and CO_2/HCO_3^- sensing in fungi. It was further demonstrated that CO_2 sensing plays a essential role in mediating fungal pathogenesis including capsule biosynthesis and melanin production, key virulence factors that are vital to cryptococcosis pathogenesis [283]. It is well known that acapsular cryptococcal cells are avirulent whilst encapsulated isolates have varying degrees of virulence [82, 83]. As *Cryptococcus* adenylate cyclases are only modestly related to mammalian adenylate cyclases [310], the development of novel therapeutic agents that target the adenylate cyclase-cyclic AMP signalling pathway could be useful in limiting *Cryptococcus* pathogenesis via the inhibition of vital virulence factors such as capsular biosynthesis.

4.4.10.2. Elastinolytic metalloproteinase

Elastin, an insoluble hydrophobic molecule, is the major component of elastic fibres and functions to maintain structural and functional integrity in the lungs. The degradation of elastin, which is highly resistant to proteolysis, is pivotal in the development of pulmonary dysfunction. Matrix metalloproteinases (MMP) have the ability to degrade elastin. Raulo *et al. (2000)* determined that MMP elastinolysis expression was increased in horses with chronic obstructive pulmonary disease (COPD), indicating that excessive elastinolytic activity is involved in the pathogenesis of COPD [311]. These authors further determined that MMP elastinolytic activity was significantly inhibited by chemically modified tetracycline-3 (CMT-3) *in vitro* [311]. The increased expression of *Cryptococcus* elastinolytic metalloproteinase may be associated with the pulmonary tissue destruction observed during severe pulmonary infection. Whether or not the inhibitory effects of CMT-3 can be translated to the treatment of human obstructive lung diseases or could be used to inhibit *Cryptococcus* elastinolytic activity during severe pulmonary infections has not been tested. Nonetheless, efficient MMP inhibitors may represent a future class of valuable drugs for use in neutralising destructive elastinolytic activity.

4.4.10.3. Glycolipid mannosyltransferase

Glycolipid mannosyltransferases are involved in the O-glycosylation of cell wall and secreted proteins. The cell surface acts as the immediate point of contact between the fungus and the host. The outer cell wall layer is enriched in mannoproteins (mannose containing glycoproteins). Both the protein and carbohydrate components of

mannoproteins have been demonstrated to be involved in fungal adhesion to host cells. O-glycosylation has been demonstrated to be necessary for the full development of *C. albicans* virulence and plays vital roles in fungal cellular adhesion and the immunomodulation of host reposes [291]. The targeted inhibition of glycolipid mannosyltransferase could limit or halt fungal cellular adhesion and host immunomodulation, which are key to pathogenesis. Coupled with antifungal treatment, glycolipid mannosyltransferase inhibition represents a future antifungal therapeutic option that could augment the ability of the host to deal with the fungal pathogen and could limit the spread of infection in the lung.

4.4.10.4. Phosphoenolpyruvate carboxykinase

Phosphoenolpyruvate carboxykinase is a central control point for the regulation of gluconeogenesis (the synthesis of glucose of from metabolic precursors). To survive and thrive in mammalian host environments fungal pathogens must be able to assimilate carbon and other available nutrients [294]. This requires a sufficient level of metabolic flexibility. It has been demonstrated that *C. albicans* has the ability to up-regulate the expression of genes involved in amino acid biosynthesis when growing in biofilms and to shift from fermentative to non-fermentative metabolism following exposure to human neutrophils and/or macrophages [312-315]. Mammalian infection has been shown to generate a high degree of metabolic heterogeneity within fungal cell populations *in vivo*. During the early stages of infection, when access to glucose is limited and as a response to phagocytosis, *C. albicans* activates gluconeogenesis. During the later stages of infection and tissue colonisation, glycolytic colonisation predominates [294]. The evidence suggests that fungal

pathogens regulate central carbon metabolism in a niche-specific manner. The targeted inhibition of gluconeogenesis, during early stage infection, via the inhibition of phosphoenolpyruvate carboxykinase activity, could therefore represent a therapeutic option if infection can be detected early. Unfortunately, the diagnosis of cryptococcosis is often delayed, particularly for *C. gattii*, which causes sporadic disease, although close monitoring of immunosuppressed patients may enable early detection of *C. neoformans*. The inhibition of fungal metabolism as a therapeutic antifungal option still demands future investigation.

4.4.10.5. Polyamine transport-related protein

Polyamines are small organic compounds with a hydrocarbon backbone and multiple positively charged amino groups spaced at regular intervals. Polyamine acquisition and biosynthesis are vital for the development of full virulence in both prokaryotic and eukaryotic human pathogens [316, 317]. Polyamine transport protein D (PotD) is a membrane-associated periplasmic substrate binding protein that binds polyamines and facilities their uptake via transmembrane proteins. Two studies by Shah *et al. (2006 and 2009)* indicated the important role of PotD in pneumococcal pathogenesis and immunity. Similar to *Cryptococcus*, *Streptococcus pneumonia* is an encapsulated human pathogen with pathogenesis initiated following colonisation of the upper respiratory tract [318]. These studies demonstrated that both the systemic and mucosal immunisation of mice with recombinant PotD resulted in a vigorous and specific antibody response that was protective against invasive pneumococcal infection [295, 319]. Mucosal immunisation resulted in significantly reduced nasopharyngeal carriage and prevented invasive disease following challenge with virulent

Streptococcus pneumonia serotypes [295]. This ability to inhibit prokaryotic disease, coupled with the known importance of PotD and polyamines in eukaryotic human pathogens, indicates the potential of this protein as a component of an effective next-generation fungal vaccine.

4.4.11. From biologically relevant protein to drug target

While these qualitatively identified proteins appear interesting with regard to protein abundance and function, their potential as drug targets relies on whether or not a protein homolog exists in the host organism. Protein sequence and structure homology is widely utilised in the scientific literature as evidence of shared protein function between species. The lack of a homologous protein in the host strongly indicates that the specific function of the fungal protein of interest could be modulated without affecting the host. There are a myriad of automated homology detection tools in existence, however the difficulties associated with homology-based function prediction have been well described in the literature [320]. Automated strategies for the assignment of protein function depend on function transfer via protein sequence, structure and interaction based inference methods.

Accurate function prediction requires the coupling of genomic, transcriptomic and proteomic sequence and expression information with prediction algorithms. The primary issue with function prediction techniques is whether inferences made by similarity comparisons actually provide a true representation of functional relatedness [321]. Thus, function prediction via homology based inference remains a significant challenge. The work completed in this study was limited by the poorly annotated

nature of the *Cryptococcus* sequence databases. Very few *Cryptococcus* proteins have been extensively modelled or indeed researched at all beyond simple amino acid sequence information and the provision of a protein name. Indeed, the vast majority of *Cryptococcus* proteins listed on UniProt are 'Predicted'. UniProt provides five levels of evidence of protein existence. These are, in descending strength, are 'evidence at protein level', 'evidence at transcript level', 'inferred from homology', 'predicted' and 'uncertain'. 'Predicted' proteins represent detected proteins for which there is no evidence for protein existence at the protein, transcript, or homology levels (http://www.uniprot.org/manual/protein_existence). The lack of comprehensive protein structural modelling and protein interactions for *Cryptococcus* protein databases severely limits the comprehensiveness of any conducted homology based function prediction.

The most stringent method of defining protein function, and thus, the potential of an identified protein as a drug target, is via *in vitro* and *in vivo* experimentation. These experiments are performed to confirm the exact function of an identified cryptococcal protein. In addition, *in vitro* and *in vivo* experimentation can deduce the physiological effects of *Cryptococcus* protein function modulation (ranging from function deletion to recombinant protein supplementation) on both the animal model utilised and on fungal pathogenesis. *In vitro* experimentation involving the fungal pathogen is useful for determining how modulating protein function affects the fungal organism, with the key question being: does protein modulation inhibit key features of pathogenesis? *In vitro* experimentation can then be followed by *in vivo* experiments in an animal model. These experiments can determine whether deletion of the mammalian homolog of the fungal protein, or introduction of recombinant fungal protein, affects the host cellular machinery. Subsequently, *in vivo* experiments involving both the host

and the infective agent can determine whether the modulation of fungal protein function successfully attenuates fungal pathogenesis and thus enables the host immune system to successfully deal with the pathogenic threat. While these experimental processes are time consuming and demanding on resources expenditure, the results obtained would provide comprehensive insight into the function of an identified protein and its potential as an anti-fungal drug target.

4.5. Conclusions

Unfortunately validation studies fell outside of the scope this study, largely because of the technical difficulties associated with *C. gattii* that delayed progress and hampered further studies, and also because the *Cryptococcus* databases crucial to proteomic analyses area as yet poorly annotated. Despite the impediments to experimentation, the identification of significant numbers of non-redundant *Cryptococcus* proteins from cultured cells and cells from pulmonary infection provided interesting qualitative datasets that offered insights into fungal pathogenesis at the protein level and highlighted a number of potentially exciting *Cryptococcus* proteins that could be exploited as drug targets. However, the proof of concept for global '–omics' analysis of this technically challenging sample type provided by this study should lead to further analysis, and potentially quantitative analysis, of fungal pathogens under *in vivo* conditions, along with continued development of novel therapeutic and diagnostic options for pathogenic fungi.

Chapter Five

Elucidating the rat host protein response to pulmonary infection with *Cryptococcus*

Despite the recognition of the lung as a primary site of Cryptococcus infection, very little is understood about the global molecular mechanisms of the pulmonary host response to fungal inhalation and pathogenesis. This study provides the first attempt at global quantitative proteomic investigation of the host response to pulmonary cryptococcosis. The elucidation of the global host protein response to pulmonary infection with Cryptococcus *was technically challenging due to the physiochemical nature of* Cryptococcus *exopolysaccharide. Advances in sample preparation described in chapter 3 permitted the use of isobaric tag for relative and absolute quantification (iTRAQ) analysis to quantitatively compare the proteomes of rat lungs infected with virulent strains of* Cryptococcus*, using naïve control lungs as a baseline. The quantitative data obtained shows how the host adapts to fungal insult and highlights potential diagnostic and therapeutic targets.*

5.1. Introduction

The lung is the essential respiration organ of mammals [322]. The primary function of the lung is to transport oxygen from the atmosphere into the bloodstream and to release carbon dioxide from the bloodstream into the atmosphere (figure 5.1). The lung serves other vital functions, including but not limited to, protecting the host against air-borne infection via mucociliary escalator actions [323] and maintaining sterility by producing mucus containing antimicrobial agents [324]. Breathing is driven by muscular action with gas exchange taking place in the alveoli, the terminal end of the respiratory tree (figure 5.1). The approximately 300 to 500 million alveoli in the human lung provides the large surface area (roughly 70 m^2) required for efficient gas exchange [325].

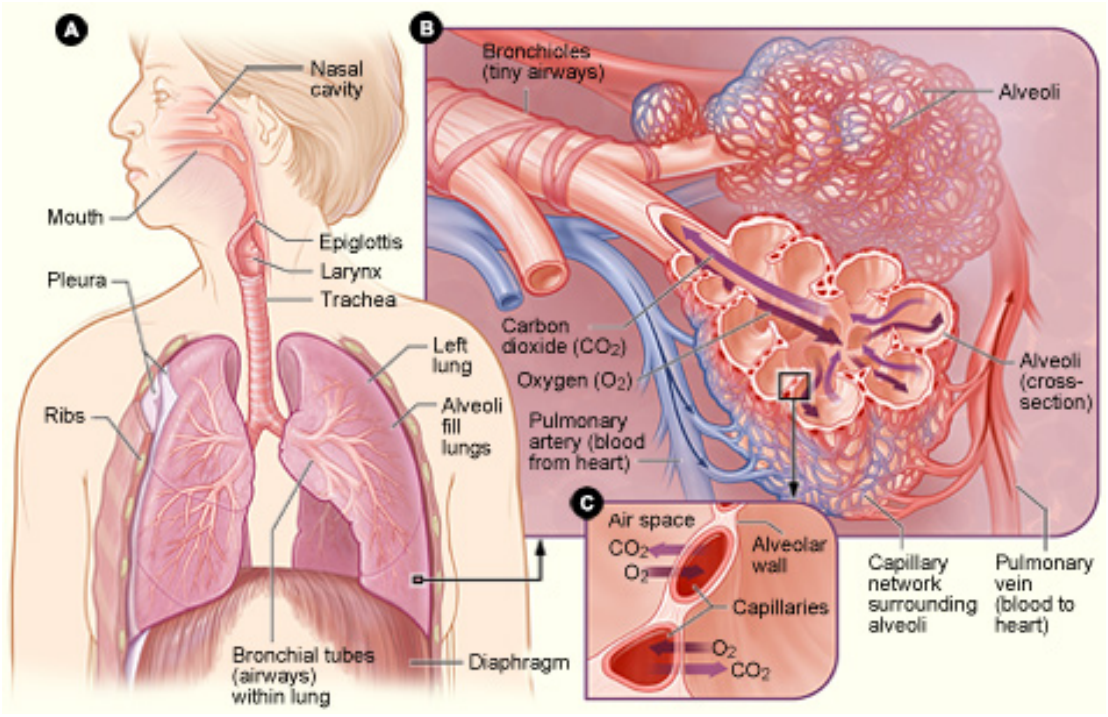

Figure 5.1: Schematic of the mammalian respiratory structures.

A) The location of the respiratory structures in the body. B) An enlarged view of the airways, alveoli and capillaries. C) Gas exchange between the capillaries and alveoli (from [326]).

The lung is susceptible to microbial pathogens that are transmitted through the air via aerosols of dust or liquids. The bodily secretions of an infected individual represent a likely source of pathogen-containing aerosols. While the zoonotic transmission of *Cryptococcus* has been documented [19, 20] it is very rare and human-to-human transmission remains undocumented. *Cryptococcus* infectious propagules are most likely to be desiccated yeast cells or basidiospores transmitted via environmentally generated aerosols. For example, infection with *C. neoformans* is commonly associated with the disturbance of soil contaminated with bird droppings, especially pigeon droppings, and *C. gattii* infection, especially the Vancouver Island outbreak, is associated with forestry [327-329]. Effective host defence against airborne pathogens depends on the rapid mechanical clearance of inhaled infective agents via the action of airway turbulence and the mucociliary escalator [330, 331]. *Cryptococcus* displays the ability to circumvent these upper airway defences and become deposited in the respiratory spaces of the lung. The success or failure of host defence against deposited *Cryptococcus* is critically regulated by cell-mediated immunity and especially T lymphocytes [35, 86, 141-144]. The predominant synthesis of Th1 and Th17 cytokines over Th2 cytokines protects mice from cryptococcal infection [147-149]. Virulent *Cryptococcus* strains are then able to circumvent the non-specific innate immune system defences, leading to fungal proliferation and metastasisation [332].

While previous studies have determined the type of innate immune response effective for the elimination of *Cryptococcus* from the host, the elucidation of the global molecular responses to *Cryptococcus* infection remains enigmatic. Hirsch *et al. (2004)* acknowledged the potential of proteomics to acquire an understanding of the complex responses of lung exposure to stimuli [333]. This review of proteomic methods of pulmonary research also acknowledged that the pulmonary sample type,

due to its inherent complexity, represented a challenging target to proteomics. Zhao *et al. (2012)* demonstrated that meaningful comparative proteomic data could be obtained from *in vivo* pulmonary infection models [334]. This study investigated the host response to viral infection using 2-D DIGE to compare the proteomes of uninfected and infected murine lung tissue. Similarly, Ohlmeier *et al. (2010)* demonstrated that differential display 2-D PAGE coupled with Western blot analysis could be utilised to identify potential human protein biomarkers involved in the pathogenesis of chronic obstructive pulmonary disease [335]. With regard to the analysis of fungal pathogens, Fekkar *et al. (2012)* investigated the ability of proteomics to discover novel diagnostic biomarkers for invasive aspergillosis using 2-D DIGE to analyse murine bronchoalveolar lavage and sera. This study was able to provide evidence for an *in vivo* complement evasion mechanism during invasive aspergillosis and provided insight the inflammatory host response to invasive aspergillosis in both the lung and sera, providing new insight into the pathophysiology of the disease [336]. Combined, these studies provide evidence for the ability of global comparative proteomics to interpret the host responses to infection and to highlight potential biomarkers. In the case of pulmonary fungal infection, analysis to date has been limited to bronchoalveolar lavage and sera. It is likely that the absence of literature concerning the comparative proteomic investigation of host pulmonary tissue during fungal infection is a result of the technical challenges associated with this sample type (discussed in chapter 3).

The work undertaken in this study attempted to utilise global comparative proteomic approaches to analyse differential gene expression at the whole organism level. Specifically, this study attempted to compare the host responses of animals infected with high virulence *C. gattii* strain R265 and low virulence *C. gattii* strain R272 and

the responses of animals infected with the two different virulent species of *Cryptococcus* (*C. neoformans* vs. *C. gattii*). This is the first global quantitative proteomic investigation of how the rat reacts to pulmonary infection with *Cryptococcus*. The underlying hypotheses of the study were that:

- Fungal growth in the pulmonary environment would induce specific protein changes in the lung proteome
- iTRAQ comparative proteomic analyses would identify these specific proteins highlighting:
    - The lung proteins that respond to infection with *Cryptococcus* of different species and different virulence levels.
    - The proteins that could form future drug targets, biomarkers and diagnostic markers.

5.2. Methods

5.2.1. *Cryptococcus* strains and number of rats infected

Table 5.1: *Cryptococcus* strains and number of rats infected

***Cryptococcus* strain**	**Number if rats infected**	
	Early stage infection	Late stage infection
KN99α (*C. neoformans* molecular type VNI)	10	N/A
R265 (*C. gattii* molecular type VGIIa, high virulence)	10	10
R272 (*C. gattii* molecular type VGIIb, low virulence)	10	10

5.2.2. Pulmonary infection model

The pulmonary infection model used was described in section 2.3.2.

5.2.3. Pulmonary tissue homogenisation

Pulmonary tissue homogenisation was completed using the method described in section 2.3.3.

5.2.4. Pulmonary sample preparation for iTRAQ analysis

Supernatants retained from 2.3.3. were divided among a suitable number of 50 mL Falcon tunes and the proteins precipitated by incubation with a 5 x volume of 100 % acetone for 30 minutes at room temperature. Following centrifugation at 3,000 *g* for 10 minutes, the acetone was discarded and the protein pellet solubilised in a suitable volume of 1 % SDS (v/v), 100 mM TEAB. The sample was then transferred to 100 kDa MWCO filters (250 μL per filter, Pall Scientific, USA) and centrifuged at 10,000 *g* until all of the solution had passed through the filter (approximately 8 hours). The sample was then buffer exchanged into 0.1 % SDS (v/v), 250 mM TEAB using Micro Bio-Spin 6 chromatography columns (Bio-Rad, USA) to remove residual LiCl prior to iTRAQ analysis.

5.2.5. 4-plex iTRAQ sample design

Tables 5.2, 5.3 and 5.4 describe the specific iTRAQ labels used to label uninfected control and infected lung protein samples for KN99α, R265 and R272 respectively. Experiments with KN99α used the 4 labels available for 4-plex iTRAQ, while experiments with R265 and R272 used 3 of the 4 the labels in each run.

Table 5.2: 4-plex iTRAQ sample design for pulmonary infection with KN99α

4-plex run #1 (two biological replicates in the same run)		
Sample	**Lung weight**	**iTRAQ label**
Uninfected control #1	0.85 g	114
Uninfected control #2	0.90 g	115
Early stage infection #1	7.03 g	116
Early stage infection #2	7.33 g	117

Table 5.3: 4-plex iTRAQ sample design for pulmonary infection with R265

4-plex run #1 (1st biological replicate)			**4-plex run #2 (2nd biological replicate)**		
Sample	**Lung weight**	**iTRAQ label**	**Sample**	**Lung weight**	**iTRAQ label**
Uninfected control	0.85 g	115	Uninfected control	0.90 g	115
Early stage infection	3.80 g	116	Early stage infection	6.19 g	116
Late stage infection	3.60 g	117	Late stage infection	5.97 g	117

Table 5.4: 4-plex iTRAQ sample design for pulmonary infection with R272

4-plex run #1 (1st biological replicate)			4-plex run #2 (2nd biological replicate)		
Sample	**Lung weight**	**iTRAQ label**	**Sample**	**Lung weight**	**iTRAQ label**
Uninfected control	0.85 g	115	Uninfected control	0.90 g	115
Early stage infection	2.10 g	116	Early stage infection	1.81 g	116
Late stage infection	0.94 g	117	Late stage infection	0.81 g	117

5.2.6. iTRAQ labelling (completed by the Australian Proteome Analysis Facility at Macquarie University)

iTRAQ was used to quantitatively profile the lung proteome during infection. 100 µL aliquots of protein samples were delivered to the Australian Proteome Analysis Facility as a liquid in 0.1 % SDS at a concentration of approximately 1 µg/µL (determined by the comparison of protein standards run on 1-D SDS-PAGE). The samples were reduced with 5 mM TCEP for 1 hour at 60 °C and alkylated with 10 mM MMTS at room temperature for 10 minutes. The protein sample was digested overnight with trypsin at 37 °C at a trypsin to protein ratio of 1:20. Digested samples were labelled with the iTRAQ reagents following the protocol provided by the vendor (Applied Biosystems, Foster City, CA). Briefly, one vial of iTRAQ labelling reagent was used for every 100 µg of protein. Ethanol was used to solubilise the iTRAQ reagent then added to the peptide sample ensuring a final organic concentration of at least 60 % (v/v). After 1 hour of iTRAQ labelling, the reaction was quenched by adding 50 µL of water. The samples were then mixed at equal ratios and dried by centrifugal evaporation.

5.2.7. Mass spectrometry (completed by the Australian Proteome Analysis Facility at Macquarie University)

Mass spectrometry was completed using the methods described in section 2.3.9.

5.3. Results

5.3.1. Rat lung weights pre and post infection

Table 5.5 lists the mean weights of lungs from control and infected rats according to the specific *Cryptococcus* strain used for infection and the infection time point.

Table 5.5: Rat lung weights

***Cryptococcus* strain**	**Infection time point**	**Mean control lung weight (±SD)**	**Mean infected lung weight (±SD)**
KN99α (*C. neoformans* molecular type VNI)	14 days	0.88 g (0.035)	7.18 g (0.212)
	42 days	N/A	N/A
R265 (*C. gattii* molecular type VGIIa)	14 days	0.88 g (0.035)	5.00 g (1.700)
	42 days	0.88 g (0.035)	4.79 g (1.676)
R272 (*C. gattii* molecular type VGIIb)	14 days	0.88 g (0.035)	1.96 g (0.205)
	42 days	0.88 g (0.035)	0.86 g (0.092)

5.3.2. Inoculation resulted in strain specific lesion formation in rat lungs

The progression of infection and lesion formation was assessed by the general appearance and health of the rats prior to euthanasia and by the macroscopic scale inspection of their lungs post euthanasia. The extent of lesion development observed

at the early and late stage infection time points was found to be highly dependent on the *Cryptococcus* strain used for pulmonary infection.

5.3.2.1. Rats infected with KN99α (C. neoformans molecular type VNI)

Early stage infection: At the 14 day time-point rats displayed symptoms typical of cryptococcosis. The rats were hunched, lethargic with ruffled fur and squinted eyes and were visibly struggling to breathe. Infected lungs were greatly increased in size compared to control lungs due to the development of large, multifocal gelatinous lesions. Infected lungs demonstrated extensive consolidation of lung fields, with little normal lung material remaining. Based on these observations, and the requirements for ethical animal treatment, experiments involving late stage infection with KN99α were abandoned. All rats infected with KN99α were humanely euthanized at day 14 (early stage infection) as per the Animal Ethic Committee protocol to prevent suffering.

5.3.2.2. Rats infected with R265 (C. gattii molecular type VGIIa)

Early stage infection: At the 14 day time-point rats appeared less lethargic than those infected with KN99α. Their fur was ruffled and breathing strained, but less so than in infections with KN99α. The dissected lungs were considerably larger than control lungs, although less so than in infection with KN99α. Compared to KN99α, lesion development was slightly reduced and there was a greater amount of apparently

normal lung material. Based on these observations, experiments designed for late stage infection with R265 were permitted to proceed to the 42-day time point.

Late stage infection: At the 42 day time point rats appeared hunched, lethargic with ruffled fur and squinted eyes and were visibly struggling to breathe, but less so than in the 14 day infections with KN99α. The dissected lungs were considerably larger than the control lungs, although less so than in infection with KN99α. Lesion development and amounts of normal tissue was similar to those observed at the 14 day time-point, however, the lungs were lighter at 42 days than at 14 days.

5.3.2.3. Rats infected with R272 (C. gattii molecular type VGIIb)

Early stage infection: At the 14 day time point rats appeared in normal health. Rats were active with apparently normal breathing patterns. The lungs were slightly larger than control lungs, though considerably smaller than 14 day R265 and KN99α. Lesion development was sparse with the majority of the lung tissue appearing normal.

Late stage infection: At the 42-day time-point rats appeared in normal health. Rats were active with apparently normal breathing patterns. The lungs were not statistically different in weight compared to the uninfected controls; however, they were significantly smaller than 14-day infections with R272. The lungs were considerably smaller than lungs infected with KN99α and 14 and 42 day R265. Lesion development was not observed and the lung tissue appeared normal.

5.3.3. Global comparative quantitative analysis of control and infected lungs

The soluble proteomes of control and infected rat lungs were compared utilizing iTRAQ. Table 5.6 details the mass spectrometric results obtained with respect to the *Cryptococcus* strain used for pulmonary infection.

Table 5.6: iTRAQ mass spectrometry results

Pulmonary infection strain	**KN99α**	**R265**		**R272**	
4-plex run	1	1	2	1	2
Mass spectrometer	Triple TOF 5600 (AB Sciex)	Qstar XL (AB Sciex)	Triple TOF 5600 (AB Sciex)	Triple TOF 5600 (AB Sciex)	Triple TOF 5600 (AB Sciex)
Spectra identified	238103	38581	197661	144955	173678
Distinct peptides	26927	9560	26213	18037	16486
Proteins detected	1152	876	1344	1017	897

5.3.4. Differentially expressed proteins common to infected lungs

Table 5.7 lists the differentially expressed proteins that were detected across all pulmonary infections with KN99α, R265 and R272. Accept for Alpha-1B-glycoprotein, the proteins were consistently increased or decreased in expression across all pulmonary infection datasets. A number of these proteins were found to have functions involved in the host immune response to infection.

Table 5.7: Differentially expressed proteins common to the pulmonary infection datasets

Accession number:	Protein name:	Expression
Q9EPH1	Alpha-1B-glycoprotein	Ambiguous
P10760	Adenosylhomocysteinase	Decreased
Q63495	Advanced glycosylation end product-specific receptor	Decreased
P47853	Biglycan	Decreased
B0BNN3	Carbonic anhydrase 1	Decreased
P27139	Carbonic anhydrase 2	Decreased
P16303	Carboxylesterase 3	Decreased
Q9EPT8	Chloride intracellular channel protein 5	Decreased
P31430	Dipeptidase 1	Decreased
P23764	Glutathione peroxidase 3	Decreased
P08010	Glutathione S-transferase Mu 2	Decreased
Q63279	Keratin, type I cytoskeletal 19	Decreased
P48679	Lamin-A	Decreased
O35763	Moesin	Decreased
Q63425	Periaxin	Decreased
P35704	Peroxiredoxin-2	Decreased
P85125	Polymerase I and transcript release factor	Decreased
Q9Z1J8	SEC14-like protein 3	Decreased
Q8VIF7	Selenium-binding protein 1	Decreased
P06761	78 kDa glucose-regulated protein	Increased
Q6RY07	Acidic mammalian chitinase	Increased
P24268	Cathepsin D	Increased
P55053	Fatty acid-binding protein, epidermal	Increased
P04642	L-lactate dehydrogenase A chain	Increased
Q6AYC4	Macrophage-capping protein	Increased
P35248	Pulmonary surfactant-associated protein D	Increased

5.3.5. Biologically relevant differentially expressed proteins

Table 5.8 and 5.9 list lung proteins selected from the list of differentially expressed proteins common to the KN99α, R265 and R272 datasets (table 5.7) according to the selection criteria for proteins of interest outlined in this study (section 4.4.6.). The proteins listed in table 5.8 increased in expression with infection while those in Table 5.9 decreased.

Table 5.8: Biologically relevant proteins with increased expression

Accession number:	Protein name:	Protein function:
P06761	78 kDa glucose-regulated protein	Maintenance of cellular homeostasis and protection from cell lysis.
Q6RY07	Acidic mammalian chitinase	Degrades chitin, promoter of allergic inflammation.
P24268	Cathepsin D	Blocks alveolar epithelial cell apoptosis.
P55053	Fatty acid-binding protein, epidermal	Involved in the synthesis of functional surfactant.
Q6AYC4	Macrophage-capping protein	Involved in macrophage motility and phagocytosis.
P35248	Pulmonary surfactant-associated protein D	Pattern recognition molecule involved in opsonisation for enhanced phagocytosis.

Table 5.9: Biologically relevant proteins with decreased expression

Accession number:	Protein name:	Protein function:
Q63495	Advanced glycosylation end product-specific receptor	Maintains the correct morphology of alveolar type I cells.
P47853	Biglycan	Anti-fibrotic.
B0BNN3	Carbonic anhydrase 1	Carbon dioxide transport out of the lungs.
P27139	Carbonic anhydrase 2	Carbon dioxide transport out of the lungs.
P23764	Glutathione peroxidase 3	Antioxidant.
O35763	Moesin	Innate immune response, TLR4-mediated pattern recognition, promotes expression of pro-inflammatory cytokines.
Q63425	Periaxin	Maintenance of peripheral nerve myelin.
P35704	Peroxiredoxin-2	Antioxidant.
Q9Z1J8	SEC14-like protein 3	Indicator of airway inflammation progression.

5.3.6. Proteins that are marginally outside the selection criteria

The proteins listed in Table 5.10 were significantly different in expression in five out of six biological replicates. These proteins represent a data subset marginally lower than the filtered 'common proteins' in the hierarchy of stringency (section 5.4.2.), indicating that this subset represents regulated proteins with a high likelihood of being biologically relevant in the context of pulmonary ailment.

Table 5.10: Differentially expressed proteins marginally outside the selection criteria

Legend:	
⇑	Significantly up-regulated in both biological replicates
↑	Significantly up-regulated in one of two biological replicates
⇓	Significantly down-regulated in both biological replicates
↓	Significantly down-regulated in one of two biological replicates

Accession number:	**Protein name:**	**Regulation state:**	**Function:**
P00697	**Lysozyme C-1**	⇑ R272, KN99α ↑R265	Antibacterial protein, glycoside hydrolase that damages the bacterial cell wall [337], associated with *Plasmodium* parasite persistence during mosquito infection [338].
P50116	**Protein S100-A9**	⇑ KN99α, R265 ↑R272	Major antifungal agent of neutrophil extracellular traps [339]; chelates divalent cations essential for fungal growth [340], promotes the inflammatory response [341], inhibits the function of wound repairing fibroblasts [342].
P08699	**Galectin-3**	⇑ KN99α, R265 ↑R272	Capable of binding a wide range of oligosaccharide structures (including *C. albicans* and cryptococcal 1,2-linked sugars, promotes fungal cell death by both indirect and direct fungicidal mechanisms [343-346].
Q9EQP5	**Prolargin**	⇓R265, R272 ↓ KN99α	Possess antimicrobial peptides that bind to negatively charged bacterial membranes promoting membrane destabilisation and consequent bacterial killing without effecting host cells [347, 348].
O35244	**Peroxiredoxin-6**	⇓ KN99α, R265 ↓R272	Antioxidant enzyme highly expressed in the lungs and a major player in the defence of lungs under oxidative stress in the lung [349, 350], catalyses the reduction of H_2O_2, E-FABP hyperoxides and phospholipid hyperoxides in cell membranes, protecting cells against apoptotic death [351].
P04764	**Alpha-enolase**	⇓R265, KN99α ↓R272	It has been suggested that the expression of alpha enolase on the surface of mammalian cells, and also pathogenic organisms, could function to concentrate plasminogen on the surface of cells, enhancing the cells ability to digest fibrous tissue and/or invade through stroma [352].
Q66H98	**Serum deprivation-response protein**	⇓ R265, KN99α ↓r272	Involved in caveolae formation and stabilisation [353, 354]. The loss of caveolae results in severe pathomorphological defects in large sections of lung alveolar septa, the tissue location where gas exchange takes place.
P85972	**Vinculin**	⇓	Maintains the mechanical integrity of the cytoskeleton and cell shape control, cells

		KN99α,R272 ↓R265	lacking vinculin are unable to produce stable lamellipodia the motor that pulls the cell forward during migration and acts as a steering device during chemotaxis [355-358].
P23785	**Granulins**	⇑R272, R265 ↑ KN99α	In wound fluids granulins acts as an anti-inflammatory via the inhibition of TNF-α activation of inflammatory cells [359].

5.3.7. Ambiguous interesting proteins

Table 5.11 lists the proteins that are more ambiguous in their statistical significance and corresponding regulation state. One or more of the biological replicates for these proteins were found to have expression that was not statistically significant (p-value >0.05), did not meet the >1.2 or <0.8 level of differential expression (as compared to the control lung baseline) or were not detected by the mass spectrometer. Despite the ambiguous nature of the data, the biological functions that these particular proteins represent are interesting and therefore worth mentioning.

Table 5.11: Proteins with ambiguous expression states among biological replicates

Legend:	
⇑	Significantly up-regulated in both biological replicates
↑	Significantly up-regulated in one of two biological replicates
⇓	Significantly down-regulated in both biological replicates
↓	Significantly down-regulated in one of two biological replicates
↔	Not differentially expressed
×	Not detected by the mass spectrometer

Accession number:	**Protein name:**	**Regulation state:**	**Function:**
P55009	**Allograft inflammatory factor 1**	⇑ KN99α ↑R272 ×R265	Plays a crucial role in the survival, migration and proinflammatory activity of macrophages [360].
P07151	**Beta-2-microglobulin**	⇑ KN99α ↑R265, R272	Essential for the cell surface expression of MHC class I, the stability of the peptide-binding groove, antigen presentation and subsequent cytotoxic T cell activation [361], factor in the genesis of pulmonary fibrosis [362-364].
P04762	**Catalase**	⇓ KN99α, R272 ↔R265	Catalyses the decomposition of hydrogen peroxide to water and oxygen, functions to prevent damage to cells and tissues as a result of exposure to hydrogen peroxide.
O88767	**Protein DJ-1**	⇓R265 ↓ KN99α ↑R272)	A stabilizer of Nuclear factor elytroid 2-related factor (NRF2). NRF2 plays a protective role during lung diseases that involve oxidative stress and inflammation via the regulation of the antioxidant defence system [365, 366].
P07632	**Superoxide dismutase [Cu-Zn]**	⇓R265 ↓ KN99α ↑ R272	Catalyses the dismutation of superoxides into oxygen and hydrogen peroxide, is strongly correlated with an increased production and release of hydrogen peroxide from alveolar macrophages represents a novel mechanism for the pathogenesis of pulmonary fibrosis [367].
P41350	**Caveolin-1**	⇓R265 ↑R272 ↑↓ KN99α	Involved in caveolae formation and stabilisation [353, 354]. The loss of caveolae results in severe pathomorphological defects in large sections of lung alveolar septa, the tissue location where gas exchange takes place.

5.4. Discussion

5.4.1. An observable strain hierarchy in response to infection

Observations of general rat health and the progression of lesion development at the early infection time-point revealed a hierarchy of infection severity. KN99α was found to be the most lethal *Cryptococcus* strain to Fisher-344 rats, followed by R265 with R272 being the least lethal. The severity of pulmonary infection with KN99α was so extreme that these infections were not permitted to proceed to the 42-day 'late stage infection' time point. Repeat infections were not possible within the timeframe of this study, however, considerably lower cell numbers would be recommended in any future KN99α inoculations. The lethality hierarchy remains consistent at the late stage infection time-point. While KN99α infection would presumably result in rat death, pulmonary infections with R265 were able to persist through to late stage infection. For rats infected with R272 general health remained stable, with no apparent lesion formation and lung weights similar to control weights. This indicates the possible resolution of infection. These macroscopic examinations are interesting and appear to display a strain-based hierarchy of infection. It was hypothesised that these strain-based differences in the degree of infection reflected the level of host immune responses and were associated with different immunological and physiological processes. The investigation of this hypothesis required the analysis of the molecular processes involved in the host response to pulmonary infection with *Cryptococcus*.

5.4.2. The selection of biologically proteins from datasets generated by iTRAQ

Only proteins found significantly altered in expression in both biological replicates (represented by individual 4-plex iTRAQ runs (5.2.5.)) of rats infected with KN99α, R265 or R272 were included as biologically relevant quantitatively different proteins. For this study statistical significance was judged according to the p-value calculated by the ProteinPilot software (AB SCIEX, USA). P-values were used as an initial indicator of whether a protein had any significance in the context of the iTRAQ investigation of pulmonary infection. The next level of selection criteria used to refine the list of biologically relevant quantitatively different proteins was whether or not they changed in expression >1.2 or <0.8 fold of their level compared to the uninfected control. These are the standard fold change cut-offs used by the Australian Proteome Analysis Facility, where the iTRAQ labelling, mass spectrometry and data acquisition and processing for this study were undertaken. Whilst this study uses the term 'up or down regulation' to describe proteins detected in increased or decreased abundance, there are a number of possible reasons for changes in protein abundance. A change in gene expression is one possibility, but protein abundance in a particular cell extract may also be altered by post-translational modification, degradation or intra-cellular localization.

The application of these two selection criteria revealed a correspondence between the previously described hierarchy of *Cryptococcus* strain lethality (5.4.1.) and a hierarchy associated with the total number of quantitatively different proteins. Rats infected with KN99α, which generated most severe pulmonary infections, generated a list of 170 quantitatively different proteins using the uninfected control lung as a baseline. The less severe infections associated with R265 resulted in 121

quantitatively different proteins while least severe infections with R272 generated the smallest protein list, with only 75 quantitatively different proteins being identified. This observed hierarchy occurred despite the fact that the total number of proteins identified for each iTRAQ run, representing the lungs infected with the different *Cryptococcus* strains, were relatively similar (table 5.6).

5.4.3. Protein function as a selection criterion

The final selection criterion for ranking proteins of interest was the determination of the specific function of an identified protein in the context of pulmonary infection and trauma. While increased or decreased protein expression coupled with statistical significance provides crucial indications as to the effect infection is having on the lung, the degree of expression does not provide a great deal of information about the likely biological effect of this regulation. An accurate assessment of the degree of protein regulation requires additional analysis to ensure accuracy. Due to the limited amount of protein obtained, this additional analysis would be difficult or impossible for the majority of our samples. In this context, to ensure that considerable time was not spent analysing irrelevant proteins, the specific function of an identified protein has been given a greater weight than the degree of positive or negative regulation.

5.4.4. Differentially expressed proteins common to infected lungs

The search for proteins of relevant function revealed that at the early infection time-point there was a subset of proteins that were common to pulmonary infections with KN99α, R265 and R272 (table 5.7). These were significantly differentially expressed in all biological replicates across all infections. Interestingly, it was observed that all

but one of these identified proteins (Alpha-1B-glycoprotein) was uniformly regulated in abundance, meaning they were consistently increased or decreased in expression in all pulmonary infection datasets. This finding strongly suggests that the basic responses to pulmonary infection with *Cryptococcus* of different species and different virulence levels are uniform, regardless of the disease outcome.

Reviews of infectious disease literature suggest that the changes in host gene expression changes are different for bacterial and fungal infections [368, 369], however, the proteins detected in this experiment represent a subset of the host innate immune system involved in the non-specific response to insult. What follows is a discussion of the function of the identified 'interesting common' proteins and what the potential consequences of therapeutic intervention against or with recombinant forms of these proteins could be in the context of pulmonary insult and infection. The proteins have been divided into groups according to the direction of protein expression and function. It should be noted that while there are clearly proteins involved in host defence within this common list, this group of proteins alone was not sufficient to define the host response to the various strains of *Cryptococcus*. Additionally, this group of proteins did not indicate whether the eventual host responses were going to be successful in controlling and eliminating the infection.

5.4.5. Differentially expressed proteins that increased in expression

5.4.5.1. Proteins involved in tissue protection after insult

5.4.5.1.1. 78 kDa glucose-regulated protein

78 kDa glucose-regulated protein (GRP78) is a resident stress protein of the endoplasmic reticulum that belongs to the Hsp70 multi-gene family. In contrast to the

stress proteins Hsp60 and Hsp70, whose surface expression promotes the lysis of injured, pathogen-infected or transformed cells, the surface expression of GRP78 confers resistance to cell lysis by cytotoxic T lymphocytes and TNF [370]. GRP78 has also been demonstrated to protect cells from death via the suppression of oxygen free radical accumulation and the stabilisation of mitochondrial function [371]. There is also evidence that the induction of GRP78 up-regulation has the potential to counterbalance the effects of idiopathic pulmonary fibrosis [372]. The observed up-regulation of GRP78 across all *Cryptococcus* infections suggests that the host is attempting to protect itself from unrelenting cellular destruction as a result of infection-associated stress. It is possible that the development and administration of a recombinant form of GRP78 could help to ameliorate the tissue destruction that occurs during pulmonary infection with *Cryptococcus*.

5.4.5.1.2. Cathepsin D

Cathepsin D is a lysosomal aspartyl protease that has been found to be up-regulated during pulmonary injury by bleomycin, a glycopeptide antibiotic, in primary cultures of rat alveolar epithelial cells [373]. Bleomycin induces sensitivity to oxygen toxicity that results in pulmonary fibrosis, impaired lung function and apoptosis. Li *et al.* (*2004)* demonstrated that apoptosis of alveolar epithelial cell due to exposure to bleomycin required the autocrine expression and proteolytic processing of angiotensinogen to angiotensin II [373]. These authors also provided evidence that cathepsin D is required for the proteolytic processing of angiotensinogen to angiotensin II, and that the blockage of cathepsin D could prevent alveolar epithelial cell apoptosis. The anti-apoptotic activity of cathepsin D could limit the extent of lung

injury, which indicates the potential suitability of this protein as a target for recombinant protein therapy.

5.4.5.2. Proteins involved in the antifungal response and inflammation

5.4.5.2.1. Acidic mammalian chitinase

C. neoformans has a tendancy to induce and promote the progression of allergic inflammation in animal models. Goldman *et al. (2006)* demonstrated that chitinases act as important mediators of IL-13-associated allergic inflammation and airway hyper-responsiveness during chronic infection with *C. neoformans* [374]. Vicencio *et al. (2008)* demonstrated an increased expression of acidic mammalian chitinase (AMCase), a hydrolytic enzyme that degrades chitin via the digestion of glycosidic bonds, in airway epithelial cells and macrophages during chronic pulmonary infection with *C. neoformans* [375]. These results strongly suggest that AMCase acts as an important promoter of allergic inflammation during cryptococcal infections. AMCase has also emerged as a potential diagnostic maker for pulmonary infection with fungal organisms. Vicencio *et a (2008)* demonstrated an increased expression of AMCase during chronic pulmoary infection that was not present with systemic infection [375]. The observable increase in AMCase protein expression has been found to act as an indicator of the initiation of pulmonary fungal infection [376]. The measurement of AMCase in patients suspected to have been exposed to infectious *Cryptococcus* species could be used as a general diagnostic for infection and a trigger for prophylactic antifungal treatment in high-risk cases.

5.4.5.3. Proteins associated with pulmonary surfactant

Pulmonary surfactant is a surface-active lipoprotein complex produced by type II alveolar cells essential for reducing the surface tension in the lungs [377]. Surfactant functions to increase lung compliance, regulates alveolar size and reduces fluid accumulation in the alveoli [377]. These properties of surfactant are afforded by the physiochemical nature of the protein and lipid constituents of the material.

5.4.5.3.1. Fatty acid-binding protein, epidermal

In the lung fatty acid-binding protein, epidermal (E-FABP) has been identified to be involved in the synthesis of dipalmitoylphosphatidylcholine. Dipalmitoylphosphatidylcholine is the most abundant phospholipid component of lung surfactant and contributes the majority of its surface tension reduction properties [378]. Resultantly, E-FABP has been established as an essential factor required for the synthesis of functional surfactant [379]. The up-regulation of E-FABP during infection indicates that the host is either actively increasing the secretion of surfactant to ameliorate the consequences of infection or is being forced to do so by the infective agent. In the latter case, increased surfactant secretion could act as vital supply of nutrients for the infective agent.

5.4.5.3.2. Pulmonary surfactant-associated protein D

Pulmonary surfactant-associated protein D (SP-D) is a hydrophilic surfactant protein that possesses important immune functions for host defence. SP-D, a member of the collectin family of proteins, functions as a pattern recognition molecule involved in the opsonisation of fungal cells for enhanced phagocytosis. This innate immune host response should lead to the destruction of the majority of the microorganism burden.

Cryptococcus cells, however, have been shown to survive within and be liberated alive from macrophages after phagocytosis, which is an important aspect of their infection process [53, 54]. The observations made in this study correlate with results produced by Geunes-Boyer *et al. (2009)* who determined that pre-treatment with SP-D prior to infection with *C. neoformans* increased both fungal phagocytosis and fungal growth in the presence of macrophages [380]. With the knowledge that infection progresses past the 14-day time point for KN99α and R265, it could be concluded that these strains represent examples where the host's immune system could be enhancing fungal pathogenesis and dissemination.

5.4.5.4. Proteins involved in tissue and cell structural modulation

5.4.5.4.1. Macrophage capping protein

The forces required for cell motility in non-muscle cells are provided via regulated dynamic shifts in the concentration and length of actin filaments. Macrophage capping protein (CAP-G) belongs to the gelsolin/villin family of proteins that function to regulate these dynamic shifts. These proteins serve to control the growth and assembly of actin filaments and are capable of determining where new forces for directional cell movement are generated [381]. CAP-G is widely expressed in mammalian cells but is most abundant in macrophages. Macrophages require barbed end actin filament assembly and regulation in order to form pseudopods to ingest and destroy foreign organisms. Witke *et al. (2001)* determined that CAP-G plays an important role in macrophage motility and phagocytosis and that the loss of macrophage capping protein function while not being lethal, resulted in the significant decrease in phagocytosis rates [382].

5.4.6. Differentially expressed proteins that decreased in expression

5.4.6.1. Molecular indicators of reduced ventilation and poor health

5.4.6.1.1. Carbonic anhydrase 1 and 2

Carbonic anhydrases, a large family of zinc metalloenzymes, catalyse the interconversion of carbon dioxide and water to bicarbonate and protons [383]. Carbonic anhydrases function in a number of vital biological processes including the transport of carbon dioxide out of the lungs, cellular respiration and acid-base balance. Coupled with our observation that infected animals were struggling to breath that indicates physical limitations to ventilation, a result of obstruction and/or the destruction of the lung tissue due to fungal infection, the down regulation of carbonic anhydrase 1 and carbonic anhydrase 2 would likely lead to the development of respiratory acidosis. If not adequately expelled through alveolar ventilation, carbon dioxide rapidly accumulates in the lungs. This causes body fluids to become overly acidic and the onset of symptoms including confusion, fatigue, lethargy and shortness of breath [384], which are all observed in rats during severe infection with *Cryptococcus*. The consistent down-regulation of carbonic anhydrase 1 and 2 coupled with the observed physical difficulties with breathing indicates that chronic infection with *Cryptococcus* reduces ventilation at a physical and molecular level.

5.4.6.1.2. Sec14-like protein 3

Sec14-like protein 3, a water-soluble 45 kDa protein secreted by alveolar epithelial cells, functions to maintain airway epithelial cell homeostasis. It has recently been demonstrated that sec14-like protein 3 expression is strongly and inversely associated with the progression of airway inflammation [385]. The decrease in sec14-like protein

3 expression in diseased lung tissue may be caused by damage to the epithelium. Indeed it is believed that the changes in sec14-like protein 3 expression may be triggered by neutrophils and then exacerbated by the infiltration of other inflammatory cells. A practical aspect of this inverse relationship is that the degree of down-regulation of sec14-like protein 3 acts as a quantitative indicator/biomarker of the progression of respiratory inflammation and tissue damage during pulmonary cryptococcosis.

5.4.6.1.3. Periaxin

Periaxin is a cytoskeleton-associated protein that appears to be required during the early deposition and maintenance of peripheral nerve myelin. It appears that periaxin functions to enhance the structural stabilisation of myelin [386]. Mice lacking periaxin, while being able to ensheath and myelinate peripheral axons, where found to subsequently develop severe demyelinating neuropathy [387]. The impairment of the transmission of peripheral nerve impulses can have severe consequences, such as the peripheral nerves being less able to activate muscles, or impairment of the relay of information from sensory cells to the brain. The possible impairment of the transmission of nerve impulses from the brain to the lung and vice versa would have a detrimental effect on the control of respiration.

5.4.6.2. Proteins involved in the antifungal response

5.4.6.2.1. Moesin

Moesin is a member of the ERM superfamily of proteins that are associated with the submembranous cytoskeleton. ERM proteins are widely expressed and localized to membranous protrusions that are important for ligand recognition, signal transduction and motility. Moesin is primarily found in the core of microextensions of leukocytes and endothelial cells where it functions in the dynamic changes in cell shape that take place during attachment, spreading and cell movement. While traditionally being identified as a structural protein, it has recently been proposed that moesin plays an important role in the innate immune response and TLR4-mediated pattern recognition. Tohme *et al. (1999)* and Zawawi *et al. (2011)* demonstrated that moesin acts as a second, independent receptor for LPS on the surface of human monocytes and that LPS binding stimulates a biological response, with the expression of pro-inflammatory cytokines [388, 389]. These data also suggested that moesin acts as a necessary co-receptor for the transduction of the CD14 signal, that is, the recognition of pathogen associated molecular patterns. The observed down regulation of this protein across the three infection types indicates that pulmonary infection with *Cryptococcus* is detrimentally affecting at least one mode of non-host material recognition.

5.4.6.3. Proteins involved in tissue and cell structural modulation

5.4.6.3.1. Advanced glycosylation end product-specific receptor

Advanced glycosylation end product-specific receptor (RAGE) is a 35 kDa transmembrane receptor of the immunoglobulin super family that functions as a pattern recognition receptor [390]. The lungs exhibit a high basal level of expression for RAGE, especially in alveolar type I cells [391, 392]. The interaction between RAGE and its ligands has been demonstrated to activate a proinflammatory effect in innate immunity [393]. RAGE, via an association with the basal cell membrane, promotes and maintains the spread-out morphology of alveolar type I cells. This morphology ensures optimal gas exchange and alveolar stability. The disruption of RAGE has been implicated in the development of a number of pulmonary disorders including cancer and fibrosis [391, 394]. RAGE presents itself as a potential target for therapeutic use, whereby the development and administration of recombinant RAGE could function to maintain pulmonary structure and gas exchange homeostasis during infection.

5.4.6.4. Proteins involved in tissue protection after insult

5.4.6.4.1. Peroxiredoxin-2

In order to minimize damage and death, cells rely on the scavenging of reactive oxygen species by enzymatic and non-enzymatic antioxidant defences. Peroxiredoxins are ubiquitously expressed enzymes that play protective roles against oxidative stress via the reduction of hydrogen peroxide and other reactive oxygen

species [395]. Peroxiredoxin 2 is a relatively abundant, predominant cytoplasmic peroxiredoxin found in mammalian cells that belongs to the 2-Cys subgroup [351]. The observation that peroxiredoxin 2 is downregulated during severe pulmonary infection strongly indicates the occurrence of an oxidant/antioxidant imbalance as a result of infection with *Cryptococcus*.

5.4.6.4.2. Glutathione peroxidase 3

Glutathione peroxidases are widely distributed enzymes that catalyse the reduction of hydrogen peroxide and other peroxides, generated during normal metabolism or oxidative stress, to their corresponding alcohols using glutathione as a substrate [395]. Glutathione peroxidase 3 is found in the plasma (it is the only known Glutathione peroxidase that exists in the extracellular space) and plays a role in maintaining the vasorelaxant and antithrombotic properties of the vascular endothelium [396]. The observed down-regulation of glutathione peroxidase 3 in all infections with *Cryptococcus* strongly indicates an imbalance in the oxidant/antioxidant system that exists during the early stages of pulmonary infection.

5.4.6.4.3. Biglycan

It has been demonstrated *in vitro* that the small leucine-rich proteoglycans decorin and biglycan have the inherent ability to bind to and inhibit the profibrotic function of TGF-β [397]. The anti-fibrotic function of decorin identified *in vitro* carries over to *in vivo* animal models. This is not the case for biglycan; indeed under certain conditions it has been suggested that biglycan could act as a profibrotic agent [397, 398]. The

divergent *in vivo* function of these two similar molecules is a result of their differing tissue localisations. Decorin is bound to collagen where it binds TGF-β and prohibits its interaction with cellular receptors. Biglycan is more closely associated with the pericellular space and cell surface. At this cellular location, biglycan binds TGF-β but does not inhibit its interaction with receptors. Inhibition of the profibrotic function of biglycan and the development and administration of recombinant decorin could act to inhibit the development of excessive fibrous connective tissue during pulmonary infection with *Cryptococcus*.

5.4.7. The case of proteins that fall outside of the selection criteria

Despite the observed hierarchy in the number of statistically significant quantitatively different proteins for the three differing strains of *Cryptococcus*, the total numbers of identified proteins from the lung material from these infections were relatively similar. Furthermore, the identified proteins evident in the original unfiltered lists were surprisingly similar. This was despite the differing infective strains used and the marked differences in ultimate disease outcome. The reasons for the vast majority of identified proteins being excluded from the 'common list' of proteins is largely a result of our experimental design and the methodology used. The decision to specifically target proteins that were statistically significant in all biological replications was intended to increase the stringency of the subsequent analysis. The reality of this approach is the loss of significant amounts of ambiguous but potentially interesting protein data.

The omitted data is ambiguous in that despite being iTRAQ labelled, identified by the mass spectrometer and exhibiting a fold change that falls within the designated

parameters of >1.2 or <0.8, the differential expression of these proteins was not significant (p-value > 0.05) in one or more of the biological replicates. This phenomenon can arise due to a number of factors, including biological variations in peptide levels due to *in vivo* degradation, or artefacts of the technique such as inefficient trypsin digestion, variable iTRAQ labelling or variations in chromatography and mass spectrometric peptide fragmentation and detection. The fact that the p-values of these identified proteins are outside the optimal threshold casts doubt on whether or not the regulation state of the proteins as indicated by iTRAQ labelling are indeed a true representation of the biological states of these proteins during infection.

The iTRAQ samples were prepared using a robust and validated method. iTRAQ has been found to be reproducible when samples are processed together and then analysed in a single iTRAQ run. The experiences encountered in this study are similar to those of other experienced iTRAQ users, including the Australian Proteome Analysis Facility, where our analyses were performed [399]. It is tempting, therefore, to conclude that the proteins identified with high confidence in one strain, but not in another are differentially processed or degraded during the course of the infection. Given the very different outcomes from the three *Cryptococcus* strains it is not unreasonable to conclude that the lung remodelling processes will also be quite different. Despite the ambiguous nature of this specific subset of the obtained data, the question remains as to whether any of these identified proteins could be used to provide either an indication of the host response to infection or therapeutic targets to combat infection. Speculations made from the analysis of this data sub-set require further investigation and experimental validation, as do any deductions made from the 'common list' of proteins. The same criteria of functional relevance were applied to

this protein group (section 5.4.2.), and their potential association with lung infection is discussed below.

5.4.8. Proteins with one or more biological replicates that was not significant

The application of the selection criteria limited the scope of analysis to 26 potentially interesting proteins. Table 5.10 lists proteins that are biologically significant in five out of six biological replicates. This data subset includes antifungal agents (Lysozyme C-1, Protein S100A9, Galectin-3, Prolargin), proteins involved in tissue protection, (Peroxiredoxin-6, Granulins), proteins involved in tissue and cell structure stabilisation (Serum deprivation-response protein, Vinculin) and a protein that is potentially involved in tissue invasion (Alpha enolase). Table 5.11 represents proteins that are more ambiguous in their statistical significance and corresponding regulation state. One or more of the biological replicates for these proteins were found to have expression that was not statistically significant (p-value >0.05), did not meet the >1.2 or <0.8 level of differential expression (as compared to the control lung baseline) or were not detected by the mass spectrometer. Despite the ambiguous nature of the data, the biological functions that these particular proteins represent are interesting. For example, they include proteins involved in the survival of macrophages (Allograft inflammatory factor 1), antigen presentation (Beta-2-microglobulin) and tissue protection (Catalase, Protein DJ-1, Superoxide dismutase [Cu-Zn], Caveolin-1 Caveolin-1). While representing interesting proteins in the context of pulmonary infection, whether these data are trustworthy is questionable. The lack of statistical significance across all the replicates indicates that there is a higher chance that their assigned expression state may be the result of factors other than a true biological

response to *Cryptococcus* pulmonary infection. It is also possible that the clarification of the molecular processes involved in the host response to *Cryptococcus* pulmonary infection requires significantly more biological replicates to "catch" the dynamic response of the host, especially given the variable extent of infection observed across the biological replicates by this study.

5.4.9. Experimental design constrains the elucidation of the host response to infection

This project represents the first attempt at the global elucidation of the host response to *Cryptococcus* pulmonary infection using quantitative proteomic analysis techniques. There have been large scale analyses carried out on lung infections and diseases, however, these were gene expression studies rather than proteomics. The complete lack of large-scale quantitative proteomics studies of lung infection probably reflects the technical difficulties associated with sample preparation. In addition, high quality, reproducible and cost effective proteomic techniques such as iTRAQ have only been widely available in the last 5 years. The experimental design of this PhD project, however, was targeted at the investigation of fungal pathogenesis during pulmonary infection. This required synchronised pulmonary infections with high fungal burdens to ensure maximal fungal cell numbers and the highest possible protein yields. A limitation of this experimental design, in terms of the elucidation of the host response to infection, was that the induction of such severe infection required inoculation with unnaturally large fungal loads followed by relatively long periods of infection. An experimental design that would enable a more realistic appraisal of the host response to *Cryptococcus* infection demands considerably increased animal

numbers and a re-evaluation of fungal load, timing of euthanasia and the analysis platforms utilised.

A more suitable infection model for the targeted study of the host response to fungal infection would include inoculations with more environmentally realistic doses of the infective agent and the inclusion of earlier, and potentially more, time-points for analysis. The common response to infection indicated by the majority of the iTRAQ data obtained indicates that this technology platform may not be ideally suited to interpreting the host response to *Cryptococcus* infections. It is likely that iTRAQ is not sensitive enough to identify relevant proteins that are present at low abundance in a very complex sample. It is also likely that analyses at time-points between 14 days and 42 days will be important in elucidating the strain-specific responses after the initial common response period. The integration of transcriptomic technology platforms into the experimental design may increase the analytical potential in future studies. Transcriptomics involves quantitative analysis of mRNAs using high-throughput techniques based on DNA microarray technology or next generation sequencing. Furthermore, transcriptomics is more applicable to the relatively small sample types generated by our experimentation as mRNA can undergo PCR amplification. Proteins and proteomics lack a PCR equivalent, and thus demand high fungal burdens.

Despite the limitations in the experimental design, a number of proteins have been identified that could potentially act as targets for recombinant protein treatment. There are a growing number of recombinantly expressed and purified proteins being investigated as clinical therapeutic agents for a myriad of diseases. One such example is the intravenous administration of angiotensin-converting enzyme 2 to inactivate angiotensin II, which resulted in the amelioration of LPS induced acute lung injury in

piglets [400]. Coupled with the administration of a suitable antifungal, such as the fungistatic fluconazole, the administration of recombinantly generated and purified forms of proteins could aid in both the inhibition of fungal pathogenesis and the amelioration of lung injury. We have identified a number of proteins that were downregulated during infection and would fall into this class of potential therapeutics. The include moesin (involved in the innate immune system), advanced glycosylation end product-specific receptor (involved in the maintenance of the lung architecture), carbonic anhydrase 1/carbonic anhydrase 2 (involved in lung homeostasis) and biglycan, glutathione peroxidase 3 or peroxiredoxin-2 (involved in tissue protection).

5.4.10. An observable increase in ambiguity at the late stage infection time-point

Inconsistent protein expression is an inherent phenomenon of quantitative proteomics using animal models and is generally indicative of the biological variation between individual members of the animal population being analysed. What was notable in the current analysis was that inconsistency dramatically increased in late stage infection compared with early stage infection. In the early stage infections with R265, 3 of the 136 (2%) significantly differentially expressed proteins were alternatively regulated in the biological replicates. The rate for R272 was slightly higher with 8 of 88 (9%) significantly differentially expressed proteins alternatively regulated. At the late stage of infection this increased to 23 of 102 identified proteins (23%) for R265 and 31 of 46 (67%) identified proteins for R272. Note that infections with KN99α were too aggressive to be permitted to continue to the late stage infection time point.

What is the cause of the rise in inconsistently regulated proteins at the late stage infection time point? Is it a consequence of the differing biological responses of individuals to the stress of infection or differing rate of recovery from infection at the late stage of infection? Unfortunately the experimental design does not permit an adequate answer to this question. At the early stage infection time-point, the proteomic analyses agree with the literature suggesting the host mounts a common response to infection regardless of strain. Between the early and late stages of infection the course of the infections preceded very differently, with KN99α animals requiring early euthanasia, R265 animals progressing to severe but not lethal infection and R272 infections resolving. It is highly likely that the time-point where the response to infection changes from synchronous to asynchronous has been missed. In a similar fashion to the issues with early stage infection, the rectification of this issue requires an improvement to experimental design to better target the host response to infection. This improved design would feature pulmonary infections initiated with more realistic inoculation sizes and an increased number of time-points, especially in the earlier stages of infection and between the early and late stage infection time-points.

5.5. Conclusions

While limited by a number of experimental design issues this study has provided evidence that a global analysis of the complex biological interactions between host and infective agent is possible. The analysis permitted inferences to be drawn regarding the potential therapeutic use of a number of differentially expressed proteins, most likely in a dual role with commercially available antifungal agents,

which could be exploited to ameliorate lung injury as a result of infection. While this study shows that global proteomic analyses of the host response to pulmonary infection with *Cryptococcus* are possible, further comprehensive analysis requires the inclusion of additional infection time points as well as integration of quantitative analytical techniques that are more sensitive than iTRAQ.

Chapter Six

The systemic response to pulmonary infection with *Cryptococcus*

The previous result chapters were restricted in focus to the investigation of Cryptococcus *pathogenesis (chapter 4) and the host responses to pathogenesis (chapter 5) in the context of the pulmonary environment. The aim of the following study was to explore the systemic host response to pulmonary infections with* Cryptococcus*. The experimental design was focused on the quantitative analysis of cytokines, chemokines and growth factors during pulmonary infection with virulent* Cryptococcus*, using naïve control lung as the baseline. This analysis was achieved using the Bio-Plex suspension array system (Bio-Rad, USA).*

6.1. Introduction

Profiling serum cytokine expression levels has been described as a powerful tool that links the systemic host immune defence system with disease pathogenesis [401]. Cytokines are cell-signalling proteins expressed and secreted by a myriad of cells, including those of the immune system. The host immune response to invading pathogens involves a tightly regulated balance between the Th1 (a proinflammatory response that stimulates the cellular immune system), Th17 (recruitment, activation and migration of neutrophils) and Th2 (a generally anti-inflammatory response that stimulates the humoral immune system) patterns of cytokine production. The outcome of infection is heavily dependent on the specific cytokine response mounted by the host after exposure to *Cryptococcus* [86]. The appropriate cytokine production profile promotes removal of the invading pathogen and damaged cells while minimalizing the detrimental impact to the host via the repair of the injured tissue. It has become apparent that the predominant synthesis of Th1 and Th17 cytokines over Th2 cytokines protects mice from cryptococcal infection [147-149]. The detection and quantitative measurement of these immune proteins could provide insight to the physiological state and the responses of the host to cryptococcal infection.

Circulating cytokines levels are generally in the low pg/mL range and are below the detection limit of mass spectrometry-based proteomics. Whilst cytokines can be detected by traditional immunoassays such as ELISA, obtaining data on many cytokines is time consuming and expensive. Multiplexed methods of cytokine detection and quantification provide a number of advantages over traditional single-cytokine measurement systems. The detection and quantification of single cytokines is of limited value given the fact that many cytokines have closely related or overlapping functions. Multiplexed methods also reduce the cost and time of analysis

and use samples more effectively than single-cytokine measurements. The Bio-Plex suspension array system, using xMAP technology licensed from Luminex Corp. by Bio-Rad [402], is one such multiplex analysis system. The technology is based on the flow cytometric analysis of fluorescently colour-coded magnetic microspheres that possess distinct spectral addresses (figure 6.1). The assay is essentially an immunoassay, similar in principle to a sandwich ELISA, supplied on colour coded magnetic beads.

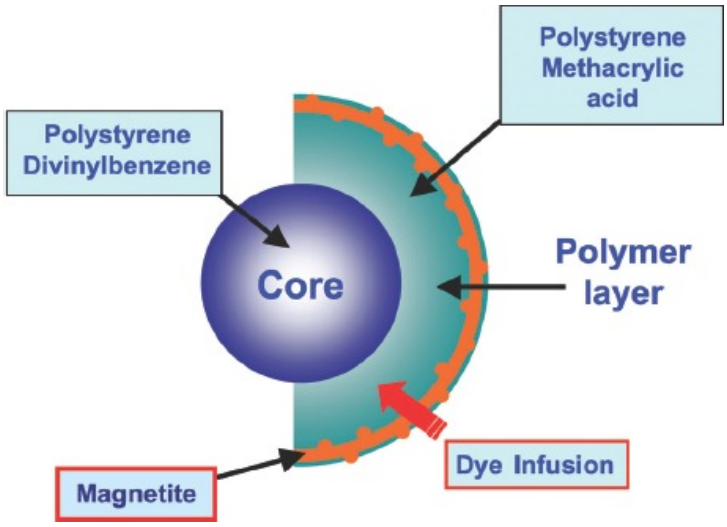

Figure 6.1: Magnetic microsphere architecture (from [234])

The Bio-Plex suspension array system is the most cited xMAP assay in the world [402, 403]. It has been used to analyse cytokine levels in human, mouse and rat biological fluids and tissues including: plasma, serum, adipose interstitial fluid, bronchoalveolar lavage fluid, blister fluid, cerebrospinal fluid, nasal lavage fluid, peritoneal fluid, synovial fluid, colon tissue, kidney tissue, nervous system tissue, spleen tissue and tissue culture supernatant [403]. Bio-Plex has also been used to analyse the supernatants of murine lung tissue homogenates generated following pulmonary infection with *C. neoformans* and *C. gattii* strains. Wormley *et al. (2007)*

investigated the cell-mediated immune responses that are generated during pulmonary infection with *C. neoformans* (H99γ), a strain engineered to produce host Th1 type cytokine interferon gamma (IFN-γ). This study demonstrated that the pro-inflammatory Th1 pattern of cytokine production was significantly higher, while the anti-inflammatory Th2 pattern of cytokine production was significantly lower, in mice infected with H99γ than those infected with wild type H99. This Th1-skewed response resulted in the elimination of primary infection and provided subsequent protection against secondary pulmonary challenge with wild type *C. neoformans*. Similarly, Wozniak *et al. (2011)* used the Bio-Plex suspension array system to demonstrate that while IL-17 may be important for the optimal protection of the host from pulmonary infection with *C. neoformans* (H99γ), the Th1 pattern of cytokine expression is sufficient for protection against infection [404]. Wang *et al. (2011)* also employed the Bio-Plex system to determine the contribution of MyD88 dependent receptors to host defences during pulmonary infection with *C. neoformans* (H99) [405]. MyD88 is an adaptor molecule required for IL-1 and IL-18 signalling pathways and is utilised by toll-like receptors for signalling [405-407]. MyD88 is vital for host defence against infection with *Cryptococcus*, with MyD88-deficient mice exhibiting decreased survival and increase pulmonary fungal burdens [408, 409].

Using lung tissue homogenates, Cheng *et al. (2009)* demonstrated that at 7 days post infection, acknowledged as the time that coincides with the onset of cell-mediated immunity in the mouse model [410], *C. gattii* strain R265 induced considerably lower levels of neutrophil infiltration and reduced inflammatory cytokine production during murine pulmonary infection compared to *C. neoformans* [411]. Cytokine analysis indicated the absence of a clear Th1 type immune response, however they were also not able to find evidence for the development of a Th2 type immune response. The

authors suggested that the hypervirulent *C. gattii* strain responsible for the outbreak of cryptococcosis on Vancouver Island was inducing less protective immunity or suppressing the protective immune responses in mice, permitting the pathogen to thrive in an environment that normally limits the progression of disease.

It has been acknowledged that mice and rats differ in their susceptibility and their immune responses to infection with *Cryptococcus* [133, 411, 412]. Furthermore, the rat model appears to be more similar to humans in susceptibility to pulmonary cryptococcosis than the mouse, and to exhibit some of the clinical features of human pulmonary cryptococcosis [238, 239]. While the previously described studies provide important insights into *Cryptococcus* virulence and the host immune responses to pulmonary infection, all were conducted in the mouse host model. The aim of the work undertaken in this study was to reveal the cytokines, chemokines and growth factors that play a role in the rat host response to *Cryptococcus* pulmonary infection. The underlying hypotheses of the study were that:

- Rats infected with *Cryptococcus* strains of assumed differing virulence would express significantly different cytokine expression profiles.
- The Bio-Plex suspension array system would identify specific cytokines, chemokines and growth factors that highlight:
    - Differences in overall cytokine expression profiles evoked by *Cryptococcus* strains of differing virulence;
    - Specific cytokines or cytokine responses that promote or eliminate infection;
    - Cytokines that could form potential future drug targets, biomarkers and diagnostic markers.

6.2. Methods

6.2.1. *In vitro* growth conditions

The *in vitro* growth conditions used were described in section 2.3.1.

6.2.2. Pulmonary infection model

The pulmonary infection model used was described in section 2.3.2.

6.2.3. Bio-Plex Pro Rat Cytokine, Chemokine, and Growth Factor Assay

6.2.3.1. Sample preparation

Aliquoted serum samples, prepared in section 6.2.2., were removed from -80 °C storage and defrosted. At the same time the buffer components of the Bio-Plex kit were removed from 4 °C storage and warmed to room temperature. The magnetic beads, standard, detection antibody and streptavidin-PE tubes were kept on ice. The standard was reconstituted with 500 µL of sample diluent and left on ice for 30 minutes. 75-100 µL of serum was then transferred to a 0.2 µm Nanosep MF Centrifugal Device with Bio-Inert Membrane (Pall Scientific, USA) and centrifuged at 9,000 g for five minutes (note: 50 µL is required per well and a loss of 5-10 µL is expected as a result of filtration). After centrifugation the columns were checked to ensure that all of the solution had passed through the filter. If not, the centrifugation process was repeated until the entire sample had passed through the filter. Samples of each filtrate were analysed using the Bio-Plex Pro™ Rat Cytokine, Chemokine and Growth Factor 24-plex Assay (Bio-Rad, USA) according to the manufacturer's

instructions. This assay kit included the following cytokines, chemokines and growth factors:

Pro-inflammatory	**Growth factors**	**Chemokines**	**Anti-inflammatory**	**Dual role cytokines**
IFN-γ	IL-7	IL-5	IL-4	IL-2
IL-1α	EPO	GRO/KC	IL-10	IL-6
IL-1β	G-CSF	MIP-1α	IL-13	
IL-12 (p70)	GM-CSF	MIP-3α		
IL-17	M-CSF	RANTES		
IL-18	VEGF			
IFN-γ				
TNF-α				

6.2.3.2. Wash station preparation

All washing procedures were performed on the Bio-Plex Pro II magnetic wash station (Bio-Rad, USA). Following the rinse procedure provided by Bio-Rad, 100 mL of ddH_2O was used to flush the wash station. The wash station was then primed using 30 mL of the Bio-Plex wash buffer.

6.2.3.3. Coupled magnetic bead preparation

Each well required 50 µL of 1 x coupled beads. The 10 x coupled beads were gently resuspended before transferring the required volume (variable depending on number of wells used during analysis). The beads were then diluted to the working solution with assay buffer and kept on ice in the dark.

6.2.3.4. Serial dilution of standards

Eight tubes were labelled S1 to S8 for the standard dilutions. 128 µL of reconstituted standard was added to the first tube (labelled S1) with 72 µL of standard diluent. The sample was then vortexed gently for 1-3 seconds. 50 µL of S1 was then transferred to S2 with 150 µL of standard diluent and then vortexed. This process was repeated until completion of the 8-tube dilution series.

6.2.3.5. Assay procedure

The diluted standards, samples and controls were equilibrated at room temperature for 20 minutes prior to use. The coupled beads were vortexed for 30 seconds at medium speed and then 50 µL transferred to the designated wells of the provided 96-well plate. The 96-well plate was then placed on the magnetic wash station and the coupled beads washed twice with Bio-Plex wash buffer. The diluted standards, samples and controls were briefly and gently vortexed and 50 µL of each were added to the designated wells. The plate was covered and incubated on a shaker at room temperature for one minute at 1,100 rpm. The shaker speed was then reduced to 300 rpm and the samples were incubated for a further 60 minutes.

Ten minutes prior to the completion of the incubation the detection antibody was prepared. Stock 10 x detection antibody was vortexed at medium speed for 20 seconds and diluted to a 1 x working solution (25 µL required per well) with detection antibody diluent. After the completion of the 60 minute shaking incubation (above) the plate was washed three times using the Bio-Plex wash station. Detection antibodies were briefly and gently vortexed and 25 µL transferred to each well. The

covered plate was then placed on the incubating shaker for one minute at 1,100 rpm, followed by 30 minutes at 300 rpm.

During this incubation period the Bio-Plex machine was set up, calibrated and the streptavidin-PE prepared. Stock 100 x streptavidin-PE was vortexed for 20 seconds at medium speed. A 1 x working solution of streptavidin-PE was then prepared with assay buffer (50 µL required per well). Finally, the Bio-Plex software was set up. The identification details for each sample were entered and all calculated standard values were double-checked to match the table supplied with the standard vial.

After completion of the antibody incubation the 96 well plate was placed on the magnetic wash station and the coupled beads washed three times with the Bio-Plex wash buffer. The working solution of streptavidin-PE was vortexed vigorously and 50 µL added to each well. The covered plate was then placed on the incubating shaker for one minute at 1,100 rpm followed by 10 minutes at 300 rpm. The plastic seal was removed, the plate placed on the magnetic wash station and the beads washed three times with the Bio-Plex wash buffer. 125 µL of assay buffer was then added to each well, and the plate was covered and placed on the incubating shaker at 1,100 rpm for 1 minute. The plate was now ready for reading. Data were acquired using the Bio-Plex 200 system with version 5.0 software (Bio-Rad, USA).

6.2.4. Linear regression models

Cytokine expression data were loaded into RStudio (RStudio Inc, USA) and a linear regression model fitted to the data using the following functions and command lines:

6.2.4.1. Loading data

The *data* function specifies the data file to be loaded into RStudio and the format of the data file.

- data=read.csv("filename.csv", header=T, as.is=T)

6.2.4.2. Stacking vectors from a Data Frame

The *stack* function is used to transform the data from a separate column form (produced by the Bio-Plex 200 system with version 5.0 software (Bio-Rad, USA)) into a single column. Essentially, stacking vectors concatenate multiple vectors into a single vector. Factors can be added to indicate where each data point, or data point subgroup, originated. The *colnames* function applies a character vector to the generic stacked data.

- datastack=stack(data[,x:y])
- datastack$Strain=rep(cyto$Strain,y)
- datastack$Time=rep(cyto$Time,y)
- datastack$Strain=as.factor(datastack$Strain)
- colnames(datastack)[2]="Cytokine"
- colnames(datastack)[1]="Fluorescence"

6.2.4.3. Fitting a linear model

The *lm* function is a sophisticated command that computes a linear model that fits the data. The *summary* function produces result summaries of the model fitting functions.

- datatrend=lm(Fluorescence~Time*Strain, subset=(Strain %in% c("KN99", "R272", "R265"))
- summary(datatrend)

6.2.4.4. Plotting the linear model

The *plot* function is a generic command for the plotting of R objects, such as the linear regression model (lm). The *points* function is a generic command that draws a sequence of points at the specified coordinates.

- plot(Fluorescence~Time, subset=(Strain==“R265”), data=datastack, col=1)
- points(Fluorescence~Time, subset=(Strain==“KN99”), data=datastack, col=2)
- points(Fluorescence~Time, subset=(Strain==“R272”), data=datastack, col=3)

6.2.4.5. Adding straight lines (intercept/slope form) to the plot

The *abline* function adds one or more straight lines, specifying the line in intercept/slope form, through the specified coordinates.

- abline(datatrend(Fluorescence~Time, subset=(Strain==“R265”), data=datastack), col=1)
- abline(datatrend(Fluorescence~Time, subset=(Strain==“KN99”), data=datastack), col=2)
- abline(datatrend(Fluorescence~Time, subset=(Strain==“R272”), data=datastack), col=3)

6.2.5. Data analysis

The average concentration of each cytokine was calculated from the biological replicates. The results are presented as the mean ± standard error of the mean (SEM). A two-tailed t-test was used to test the significance between the average concentrations of each cytokine in the disease samples compared to the control samples. P-values <0.05 were considered statistically significant. Only the cytokines that were observed at significantly different concentrations between control and test conditions are presented.

6.3. Results

6.3.1. Cytokine response to pulmonary cryptococcosis: global trends

The fitting of linear regression models to the entirety of the cytokine expression data indicated that the systemic host response to pulmonary infection with *C. gattii* R265 (high virulence) generated a statistically similar cytokine expression profile to that of *C. gattii* R272 (low virulence) (figure 6.2). This was of interest given the differing pulmonary fungal burdens and disease outcomes for animals infected with R265 or R272. Rats infected with R272 appeared in general good health throughout the six-weeks of infection and had minimal lesion development at early stage infection and the complete lack of observable lesions at late stage infection. In contrast, animals infected with R265 exhibited poor health and had large multifocal gelatinous lesions with little remaining normal lung tissue in the affected lungs at both the early and late stage infection time points (section 5.3.2.). Pulmonary infection with *C. neoformans* strain KN99α generated cytokine, chemokine and growth factor expression levels that were significantly higher than those generated by R265 and R272 (figure 6.2). This coincides with the extreme progression of pulmonary infection observed for rats infected with the KN99α.

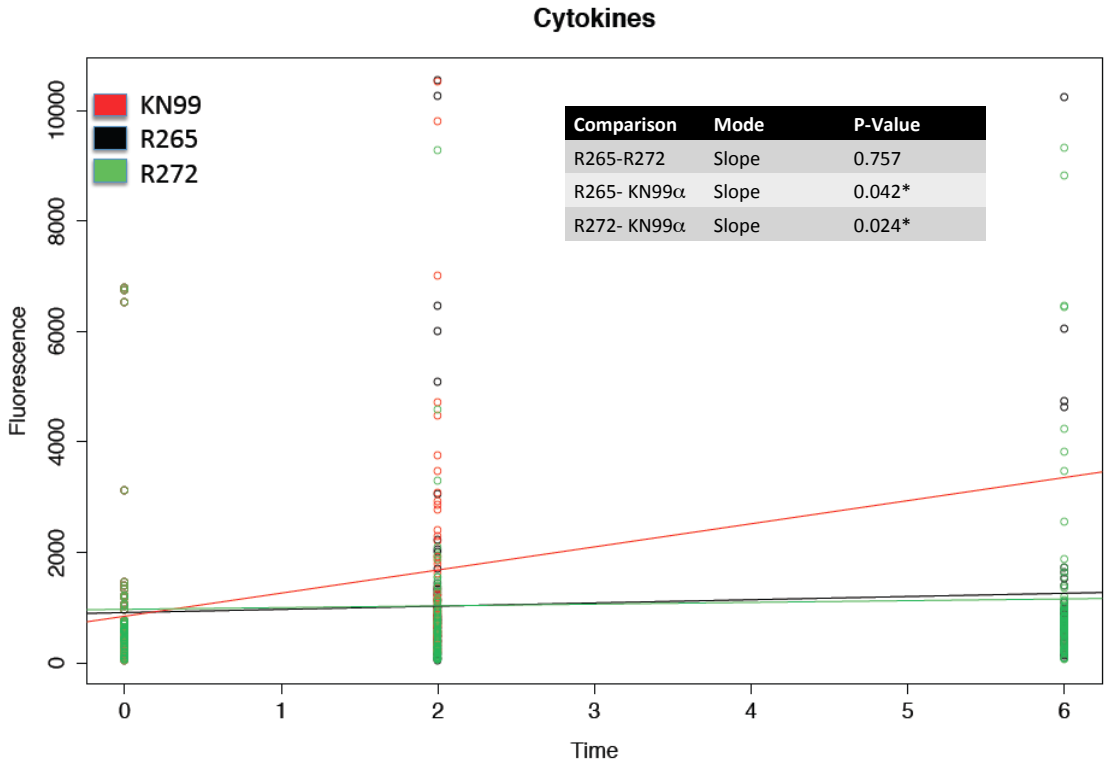

Figure 6.2: Plot generated by RStudio after fitting a linear regression model to the global cytokine, chemokine and growth factor expression data for control and infected rat lung.

P-values refer to whether the slopes, which provide an indication of the cytokine expression trend, are significantly different when comparing strains.

6.3.2. Pro-inflammatory cytokine expression during pulmonary infection

Linear regression models indicated that rats infected with KN99α had significantly higher expression of pro-inflammatory cytokines than those infected with R265 and R272 (figure 6.3). Similar to the global cytokine, chemokine and growth factor data, the expression level of pro-inflammatory cytokines for infections with R265 and R272 were statistically indistinguishable (figure 6.3). These data indicate that a pro-inflammatory environment is promoted by pulmonary infection with virulent strains of *Cryptococcus*.

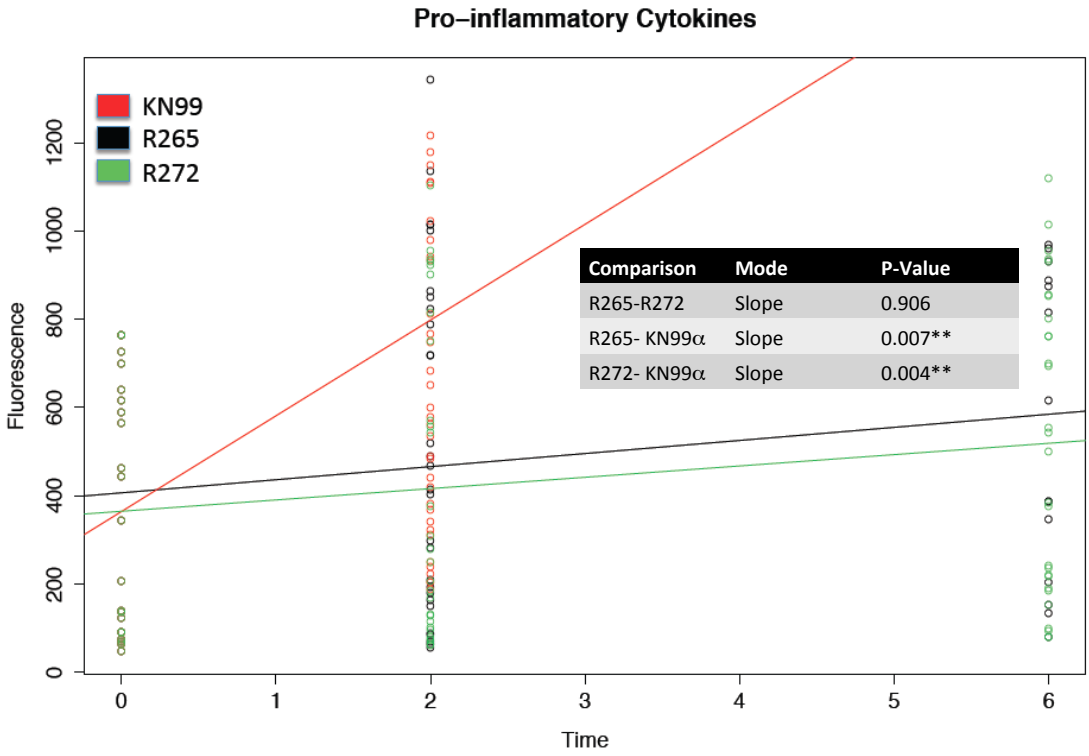

Figure 6.3: Plot generated by RStudio after fitting a linear regression model to the pro-inflammatory cytokine expression data for control and infected rat lung.

P-values refer to whether the slopes, which provide an indication of the cytokine expression trend, are significantly different when comparing strains.

6.3.3. Anti-inflammatory cytokine, chemokine, growth factor and dual role cytokine expression during pulmonary infection

No significant differences in the overall expression of anti-inflammatory, growth factor or dual role cytokines were seen across infections (figure 6.4). There was a significant difference in chemokine expression trends between KN99α and R272 (figure 6.4). For the dual role cytokines, the comparison of KN99α with R265 (p-value 0.069) and R272 (p-value 0.062) were close to statistical significance.

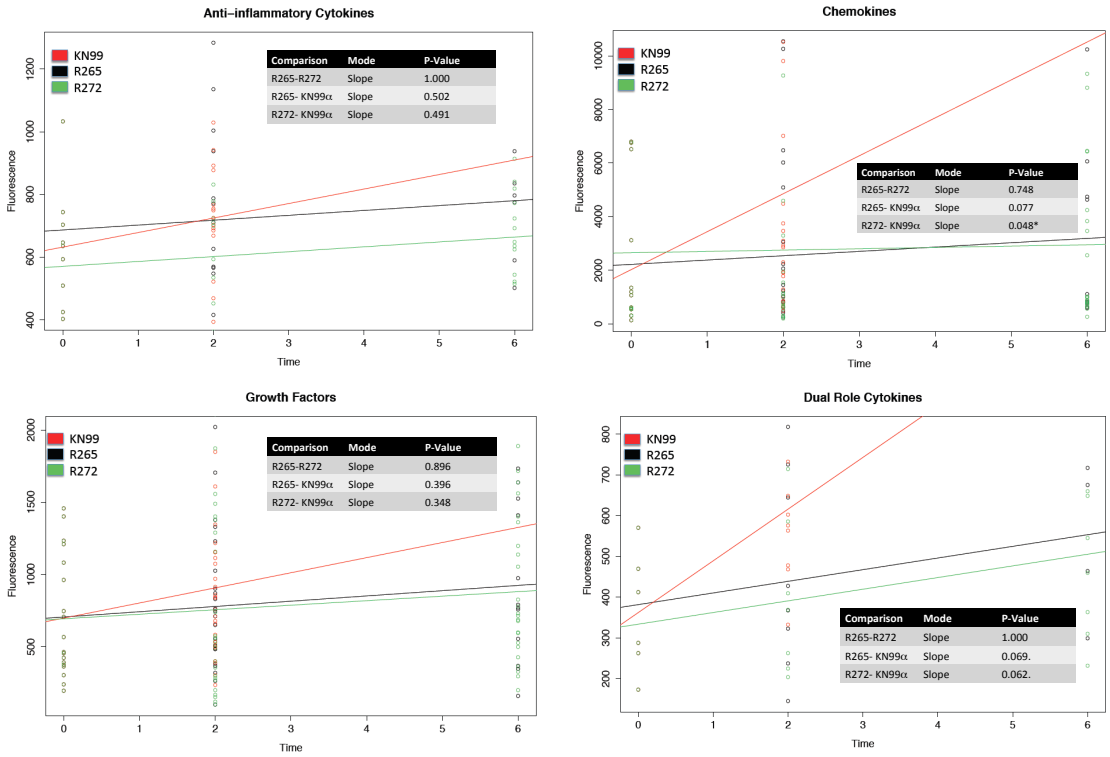

Figure 6.4: Plots generated by RStudio after fitting linear regression models to the anti-inflammatory, chemokine, growth factors and dual role cytokine expression data for control and infected rat lung.

P-values refer to whether the slopes, which provide an indication of the cytokine expression trend, are significantly different when comparing strains.

6.3.4. Differentially expressed cytokines as a result of pulmonary infection with *Cryptococcus*

There was a trend of increased expression for each of the 23 cytokines analysed in rats infected with KN99α, at the early infection time point, although not all cytokines increased significantly. This observed system-wide disruption of normal cytokine expression indicates that aggressive pulmonary infection with KN99α disrupts the systemic homeostasis of the infected animal. The cytokines significantly increased in expression were IL-1α, IL-17, IFN-γ, MIP-1α and TNF-α (figure 6.5). Similar to the

KN99α dataset, only a small subset of the cytokines analysed at early and late stage infection with strain R265 were significantly different in expression. These cytokines were IL-5, IL-17, GRO/KC and MIP-1α, all of which were increased in expression (figure 6.5). The subset of cytokines significantly different in expression for R272 was smaller than for KN99α or R265 and included IL-β, IL-12 and RANTES, all of which were increased in expression (figure 6.5).

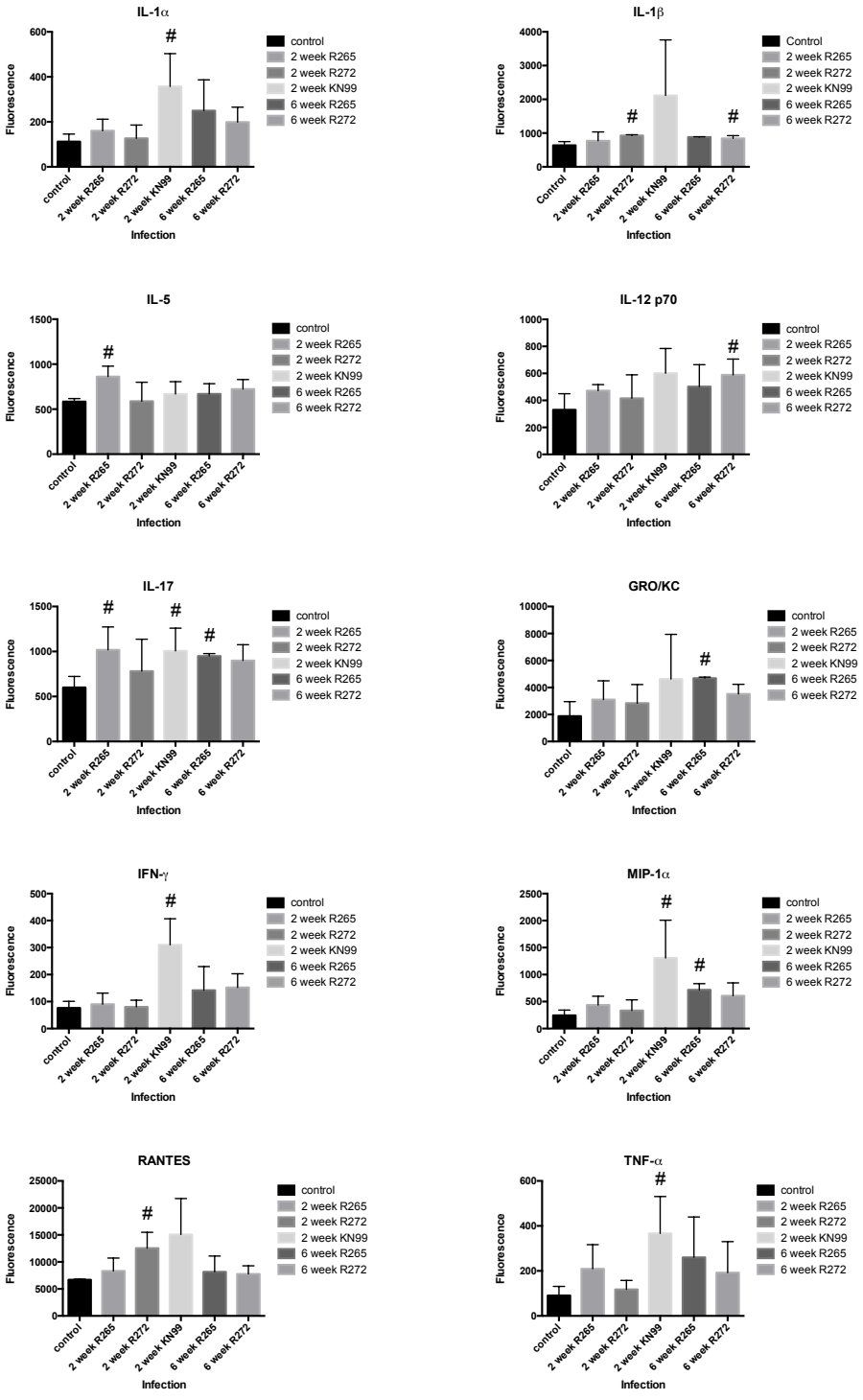

Figure 6.5: Cytokines, chemokines and growth factors found to be significantly different in expression when comparing serum from rats with pulmonary *Cryptococcus* infection to serum from naïve rats.

The cytokines graphed are presented as mean ± standard deviation (n=5) for the control and each infection time point. # indicates the statistically significant strains and time points.

6.4. Discussion

6.4.1. Experimental design considerations

Wormley *et al. (2007)*, Wozniak *et al. (2011)* and Wang *et al. (2011)* demonstrated the ability of the Bio-Plex suspension array system to provide valuable insights to the murine immune responses to pulmonary infection with *C. neoformans* [145, 404, 405]. The vital difference between this study and the aforementioned studies was the severity of pulmonary infection. Wormley *et al. (2007)*, Wozniak *et al. (2011)* and Wang *et al. (2011)* did not report the extreme degree of pulmonary fungal burden as observed for virulent strains of *Cryptococcus* for this study. Given that rats have been observed to be more resistant to pulmonary infection than mice in models of fungal pneumonia [133], the heightened severity of infection observed for this study is likely due to the use of an infectious inoculum aimed a producing maximal pulmonary disease. *Krockenberger et al. (2010)* determined that rats consistently became ill or died following inoculation with $\geq 10^7$ CFU mL^{-1} [239]. The experimental design of this thesis was primarily concerned with obtaining sufficient *Cryptococcus* for quantitative proteome analysis. This led to compromises with respect to obtaining pulmonary tissue samples and datasets. Thus, this study used inoculations of 10^8 CFU mL^{-1} to ensure that pulmonary infection was severe enough to generate fungal burdens sufficient for downstream quantitative proteomic analysis. In contrast, the mouse based studies used inoculation concentrations (10^4 to 10^5 CFU mL^{-1}), consistent with the generation of standard infection in mice. The use of such a high inoculum in this study has resulted in a more progressive pulmonary infection than previously observed [145, 404, 405]. The consequence of increased fungal cell numbers, especially in the pulmonary environment, is the generation of significant amounts of capsular polysaccharide and exopolysaccharide. This is a possible

explanation for the absence of any detailed polysaccharide contamination noted by previous studies.

Cytokines exist at nanomolar to picomolar concentrations that vary significantly in response to trauma or infection. Considering the severe technical issues previously encountered with *Cryptococcus* capsular polysaccharides and exopolysaccharides (chapters 3, 4 and 5) it was likely that any cytokine data obtained from lung homogenates of severely infected rat lungs would be compromised by polysaccharide contamination. It was predicted that the attempted replication of the analysis of supernatants from tissue homogenates would introduce serious analytical challenges. In the place of tissue homogenates, the serum of uninfected control and infected rats was analysed using the Bio-Plex suspension array system. While this did not provide localised tissue information regarding the cytokine profile of the lungs during infection, it had the advantage of providing insight to the systemic response to pulmonary fungal infection.

6.4.2. Linear regression models and the cytokine response to infection

To interpret the general trend of cytokine expression, globally and according to functional categories, linear regression models were fitted to the data. Linear regression models are a type of trend estimation that fits a linear model to the data, independently of anything known about the system being analysed. This provides inferences about the general direction of cytokine expression over time, whether the trend is random or not, and permits comparisons and interpretations on specific sub-populations of the data.

It was originally hypothesized that the systemic cytokine expression profiles generated in response to pulmonary infection with strains of *C. gattii* assumed to be of low (R272) or high (R265) virulence would be significantly different. It was further hypothesized that these differences would provide an indication of the specific cytokine profile that induces the progression or regression of pulmonary infection. The fitting of linear regression models to the cytokine expression data revealed that that the reality of infection does not fit this hypothesis. Linear regression models indicated that the host generates statistically similar overall cytokine expression profiles in response to pulmonary infections with *C. gattii* strains of either high or low virulence. A clear limitation to the fitted linear regression models is that they do not provide an explanation for the differences in pulmonary fungal burden and disease outcome observed for rats infected with these differing strains of *C. gattii*.

This study also hypothesized that there would be an observable difference in the systemic cytokine expression profiles generated in response to pulmonary infection with *C. gattii* vs. *C. neoformans*. The linear regression models fitted to these datasets demonstrated a significant increase in global cytokine, pro-inflammatory cytokine and chemokine expression in response to pulmonary infection with *C. neoformans* strain KN99α compared to infection with *C. gattii* strains. Increases in the expression of cytokines involved in generating an inflammatory environment can be correlated to the extreme degree of symptoms observed for rats infected KN99α. What linear regression models fail to provide is insight with regard to the specific molecules that are responsible for the observable trends and biological outcomes of cytokine expression.

6.4.3. More than regression models

Linear regression models were used to provide general information about the trend of cytokine, chemokine and growth factor expression over time in a strain-specific manner. While expression trends can provide useful inferences about how changes observed during experimentation correlate with the data generated, this form of statistical analysis does not provide specific information that aids in the elucidation of what is causing the correlation. Specifically, this study found that pulmonary infections with R265 and R272 resulted in markedly different pulmonary fungal burdens and disease outcomes, but the linear regression models applied to the cytokine expression data indicated that the host generated similar cytokine expression profiles. It was therefore hypothesised that the analysis of individual cytokines significantly changed in expression would provide insight to the molecular mechanisms responsible for the cytokine expression trends and biological outcomes associated pulmonary cryptococcosis. What follows is the analysis and discussion of the significantly differentially expressed cytokines.

6.4.3.1. IL-1α

IL-1α expression is central to the initiation and persistence of inflammation and the promotion of fever and sepsis [413]. IL-1α is produced largely by activated macrophages; however, neutrophils, epithelial cells and endothelial cells also produce IL-1α. Botelho *et al. (2011)* determined that IL-1α is central to the initiation and exacerbation of smoke-induced neutrophilic inflammation, independently of IL-1β [414]. Botelho *et al. (2011)* also provided evidence that IL-1α is expressed in stable chronic obstructive pulmonary disease (COPD) but that IL-1α expression is increased

in correlation to COPD exacerbation [414]. The current study demonstrated that IL-1α expression was significantly increased at the early stage infection time point of pulmonary infection with KN99α compared to uninfected controls. This suggests the possibility that, in concert with a suitably effective antifungal agent being used to eliminate the fungal pathogen, the targeted inhibition of IL-1α could represent a therapeutic option for the amelioration of the excessive inflammation observed during severe pulmonary infection with highly virulent strains of *Cryptococcus*.

6.4.3.2. IL-1β

Produced by activated macrophages as a pro-protein, IL-1β is proteolytically processed to its active form by caspase 1. The expression of IL-1β is strongly correlated with the expression of the pro-inflammatory cytokine TNF-α in alveolar macrophages. IL-1β is a potent pro-inflammatory cytokine that is vital to processes such as the initial response to infection or sepsis and in systemic diseases [413]. There is evidence that the high expression of IL-1β is inversely related to pulmonary function [415]. Churg *et al.* demonstrated that IL-1β plays a crucial role in the development of murine emphysema and small airway remodelling and suggested that the amelioration of the IL-1β pro-inflammatory response could limit the amount of tissue damage associated with COPD [416]. Similar to COPD, pulmonary infections with virulent strains of *Cryptococcus* are associated with significant tissue remodelling and damage. This study demonstrated that IL-1β expression was significantly increased at early and late stage infection with R272. As with IL-1α, with a suitably effective antifungal agent, the targeted inhibition of IL-1β function

during pulmonary infection with *Cryptococcus* could act to ameliorate the tissue damage associated with the pro-inflammatory response to fungal infection.

6.4.3.3. IL-5

IL-5 is a chemokine (cytokines that have the ability to induce directed chemotaxis in nearby responsive cells) generated by Th2 cells and mast cells. IL-5 has been identified as a key player in the recruitment of eosinophil granulocytes to the site of physiological stimulus during immune responses to respiratory allergens and infections [417]. Eosinophils are not found in the lung under normal conditions and the observation of pulmonary eosinophilia is generally indicative of disease [418]. Eosinophil activation and subsequent degranulation leads to the release of a number of cationic granule proteins, reactive oxygen species, lipid modulators, enzymes, growth factors and cytokines that are either directly toxic to the infective agent, and the host, or promote a toxic environment for pathogen eradication. Eosinophils have also been implicated in antigen presentation to T-cells [419].

Domachowske *et al. (2002)* demonstrated that phenotypically normal eosinophils could be recruited to sites of physiological stimulus in an environment completely devoid of IL-5 [420]. This suggests the presence of distinct subsets of IL-5-dependent and independent eosinophils at the site of physiological stimulus under normal physiological conditions. Similarly, Foster *et al. (2001)* concluded that IL-5 is primarily responsible for the allergen-induced expansion of pre-existing eosinophil populations [421]. Coupled, these findings suggest that IL-5 plays a prominent role in eosinophil activation, maturation and survival rather than in direct eosinophil recruitment. Domachowske *et al. (2002)* even speculated that IL-5 might play a role

in the more negative aspects of eosinophil biology. IL-5 has been implicated in eosinophil overproduction and the prolonged viability of eosinophils in asthmatic and allergic lung tissue. This study demonstrated that the expression of IL-5 was significantly increased at early stage infection with R265. An improved understanding of the role of IL-5 in eosinophil recruitment and function could permit the future regulation of the eosinophilic inflammatory response to the benefit of the host.

6.4.3.4. IL-12 p70

IL-12 p70 is a heterodimeric cytokine, consisting of the two subunits p35 and p40, produced by dendritic cells and phagocytes after microbial or cytokine stimulation [422]. IL-12 p70, which is also known as T cell stimulating factor, is directly involved in the differentiation of naïve T cells into Th1 cells and the subsequent generation of a proinflammatory environment [423]. IL-12 p70 induces the production of IFN-γ and TNF-α from T cells (CD8+ cytotoxic T lymphocytes) and natural killer cells. This cytokine also reduces IL-4, an anti-inflammatory cytokine that induces the differentiation of naïve helper T cells to Th2 cells. The production of IFN-γ leads to both the killing of targeted cells, be it foreign or host cells, and anti-angiogenic activities [424].

Duckett *et al. (2005)* demonstrated that intact IL-12 p70 was pivotal for the protection of mice against pulmonary infection with the gram-negative bacterium *F. tularensis* [425]. Pre-treatment with exogenous IL-12 p70, which acts as a strong inducer of IFN-γ in the lungs, provided increased protection against lethal respiratory bacterial infections. Inoculation with IL-12 p70 did not prevent dissemination nor did it influence survival during an already established infection [425]. The protective immunity provided by IL-12 p70 pre-treatment was dependent on the presence of

IFN-γ and CD8 cells. While the precise mechanisms for IL-12 p70 activated CD8 T cell protection from intracellular bacterial infection remains enigmatic, it has been speculated that infection is controlled by the lysis of infected macrophages. Similar to *Cryptococcus, F. tularensis* is an intracellular pathogen that targets macrophages. It is speculated that the destruction of a niche growth environment, that is, host macrophages, limits the potential of infectious agent pathogenesis. Kawakami *et al. (1996)* demonstrated that the early administration of IL-12-induced IFN-γ production in the lungs of mice infected with *C. neoformans* led to increased murine survival rates [426]. This study demonstrated that expression of IL-12 p70 was significantly increased at late stage infection with R272. At this time point infection appeared to be resolved. These results indicate that the pre-treatment of individuals from environments of high infection risk with IL-12 p70 represents a potential preventative therapeutic option to limit *Cryptococcus* infection.

6.4.3.5. IL-17

IL-17, which is also known as IL-17A, is a pro-inflammatory cytokine produced by Th17 type cells, γδ T cells, $CD8^+$ T cells, NKT cells, NK cells and neutrophils [404]. IL-17 is the defining cytokine for Th17 cells. The secretion of IL-17 generates a positive feedback loop causing undifferentiated CD4+ cells to differentiate into TH17 cells. Th17 cells are potent inducers of inflammatory mediators such as TNF-α, IL-1β, and IL-6. IL-17 also acts as a potent mediator of chemokine production that recruits monocytes and neutrophils to the site of inflammation in a similar fashion to IFN-γ. It has been demonstrated that Th17 cells are able to bridge the innate and adaptive immune responses [427]. Th17 cells act as a "backstop" for the immune system in that they are recruited when the Th1 and Th2 cells cannot eliminate pathogens [428].

The role that Th17 cells and IL-17 play with regard to susceptibility or resistance to fungal infections remains enigmatic. It has been demonstrated that the neutralization of IL-17 during oral candidiasis [429] and pulmonary aspergillosis [430] results in decreased neutrophil infiltration, reduced levels of chemokines and antimicrobial expression and increased fungal burden [427]. Conversely, it has been demonstrated that Th17 cell activation promotes deleterious inflammation and defective fungal clearance in pulmonary aspergillosis and gastrointestinal candidiasis [431, 432]. Wormley *et al. (2007)* demonstrated that mice infected with IFN-γ-producing, but not wild type, *C. neoformans* (H99) had an increased production of IL-17 that elicited protective host immunity against pulmonary cryptococcosis [145]. Wozniak *et al. (2011)* confirmed that IL-17 expression, which was increased during infection and resulted in the resolution of acute infection with wild-type *C. neoformans*, was dependent on IFN-γ receptor signalling. Additionally, Wozniak *et al. (2011)* suggest that the observed immune response to infection with *C. neoformans* was more likely associated with the Th1 type immune response than the Th17 type immune response [404]. This study demonstrated that IL-17 expression was significantly increased at early stage infection with KN99α and R265 and at late stage infection with R265. The observed increase in IL-17 expression may represent an attempt by the host to provide a "backstop" or supplementary effector for the immune system due to the failure of the Th1 type host response to effectively eliminate the most virulent infective agents.

6.4.3.6. GRO/KC

GRO/KC expression was significantly increased in expression at late stage infection with R265. GRO/KC, which is also known as CXCL1, is a potent neutrophil

chemoattractant that has been found to be essential to the recruitment of neutrophils to the lungs during pathogen infection [433]. Inbred SJL/J mice generate a heightened pro-inflammatory response to infection and are resistant to infection with *Cryptococcus*. Guillot *et al. (2008)* determined that inbred SJL/J mice significantly increased the expression of TNF-α and KC/GRO during infection [434]. As previously discussed, the Th1 type immune response is protective against infection with *Cryptococcus*. While it is known that TNF-α is a proinflammatory cytokine that promotes the Th1 type immune response, the exact role of the neutrophil chemokine KC/GRO in host defence against fungal infection is far from clear.

6.4.3.7. IFN-γ

IFN-γ is a crucial pro-inflammatory cytokine whose expression defines Th1 type immune cells and promotes the Th1 type immune response. IFN-γ is produced by a myriad of cells including CD4+ T helper cell type 1 lymphocytes, CD8+ cytotoxic lymphocytes, NK cells, B cells, NKT cells and professional antigen presenting cells (i.e. macrophages, dendritic cells) [435]. An increase in IFN-γ production is generally associated with a greater resistance to bacterial, viral and fungal infections. IFN-γ production is initiated by macrophage pathogen recognition that induces macrophage secretion of both IL-12 and chemokines. The chemokines recruit immune cells to the site of inflammation while IL-12 secretion promotes IFN-γ synthesis by these recruited immune cells. The expression of IL-12 and IL-18 further promotes the synthesis of IFN-γ in macrophages, NK cells and T cells [435].

Using strains of *C. neoformans* engineered to produce host IFN-γ, Wormley *et al. (2007)* [404] and Hardison *et al. (2010)* [436] independently demonstrated that the

expression of IFN-γ stimulated the local Th1-type cell mediated immunity. The result was the development of protective host immunity against pulmonary infection. Conversely, animals infected with wild type strains of *C. neoformans* generated a Th2-type response to infection, resulting in the progression of disease [145, 436]. This study found IFN-γ to be significantly increased in expression at early stage infection with KN99α. The induction of IFN-γ production, or the development of a recombinant IFN-γ therapeutic, to generate the Th1-type response to infection has the potential to act as a therapeutic option for protection against pulmonary infection with virulent strains of *Cryptococcus*.

6.4.3.8. MIP-1α

Macrophage Inflammatory Protein 1-alpha (MIP-1α) expression was significantly increased at early stage infection with KN99α and late stage infection with R265. MIP-1α is a pro-inflammatory chemokine generated by macrophages, dendritic cells and lymphocytes after stimulation by pathogen endotoxins. MIP-1α plays a major role in the recruitment and activation of a myriad of immune cells, including granulocytes (such as neutrophils, eosinophils and basophils) as well as T cells and natural killer cells, to the site of physiochemical stimulation [437]. MIP-1α also induces the synthesis and expression of other proinflammatory cytokines such as IL-1, IL-6 and TNF-α from fibroblasts and macrophages. Fittingly, MIP-1α is crucial for the effective and efficient immune response towards infection and inflammation [438].

6.4.3.9. RANTES

Regulated on Activation, Normal T cell Expressed and Secreted (RANTES) was increased in expression at early stage infection with R272. RANTES is a vital pro-inflammatory chemokine that acts to recruit leukocytes to the site of infection and/or inflammation. RANTES appears to have a dual role with regard to Th1 and Th2 type immune responses. This chemokine has been implicated in both the IFN-γ dominant Th1 response and also in eosinophilic disease that is driven by Th2 type responses [439-441]. There is, however, strong evidence that RANTES is essential for driving inflammation during respiratory syncytial virus infection [441] and in the recruitment of Th1 cells to the lungs for protective granuloma formation during pulmonary infection with *Mycobacterium tuberculosis* [442]. Blocking the action of RANTES could be beneficial in mitigating the detrimental effects of an overbearing pro-inflammatory immune response. Conversely, supplementing the immune system with RANTES during the early stages of infection could result in the more efficient recruitment of immune cells to the site of infection/inflammation, the promotion of the IFN-γ dominant Th1 response and the eradication of disease. Due to the apparent divergent roles of RANTES in relation promotion of either the Th1 or Th2 type response, the exact therapeutic potential of this cytokine for infections with *Cryptococcus* remains enigmatic.

6.4.3.10. TNF-α

Tumor necrosis factor (TNF-α) expression was significantly increased at early stage infection with KN99α. TNF-α is a potent pro-inflammatory protein produced by activated macrophages, CD4+ lymphocytes and NK cells. TNF-α is an endogenous

pyrogen that is involved in the regulation of immune cells and acts to induce apoptotic cell death, sepsis, cachexia and inflammation. The expression of TNF-α, and the subsequent induction of systemic inflammation, acts to inhibit pathogen replication. TNF-α is a key member of the group of cytokines that stimulate the acute phase response. The maximal production of TNF-α during fungal pulmonary infections is dependent on the presence of IL-12 and IL-18.

Filler *et al. (2005)* demonstrated that TNF-α knockout mice are susceptible to fungal pulmonary infection [443]. While macrophage and neutrophil recruitment appeared normal, the recruited immune cells were unable to comprehensively deal with the pathogenic fungi. These data suggest that TNF-α is essential for the promotion of a Th1 type immune response and the enhancement of leukocyte killing of pathogenic organisms. Mehrad *et al. (1999)* determined that mice treated with anti-TNF-α antibodies exhibited diminished neutrophil recruitment to the sight of infection during pulmonary fungal infection [444]. Coupled, these studies suggest that TNF-α is vital for the recruitment of immune cells to the sight of fungal infection and for augmenting the antifungal capacity of the recruited immune cells.

6.4. Conclusions

The analysis of host cytokine expression in response to pulmonary infection with virulent *Cryptococcus* strains indicated that the systemic response to pulmonary infection is largely a Th1 type and/or Th17 type immune response. A pro-inflammatory Th1 type cell mediated immune response, which is augmented by the generation of the Th17 immune response, is believed to be essential for protection of

the host from infection with virulent intracellular pathogens, including *Cryptococcus*. This study observed a significant increase in the expression of a number of cytokines reported to be fundamental to the initiation and promotion of pro-inflammatory Th1 and Th17 immune responses. While infection with low virulence R272 was eradicated by late stage infection, pulmonary infections generated with the highly virulent KN99α and R265 strains of *Cryptococcus* progressed aggressively. These observations suggest that Th1 and Th17 type immune responses are unable to resolve infections with highly virulent strains of *Cryptococcus*.

Similar to the study conducted by Cheng *et al. (2009),* this study indicated that the host is able to detect *C. neoformans* more readily than *C. gattii*, regardless of *C. gattii* type. Cheng *et al. (2009)* demonstrated that *C. gattii* induced lower levels of neutrophil infiltration and reduced inflammatory cytokine production during murine pulmonary infection compared to *C. neoformans* [411]. While lacking pulmonary infiltration data, the current study highlighted a significant increase in global, pro-inflammatory cytokine and chemokine expression in response to pulmonary infection with *C. neoformans* strain KN99α compared to infection with *C. gattii* strains. Cheng *et al. (2009)* correlated reduced inflammatory cytokine production during pulmonary infection with *C. gattii* to the apparent generation of the less protective Th2 type immune response. It is more likely in the current study that the significant increase in inflammatory cytokine production in response to KN99α is due to a Th1 overreaction. A major caveat to the findings made by this study is that infection was produced by a large inoculum of *Cryptococcus* cells, which may have overwhelmed the host response and triggered a damaging, overactive Th1 response. Replication of this study with more appropriate infective doses is required to elucidate how cytokine expression relates to the outcome of infection.

The extreme nature of the observed pulmonary fungal burdens and disease outcomes for infections with KN99α and R265 suggest that the Th1 and Th17 immune responses may actually be promoting fungal pathogenesis. It has been previously demonstrated that the incubation of rabbit pulmonary macrophages with TNF-α, a potent pro-inflammatory cytokine assumed to be paramount to host protection from fungal infection, led to increased *A. fumigatus* phagocytosis rates and enhanced fungal clearance [445]. Unlike *A. fumigatus, Cryptococcus* can survive and undergo phenotypic switching within macrophages, enhancing the development of the virulence factors paramount to fungal replication and dissemination. Unfortunately this study, either by the analysis of cytokine expression trends or individual cytokine expression, was unable to determine what affords the highly virulent KN99α and R265 strains with the survival advantages apparently lacking in the eradicated low virulence R272. Elucidation of these survival advantages requires the *in vivo* analysis, be it genomic, transcriptomic or proteomic, of the *Cryptococcus* infective agent, which has proven to be technically challenging.

Chapter Seven

General discussion

This chapter discusses the findings of this doctoral thesis and proposes further work that warrants pursuing.

7.1. Fungal pathogens - the emerging threat

Fungal diseases represent an emerging threat to human, animal and plant health. The chilling statement made by microbiologist and immunologist Arturo Casadevall that "Fungi are the only group of organisms that have been convincingly shown to cause extinction" [446] exemplifies the dire consequences of unmitigated fungal disease [447]. *C. gattii* has emerged as pathogenic fungus of concern. In 1999, highly virulent strains of *C. gattii* were identified as causing widespread pulmonary infection and the death of otherwise healthy hosts on Vancouver Island, British Columbia, Canada [448]. Since 1999, *C. gattii* has caused an expanding epidemic of human and animal infection and death. As of December 2010, *C. gattii* was associated with 338 confirmed human infections and 40 deaths [40, 447, 448]. The Vancouver Island outbreak represents the largest documented population of *C. gattii* infected people in the world [447, 449]. The initial outbreak on Vancouver Island has spread to mainland British Columbia and further south into the Pacific northwest of the United States of America [40]. Disease as a result of *C. gattii* infection is currently under public health surveillance in the United States of America, becoming reportable as of Autumn 2011 in Oregon and Washington [450]. This means that healthcare providers and laboratories must collect and retain specific information on each case and report the information to the appropriate public health authority.

This study set out to identify the global proteome changes that occur in *Cryptococcus* and mammalian host lung tissue during pulmonary infection with *Cryptococcus* of different species and different virulence levels using quantitative proteomic analysis platforms. It was hypothesised that the identification of significantly expressed, biologically relevant *Cryptococcus* or mammalian proteins could be exploited as

future therapeutic or diagnostic targets. The use of the mammalian model of infection to determine the *in vivo* molecular mechanisms of fungal pathogenesis and the host response to infection introduced several significant technical challenges. These technical challenges inhibited the integration of alternative "-omics" analyses, such as genomics and transcriptomics, with proteomics to further elucidate fungal pathogenesis and host-pathogen interactions.

7.2. The elucidation of *Cryptococcus* pathogenesis and the host response to infection requires a holistic approach

Combined, the emergence of highly virulent strains of *C. gattii* in environments outside their geographical niche and the limited availability of diagnostic and treatment strategies for infection with *Cryptococcus*, have prompted research into this previously overlooked fungal pathogen. There is particular interest in determining the molecular mechanisms responsible for fungal pathogenesis, and the host response to fungal infection. Most studies of fungal pathogenesis have taken a reductionist perspective, whereby a specific molecular process is studied in isolation, with limited analysis of the broader biological system. Understanding invasive fungal infection requires the comprehensive investigation of the complex interactions between host and the pathogen. This requires the quantitative analysis of a large number of functionally diverse genes, proteins and metabolites [451]. Systems biology is an emerging approach to biomedical and biological research. This generally involves biology-based interdisciplinary experimentation that focuses on the holistic analysis of the complex interactions within biological systems [452]. The evolution of

integrated, high-throughput, systems-oriented approaches to understanding the mechanisms that underlie infection and immune response are improving the analysis of these complex systems [453].

To date the *in vivo* study of the interplay between fungal pathogens and the host at the level of the genome, transcriptome and proteome remains limited [451]. The primary challenges are the highly complex nature of pathogen-host interactions and the limited number of methods available for the separation of fungal and host material (that is, DNA, RNA and protein) [451]. Most "-omics" studies of fungal pathogenesis have focused on fungi grown under controlled *in vitro* or *ex vivo* conditions. While these studies have been able to use global comparative analysis platforms to identify genes [454-459], proteins [272, 460, 461] and pathways of relevance to human-pathogenic fungi, such as *Aspergillus fumigatus, Candida albicans* and *Cryptococcus*, they cannot capture the complexity of *in vivo* infection. Several studies have attempted to broaden their analysis by determining the proteome changes that occur in cultured host cells after exposure to fungal pathogens in tandem with the investigation of the proteome changes that occur in the fungus itself [462-464]. While increasing the perspective of analysis, this *in vitro* approach does not replicate the complex host environment and thus limits the interpretation of how fungi respond to *in vivo* infection. The current study attempted to use a systems biology approach, focused primarily on proteomic analyses, to study *Cryptococcus* pathogenesis and the host reposes to pulmonary infection using the rat model.

7.3. *Cryptococcus* protein extraction protocols - a work in progress

The research presented in this thesis demonstrated that lyophilisation of *Cryptococcus* reduced the high level of structural integrity provided by the polysaccharide capsule, allowing for subsequent mechanical cellular disruption. This study also demonstrated that phenol protein extraction could largely prevent the inhibitory effects of non-protein capsule contamination. Despite these advances, the optimal removal of non-protein contaminants remains the primary issue associated with *Cryptococcus* obtained from pulmonary infection. Additionally, this study demonstrated that despite extensive washing procedures rat proteins continued to contaminate the preparation of intracellular *Cryptococcus* proteins from pulmonary infection. The co-identification of rat and *Cryptococcus* proteins gave clear evidence that the proteomes remained mixed.

Despite these technical challenges, this is the first study to successfully extract and identify intracellular *Cryptococcus* proteins from mammalian pulmonary infection. One of the most significant achievements of this study was the proof of concept for the global "-omics" analysis of *Cryptococcus* obtained from *in vivo* sources. Furthermore, the qualitative comparison of *in vitro* and *in vivo C. gattii* offered insights into fungal pathogenesis at the protein level and highlighted a number of *Cryptococcus* proteins that could be exploited as potential drug targets, biomarkers and diagnostic markers. Future work from this study should include continued protocol development aimed at the complete amelioration of polysaccharide contamination and contaminating rat proteins. This requires further research to discover more suitable disassociating agents that can be used before and after cellular disruption, or the development of suitable de-capsulation techniques prior to cellular

disruption. The advances made should lead to future quantitative analyses of *Cryptococcus*, and other fungal pathogens, under *in vivo* conditions.

7.4. Comparative proteomics revealed lung proteins of biological relevance

During *in vitro* and *in vivo* growth *Cryptococcus* continuously sheds polysaccharide capsule into the extracellular surroundings. These exopolysaccharides represent a significant non-protein contaminant that inhibited the proteomic analysis of host tissue infected with *Cryptococcus*. Acidic protein extraction protocols reduced the effects of exopolysaccharide contamination, and it would be of interest to now determine whether phenol extraction of proteins could more effectively remove the exopolysaccharides. Unfortunately, experiments involving phenol protein extraction were undertaken after the completion of the work involving the iTRAQ analysis of control and infected host tissue.

iTRAQ comparative proteomics suggested that the fundamental response of the host to pulmonary infection with *Cryptococcus* is uniform, regardless of infecting species, level of virulence, or disease outcome. This study highlighted the potential of inhibiting *Cryptococcus* pathogenesis by supplementation of the host with recombinant lung proteins. The work in this study provides further evidence that global proteomic approaches can be used to identify potential drug targets, biomarkers and diagnostic markers from *in vivo* mammalian infection models. Future work based on this study would involve the validation of expression states for the proteins identified as being biologically relevant. This can be achieved using 2-D PAGE,

Western blot or multiple reaction monitoring (targeted quantitative mass spectrometry) [465, 466]. Validation work would then be followed by *in vitro* and *in vivo* experimentation to deduce the physiological effects of protein function modulation (ranging from function deletion to recombinant protein supplementation) on both the animal model utilised and on fungal pathogenesis. While these experimental processes are time consuming and demanding on resources, the results obtained would provide comprehensive insight into the function of an identified protein and its potential as a drug target.

7.5. The systemic cytokine response to infection

In the current study, infection with *C. neoformans* resulted in significant increases in global cytokine, pro-inflammatory cytokine and chemokine expression compared to infection with *C. gattii*. This agrees with previous studies that have suggested that the host more readily detects *C. neoformans* than *C. gattii* [411]. Unfortunately, the current study was unable to determine why the highly virulent strains KN99α and R265 had a survival advantage over the low virulence strain R272, which was eradicated. Pulmonary infection with virulent *Cryptococcus* progressed, despite an increase in expression of cytokines, chemokines and growth factors that should result in the infection inhibition and/or eradication of infection. This study indicates that host response alone cannot eradicate disease with highly virulent strains of *Cryptococcus*. The eradication of infection with highly virulent strains of *Cryptococcus* requires effective diagnostic and treatment strategies. The development of said strategies has not kept pace with the emergence of cryptococcosis. The discovery of novel therapies requires an improved understanding of host-pathogen

interactions, which could be accomplished via future integrated "-omics" analyses of how *Cryptococcus* behaves under host conditions.

7.6. Is there a relationship between pulmonary *Cryptococcus* infection and COPD?

Chronic obstructive pulmonary disease (COPD) is defined by characteristically low airflow on lung function tests that is poorly reversible and progressively worse over time [467, 468]. In reality COPD refers to two main conditions, emphysema and chronic bronchitis [467]. Emphysema is a long-term progressive condition where the tissue supporting the physical shape and function of alveolar and surrounding tissue is destroyed [366]. Chronic bronchitis, the chronic inflammation of the bronchi, increases the thickness of the walls of the airways and induces the overproduction of mucus, both of which can lead to airway obstruction. The severity of COPD has been directly linked to the presence of an oxidant/antioxidant imbalance in lungs, with an increased oxidant burden contributing to epithelial damage [469]. COPD has become a global epidemic and is likely to become the third largest cause of death worldwide by 2020 [470]. Traditionally, COPD is caused by the inhalation of noxious particles or gases that trigger abnormal inflammatory responses in the lung [471].

Observations made by this study, of general rat health and the progression of infection at the early and late stage infection time points, suggest that pulmonary infection with virulent strains of *Cryptococcus* could fall under the general description of COPD. Fungi are not considered classical irritants associated with the development of COPD,

however, pulmonary infections with virulent *Cryptococcus* strains generates symptoms consistent with COPD:

- There is a severe limitation to the normal functions of the pulmonary system that gets worse over time.
- The physiology of the lungs is affected. This was indicated by the comparison of uninfected control and diseased lung morphology at the macroscopic scale and by iTRAQ data that identified proteins involved in cell and tissue remodelling. Similarly to emphysema, alteration of the physical nature of the lungs induced by infection with *Cryptococcus* corresponds with a high level of tissue damage and destruction.
- Similar to chronic bronchitis, infection with virulent *Cryptococcus* strains induces acute and chronic inflammation in the lung tissue and associated airways. Additionally, this study identified proteins (including cytokines) that indicate the progression of airway inflammation.
- iTRAQ data obtained in this study indicated that there was an increased oxidant burden in the pulmonary environment, which is known to exacerbate COPD.

While not entirely falling under the scope of COPD, observations by this study at the macroscopic and molecular level suggest that rat pulmonary infection with virulent *Cryptococcus* strains exhibit the signs and symptoms associated with COPD. This suggests that that pulmonary cryptococcosis could be considered a type of COPD. As with cryptococcosis, COPD has no cure. Furthermore, diagnosis of COPD is limited to lung function tests, chest X-ray or CT scans and arterial blood gas tests that only indicate disease once symptoms are severe [472]. The amelioration of COPD and cryptococcosis requires diagnostic advancements that are capable of identify early

stage disease. Subsequent induction of therapeutic options in early stage disease would limit the development of severe pulmonary tissue inflammation and destruction that are associated with these emerging diseases.

7.7. Conclusions

The most significant achievements made by this study were the advances in protocol development. This study also demonstrates that systems-oriented approaches to understanding invasive *Cryptococcus* infection have the ability to identify molecules of biological relevance to pulmonary cryptococcosis. It is hoped that, given continued protocol development, the advances made by the current study will permit future integration of proteomics analyses of *in vivo* fungal infection with genomics, transcriptomics and other alternative "-omics" analysis platforms. The integrated "-omics" analysis of fungal pathogens and the host responses to infection under *in vivo* conditions should make it possible to uncover the molecular and cellular dynamics of the complex host-pathogen interactions. Additionally, it is hoped that these future integrated studies will lead to the development of novel therapeutic and diagnostic options that are so desperately required to meet the growing threat of emerging fungal pathogens.

Chapter Eight

References

1. Jiang, B., H. Bussey, and T. Roemer, *Novel strategies in antifungal lead discovery.* Current Opinion in Microbiology, 2002. **5**(5): p. 466-471.
2. Casadevall, A. and P.J. R., *Cryptococcus neoformans*. 1999, Washington, DC: ASM Press.
3. Carter, D., et al., *Fungal proteins important in animal infection*, 2009, National Health and Medical Research Council: University of Sydney, Australia.
4. Kamareddine, L., et al., *Expression of trypsin modulating oostatic factor (TMOF) in an entomopathogenic fungus increases its virulence towards Anopheles gambiae and reduces fecundity in the target mosquito.* Parasit Vectors, 2013. **6**: p. 22.
5. Weingarten, P., et al., *Application of proteomics and protein analysis for biomarker and target finding for immunotherapy.* Methods Mol Med, 2005. **109**: p. 155-74.
6. Wang, K., et al., *Chemistry-based functional proteomics for drug target deconvolution.* Expert Rev Proteomics, 2012. **9**(3): p. 293-310.
7. Kniemeyer, O., et al., *Identification of virulence determinants of the human pathogenic fungi Aspergillus fumigatus and Candida albicans by proteomics.* Int J Med Microbiol, 2011. **301**(5): p. 368-77.
8. Cooper, R.A. and D.J. Carucci, *Proteomic approaches to studying drug targets and resistance in Plasmodium.* Curr Drug Targets Infect Disord, 2004. **4**(1): p. 41-51.
9. Sleno, L. and A. Emili, *Proteomic methods for drug target discovery.* Curr Opin Chem Biol, 2008. **12**(1): p. 46-54.
10. Kirk, P.M., Cannon, P. F., Minter, D. W. and Stalpers, J . A., ed. *Dictionary of the Fungi*. 2008, CABI Publishing.
11. Hawksworth, D.L., *The fungal dimension of biodiversity: magnitude, significance and conservation.* Mycological Research, 1991. **95**(6): p. 641-55.
12. Steenbergen, J.N. and A. Casadevall, *The origin and maintenance of virulence for the human pathogenic fungus Cryptococcus neoformans.* Microbes Infect, 2003. **5**(7): p. 667-75.
13. Taylor, L.H., S.M. Latham, and M.E. Woolhouse, *Risk factors for human disease emergence.* Philosophical transactions of the Royal Society of London. Series B, Biological sciences, 2001. **356**(1411): p. 983-9.
14. Findley, K., et al., *Phylogeny and phenotypic characterization of pathogenic Cryptococcus species and closely related saprobic taxa in the Tremellales.* Eukaryot Cell, 2009. **8**(3): p. 353-61.
15. Lester, S.J., et al., *Cryptococcosis: update and emergence of Cryptococcus gattii.* Vet Clin Pathol, 2011. **40**(1): p. 4-17.
16. Casadevall, A. and J.R. Perfect, *Cryptococcus neoformans*. 1998, Washington, DC: American Society for Microbiology.
17. Kwon-Chung, K.J. and J.C. Rhodes, *Encapsulation and melanin formation as indicators of virulence in Cryptococcus neoformans.* Infect Immun, 1986. **51**(1): p. 218-23.
18. Blaschke-Hellmessen, R., *[Cryptococcus species--etiological agents of zoonoses or sapronosis?].* Mycoses, 2000. **43 Suppl 1**: p. 48-60.
19. Lagrou, K., et al., *Zoonotic transmission of Cryptococcus neoformans from a magpie to an immunocompetent patient.* J Intern Med, 2005. **257**(4): p. 385-8.

20. Nosanchuk, J.D., et al., *Evidence of zoonotic transmission of Cryptococcus neoformans from a pet cockatoo to an immunocompromised patient.* Ann Intern Med, 2000. **132**(3): p. 205-8.
21. Idnurm, A., et al., *Deciphering the model pathogenic fungus Cryptococcus neoformans.* Nature reviews. Microbiology, 2005. **3**(10): p. 753-64.
22. Lortholary, O., et al., *Long-term outcome of AIDS-associated cryptococcosis in the era of combination antiretroviral therapy.* AIDS, 2006. **20**(17): p. 2183-91.
23. Zaragoza, O., et al., *Fungal cell gigantism during mammalian infection.* PLoS Pathog, 2010. **6**(6): p. e1000945.
24. Idnurm, A., et al., *Deciphering the model pathogenic fungus Cryptococcus neoformans.* Nat Rev Microbiol, 2005. **3**(10): p. 753-64.
25. Xu, J., R. Vilgalys, and T.G. Mitchell, *Multiple gene genealogies reveal recent dispersion and hybridization in the human pathogenic fungus Cryptococcus neoformans.* Mol Ecol, 2000. **9**(10): p. 1471-81.
26. Kwon-Chung, K.J., et al., *Proposal to conserve the name Cryptococcus gattii against C. hondurianus and C. bacillisporus (Basidiomycota, Hymenomycetes, Tremellomycetidae).* Taxon, 2002. **51**: p. 804-6.
27. Kwon-Chung, K.J. and A. Varma, *Do major species concepts support one, two or more species within Cryptococcus neoformans?* FEMS Yeast Res, 2006. **6**(4): p. 574-87.
28. Sorrell, T.C., *Cryptococcus neoformans variety gattii.* Med Mycol, 2001. **39**(2): p. 155-68.
29. Fraser, J.A., et al., *Recapitulation of the sexual cycle of the primary fungal pathogen Cryptococcus neoformans var. gattii: implications for an outbreak on Vancouver Island, Canada.* Eukaryot Cell, 2003. **2**(5): p. 1036-45.
30. Garcia-Hermoso, D., G. Janbon, and F. Dromer, *Epidemiological evidence for dormant Cryptococcus neoformans infection.* J Clin Microbiol, 1999. **37**(10): p. 3204-9.
31. Ellis, D.H. and T.J. Pfeiffer, *Natural habitat of Cryptococcus neoformans var. gattii.* J Clin Microbiol, 1990. **28**(7): p. 1642-4.
32. MacDougall, L., et al., *Spread of Cryptococcus gattii in British Columbia, Canada, and detection in the Pacific Northwest, USA.* Emerg Infect Dis, 2007. **13**(1): p. 42-50.
33. Kwon-Chung, K.J. and J.E. Bennett, *High prevalence of Cryptococcus neoformans var. gattii in tropical and subtropical regions.* Zentralbl Bakteriol Mikrobiol Hyg A, 1984. **257**(2): p. 213-8.
34. Lindberg, J., et al., *Cryptococcus gattii risk for tourists visiting Vancouver Island, Canada.* Emerg Infect Dis, 2007. **13**(1): p. 178-9.
35. Ma, H., *Intracellular parasitism of macrophages by Cryptococcus*, in *School of Biosciences*2009, The University of Birmingham: Birmingham. p. 192.
36. Faganello, J., et al., *Identification of genomic differences between Cryptococcus neoformans and Cryptococcus gattii by Representational Difference Analysis (RDA).* Med Mycol, 2009. **47**(6): p. 584-91.
37. Kidd, S.E., et al., *Comparative gene genealogies indicate that two clonal lineages of Cryptococcus gattii in British Columbia resemble strains from other geographical areas.* Eukaryot Cell, 2005. **4**(10): p. 1629-38.
38. Vanbreuseghem, R. and M. Takashio, *An atypical strain of Cryptococcus neoformans (San Felice) Vuillemin 1894. II. Cryptococcus neoformans var.*

gattii var. nov. Annales des societes belges de medecine tropicale, de parasitologie, et de mycologie, 1970. **50**(6): p. 695-702.
39. Byrnes, E.J., 3rd, et al., *Molecular evidence that the range of the Vancouver Island outbreak of Cryptococcus gattii infection has expanded into the Pacific Northwest in the United States.* The Journal of infectious diseases, 2009. **199**(7): p. 1081-6.
40. Datta, K., et al., *Spread of Cryptococcus gattii into Pacific Northwest region of the United States.* Emerg Infect Dis, 2009. **15**(8): p. 1185-91.
41. Kidd, S.E., et al., *Cryptococcus gattii dispersal mechanisms, British Columbia, Canada.* Emerg Infect Dis, 2007. **13**(1): p. 51-7.
42. Fraser, J.A., et al., *Same-sex mating and the origin of the Vancouver Island Cryptococcus gattii outbreak.* Nature, 2005. **437**(7063): p. 1360-4.
43. Kidd, S.E., et al., *A rare genotype of Cryptococcus gattii caused the cryptococcosis outbreak on Vancouver Island (British Columbia, Canada).* Proc Natl Acad Sci U S A, 2004. **101**(49): p. 17258-63.
44. Khasnis, A.A. and M.D. Nettleman, *Global warming and infectious disease.* Archives of medical research, 2005. **36**(6): p. 689-96.
45. St Louis, M.E. and J.J. Hess, *Climate change: impacts on and implications for global health.* American journal of preventive medicine, 2008. **35**(5): p. 527-38.
46. Zell, R., *Global climate change and the emergence/re-emergence of infectious diseases.* International journal of medical microbiology : IJMM, 2004. **293 Suppl 37**: p. 16-26.
47. Casadevall, A., *Fungal virulence, vertebrate endothermy, and dinosaur extinction: is there a connection?* Fungal Genet Biol, 2005. **42**(2): p. 98-106.
48. Garcia-Solache, M.A. and A. Casadevall, *Global Warming Will Bring New Fungal Diseases for Mammals.* mBio, 2010. **1**(1).
49. Chayakulkeeree, M. and J.R. Perfect, *Cryptococcosis.* Infect Dis Clin North Am, 2006. **20**(3): p. 507-44, v-vi.
50. Hatch, T.F., *Distribution and deposition of inhaled particles in respiratory tract.* Bacteriol Rev, 1961. **25**: p. 237-40.
51. Buchanan, K.L. and J.W. Murphy, *What makes Cryptococcus neoformans a pathogen?* Emerg Infect Dis, 1998. **4**(1): p. 71-83.
52. Tucker, S.C. and A. Casadevall, *Replication of Cryptococcus neoformans in macrophages is accompanied by phagosomal permeabilization and accumulation of vesicles containing polysaccharide in the cytoplasm.* Proc Natl Acad Sci U S A, 2002. **99**(5): p. 3165-70.
53. Ma, H., et al., *Expulsion of live pathogenic yeast by macrophages.* Curr Biol, 2006. **16**(21): p. 2156-60.
54. Alvarez, M. and A. Casadevall, *Phagosome extrusion and host-cell survival after Cryptococcus neoformans phagocytosis by macrophages.* Curr Biol, 2006. **16**(21): p. 2161-5.
55. Feldmesser, M., S. Tucker, and A. Casadevall, *Intracellular parasitism of macrophages by Cryptococcus neoformans.* Trends Microbiol, 2001. **9**(6): p. 273-8.
56. Alvarez, M. and A. Casadevall, *Cell-to-cell spread and massive vacuole formation after Cryptococcus neoformans infection of murine macrophages.* BMC Immunol, 2007. **8**: p. 16.
57. Ma, H., et al., *Direct cell-to-cell spread of a pathogenic yeast.* BMC Immunol, 2007. **8**: p. 15.

58. Santangelo, R., et al., *Role of extracellular phospholipases and mononuclear phagocytes in dissemination of cryptococcosis in a murine model.* Infect Immun, 2004. **72**(4): p. 2229-39.
59. Charlier, C., et al., *Evidence of a role for monocytes in dissemination and brain invasion by Cryptococcus neoformans.* Infect Immun, 2009. **77**(1): p. 120-7.
60. Chretien, F., et al., *Pathogenesis of cerebral Cryptococcus neoformans infection after fungemia.* J Infect Dis, 2002. **186**(4): p. 522-30.
61. Huang, S.H. and A.Y. Jong, *Cellular mechanisms of microbial proteins contributing to invasion of the blood-brain barrier.* Cell Microbiol, 2001. **3**(5): p. 277-87.
62. Chang, Y.C., et al., *Cryptococcal yeast cells invade the central nervous system via transcellular penetration of the blood-brain barrier.* Infect Immun, 2004. **72**(9): p. 4985-95.
63. Velagapudi, R., et al., *Spores as infectious propagules of Cryptococcus neoformans.* Infect Immun, 2009. **77**(10): p. 4345-55.
64. Su, C., et al., *Recent expansion of Toxoplasma through enhanced oral transmission.* Science, 2003. **299**(5605): p. 414-6.
65. Grigg, M.E., et al., *Success and virulence in Toxoplasma as the result of sexual recombination between two distinct ancestries.* Science, 2001. **294**(5540): p. 161-5.
66. Ngamskulrungroj, P., et al., *Association between fertility and molecular sub-type of global isolates of Cryptococcus gattii molecular type VGII.* Med Mycol, 2008. **46**(7): p. 665-73.
67. Goddard, M.R., H.C. Godfray, and A. Burt, *Sex increases the efficacy of natural selection in experimental yeast populations.* Nature, 2005. **434**(7033): p. 636-40.
68. Grimberg, B. and C. Zeyl, *The effects of sex and mutation rate on adaptation in test tubes and to mouse hosts by Saccharomyces cerevisiae.* Evolution; international journal of organic evolution, 2005. **59**(2): p. 431-8.
69. Wickes, B.L., et al., *Dimorphism and haploid fruiting in Cryptococcus neoformans: association with the alpha-mating type.* Proc Natl Acad Sci U S A, 1996. **93**(14): p. 7327-31.
70. Tscharke, R.L., et al., *Haploid fruiting in Cryptococcus neoformans is not mating type alpha-specific.* Fungal Genet Biol, 2003. **39**(3): p. 230-7.
71. Steen, B.R., et al., *Temperature-regulated transcription in the pathogenic fungus Cryptococcus neoformans.* Genome research, 2002. **12**(9): p. 1386-400.
72. Rosa e Silva, L.K., et al., *Identification of novel temperature-regulated genes in the human pathogen Cryptococcus neoformans using representational difference analysis.* Research in microbiology, 2008. **159**(3): p. 221-9.
73. Kraus, P.R., et al., *Identification of Cryptococcus neoformans temperature-regulated genes with a genomic-DNA microarray.* Eukaryotic cell, 2004. **3**(5): p. 1249-60.
74. Odom, A., et al., *Calcineurin is required for virulence of Cryptococcus neoformans.* EMBO J, 1997. **16**(10): p. 2576-89.
75. Yeh, H. and J.F. Markmann, *Transplantation: Are calcineurin inhibitors safer than mTOR inhibitors?* Nat Rev Nephrol, 2013. **9**(1): p. 11-3.
76. Vincenti, F., *Are calcineurin inhibitors-free regimens ready for prime time?* Kidney Int, 2012. **82**(10): p. 1054-60.

77. Steinbach, W.J., et al., *Harnessing calcineurin as a novel anti-infective agent against invasive fungal infections.* Nat Rev Microbiol, 2007. **5**(6): p. 418-30.
78. Cox, G.M., et al., *Extracellular phospholipase activity is a virulence factor for Cryptococcus neoformans.* Mol Microbiol, 2001. **39**(1): p. 166-75.
79. Cox, G.M., et al., *Urease as a virulence factor in experimental cryptococcosis.* Infect Immun, 2000. **68**(2): p. 443-8.
80. Missall, T.A., M.E. Pusateri, and J.K. Lodge, *Thiol peroxidase is critical for virulence and resistance to nitric oxide and peroxide in the fungal pathogen, Cryptococcus neoformans.* Mol Microbiol, 2004. **51**(5): p. 1447-58.
81. Jacobson, E.S., N.D. Jenkins, and J.M. Todd, *Relationship between superoxide dismutase and melanin in a pathogenic fungus.* Infect Immun, 1994. **62**(9): p. 4085-6.
82. Fromtling, R.A., H.J. Shadomy, and E.S. Jacobson, *Decreased virulence in stable, acapsular mutants of cryptococcus neoformans.* Mycopathologia, 1982. **79**(1): p. 23-9.
83. Chang, Y.C. and K.J. Kwon-Chung, *Complementation of a capsule-deficient mutation of Cryptococcus neoformans restores its virulence.* Mol Cell Biol, 1994. **14**(7): p. 4912-9.
84. Kwon-Chung, J.K. and J.E. Bennett, *Medical Mycology*. 1992, Philadelphia: Lea & Febiger.
85. Pool, A., et al., *Neurovirulence of Cryptococcus neoformans determined by time course of capsule accumulation and total volume of capsule in the brain.* J Neurovirol, 2013. **19**(3): p. 228-38.
86. Voelz, K. and R.C. May, *Cryptococcal interactions with the host immune system.* Eukaryot Cell, 2010. **9**(6): p. 835-46.
87. Monari, C., F. Bistoni, and A. Vecchiarelli, *Glucuronoxylomannan exhibits potent immunosuppressive properties.* FEMS Yeast Res, 2006. **6**(4): p. 537-42.
88. Gates, M.A., P. Thorkildson, and T.R. Kozel, *Molecular architecture of the Cryptococcus neoformans capsule.* Mol Microbiol, 2004. **52**(1): p. 13-24.
89. Maxson, M.E., et al., *Radial mass density, charge, and epitope distribution in the Cryptococcus neoformans capsule.* Eukaryot Cell, 2007. **6**(1): p. 95-109.
90. McFadden, D.C., et al., *Capsule structural heterogeneity and antigenic variation in Cryptococcus neoformans.* Eukaryot Cell, 2007. **6**(8): p. 1464-73.
91. Reese, A.J. and T.L. Doering, *Cell wall alpha-1,3-glucan is required to anchor the Cryptococcus neoformans capsule.* Mol Microbiol, 2003. **50**(4): p. 1401-9.
92. Reese, A.J., et al., *Loss of cell wall alpha(1-3) glucan affects Cryptococcus neoformans from ultrastructure to virulence.* Mol Microbiol, 2007. **63**(5): p. 1385-98.
93. Bose, I., et al., *A yeast under cover: the capsule of Cryptococcus neoformans.* Eukaryot Cell, 2003. **2**(4): p. 655-63.
94. Zaragoza, O. and A. Casadevall, *Experimental modulation of capsule size in Cryptococcus neoformans.* Biol Proced Online, 2004. **6**: p. 10-15.
95. Zaragoza, O., B.C. Fries, and A. Casadevall, *Induction of capsule growth in Cryptococcus neoformans by mammalian serum and CO(2).* Infect Immun, 2003. **71**(11): p. 6155-64.
96. McFadden, D., O. Zaragoza, and A. Casadevall, *The capsular dynamics of Cryptococcus neoformans.* Trends in microbiology, 2006. **14**(11): p. 497-505.

97. Frases, S., et al., *Capsule of Cryptococcus neoformans grows by enlargement of polysaccharide molecules.* Proc Natl Acad Sci U S A, 2009. **106**(4): p. 1228-33.
98. Yoneda, A. and T.L. Doering, *Regulation of Cryptococcus neoformans capsule size is mediated at the polymer level.* Eukaryot Cell, 2008. **7**(3): p. 546-9.
99. Zaragoza, O., et al., *The polysaccharide capsule of the pathogenic fungus Cryptococcus neoformans enlarges by distal growth and is rearranged during budding.* Mol Microbiol, 2006. **59**(1): p. 67-83.
100. Zaragoza, O., et al., *Capsule enlargement in Cryptococcus neoformans confers resistance to oxidative stress suggesting a mechanism for intracellular survival.* Cell Microbiol, 2008. **10**(10): p. 2043-57.
101. Garcia-Rivera, J., et al., *Cryptococcus neoformans CAP59 (or Cap59p) is involved in the extracellular trafficking of capsular glucuronoxylomannan.* Eukaryot Cell, 2004. **3**(2): p. 385-92.
102. Maxson, M.E., et al., *The volume and hydration of the Cryptococcus neoformans polysaccharide capsule.* Fungal Genet Biol, 2007. **44**(3): p. 180-6.
103. McFadden, D., O. Zaragoza, and A. Casadevall, *The capsular dynamics of Cryptococcus neoformans.* Trends Microbiol, 2006. **14**(11): p. 497-505.
104. Staib, F., *Cryptococcus neoformans und Guizotia abyssinica* Zeitschrift fur Hygiene, 1962. **148**: p. 466-75.
105. Shaw, C.E. and L. Kapica, *Production of diagnostic pigment by phenoloxidase activity of cryptococcus neoformans.* Appl Microbiol, 1972. **24**(5): p. 824-30.
106. Ngamskulrungroj, P. and W. Meyer, *Melanin production at 37°C is linked to the high virulent Cryptococcus gattii Vancouver Island outbreak genotype VGIIa.* Australasian Mycologist 2009. **28**: p. 9-15.
107. Polacheck, I., Y. Platt, and J. Aronovitch, *Catecholamines and virulence of Cryptococcus neoformans.* Infect Immun, 1990. **58**(9): p. 2919-22.
108. Wong, B., et al., *Production of the hexitol D-mannitol by Cryptococcus neoformans in vitro and in rabbits with experimental meningitis.* Infect Immun, 1990. **58**(6): p. 1664-70.
109. Chaturvedi, V., et al., *Stress tolerance and pathogenic potential of a mannitol mutant of Cryptococcus neoformans.* Microbiology, 1996. **142 (Pt 4)**: p. 937-43.
110. Gordon, M.A. and D.K. Vedder, *Serologic tests in diagnosis and prognosis of cryptococcosis.* JAMA, 1966. **197**(12): p. 961-7.
111. Frases, S., et al., *Cryptococcus neoformans capsular polysaccharide and exopolysaccharide fractions manifest physical, chemical, and antigenic differences.* Eukaryot Cell, 2008. **7**(2): p. 319-27.
112. Denning, D.W., et al., *Elevated cerebrospinal fluid pressures in patients with cryptococcal meningitis and acquired immunodeficiency syndrome.* Am J Med, 1991. **91**(3): p. 267-72.
113. D'Souza, C.A. and J. Heitman, *It infects me, it infects me not: phenotypic switching in the fungal pathogen Cryptococcus neoformans.* J Clin Invest, 2001. **108**(11): p. 1577-8.
114. Fries, B.C. and A. Casadevall, *Serial isolates of Cryptococcus neoformans from patients with AIDS differ in virulence for mice.* The Journal of infectious diseases, 1998. **178**(6): p. 1761-6.

115. Fries, B.C., et al., *Phenotypic switching of Cryptococcus neoformans occurs in vivo and influences the outcome of infection.* J Clin Invest, 2001. **108**(11): p. 1639-48.
116. Jain, N., et al., *Phenotypic switching in a Cryptococcus neoformans variety gattii strain is associated with changes in virulence and promotes dissemination to the central nervous system.* Infect Immun, 2006. **74**(2): p. 896-903.
117. Jain, N. and B.C. Fries, *Phenotypic switching of Cryptococcus neoformans and Cryptococcus gattii.* Mycopathologia, 2008. **166**(4): p. 181-8.
118. Guerrero, A., et al., *Phenotypic switching in Cryptococcus neoformans.* Microbiology, 2006. **152**(Pt 1): p. 3-9.
119. Casadevall, A., J.N. Steenbergen, and J.D. Nosanchuk, *'Ready made' virulence and 'dual use' virulence factors in pathogenic environmental fungi--the Cryptococcus neoformans paradigm.* Curr Opin Microbiol, 2003. **6**(4): p. 332-7.
120. Steenbergen, J.N., H.A. Shuman, and A. Casadevall, *Cryptococcus neoformans interactions with amoebae suggest an explanation for its virulence and intracellular pathogenic strategy in macrophages.* Proc Natl Acad Sci U S A, 2001. **98**(26): p. 15245-50.
121. Janeway, C.A.J., *Evolution of the immune system: past, present and future*, in *Immunobiology*, C.A.J. Janeway, et al., Editors. 2001, Garland Publishing: New York. p. 567-611.
122. Del Poeta, M., *Role of phagocytosis in the virulence of Cryptococcus neoformans.* Eukaryot Cell, 2004. **3**(5): p. 1067-75.
123. Shoham, S. and S.M. Levitz, *The immune response to fungal infections.* Br J Haematol, 2005. **129**(5): p. 569-82.
124. Sabiiti, W., R.C. May, and E.R. Pursall, *Experimental models of cryptococcosis.* Int J Microbiol, 2012. **2012**: p. 626745.
125. Baum, G.L. and D. Artis, *Characterization of the Growth Inhibition Factor for Cryptococcus Neoformans (Gifc) in Human Serum.* Am J Med Sci, 1963. **246**: p. 53-7.
126. Baum, G.L. and D. Artis, *Fungistatic effects of cell free human serum.* Am J Med Sci, 1961. **242**: p. 761-70.
127. Baum, G.L. and D. Artis, *Growth inhibition of Cryptococcus neoformans by cell free human serum.* Am J Med Sci, 1961. **241**: p. 613-6.
128. Hendry, A.T. and A. Bakerspigel, *Factors affecting serum inhibited growth of Candida albicans and Cryptococcus neoformans.* Sabouraudia, 1969. **7**(3): p. 219-29.
129. Igel, H.J. and R.P. Bolande, *Humoral defense mechanisms in cryptococcosis: substances in normal human serum, saliva, and cerebrospinal fluid affecting the growth of Cryptococcus neoformans.* The Journal of infectious diseases, 1966. **116**(1): p. 75-83.
130. Nassar, F., E. Brummer, and D.A. Stevens, *Different components in human serum inhibit multiplication of Cryptococcus neoformans and enhance fluconazole activity.* Antimicrob Agents Chemother, 1995. **39**(11): p. 2490-3.
131. Szilagyi, G., F. Reiss, and J.C. Smith, *The anticryptococcal factor of blood serum. A preliminary report.* J Invest Dermatol, 1966. **46**(3): p. 306-8.
132. Schelenz, S., et al., *Binding of host collectins to the pathogenic yeast Cryptococcus neoformans: human surfactant protein D acts as an agglutinin for acapsular yeast cells.* Infect Immun, 1995. **63**(9): p. 3360-6.

133. Shao, X., et al., *An innate immune system cell is a major determinant of species-related susceptibility differences to fungal pneumonia.* J Immunol, 2005. **175**(5): p. 3244-51.
134. Watford, W.T., A.J. Ghio, and J.R. Wright, *Complement-mediated host defense in the lung.* Am J Physiol Lung Cell Mol Physiol, 2000. **279**(5): p. L790-8.
135. Diamond, R.D., et al., *The role of late complement components and the alternate complement pathway in experimental cryptococcosis.* Proc Soc Exp Biol Med, 1973. **144**(1): p. 312-5.
136. Panepinto, J.C., et al., *Binding of serum mannan binding lectin to a cell integrity-defective Cryptococcus neoformans ccr4Delta mutant.* Infect Immun, 2007. **75**(10): p. 4769-79.
137. Kozel, T.R., et al., *Influence of opsonization conditions on C3 deposition and phagocyte binding of large- and small-capsule Cryptococcus neoformans cells.* Infect Immun, 1996. **64**(6): p. 2336-8.
138. Washburn, R.G., et al., *Differences in Cryptococcus neoformans capsular polysaccharide structure influence assembly of alternative complement pathway C3 convertase on fungal surfaces.* Mol Immunol, 1991. **28**(4-5): p. 465-70.
139. Young, B.J. and T.R. Kozel, *Effects of strain variation, serotype, and structural modification on kinetics for activation and binding of C3 to Cryptococcus neoformans.* Infect Immun, 1993. **61**(7): p. 2966-72.
140. Sahu, A., T.R. Kozel, and M.K. Pangburn, *Specificity of the thioester-containing reactive site of human C3 and its significance to complement activation.* Biochem J, 1994. **302 (Pt 2)**: p. 429-36.
141. Lim, T.S. and J.W. Murphy, *Transfer of immunity to cryptococcosis by T-enriched splenic lymphocytes from Cryptococcus neoformans-sensitized mice.* Infect Immun, 1980. **30**(1): p. 5-11.
142. Hill, J.O. and A.G. Harmsen, *Intrapulmonary growth and dissemination of an avirulent strain of Cryptococcus neoformans in mice depleted of CD4+ or CD8+ T cells.* The Journal of experimental medicine, 1991. **173**(3): p. 755-8.
143. Huffnagle, G.B., J.L. Yates, and M.F. Lipscomb, *Immunity to a pulmonary Cryptococcus neoformans infection requires both CD4+ and CD8+ T cells.* The Journal of experimental medicine, 1991. **173**(4): p. 793-800.
144. Mody, C.H., et al., *Depletion of CD4+ (L3T4+) lymphocytes in vivo impairs murine host defense to Cryptococcus neoformans.* J Immunol, 1990. **144**(4): p. 1472-7.
145. Wormley, F.L., Jr., et al., *Protection against cryptococcosis by using a murine gamma interferon-producing Cryptococcus neoformans strain.* Infect Immun, 2007. **75**(3): p. 1453-62.
146. Kawakami, K., et al., *T cell-dependent activation of macrophages and enhancement of their phagocytic activity in the lungs of mice inoculated with heat-killed Cryptococcus neoformans: involvement of IFN-gamma and its protective effect against cryptococcal infection.* Microbiol Immunol, 1995. **39**(2): p. 135-43.
147. Altfeld, M., et al., *T(H)1 to T(H)2 shift of cytokines in peripheral blood of HIV-infected patients is detectable by reverse transcriptase polymerase chain reaction but not by enzyme-linked immunosorbent assay under nonstimulated conditions.* J Acquir Immune Defic Syndr, 2000. **23**(4): p. 287-94.

148. Arora, S., et al., *Role of IFN-gamma in regulating T2 immunity and the development of alternatively activated macrophages during allergic bronchopulmonary mycosis.* J Immunol, 2005. **174**(10): p. 6346-56.
149. Singh, N., et al., *Pulmonary cryptococcosis in solid organ transplant recipients: clinical relevance of serum cryptococcal antigen.* Clin Infect Dis, 2008. **46**(2): p. e12-8.
150. Nanno, M., et al., *gammadelta T cells: firefighters or fire boosters in the front lines of inflammatory responses.* Immunol Rev, 2007. **215**: p. 103-13.
151. Wozniak, K.L., J.M. Vyas, and S.M. Levitz, *In vivo role of dendritic cells in a murine model of pulmonary cryptococcosis.* Infect Immun, 2006. **74**(7): p. 3817-24.
152. Uezu, K., et al., *Accumulation of gammadelta T cells in the lungs and their regulatory roles in Th1 response and host defense against pulmonary infection with Cryptococcus neoformans.* J Immunol, 2004. **172**(12): p. 7629-34.
153. Mednick, A.J., et al., *Neutropenia alters lung cytokine production in mice and reduces their susceptibility to pulmonary cryptococcosis.* Eur J Immunol, 2003. **33**(6): p. 1744-53.
154. Bolanos, B. and T.G. Mitchell, *Phagocytosis of Cryptococcus neoformans by rat alveolar macrophages.* J Med Vet Mycol, 1989. **27**(4): p. 203-17.
155. Levitz, S.M., *Macrophage-Cryptococcus interactions.* Immunol Ser, 1994. **60**: p. 533-43.
156. Feldmesser, M., et al., *Cryptococcus neoformans is a facultative intracellular pathogen in murine pulmonary infection.* Infect Immun, 2000. **68**(7): p. 4225-37.
157. Goldman, D.L., et al., *Persistent Cryptococcus neoformans pulmonary infection in the rat is associated with intracellular parasitism, decreased inducible nitric oxide synthase expression, and altered antibody responsiveness to cryptococcal polysaccharide.* Infect Immun, 2000. **68**(2): p. 832-8.
158. Ma, H. and R.C. May, *Virulence in Cryptococcus species.* Adv Appl Microbiol, 2009. **67**: p. 131-90.
159. Huffnagle, G.B., *Role of cytokines in T cell immunity to a pulmonary Cryptococcus neoformans infection.* Biol Signals, 1996. **5**(4): p. 215-22.
160. Koguchi, Y. and K. Kawakami, *Cryptococcal infection and Th1-Th2 cytokine balance.* Int Rev Immunol, 2002. **21**(4-5): p. 423-38.
161. Hill, J.O., *CD4+ T cells cause multinucleated giant cells to form around Cryptococcus neoformans and confine the yeast within the primary site of infection in the respiratory tract.* The Journal of experimental medicine, 1992. **175**(6): p. 1685-95.
162. Kobayashi, M., et al., *Granulomatous and cytokine responses to pulmonary Cryptococcus neoformans in two strains of rats.* Mycopathologia, 2001. **151**(3): p. 121-30.
163. Rivera, J., et al., *Antibody efficacy in murine pulmonary Cryptococcus neoformans infection: a role for nitric oxide.* J Immunol, 2002. **168**(7): p. 3419-27.
164. Levitz, S.M. and M.P. Dupont, *Phenotypic and functional characterization of human lymphocytes activated by interleukin-2 to directly inhibit growth of Cryptococcus neoformans in vitro.* J Clin Invest, 1993. **91**(4): p. 1490-8.
165. Ma, L.L., et al., *NK cells use perforin rather than granulysin for anticryptococcal activity.* J Immunol, 2004. **173**(5): p. 3357-65.

166. Ma, L.L., et al., *CD8 T cell-mediated killing of Cryptococcus neoformans requires granulysin and is dependent on CD4 T cells and IL-15.* J Immunol, 2002. **169**(10): p. 5787-95.
167. Zheng, C.F., et al., *Cytotoxic CD4+ T cells use granulysin to kill Cryptococcus neoformans, and activation of this pathway is defective in HIV patients.* Blood, 2007. **109**(5): p. 2049-57.
168. Galanis, E., et al., *Clinical presentation, diagnosis and management of Cryptococcus gattii cases: Lessons learned from British Columbia.* Can J Infect Dis Med Microbiol, 2009. **20**(1): p. 23-8.
169. Oliveira Fde, M., et al., *Cryptococcus gattii fungemia: report of a case with lung and brain lesions mimicking radiological features of malignancy.* Revista do Instituto de Medicina Tropical de Sao Paulo, 2007. **49**(4): p. 263-5.
170. Sato, Y., et al., *Rapid diagnosis of cryptococcal meningitis by microscopic examination of centrifuged cerebrospinal fluid sediment.* J Neurol Sci, 1999. **164**(1): p. 72-5.
171. Kanjanavirojkul, N., C. Sripa, and A. Puapairoj, *Cytologic diagnosis of Cryptococcus neoformans in HIV-positive patients.* Acta Cytol, 1997. **41**(2): p. 493-6.
172. Perfect, J.R., et al., *Clinical practice guidelines for the management of cryptococcal disease: 2010 update by the infectious diseases society of america.* Clin Infect Dis, 2010. **50**(3): p. 291-322.
173. Saag, M.S., et al., *Practice guidelines for the management of cryptococcal disease. Infectious Diseases Society of America.* Clin Infect Dis, 2000. **30**(4): p. 710-8.
174. Rolston, K.V., *Editorial Commentary: Cryptococcosis due to Cryptococcus gattii.* Clin Infect Dis, 2013. **57**(4): p. 552-4.
175. Dromer, F., et al., *Major role for amphotericin B-flucytosine combination in severe cryptococcosis.* PLoS One, 2008. **3**(8): p. e2870.
176. Laniado-Laborin, R. and M.N. Cabrales-Vargas, *Amphotericin B: side effects and toxicity.* Rev Iberoam Micol, 2009. **26**(4): p. 223-7.
177. Adler-Moore, J. and R.T. Proffitt, *AmBisome: liposomal formulation, structure, mechanism of action and pre-clinical experience.* J Antimicrob Chemother, 2002. **49 Suppl 1**: p. 21-30.
178. Baginski, M. and J. Czub, *Amphotericin B and Its New Derivatives - Mode of Action.* Curr Drug Metab, 2009.
179. Vermes, A., H.J. Guchelaar, and J. Dankert, *Flucytosine: a review of its pharmacology, clinical indications, pharmacokinetics, toxicity and drug interactions.* J Antimicrob Chemother, 2000. **46**(2): p. 171-9.
180. Sanfelice, F., *Contributo alla morfologia e biologia dei blastomiceti che si sviluppano nei succhi di alcuni frutti.* Ann. Igien., 1894. **4**: p. 463-95.
181. Busse, O., *Ueber parasitare zelleninschlusse und ihre zuchtung.* Zentralbl. Bakteriol., 1894. **16**: p. 175-80.
182. Buschke, A., *Ueber eine durch Coccidien Hervergerufene Krankheit des menschen.* Deutsche Med. Wochenschr., 1895. **21**(3): p. 14.
183. Park, B.J., et al., *Estimation of the current global burden of cryptococcal meningitis among persons living with HIV/AIDS.* AIDS, 2009. **23**(4): p. 525-30.
184. Levitz, S.M. and T. Boekhout, *Cryptococcus: the once-sleeping giant is fully awake.* FEMS Yeast Res, 2006. **6**(4): p. 461-2.

185. Honore, B., M. Ostergaard, and H. Vorum, *Functional genomics studied by proteomics.* Bioessays, 2004. **26**(8): p. 901-15.
186. Griffin, T.J., et al., *Complementary profiling of gene expression at the transcriptome and proteome levels in Saccharomyces cerevisiae.* Mol Cell Proteomics, 2002. **1**(4): p. 323-33.
187. Gygi, S.P., et al., *Correlation between protein and mRNA abundance in yeast.* Mol Cell Biol, 1999. **19**(3): p. 1720-30.
188. Futcher, B., et al., *A sampling of the yeast proteome.* Mol Cell Biol, 1999. **19**(11): p. 7357-68.
189. Miklos, G.L. and R. Maleszka, *Microarray reality checks in the context of a complex disease.* Nat Biotechnol, 2004. **22**(5): p. 615-21.
190. Waters, K.M., J.G. Pounds, and B.D. Thrall, *Data merging for integrated microarray and proteomic analysis.* Brief Funct Genomic Proteomic, 2006. **5**(4): p. 261-72.
191. Banks, R.E., et al., *Proteomics: new perspectives, new biomedical opportunities.* Lancet, 2000. **356**(9243): p. 1749-56.
192. Rupp, S., *Proteomics on its way to study host-pathogen interaction in Candida albicans.* Curr Opin Microbiol, 2004. **7**(4): p. 330-5.
193. Bantscheff, M., et al., *Quantitative mass spectrometry in proteomics: a critical review.* Anal Bioanal Chem, 2007. **389**(4): p. 1017-31.
194. Stasyk, T., and Huber, L.A., *Zooming in: fractionation strategies in proteomics.* Proteomics, 2004. **4**(12): p. 3704-16.
195. Righetti, P.G., Castagna, A., Antonioli, P. and Boschetti, E., *Prefractionation techniques in proteome analysis: the mining tools of the third millennium.* Electrophoresis, 2005. **26**(2): p. 297-319.
196. Washburn, M.P., *Utilisation of proteomics datasets generated via multidimensional protein identification technology (MudPIT).* Brief Funct Genomic Proteomic, 2004. **3**(3): p. 280-6.
197. Park, Y.M., Kim, J. Y., Kwon, K. H., Lee, S. K., Kim, Y. H., Kim, S. Y., Park, G. W., Lee, J. H., Lee, B. and Yoo, J. S., *Profiling human brain proteome by multi-dimensional separations coupled with MS.* Proteomics, 2006. **6**(18): p. 4978-86.
198. Minden, J., *Comparative proteomics and difference gel electrophoresis.* Biotechniques, 2007. **43**(6): p. 739, 741, 743 passim.
199. Herbert, B., et al., *Reduction and alkylation of proteins in preparation of two-dimensional map analysis: why, when, and how?* Electrophoresis, 2001. **22**(10): p. 2046-57.
200. O'Farrell, P.H., *High resolution two-dimensional electrophoresis of proteins.* J Biol Chem, 1975. **250**(10): p. 4007-21.
201. Celis, J.E. and P. Gromov, *2D protein electrophoresis: can it be perfected?* Curr Opin Biotechnol, 1999. **10**(1): p. 16-21.
202. Hanash, S.M., *Biomedical applications of two-dimensional electrophoresis using immobilized pH gradients: current status.* Electrophoresis, 2000. **21**(6): p. 1202-9.
203. Pedersen, S.K., et al., *Unseen proteome: mining below the tip of the iceberg to find low abundance and membrane proteins.* J Proteome Res, 2003. **2**(3): p. 303-11.
204. Friedman, D.B., and Lilley, K. S., *Optimizing the difference gel electrophoresis (DIGE) technology.* Methods Mol Biol, 2008. **428**: p. 93-124.

205. Unlu, M., M.E. Morgan, and J.S. Minden, *Difference gel electrophoresis: a single gel method for detecting changes in protein extracts.* Electrophoresis, 1997. **18**(11): p. 2071-7.
206. Marouga, R., S. David, and E. Hawkins, *The development of the DIGE system: 2D fluorescence difference gel analysis technology.* Anal Bioanal Chem, 2005. **382**(3): p. 669-78.
207. Zhou, G., et al., *2D differential in-gel electrophoresis for the identification of esophageal scans cell cancer-specific protein markers.* Mol Cell Proteomics, 2002. **1**(2): p. 117-24.
208. Shaw, J., et al., *Evaluation of saturation labelling two-dimensional difference gel electrophoresis fluorescent dyes.* Proteomics, 2003. **3**(7): p. 1181-95.
209. Van den Bergh, G. and L. Arckens, *Fluorescent two-dimensional difference gel electrophoresis unveils the potential of gel-based proteomics.* Curr Opin Biotechnol, 2004. **15**(1): p. 38-43.
210. Herbert, B., et al., *Sample Preparation and Prefractionation Techniques for Electrophoresis-Based Proteomics*, in *Proteome Research: Concepts, Technology and Application*, M.R. Wilkins, et al., Editors. 2007, Springer-Verlag Berlin Heidelberg: New York. p. (15-40).
211. Zhang, W., et al., *Affinity enrichment of plasma membrane for proteomics analysis.* Electrophoresis, 2003. **24**(16): p. 2855-63.
212. Ghaemmaghami, S., et al., *Global analysis of protein expression in yeast.* Nature, 2003. **425**(6959): p. 737-41.
213. Patton, W.F., *Detection technologies in proteome analysis.* Journal of Chromatography B, 2002. **771**: p. 3-31.
214. Minden, J. and A. Waggoner, *Difference gel electrophoresis using matched multiple dyes*, in *Kirkpatrick & Lockhart LLP*2000, Carnegie Mellon University: United States of America.
215. Gorg, A., et al., *2-DE with IPGs.* Electrophoresis, 2009. **30 Suppl 1**: p. S122-32.
216. Gygi, S.P., et al., *Quantitative analysis of complex protein mixtures using isotope-coded affinity tags.* Nat Biotechnol, 1999. **17**(10): p. 994-9.
217. Oda, Y., et al., *Accurate quantitation of protein expression and site-specific phosphorylation.* Proc Natl Acad Sci U S A, 1999. **96**(12): p. 6591-6.
218. Pasa-Tolic, L., et al., *High Throughput Proteome-Wide Precision Measurements of Protein Expression using Mass Spectrometry.* Journal of the American Chemical Society 1999. **121**: p. 7949-50.
219. Speers, A.E., and Wu, C.C., *Proteomics of integral membrane proteins--theory and application.* Chem Rev, 2007. **107**(8): p. 3687-714.
220. Aggarwal, K., Choe, L. H., and Lee, K. H., *Shotgun proteomics using the iTRAQ isobaric tags.* Brief Funct Genomic Proteomic, 2006. **5**(2): p. 112-20.
221. Carvalho, P.C., et al., *Identifying differences in protein expression levels by spectral counting and feature selection.* Genet Mol Res, 2008. **7**(2): p. 342-56.
222. Choi, H., D. Fermin, and A.I. Nesvizhskii, *Significance analysis of spectral count data in label-free shotgun proteomics.* Mol Cell Proteomics, 2008. **7**(12): p. 2373-85.
223. Gammulla, C.G., et al., *Differential metabolic response of cultured rice (Oryza sativa) cells exposed to high- and low-temperature stress.* Proteomics, 2010. **10**(16): p. 3001-19.
224. Aggarwal, K., L.H. Choe, and K.H. Lee, *Shotgun proteomics using the iTRAQ isobaric tags.* Brief Funct Genomic Proteomic, 2006. **5**(2): p. 112-20.

225. Institute, B. *iTRAQ*. 2013 [cited 2013 26/08/2013]; Available from: http://www.broadinstitute.org/scientific-community/science/platforms/proteomics/itraq.
226. Wiese, S., *Protein labeling by iTRAQ: A new tool for quantitative mass spectrometry in proteome research (vol 7, pg 340, 2007).* Proteomics, 2007. **7**(6): p. 1004-1004.
227. Applied Biosystems, *Amine-Modifying Labeling Reagents for Multiplexed Relative and Absolute Protein Quantification - Chemistry Reference Guide*. 2004.
228. Pichler, P., et al., *Peptide labeling with isobaric tags yields higher identification rates using iTRAQ 4-plex compared to TMT 6-plex and iTRAQ 8-plex on LTQ Orbitrap.* Anal Chem, 2010. **82**(15): p. 6549-58.
229. Tjalsma, H., R.M. Schaeps, and D.W. Swinkels, *Immunoproteomics: From biomarker discovery to diagnostic applications.* Proteomics Clin Appl, 2008. **2**(2): p. 167-80.
230. Jungblut, P.R., *Proteome analysis of bacterial pathogens.* Microbes Infect, 2001. **3**(10): p. 831-40.
231. Towbin, H., T. Staehelin, and J. Gordon, *Electrophoretic transfer of proteins from polyacrylamide gels to nitrocellulose sheets: procedure and some applications.* Proc Natl Acad Sci U S A, 1979. **76**(9): p. 4350-4.
232. Jobbins, S., et al., *An immunoproteomic approach to elucidating the pathogenesis of Cryptococcosis caused by Cryptococcus gattii.* J Proteome Res, 2010.
233. Bio-Rad, *Bio-Plex Pro™ Cytokine, Chemokine and Growth Factor Assays: Instruction Manual*, 2013, Bio-Rad Laboratories, Inc.: USA.
234. Bio-Rad. *Bio-Plex® Assays*. 2013 [cited 2013 2/3/13]; Available from: http://www.bio-rad.com/en-au/applications-technologies/bio-plex-multiplex-immunoassays.
235. Seidl, M., *Cryptococcus gattii.* The Environmental Reporter, 2012. **10**(3).
236. Jiang, B., H. Bussey, and T. Roemer, *Novel strategies in antifungal lead discovery.* Curr Opin Microbiol, 2002. **5**(5): p. 466-71.
237. Nielsen, K., et al., *Sexual cycle of Cryptococcus neoformans var. grubii and virulence of congenic a and alpha isolates.* Infection and immunity, 2003. **71**(9): p. 4831-41.
238. Carroll, S.F., L. Guillot, and S.T. Qureshi, *Mammalian model hosts of cryptococcal infection.* Comp Med, 2007. **57**(1): p. 9-17.
239. Krockenberger, M.B., et al., *Pathogenesis of Pulmonary Cryptococcus gattii Infection: A Rat Model.* Mycopathologia, 2010.
240. Bhadauria, V., et al., *Advances in fungal proteomics.* Microbiol Res, 2007. **162**(3): p. 193-200.
241. Carberry, S. and S. Doyle, *Proteomic studies in biomedically and industrially relevant fungi.* Cytotechnology, 2007. **53**(1-3): p. 95-100.
242. Shimizu, M. and H. Wariishi, *Development of a sample preparation method for fungal proteomics.* FEMS Microbiol Lett, 2005. **247**(1): p. 17-22.
243. Hu, G., et al., *Metabolic adaptation in Cryptococcus neoformans during early murine pulmonary infection.* Mol Microbiol, 2008. **69**(6): p. 1456-75.
244. Kyhse-Andersen, J., *Electroblotting of multiple gels: a simple apparatus without buffer tank for rapid transfer of proteins from polyacrylamide to nitrocellulose.* J Biochem Biophys Methods, 1984. **10**(3-4): p. 203-9.

245. Tan, A.K., *Increased transfer efficiency using a discontinuous buffer system with the Trans-Blot® SD semi-dry electrophoretic transfer cell*, in *Protein Blotting*, Bio-Rad, Editor, Bio-Rad Laboratories: Hercules, CA, USA.
246. Schafer-Nielsen, C., P.J. Svendsen, and C. Rose, *Separation of macromolecules in isotachophoresis systems involving single or multiple counterions.* J Biochem Biophys Methods, 1980. **3**(2): p. 97-128.
247. Bio-Rad, *Protein blotting guide: a guide to transfer and detection*, Bio-Rad Laboratories: Hercules, CA, USA.
248. Cong, W., . Hwang, S., Jin, L., Choi, J, *Detection of Proteins on Blots Using Direct Blue 71*, in *The Protein Protocols Handbook*, J.M. Walker, Editor. 2009, Humana Press Inc.: Totowa. p. 729-35.
249. Carpentier, S.C., et al., *Preparation of protein extracts from recalcitrant plant tissues: an evaluation of different methods for two-dimensional gel electrophoresis analysis.* Proteomics, 2005. **5**(10): p. 2497-507.
250. Goren, M.B. and G.M. Middlebrook, *Protein conjugates of polysaccharide from Cryptococcus neoforman s.* Journal of immunology, 1967. **98**(5): p. 901-13.
251. Gates, M.A., P. Thorkildson, and T.R. Kozel, *Molecular architecture of the Cryptococcus neoformans capsule.* Molecular microbiology, 2004. **52**(1): p. 13-24.
252. Maxson, M.E., et al., *The volume and hydration of the Cryptococcus neoformans polysaccharide capsule.* Fungal genetics and biology : FG & B, 2007. **44**(3): p. 180-6.
253. Herbert, B.R., et al., *Improved 2-DE of microorganisms after acidic extraction.* Electrophoresis, 2006. **27**(8): p. 1630-40.
254. Hofmeister, F., *About the science of the effect of salts.* Archive for Experimental Pathology and Pharmacology, 1888. **24**: p. 247-260.
255. Baldwin, R.L., *How Hofmeister ion interactions affect protein stability.* Biophys J, 1996. **71**(4): p. 2056-63.
256. Zhang, Y., and Cremer, P. S., *Interactions between macromolecules and ions: The Hofmeister series.* Curr Opin Chem Biol, 2006. **10**(6): p. 658-63.
257. Zaragoza, O., et al., *The polysaccharide capsule of the pathogenic fungus Cryptococcus neoformans enlarges by distal growth and is rearranged during budding.* Molecular microbiology, 2006. **59**(1): p. 67-83.
258. Frases, S., et al., *Capsule of Cryptococcus neoformans grows by enlargement of polysaccharide molecules.* Proceedings of the National Academy of Sciences of the United States of America, 2009. **106**(4): p. 1228-33.
259. McFadden, D.C., M. De Jesus, and A. Casadevall, *The physical properties of the capsular polysaccharides from Cryptococcus neoformans suggest features for capsule construction.* The Journal of biological chemistry, 2006. **281**(4): p. 1868-75.
260. Weber, M., M. Weber, and M. Kleine-Boymann, *Phenol*, in *Ullmann's Encyclopedia of Industrial Chemistry*. 2004: Gladbeck, Germany.
261. Faurobert, M., E. Pelpoir, and J. Chaib, *Phenol extraction of proteins for proteomic studies of recalcitrant plant tissues.* Methods Mol Biol, 2007. **355**: p. 9-14.
262. Hurkman, W.J. and C.K. Tanaka, *Solubilization of plant membrane proteins for analysis by two-dimensional gel electrophoresis.* Plant Physiol, 1986. **81**(3): p. 802-6.

263. Saravanan, R.S. and J.K. Rose, *A critical evaluation of sample extraction techniques for enhanced proteomic analysis of recalcitrant plant tissues.* Proteomics, 2004. **4**(9): p. 2522-32.
264. Fan, W., et al., *Cryptococcus neoformans gene expression during murine macrophage infection.* Eukaryotic Cell, 2005. **4**(8): p. 1420-1433.
265. Steen, B.R., et al., *Cryptococcus neoformans gene expression during experimental cryptococcal meningitis.* Eukaryotic Cell, 2003. **2**: p. 1336-1349.
266. Kraus, P.R., et al., *Identification of Cryptococcus neoformans temperature-regulated genes with a genomic-DNA microarray.* Eukaryotic Cell, 2004. **3**(5): p. 1249-1260.
267. Kumar, A., et al., *An integrated approach for finding overlooked genes in yeast.* Nature Biotechnology, 2002. **20**(1): p. 58-63.
268. da Silva, B.A., et al., *Proteomic analysis of the secretions of Pseudallescheria boydii, a human fungal pathogen with unknown genome.* J Proteome Res, 2012. **11**(1): p. 172-88.
269. Mulyar, O.A., A.C. Teng, and A.O. Gramolini, *A proteomic interrogation of Cryptococcus neoformans: interaction networks for calcineurin in a heated environment.* Expert Rev Proteomics, 2012. **9**(1): p. 13-5.
270. Fitzpatrick, D.A., et al., *A fungal phylogeny based on 42 complete genomes derived from supertree and combined gene analysis.* BMC Evol Biol, 2006. **6**: p. 99.
271. Martins, L.M., et al., *Immunoproteomics and immunoinformatics analysis of Cryptococcus gattii: novel candidate antigens for diagnosis.* Future Microbiol, 2013. **8**(4): p. 549-63.
272. Chong, H.S., et al., *Time-course proteome analysis reveals the dynamic response of Cryptococcus gattii cells to fluconazole.* PLoS One, 2012. **7**(8): p. e42835.
273. Crestani, J., et al., *Proteomic profiling of the influence of iron availability on Cryptococcus gattii.* J Proteome Res, 2012. **11**(1): p. 189-205.
274. Szmolla, R., *Regulatory digestive proteases in the pathomechanism of chronic pancreatitis*, in *Molecular Medical Sciences*2007, Semmelweis University.
275. Rydengard, V., et al., *Histidine-rich glycoprotein protects from systemic Candida infection.* PLoS Pathog, 2008. **4**(8): p. e1000116.
276. Jinwal, U.K., et al., *The Hsp90 kinase co-chaperone Cdc37 regulates tau stability and phosphorylation dynamics.* The Journal of biological chemistry, 2011. **286**(19): p. 16976-83.
277. Lin, C.M., et al., *Microtubule actin crosslinking factor 1b: a novel plakin that localizes to the Golgi complex.* J Cell Sci, 2005. **118**(Pt 16): p. 3727-38.
278. Hyodo, T., et al., *Misshapen-like kinase 1 (MINK1) is a novel component of striatin-interacting phosphatase and kinase (STRIPAK) and is required for the completion of cytokinesis.* The Journal of biological chemistry, 2012. **287**(30): p. 25019-29.
279. Hassel, D., et al., *Nexilin mutations destabilize cardiac Z-disks and lead to dilated cardiomyopathy.* Nat Med, 2009. **15**(11): p. 1281-8.
280. Mattioli, E., et al., *Prelamin A-mediated recruitment of SUN1 to the nuclear envelope directs nuclear positioning in human muscle.* Cell death and differentiation, 2011. **18**(8): p. 1305-15.
281. Broadhurst, M.J., et al., *Upregulation of retinal dehydrogenase 2 in alternatively activated macrophages during retinoid-dependent type-2 immunity to helminth infection in mice.* PLoS Pathog, 2012. **8**(8): p. e1002883.

282. Li, D. and R. Roberts, *WD-repeat proteins: structure characteristics, biological function, and their involvement in human diseases.* Cell Mol Life Sci, 2001. **58**(14): p. 2085-97.
283. Klengel, T., et al., *Fungal adenylyl cyclase integrates CO2 sensing with cAMP signaling and virulence.* Curr Biol, 2005. **15**(22): p. 2021-6.
284. Rodrigues, M.L., et al., *Extracellular vesicles produced by Cryptococcus neoformans contain protein components associated with virulence.* Eukaryot Cell, 2008. **7**(1): p. 58-67.
285. Johnson, S.S., et al., *Regulation of yeast nutrient permease endocytosis by ATP-binding cassette transporters and a seven-transmembrane protein, RSB1.* The Journal of biological chemistry, 2010. **285**(46): p. 35792-802.
286. Schmitz-Esser, S., et al., *ATP/ADP translocases: a common feature of obligate intracellular amoebal symbionts related to Chlamydiae and Rickettsiae.* J Bacteriol, 2004. **186**(3): p. 683-91.
287. Dinamarco, T.M., et al., *Functional characterization of an Aspergillus fumigatus calcium transporter (PmcA) that is essential for fungal infection.* PLoS One, 2012. **7**(5): p. e37591.
288. Karagiannis, J., R. Oulton, and P.G. Young, *The Scw1 RNA-binding domain protein regulates septation and cell-wall structure in fission yeast.* Genetics, 2002. **162**(1): p. 45-58.
289. Markaryan, A., et al., *Purification and characterization of an elastinolytic metalloprotease from Aspergillus fumigatus and immunoelectron microscopic evidence of secretion of this enzyme by the fungus invading the murine lung.* Infect Immun, 1994. **62**(6): p. 2149-57.
290. Aspenstrom, P., *Formin-binding proteins: modulators of formin-dependent actin polymerization.* Biochimica et biophysica acta, 2010. **1803**(2): p. 174-82.
291. Munro, C.A., et al., *Mnt1p and Mnt2p of Candida albicans are partially redundant alpha-1,2-mannosyltransferases that participate in O-linked mannosylation and are required for adhesion and virulence.* The Journal of biological chemistry, 2005. **280**(2): p. 1051-60.
292. de Smet, B.J.G.L., et al., *Nonmuscle myosin heavy chain-B expression in balloon-dilated and stented arteries: a study in the atherosclerotic Yucatan micropig.* Netherlands Heart Journal, 2005. **13**(6): p. 224-232.
293. Audhya, A., M. Foti, and S.D. Emr, *Distinct roles for the yeast phosphatidylinositol 4-kinases, Stt4p and Pik1p, in secretion, cell growth, and organelle membrane dynamics.* Mol Biol Cell, 2000. **11**(8): p. 2673-89.
294. Barelle, C.J., et al., *Niche-specific regulation of central metabolic pathways in a fungal pathogen.* Cell Microbiol, 2006. **8**(6): p. 961-71.
295. Shah, P., et al., *Mucosal immunization with polyamine transport protein D (PotD) protects mice against nasopharyngeal colonization with Streptococcus pneumoniae.* Exp Biol Med (Maywood), 2009. **234**(4): p. 403-9.
296. Nogueira, E., et al., *SOK1 translocates from the Golgi to the nucleus upon chemical anoxia and induces apoptotic cell death.* The Journal of biological chemistry, 2008. **283**(23): p. 16248-58.
297. Strange, K., J. Denton, and K. Nehrke, *Ste20-type kinases: evolutionarily conserved regulators of ion transport and cell volume.* Physiology (Bethesda), 2006. **21**: p. 61-8.
298. Mirzaei, M., et al., *Differential regulation of aquaporins, small GTPases and V-ATPases proteins in rice leaves subjected to drought stress and recovery.* Proteomics, 2012. **12**(6): p. 864-77.

299. Blaber, S.P., et al., *Analysis of in vitro secretion profiles from adipose-derived cell populations.* J Transl Med, 2012. **10**: p. 172.
300. Seed, J.R., *Protozoa: Pathogens and Defenses*, in *Medical Microbiology*, S. Baron, Editor. 1996, University of Texas Medical Branch: Galveston, Texas, USA.
301. Gill, C., et al., *A qualitative and quantitative proteomic study of human microdialysate and the cutaneous response to injury.* AAPS J, 2011. **13**(2): p. 309-17.
302. Mataija-Botelho, D., et al., *A qualitative proteome investigation of the sediment portion of human urine: Implications in the biomarker discovery process.* Proteomics Clin Appl, 2009. **3**(1): p. 95-105.
303. Jeffery, C.J., *Moonlighting proteins--an update.* Mol Biosyst, 2009. **5**(4): p. 345-50.
304. Jeffery, C.J., *Moonlighting proteins.* Trends Biochem Sci, 1999. **24**(1): p. 8-11.
305. Piatigorsky, J., et al., *Gene sharing by delta-crystallin and argininosuccinate lyase.* Proc Natl Acad Sci U S A, 1988. **85**(10): p. 3479-83.
306. Kudla, G., et al., *Coding-sequence determinants of gene expression in Escherichia coli.* Science, 2009. **324**(5924): p. 255-8.
307. Neame, E., *Structure versus codon bias.* Nature Reviews Genetics, 2009. **10**.
308. Chun, C.D., O.W. Liu, and H.D. Madhani, *A link between virulence and homeostatic responses to hypoxia during infection by the human fungal pathogen Cryptococcus neoformans.* PLoS Pathog, 2007. **3**(2): p. e22.
309. Alspaugh, J.A., et al., *Adenylyl cyclase functions downstream of the Galpha protein Gpa1 and controls mating and pathogenicity of Cryptococcus neoformans.* Eukaryot Cell, 2002. **1**(1): p. 75-84.
310. Buck, J., et al., *Cytosolic adenylyl cyclase defines a unique signaling molecule in mammals.* Proc Natl Acad Sci U S A, 1999. **96**(1): p. 79-84.
311. Raulo, S.M., T.A. Sorsa, and P.S. Maisi, *Concentrations of elastinolytic metalloproteinases in respiratory tract secretions of healthy horses and horses with chronic obstructive pulmonary disease.* Am J Vet Res, 2000. **61**(9): p. 1067-73.
312. Garcia-Sanchez, S., et al., *Global roles of Ssn6 in Tup1- and Nrg1-dependent gene regulation in the fungal pathogen, Candida albicans.* Mol Biol Cell, 2005. **16**(6): p. 2913-25.
313. Lorenz, M.C., J.A. Bender, and G.R. Fink, *Transcriptional response of Candida albicans upon internalization by macrophages.* Eukaryot Cell, 2004. **3**(5): p. 1076-87.
314. Rubin-Bejerano, I., et al., *Phagocytosis by neutrophils induces an amino acid deprivation response in Saccharomyces cerevisiae and Candida albicans.* Proc Natl Acad Sci U S A, 2003. **100**(19): p. 11007-12.
315. Fradin, C., et al., *Granulocytes govern the transcriptional response, morphology and proliferation of Candida albicans in human blood.* Mol Microbiol, 2005. **56**(2): p. 397-415.
316. Shah, P. and E. Swiatlo, *A multifaceted role for polyamines in bacterial pathogens.* Mol Microbiol, 2008. **68**(1): p. 4-16.
317. Valdes-Santiago, L., et al., *Polyamine metabolism in fungi with emphasis on phytopathogenic species.* J Amino Acids, 2012. **2012**: p. 837932.

318. Fedson, D.S. and J.A. Scott, *The burden of pneumococcal disease among adults in developed and developing countries: what is and is not known.* Vaccine, 1999. **17 Suppl 1**: p. S11-8.
319. Shah, P. and E. Swiatlo, *Immunization with polyamine transport protein PotD protects mice against systemic infection with Streptococcus pneumoniae.* Infect Immun, 2006. **74**(10): p. 5888-92.
320. Loewenstein, Y., et al., *Protein function annotation by homology-based inference.* Genome biology, 2009. **10**(2): p. 207.
321. Tress, M., et al., *Assessment of predictions submitted for the CASP7 domain prediction category.* Proteins, 2007. **69 Suppl 8**: p. 137-51.
322. Gray, H., *The Classic 1860 Edition: Gray's Anatomy*. 2008, Heatherton, Victoria, Australia: Hinkler Books Pty Ltd.
323. Vareille, M., et al., *The airway epithelium: soldier in the fight against respiratory viruses.* Clin Microbiol Rev, 2011. **24**(1): p. 210-29.
324. Travis, S.M., et al., *Activity of abundant antimicrobials of the human airway.* Am J Respir Cell Mol Biol, 1999. **20**(5): p. 872-9.
325. Notter, R., H., *Lung surfactants: basic science and clinical applications*. 2000, New York, N.Y: Marcel Dekker.
326. National Heart, L.a.B.I. *The Respiratory System*. 2012 17/07/12 [cited 2013 12th August]; Available from: http://www.nhlbi.nih.gov/health/health-topics/topics/hlw/system.html.
327. Chowdhary, A., et al., *Temperate climate niche for Cryptococcus gattii in Northern Europe.* Emerg Infect Dis, 2012. **18**(1): p. 172-4.
328. Chae, H.S., et al., *Classification of Cryptococcus neoformans and yeast-like fungus isolates from pigeon droppings by colony phenotyping and ITS genotyping and their seasonal variations in Korea.* Avian Dis, 2012. **56**(1): p. 58-64.
329. Bartlett, K., et al., *Investigation of Occupational Exposures to Forestry Workers from Environmental Cryptococcus neoformans var. gattii*, 2006, WorkSafeBC: Richmond, B.C., Canada.
330. Martin, T.R. and C.W. Frevert, *Innate immunity in the lungs.* Proc Am Thorac Soc, 2005. **2**(5): p. 403-11.
331. Livraghi-Butrico, A., et al., *Mucus clearance, MyD88-dependent and MyD88-independent immunity modulate lung susceptibility to spontaneous bacterial infection and inflammation.* Mucosal Immunol, 2012. **5**(4): p. 397-408.
332. Qiu, Y., et al., *Immune modulation mediated by cryptococcal laccase promotes pulmonary growth and brain dissemination of virulent Cryptococcus neoformans in mice.* PLoS One, 2012. **7**(10): p. e47853.
333. Hirsch, J., et al., *Proteomics: current techniques and potential applications to lung disease.* Am J Physiol Lung Cell Mol Physiol, 2004. **287**(1): p. L1-23.
334. Zhao, D., et al., *Proteomic analysis of the lungs of mice infected with different pathotypes of H5N1 avian influenza viruses.* Proteomics, 2012. **12**(12): p. 1970-82.
335. Ohlmeier, S., et al., *Proteomics of human lung tissue identifies surfactant protein A as a marker of chronic obstructive pulmonary disease.* J Proteome Res, 2008. **7**(12): p. 5125-32.
336. Fekkar, A., et al., *DIGE enables the detection of a putative serum biomarker of fungal origin in a mouse model of invasive aspergillosis.* J Proteomics, 2012. **75**(9): p. 2536-49.

337. Narmadha, G., et al., *Characterization of a novel lysozyme-like 4 gene in the rat.* PLoS One, 2011. **6**(11): p. e27659.
338. Kajla, M.K., et al., *A new role for an old antimicrobial: lysozyme c-1 can function to protect malaria parasites in Anopheles mosquitoes.* PLoS One, 2011. **6**(5): p. e19649.
339. Ma, J., et al., *Morphine disrupts interleukin-23 (IL-23)/IL-17-mediated pulmonary mucosal host defense against Streptococcus pneumoniae infection.* Infect Immun, 2010. **78**(2): p. 830-7.
340. Bianchi, M., et al., *Restoration of anti-Aspergillus defense by neutrophil extracellular traps in human chronic granulomatous disease after gene therapy is calprotectin-dependent.* J Allergy Clin Immunol, 2011. **127**(5): p. 1243-52 e7.
341. Ehrchen, J.M., et al., *The endogenous Toll-like receptor 4 agonist S100A8/S100A9 (calprotectin) as innate amplifier of infection, autoimmunity, and cancer.* J Leukoc Biol, 2009. **86**(3): p. 557-66.
342. Yui, S., Y. Nakatani, and M. Mikami, *Calprotectin (S100A8/S100A9), an inflammatory protein complex from neutrophils with a broad apoptosis-inducing activity.* Biol Pharm Bull, 2003. **26**(6): p. 753-60.
343. Krzeslak, A. and A. Lipinska, *Galectin-3 as a multifunctional protein.* Cell Mol Biol Lett, 2004. **9**(2): p. 305-28.
344. Ruas, L.P., et al., *Lack of galectin-3 drives response to Paracoccidioides brasiliensis toward a Th2-biased immunity.* PLoS One, 2009. **4**(2): p. e4519.
345. Kohatsu, L., et al., *Galectin-3 induces death of Candida species expressing specific beta-1,2-linked mannans.* J Immunol, 2006. **177**(7): p. 4718-26.
346. Masuoka, J., *Surface glycans of Candida albicans and other pathogenic fungi: physiological roles, clinical uses, and experimental challenges.* Clin Microbiol Rev, 2004. **17**(2): p. 281-310.
347. Tossi, A., L. Sandri, and A. Giangaspero, *Amphipathic, alpha-helical antimicrobial peptides.* Biopolymers, 2000. **55**(1): p. 4-30.
348. Malmsten, M., M. Davoudi, and A. Schmidtchen, *Bacterial killing by heparin-binding peptides from PRELP and thrombospondin.* Matrix Biol, 2006. **25**(5): p. 294-300.
349. Trudel, S., et al., *Peroxiredoxin 6 fails to limit phospholipid peroxidation in lung from Cftr-knockout mice subjected to oxidative challenge.* PLoS One, 2009. **4**(6): p. e6075.
350. Wang, Y., et al., *Transgenic mice overexpressing peroxiredoxin 6 show increased resistance to lung injury in hyperoxia.* Am J Respir Cell Mol Biol, 2006. **34**(4): p. 481-6.
351. Eismann, T., et al., *Peroxiredoxin-6 protects against mitochondrial dysfunction and liver injury during ischemia-reperfusion in mice.* Am J Physiol Gastrointest Liver Physiol, 2009. **296**(2): p. G266-74.
352. Liu, K. and N. Shih, *The Role of Enolase in Tissue Invasion and Metastasis of Pathogens and Tumor Cells.* Journal of Cancer Molecules, 2007. **3**(2): p. 45-48.
353. Briand, N., I. Dugail, and S. Le Lay, *Cavin proteins: New players in the caveolae field.* Biochimie, 2011. **93**(1): p. 71-7.
354. Drab, M., et al., *Loss of caveolae, vascular dysfunction, and pulmonary defects in caveolin-1 gene-disrupted mice.* Science, 2001. **293**(5539): p. 2449-52.

355. Pollard, T.D. and G.G. Borisy, *Cellular motility driven by assembly and disassembly of actin filaments.* Cell, 2003. **112**(4): p. 453-65.
356. Tucker-Kellogg, L. *Lamellipodia and Lamella: Basic Description*. 2012 July 2012 [cited 2012 4/8/12]; Available from: http://www.mechanobio.info/Home/Dynamic-Structures-in-Mechanosensing/lamellipodia/.
357. Le Clainche, C. and M.F. Carlier, *Regulation of actin assembly associated with protrusion and adhesion in cell migration.* Physiol Rev, 2008. **88**(2): p. 489-513.
358. Goldmann, W.H. and D.E. Ingber, *Intact vinculin protein is required for control of cell shape, cell mechanics, and rac-dependent lamellipodia formation.* Biochemical and biophysical research communications, 2002. **290**(2): p. 749-55.
359. He, Z. and A. Bateman, *Progranulin (granulin-epithelin precursor, PC-cell-derived growth factor, acrogranin) mediates tissue repair and tumorigenesis.* J Mol Med (Berl), 2003. **81**(10): p. 600-12.
360. Yang, Z.F., et al., *Allograft inflammatory factor-1 (AIF-1) is crucial for the survival and pro-inflammatory activity of macrophages.* International immunology, 2005. **17**(11): p. 1391-7.
361. Cook, A.L., C.M. Johnson, and M.B. Brown, *Beta 2 microglobulin and resistance to murine respiratory mycoplasmosis.* Contemp Top Lab Anim Sci, 2004. **43**(3): p. 18-24.
362. Capoluongo, E., et al., *Increased levels of IGF-1 and beta2-microglobulin in epithelial lining fluid of preterm newborns developing chronic lung disease. effects of rhG-CSF.* Int J Immunopathol Pharmacol, 2006. **19**(1): p. 57-66.
363. Ivanova, M.I., et al., *Role of the C-terminal 28 residues of beta2-microglobulin in amyloid fibril formation.* Biochemistry, 2003. **42**(46): p. 13536-40.
364. Nishimaki, S., et al., *Urinary beta 2-microglobulin in premature infants with chorioamnionitis and chronic lung disease.* J Pediatr, 2003. **143**(1): p. 120-2.
365. Rangasamy, T., et al., *Genetic ablation of Nrf2 enhances susceptibility to cigarette smoke-induced emphysema in mice.* J Clin Invest, 2004. **114**(9): p. 1248-59.
366. Malhotra, D., et al., *Decline in NRF2-regulated antioxidants in chronic obstructive pulmonary disease lungs due to loss of its positive regulator, DJ-1.* American journal of respiratory and critical care medicine, 2008. **178**(6): p. 592-604.
367. He, C., et al., *Mitochondrial Cu,Zn-superoxide dismutase mediates pulmonary fibrosis by augmenting H2O2 generation.* The Journal of biological chemistry, 2011. **286**(17): p. 15597-607.
368. Engelmann, I., et al., *A comprehensive analysis of gene expression changes provoked by bacterial and fungal infection in C. elegans.* PLoS One, 2011. **6**(5): p. e19055.
369. Pukkila-Worley, R., F.M. Ausubel, and E. Mylonakis, *Candida albicans infection of Caenorhabditis elegans induces antifungal immune defenses.* PLoS Pathog, 2011. **7**(6): p. e1002074.
370. Delpino, A. and M. Castelli, *The 78 kDa glucose-regulated protein (GRP78/BIP) is expressed on the cell membrane, is released into cell culture medium and is also present in human peripheral circulation.* Biosci Rep, 2002. **22**(3-4): p. 407-20.

371. Yu, Z., et al., *The endoplasmic reticulum stress-responsive protein GRP78 protects neurons against excitotoxicity and apoptosis: suppression of oxidative stress and stabilization of calcium homeostasis.* Exp Neurol, 1999. **155**(2): p. 302-14.
372. Korfei, M., et al., *Comparative proteomic analysis of lung tissue from patients with idiopathic pulmonary fibrosis (IPF) and lung transplant donor lungs.* J Proteome Res, 2011. **10**(5): p. 2185-205.
373. Li, X., et al., *Essential role for cathepsin D in bleomycin-induced apoptosis of alveolar epithelial cells.* Am J Physiol Lung Cell Mol Physiol, 2004. **287**(1): p. L46-51.
374. Goldman, D.L., et al., *Enhanced allergic inflammation and airway responsiveness in rats with chronic Cryptococcus neoformans infection: potential role for fungal pulmonary infection in the pathogenesis of asthma.* The Journal of infectious diseases, 2006. **193**(8): p. 1178-86.
375. Vicencio, A.G., et al., *Pulmonary cryptococcosis induces chitinase in the rat.* Respir Res, 2008. **9**: p. 40.
376. Vega, K. and M. Kalkum, *Chitin, chitinase responses, and invasive fungal infections.* Int J Microbiol, 2012. **2012**: p. 920459.
377. Akella, A. and S.B. Deshpande, *Pulmonary surfactants and their role in pathophysiology of lung disorders.* Indian J Exp Biol, 2013. **51**(1): p. 5-22.
378. Guthmann, F., et al., *Phenotype of palmitic acid transport and of signalling in alveolar type II cells from E/H-FABP double-knockout mice: contribution of caveolin-1 and PPARgamma.* Biochimica et biophysica acta, 2004. **1636**(2-3): p. 196-204.
379. Grau, V., et al., *Epidermal fatty acid-binding protein is increased in rat lungs following in vivo treatment with keratinocyte growth factor.* Int J Biochem Cell Biol, 2006. **38**(2): p. 279-87.
380. Geunes-Boyer, S., et al., *Surfactant protein D increases phagocytosis of hypocapsular Cryptococcus neoformans by murine macrophages and enhances fungal survival.* Infect Immun, 2009. **77**(7): p. 2783-94.
381. Kwiatkowski, D.J., *Functions of gelsolin: motility, signaling, apoptosis, cancer.* Current opinion in cell biology, 1999. **11**(1): p. 103-8.
382. Witke, W., et al., *Comparisons of CapG and gelsolin-null macrophages: demonstration of a unique role for CapG in receptor-mediated ruffling, phagocytosis, and vesicle rocketing.* The Journal of cell biology, 2001. **154**(4): p. 775-84.
383. Badger, M.R. and G.D. Price, *The Role of Carbonic Anhydrase in Photosynthesis.* Annual Review of Plant Physiology and Plant Molecular Biology, 1994. **45**: p. 369-392.
384. Health, P. *Respiratory acidosis*. 2011 16/8/11 [cited 2012 13/8/12]; Available from: http://www.ncbi.nlm.nih.gov/pubmedhealth/PMH0001154/.
385. Shan, L., et al., *Inverse relationship between Sec14l3 mRNA/protein expression and allergic airway inflammation.* Eur J Pharmacol, 2009. **616**(1-3): p. 293-300.
386. Takashima, H., et al., *Periaxin mutations cause a broad spectrum of demyelinating neuropathies.* Ann Neurol, 2002. **51**(6): p. 709-15.
387. Gillespie, C.S., et al., *Peripheral demyelination and neuropathic pain behavior in periaxin-deficient mice.* Neuron, 2000. **26**(2): p. 523-31.

388. Zawawi, K.H., et al., *Moesin-induced signaling in response to lipopolysaccharide in macrophages.* J Periodontal Res, 2010. **45**(5): p. 589-601.
389. Tohme, Z.N., S. Amar, and T.E. Van Dyke, *Moesin functions as a lipopolysaccharide receptor on human monocytes.* Infect Immun, 1999. **67**(7): p. 3215-20.
390. Neeper, M., et al., *Cloning and expression of a cell surface receptor for advanced glycosylation end products of proteins.* The Journal of biological chemistry, 1992. **267**(21): p. 14998-5004.
391. Buckley, S.T. and C. Ehrhardt, *The receptor for advanced glycation end products (RAGE) and the lung.* J Biomed Biotechnol, 2010. **2010**: p. 917108.
392. Dahlin, K., et al., *Identification of genes differentially expressed in rat alveolar type I cells.* Am J Respir Cell Mol Biol, 2004. **31**(3): p. 309-16.
393. Bierhaus, A., et al., *Diabetes-associated sustained activation of the transcription factor nuclear factor-kappaB.* Diabetes, 2001. **50**(12): p. 2792-808.
394. Bartling, B., et al., *Down-regulation of the receptor for advanced glycation end-products (RAGE) supports non-small cell lung carcinoma.* Carcinogenesis, 2005. **26**(2): p. 293-301.
395. Nordberg, J. and E.S. Arner, *Reactive oxygen species, antioxidants, and the mammalian thioredoxin system.* Free Radic Biol Med, 2001. **31**(11): p. 1287-312.
396. Jin, R.C., et al., *Glutathione peroxidase-3 deficiency promotes platelet-dependent thrombosis in vivo.* Circulation, 2011. **123**(18): p. 1963-73.
397. Kolb, M., et al., *Proteoglycans decorin and biglycan differentially modulate TGF-beta-mediated fibrotic responses in the lung.* Am J Physiol Lung Cell Mol Physiol, 2001. **280**(6): p. L1327-34.
398. Li, Y., et al., *Decorin gene transfer promotes muscle cell differentiation and muscle regeneration.* Mol Ther, 2007. **15**(9): p. 1616-22.
399. Song, X., et al., *iTRAQ experimental design for plasma biomarker discovery.* J Proteome Res, 2008. **7**(7): p. 2952-8.
400. Treml, B., et al., *Recombinant angiotensin-converting enzyme 2 improves pulmonary blood flow and oxygenation in lipopolysaccharide-induced lung injury in piglets.* Crit Care Med, 2010. **38**(2): p. 596-601.
401. Dabitao, D., et al., *Multiplex measurement of proinflammatory cytokines in human serum: comparison of the Meso Scale Discovery electrochemiluminescence assay and the Cytometric Bead Array.* J Immunol Methods, 2011. **372**(1-2): p. 71-7.
402. Houser, B., *Bio-Rad's Bio-Plex(R) suspension array system, xMAP technology overview.* Arch Physiol Biochem, 2012. **118**(4): p. 192-6.
403. Bio-Rad, *Bio-Plex™ Cytokine Assay References*, 2006, Bio-Rad Laboritories, Inc.: Hercules, CA.
404. Wozniak, K.L., et al., *Role of IL-17A on resolution of pulmonary C. neoformans infection.* PLoS One, 2011. **6**(2): p. e17204.
405. Wang, J.P., et al., *Contributions of the MyD88-dependent receptors IL-18R, IL-1R, and TLR9 to host defenses following pulmonary challenge with Cryptococcus neoformans.* PLoS One, 2011. **6**(10): p. e26232.
406. Adachi, O., et al., *Targeted disruption of the MyD88 gene results in loss of IL-1- and IL-18-mediated function.* Immunity, 1998. **9**(1): p. 143-50.

407. Burns, K., et al., *MyD88, an adapter protein involved in interleukin-1 signaling.* J Biol Chem, 1998. **273**(20): p. 12203-9.
408. Biondo, C., et al., *MyD88 and TLR2, but not TLR4, are required for host defense against Cryptococcus neoformans.* Eur J Immunol, 2005. **35**(3): p. 870-8.
409. Yauch, L.E., et al., *Involvement of CD14, toll-like receptors 2 and 4, and MyD88 in the host response to the fungal pathogen Cryptococcus neoformans in vivo.* Infect Immun, 2004. **72**(9): p. 5373-82.
410. Wormley, F.L., Jr., G.M. Cox, and J.R. Perfect, *Evaluation of host immune responses to pulmonary cryptococcosis using a temperature-sensitive C. neoformans calcineurin A mutant strain.* Microb Pathog, 2005. **38**(2-3): p. 113-23.
411. Cheng, P.Y., A. Sham, and J.W. Kronstad, *Cryptococcus gattii isolates from the British Columbia cryptococcosis outbreak induce less protective inflammation in a murine model of infection than Cryptococcus neoformans.* Infect Immun, 2009. **77**(10): p. 4284-94.
412. Goldman, D., S.C. Lee, and A. Casadevall, *Pathogenesis of pulmonary Cryptococcus neoformans infection in the rat.* Infect Immun, 1994. **62**(11): p. 4755-61.
413. Dinarello, C.A., *Immunological and inflammatory functions of the interleukin-1 family.* Annu Rev Immunol, 2009. **27**: p. 519-50.
414. Botelho, F.M., et al., *IL-1alpha/IL-1R1 expression in chronic obstructive pulmonary disease and mechanistic relevance to smoke-induced neutrophilia in mice.* PLoS One, 2011. **6**(12): p. e28457.
415. Ekberg-Jansson, A., et al., *Neutrophil-associated activation markers in healthy smokers relates to a fall in DL(CO) and to emphysematous changes on high resolution CT.* Respir Med, 2001. **95**(5): p. 363-73.
416. Churg, A., et al., *The role of interleukin-1beta in murine cigarette smoke-induced emphysema and small airway remodeling.* Am J Respir Cell Mol Biol, 2009. **40**(4): p. 482-90.
417. Corren, J., *Anti-interleukin-5 antibody therapy in asthma and allergies.* Curr Opin Allergy Clin Immunol, 2011. **11**(6): p. 565-70.
418. Simon, D., A. Wardlaw, and M.E. Rothenberg, *Organ-specific eosinophilic disorders of the skin, lung, and gastrointestinal tract.* J Allergy Clin Immunol, 2010. **126**(1): p. 3-13; quiz 14-5.
419. Shi, H.Z., *Eosinophils function as antigen-presenting cells.* J Leukoc Biol, 2004. **76**(3): p. 520-7.
420. Domachowske, J.B., et al., *Pulmonary eosinophilia in mice devoid of interleukin-5.* J Leukoc Biol, 2002. **71**(6): p. 966-72.
421. Foster, P.S., et al., *Elemental signals regulating eosinophil accumulation in the lung.* Immunol Rev, 2001. **179**: p. 173-81.
422. Olleros, M.L., et al., *Interleukin-12p40 overexpression promotes interleukin-12p70 and interleukin-23 formation but does not affect bacille Calmette-Guerin and Mycobacterium tuberculosis clearance.* Immunology, 2007. **122**(3): p. 350-61.
423. Dubin, P.J. and J.K. Kolls, *IL-23 mediates inflammatory responses to mucoid Pseudomonas aeruginosa lung infection in mice.* Am J Physiol Lung Cell Mol Physiol, 2007. **292**(2): p. L519-28.
424. Langrish, C.L., et al., *IL-12 and IL-23: master regulators of innate and adaptive immunity.* Immunol Rev, 2004. **202**: p. 96-105.

425. Duckett, N.S., et al., *Intranasal interleukin-12 treatment for protection against respiratory infection with the Francisella tularensis live vaccine strain.* Infect Immun, 2005. **73**(4): p. 2306-11.
426. Kawakami, K., et al., *IL-12 protects mice against pulmonary and disseminated infection caused by Cryptococcus neoformans.* Clin Exp Immunol, 1996. **104**(2): p. 208-14.
427. Peck, A. and E.D. Mellins, *Precarious balance: Th17 cells in host defense.* Infect Immun, 2010. **78**(1): p. 32-8.
428. Korn, T., et al., *IL-17 and Th17 Cells.* Annu Rev Immunol, 2009. **27**: p. 485-517.
429. Conti, H.R., et al., *Th17 cells and IL-17 receptor signaling are essential for mucosal host defense against oral candidiasis.* J Exp Med, 2009. **206**(2): p. 299-311.
430. Werner, J.L., et al., *Requisite role for the dectin-1 beta-glucan receptor in pulmonary defense against Aspergillus fumigatus.* J Immunol, 2009. **182**(8): p. 4938-46.
431. Netea, M.G., et al., *Differential role of IL-18 and IL-12 in the host defense against disseminated Candida albicans infection.* Eur J Immunol, 2003. **33**(12): p. 3409-17.
432. Bozza, S., et al., *Immune sensing of Aspergillus fumigatus proteins, glycolipids, and polysaccharides and the impact on Th immunity and vaccination.* J Immunol, 2009. **183**(4): p. 2407-14.
433. Cai, S., et al., *CXCL1 regulates pulmonary host defense to Klebsiella Infection via CXCL2, CXCL5, NF-kappaB, and MAPKs.* J Immunol, 2010. **185**(10): p. 6214-25.
434. Guillot, L., et al., *Enhanced innate immune responsiveness to pulmonary Cryptococcus neoformans infection is associated with resistance to progressive infection.* Infect Immun, 2008. **76**(10): p. 4745-56.
435. Schroder, K., et al., *Interferon-gamma: an overview of signals, mechanisms and functions.* J Leukoc Biol, 2004. **75**(2): p. 163-89.
436. Hardison, S.E., et al., *Pulmonary infection with an interferon-gamma-producing Cryptococcus neoformans strain results in classical macrophage activation and protection.* The American journal of pathology, 2010. **176**(2): p. 774-85.
437. Van de Walle, G.R., K. Sakamoto, and N. Osterrieder, *CCL3 and viral chemokine-binding protein gg modulate pulmonary inflammation and virus replication during equine herpesvirus 1 infection.* J Virol, 2008. **82**(4): p. 1714-22.
438. Lindell, D.M., et al., *Macrophage inflammatory protein 1alpha/CCL3 is required for clearance of an acute Klebsiella pneumoniae pulmonary infection.* Infect Immun, 2001. **69**(10): p. 6364-9.
439. Gonzalo, J.A., et al., *Critical involvement of the chemotactic axis CXCR4/stromal cell-derived factor-1 alpha in the inflammatory component of allergic airway disease.* J Immunol, 2000. **165**(1): p. 499-508.
440. Grone, H.J., et al., *Met-RANTES reduces vascular and tubular damage during acute renal transplant rejection: blocking monocyte arrest and recruitment.* FASEB J, 1999. **13**(11): p. 1371-83.
441. Culley, F.J., et al., *Role of CCL5 (RANTES) in viral lung disease.* J Virol, 2006. **80**(16): p. 8151-7.

442. Vesosky, B., et al., *CCL5 participates in early protection against Mycobacterium tuberculosis.* J Leukoc Biol, 2010. **87**(6): p. 1153-65.
443. Filler, S.G., M.R. Yeaman, and D.C. Sheppard, *Tumor necrosis factor inhibition and invasive fungal infections.* Clin Infect Dis, 2005. **41 Suppl 3**: p. S208-12.
444. Mehrad, B., R.M. Strieter, and T.J. Standiford, *Role of TNF-alpha in pulmonary host defense in murine invasive aspergillosis.* J Immunol, 1999. **162**(3): p. 1633-40.
445. Roilides, E., et al., *Tumor necrosis factor alpha enhances antifungal activities of polymorphonuclear and mononuclear phagocytes against Aspergillus fumigatus.* Infect Immun, 1998. **66**(12): p. 5999-6003.
446. Casadevall, A. *Emerging fugal pathogens-past, present and future* in *Fungal diseases: an emerging threat to human, animal and plant health*. 2010. Institute of Medicine, Washington D. C.
447. *Fungal Diseases: An Emerging Threat to Human, Animal, and Plant Health: Workshop Summary*. 2011: The National Academies Press.
448. Galanis, E., et al., *Epidemiology of Cryptococcus gattii, British Columbia, Canada, 1999-2007.* Emerg Infect Dis, 2010. **16**(2): p. 251-7.
449. Datta, K., K.H. Bartlett, and K.A. Marr, *Cryptococcus gattii: Emergence in Western North America: Exploitation of a Novel Ecological Niche.* Interdiscip Perspect Infect Dis, 2009. **2009**: p. 176532.
450. Prevention, C.f.D.C.a. *C. gattii cryptococcosis statistics*. 2012 15/03/2012 [cited 2013 20/08/2013]; Available from: http://www.cdc.gov/fungal/cryptococcosis-gattii/statistics.html.
451. Horn, F., et al., *Systems biology of fungal infection.* Front Microbiol, 2012. **3**: p. 108.
452. Wanjek, C., *Systems biology as defined by NIH: an intellectual resource for integrative biology.* The NIH Catalyst, 2011. **19**(6).
453. Santamaria, R., et al., *Systems biology of infectious diseases: a focus on fungal infections.* Immunobiology, 2011. **216**(11): p. 1212-27.
454. Butler, G., et al., *Evolution of pathogenicity and sexual reproduction in eight Candida genomes.* Nature, 2009. **459**(7247): p. 657-62.
455. Dujon, B., *Yeast evolutionary genomics.* Nat Rev Genet, 2010. **11**(7): p. 512-24.
456. Moran, G.P., D.C. Coleman, and D.J. Sullivan, *Comparative genomics and the evolution of pathogenicity in human pathogenic fungi.* Eukaryot Cell, 2011. **10**(1): p. 34-42.
457. Cairns, T., F. Minuzzi, and E. Bignell, *The host-infecting fungal transcriptome.* FEMS Microbiol Lett, 2010. **307**(1): p. 1-11.
458. Gibbons, J.G., et al., *Global transcriptome changes underlying colony growth in the opportunistic human pathogen Aspergillus fumigatus.* Eukaryot Cell, 2012. **11**(1): p. 68-78.
459. Upadhya, R., et al., *Global transcriptome profile of Cryptococcus neoformans during exposure to hydrogen peroxide induced oxidative stress.* PLoS One, 2013. **8**(1): p. e55110.
460. Cagas, S.E., et al., *Profiling the Aspergillus fumigatus proteome in response to caspofungin.* Antimicrob Agents Chemother, 2011. **55**(1): p. 146-54.
461. Bruns, S., et al., *Functional genomic profiling of Aspergillus fumigatus biofilm reveals enhanced production of the mycotoxin gliotoxin.* Proteomics, 2010. **10**(17): p. 3097-107.

462. Martinez-Solano, L., et al., *Differential protein expression of murine macrophages upon interaction with Candida albicans.* Proteomics, 2006. **6 Suppl 1**: p. S133-44.
463. Martinez-Solano, L., et al., *Proteomics of RAW 264.7 macrophages upon interaction with heat-inactivated Candida albicans cells unravel an anti-inflammatory response.* Proteomics, 2009. **9**(11): p. 2995-3010.
464. Shin, Y.K., K.Y. Kim, and Y.K. Paik, *Alterations of protein expression in macrophages in response to Candida albicans infection.* Mol Cells, 2005. **20**(2): p. 271-9.
465. Jin, J., et al., *Differential proteome profiling using iTRAQ in microalbuminuric and normoalbuminuric type 2 diabetic patients.* Exp Diabetes Res, 2012. **2012**: p. 168602.
466. Ghosh, D., et al., *iTRAQ based quantitative proteomics approach validated the role of calcyclin binding protein (CacyBP) in promoting colorectal cancer metastasis.* Mol Cell Proteomics, 2013. **12**(7): p. 1865-80.
467. Health, U.S.N.I.o. *What is COPD*. 2012 June 2012 [cited 2012 1/8/12]; Available from: http://www.nhlbi.nih.gov/health/health-topics/topics/copd/.
468. Nathell, L., et al., *COPD diagnosis related to different guidelines and spirometry techniques.* Respir Res, 2007. **8**: p. 89.
469. Rahman, I. and W. MacNee, *Role of oxidants/antioxidants in smoking-induced lung diseases.* Free Radic Biol Med, 1996. **21**(5): p. 669-81.
470. Lopez, A.D., et al., *Chronic obstructive pulmonary disease: current burden and future projections.* The European respiratory journal : official journal of the European Society for Clinical Respiratory Physiology, 2006. **27**(2): p. 397-412.
471. Rabe, K.F., et al., *Global strategy for the diagnosis, management, and prevention of chronic obstructive pulmonary disease: GOLD executive summary.* American journal of respiratory and critical care medicine, 2007. **176**(6): p. 532-55.
472. Health, U.S.N.I.o. *How is COPD Diagnosed*. 2012 July 31, 2013 [cited 2013 17/6/13]; Available from: http://www.nhlbi.nih.gov/health/health-topics/topics/copd/diagnosis.html.